

**Role of cellular dynamics, adhesion and polarity  
in the context of primordial germ cell migration  
in *Xenopus laevis* embryos**

PhD Thesis in partial fulfilment of the requirements  
for the degree “Doctor rerum naturalium (Dr.rer.nat)”  
in the Molecular Biology Program at the Georg August  
University Göttingen, Faculty of Biology

Submitted by

Aliaksandr Dzementsei

Born in Minsk, Belarus

April 2013

## **Affidavit**

Herewith I declare that I prepared the PhD thesis “Functional dynamics of cell-cell contact formation and cell polarity in the context of primordial germ cell migration in *Xenopus laevis* embryos” on my own and with no other sources and aids than quoted.

31.04.2013

Submission date

---

Aliaksandr Dzementsei

## List of Publications

Dzementsei<sup>1</sup> A., Schneider<sup>1</sup> D., Janshoff A. and Pieler T. Migratory and adhesive properties of *Xenopus laevis* primordial germ cells in vitro. Submitted.

Dzementsei A. and Pieler T. "Primordial germ cell migration". In *Xenopus Development*, edited by Kloc M. and Kubiak J. Z., Wiley Publishing, Inc. Accepted.

Tarbashevich K., Dzementsei A., Pieler T. 2011. A novel function for KIF13B in germ cell migration. *Dev Biol.* 349(2):169-178.

---

**TABLE OF CONTENTS**

ACKNOWLEDGEMENTS .....	8
ABSTRACT .....	9
LIST OF FIGURES .....	10
LIST OF TABLES .....	13
1. INTRODUCTION.....	14
1.1 Specification of PGCs .....	14
1.2 PGC development in different model organisms .....	16
1.2.1 PGC development in <i>C. elegans</i> .....	16
1.2.2 PGC development in <i>Drosophila</i> .....	18
1.2.3 PGC development in zebrafish .....	20
1.2.4 PGC development in mouse .....	21
1.2.5 PGC development in <i>Xenopus</i> .....	22
1.3 Control of active PGC migration in <i>Drosophila</i> , zebrafish and mouse.....	24
1.3.1 PGC migration in <i>Drosophila</i> .....	24
1.3.2 PGC migration in zebrafish .....	27
1.3.3 PGC migration in mouse .....	29
1.4 PGC migration in <i>Xenopus</i> .....	30
1.4.1 Labeling and identification of PGCs in <i>Xenopus</i> embryos.....	30
1.4.2 Blebbing-associated motility as a basis for PGC migration in the endoderm .....	31
1.4.3 Signaling pathways involved in PGC migration in <i>Xenopus</i> .....	34
1.4.4 Role of cell adhesion in <i>Xenopus</i> PGC migration .....	38
2. MATERIALS AND METHODS.....	41
2.1 Model Organism .....	41
2.2 Bacteria .....	41
2.3 Cell line .....	41
2.4 Buffers and media .....	41
2.5 DNA constructs, vectors and oligonucleotides .....	42
2.5.1 Vectors.....	42
2.5.2 Expression constructs .....	43
2.5.3 Marker constructs .....	43
2.5.4 Candidate PGC specific genes.....	44

---

2.5.5 Sequencing and cloning primers .....	44
2.5.6 Morpholino oligonucleotides .....	45
2.6 DNA-methods .....	45
2.6.1 DNA isolation and purification .....	45
2.6.2 DNA restriction digest .....	45
2.6.3 Agarose-gel electrophoresis (Sharp et al., 1973) .....	46
2.6.4 Standart Polymerase chain reaction (PCR) (Mullis et al., 1986) .....	46
2.6.5 DNA-sequencing and sequence analysis .....	46
2.6.6 Purification of DNA fragments .....	47
2.6.7 Ligation of DNA fragments .....	47
2.6.8 Transformation .....	47
2.6.9 Verification of the integration of a DNA fragment of interest .....	47
2.7 RNA-methods .....	48
2.7.1 in vitro transcription of labelled RNA probe for in situ hybridization.....	48
2.7.2 in vitro transcription of capped-mRNA for microinjections.....	48
2.7.3 Purification of synthetic RNAs .....	48
2.7.4 Isolation of total RNA .....	48
2.7.5 Semiquantitative Reverse-Transcription PCR (RT-PCR) .....	49
2.7.6 Quantitative RT-PCR analysis.....	49
2.7.7 Whole transcriptome analysis.....	50
2.8 Protein methods .....	51
2.8.1 In vitro translation of the proteins and immunoprecipitation.....	51
2.8.2 Western blotting.....	51
2.9 Preparation and manipulation of <i>Xenopus laevis</i> embryos .....	51
2.9.1 Preparation of <i>Xenopus laevis</i> testis .....	51
2.9.2 Embryo injections and culture.....	52
2.9.3 Whole-mount in situ hybridization (WMISH).....	52
2.9.4 Bleaching .....	55
2.9.5 Clearing of the endoderm .....	55
2.9.6 TUNEL-staining .....	56
2.10 PGC cultivation .....	56
2.10.1 Labelling and isolation of PGCs and somatic endodermal cells .....	56
2.10.2 Cultivation of PGCs on a layer of HEK 293.....	56

---

2.10.3 Cultivation of PGCs in between two layers of endodermal cells .....	57
2.10.4 Cultivation of PGCs in extracellular matrix.....	57
2.10.5 Cultivation of PGC imbedded in agarose gel .....	57
2.10.6 Under-agarose migration assay.....	57
2.11 Biophysical methods.....	58
2.11.1 Electric cell-substrate impedance sensing .....	58
2.11.2 Time-lapse image analysis .....	58
2.11.3 Single-cell force spectroscopy .....	59
3. RESULTS .....	60
3.1 Isolated <i>X. laevis</i> PGCs can migrate <i>in vitro</i> in the confined environment via bleb-associated mechanism without specific adhesion to the substrate .....	60
3.1.1 Cultivation of <i>X. laevis</i> PGCs on the cellular substrates .....	60
3.1.2 Cultivation of <i>X. laevis</i> PGCs on the artificial substrates.....	61
3.1.3 Bleb-associated motility of PGCs in the under-agarose migration assay.....	64
3.2 PGCs isolated from neurula stage can migrate in the under-agarose migration assay, but migration efficiency is increased at the tailbud stage .....	67
3.3 PGCs isolated from tailbud stage <i>Xenopus laevis</i> embryos show higher plasma membrane dynamics in comparison to neurula stage due to increased formation of bleb-like protrusions.....	71
3.3.1 Analysis of cellular dynamics by electric cell-substrate impedance sensing .....	71
3.3.2 Time-lapse image analysis of isolated PGCs.....	73
3.4 Adhesion of PGCs to surrounding somatic endodermal cells and fibronectin decreases at the tailbud stage of embryonic development.....	74
3.4.1 Measurement of cell-cell adhesion forces .....	76
3.4.2 Measurement of cell adhesion to fibronectin and collagen I .....	76
3.5 Differential transcriptome analysis of PGCs and somatic endodermal cells isolated from tailbud and neurula stage embryos.....	78
3.5.1 Strategy used for the whole transcriptome analysis of PGCs and somatic endodermal cells .....	78
3.5.2 Evaluation of the sequencing results .....	79
3.5.3 Analysis of candidate PGC-specific transcripts by WMISH.....	81
3.6 Expression of several adhesion molecules is downregulated during PGC transition to the active migration .....	81
3.6.1 Transcriptom analysis to identify differential gene expression in pre-migratory and migratory PGCs .....	81

---

3.6.2 Quantitative RT-PCR analysis of candidate adhesion molecules expression in PGCs .....	84
3.7 <i>xKIF13B</i> mRNA is present in germ plasm and PGCs up to tailbud stages, but its translation is not required for PGC development before active migration .....	86
3.8 <i>Xenopus</i> homologues of Centaurin- $\alpha$ 1 and Syntabulin are not likely to be involved to be involved in the interaction with <i>xKIF13B</i> in PGCs .....	87
3.8.1 Known interaction partner of <i>xKIF13B</i> , Centaurin- $\alpha$ 1, is not expressed in <i>X. laevis</i> PGCs .....	87
3.8.2 <i>xSyntabulin</i> as a potential binding partner of <i>xKIF13B</i> in PGCs .....	88
4. DISCUSSION .....	95
4.1 Polarization and directional migration of <i>X. laevis</i> PGCs <i>in vitro</i> .....	95
4.1.1 <i>In vitro</i> PGC migration in the presence of different substrates .....	95
4.1.2 Role of PIP3 in PGC polarization .....	97
4.2 Role of cellular dynamics in the transition to active migration .....	99
4.3 Cell-cell and cell-extracellular matrix adhesion in active migration .....	100
4.3.1 Role of adhesion during PGC migration .....	100
4.3.2 Quantification of cell-cell and cell-extracellular matrix adhesion of PGCs .....	101
4.4 Differential gene expression in PGCs .....	102
4.4.1 Regulation of gene expression in PGCs among different species .....	102
4.4.2 Strategy for the next generation sequencing analysis .....	104
4.4.3 Annotation of the next generation sequencing results .....	105
4.4.4 Analysis of the differential gene expression .....	105
4.4.5 Differential gene expression in migratory and pre-migratory PGCs .....	107
4.5 Role of <i>xKIF13B</i> in the active PGC migration .....	108
4.5.1 <i>xKIF13B</i> in the early stages of <i>X. laevis</i> embryogenesis .....	108
4.5.2 <i>xCentaurin-<math>\alpha</math>1</i> as a candidate interaction partner for <i>xKIF13B</i> .....	110
4.5.3 <i>xSyntabulin</i> as a candidate interaction partner for <i>xKIF13B</i> .....	111
5. SUMMARY AND CONCLUSIONS .....	114
6. BIBLIOGRAPHY .....	115
Supplementary material .....	129
Curriculum vitae .....	137

---

## ACKNOWLEDGEMENTS

First of all I want to express a deep gratitude to my supervisor Prof. Dr. Tomas Pieler for giving me an opportunity to work on this project, and for the great guidance and support over these years.

I would also like to thank Dr. Katsiaryna Tarbashevich who started this project, motivated me to continue this work and introduced a lot of nice techniques.

I am very grateful to the members of my thesis committee, Prof. Dr. Andreas Wodarz and Prof. Dr. Michael Kessel, for critical evaluation and valuable suggestions done for this project during committee meetings.

I'm very thankful to the entire Developmental Biology team for creating a great environment and all the help and support. I especially want to thank members of "Transport" group, Dr. Maïke Claussen, Marion Dornwell, Juliane Wellner and Diana Obermann.

I want to thank our collaborators, Prof. Dr. Andreas Janshoff and D. Schnieder, for providing great tools to study isolated cells and for the help in design and evaluation of experiments.

I would also like to thank The Transcriptome Analysis Laboratory (TAL), especially Dr. Gabriela Salinas-Riester for the help with experimental design for whole transcriptome analysis, Fabian Ludewig and Susanne Luthin for the help with sample preparation and Lennart Opitz for bioinformatical analysis.

I want to thank Avani Shukla for the contribution in the study of xSyntabulin during her lab rotation project in our lab.

I would like to acknowledge the International MSc/PhD program in Molecular Biology, and particularly Dr. Steffen Burkhardt, for giving me an opportunity to study at the Göttingen University and for the excellent coordination and support during all these years.

Last but not least I want to deeply thank my family and Olena Steshenko for the love and moral support that encourages me wherever I go and whatever I do in my life.

This research was partially supported by a grant from the Deutsche Forschungsgemeinschaft (DFG) to Prof. Dr. Tomas Pieler and Prof. Dr. Andreas Janshoff (FOR 1756).



## ABSTRACT

Directional cell migration is an intensively studied process relevant for both normal development of an organism as well as for a number of pathological conditions such as chronic inflammation and cancer. Primordial germ cells (PGCs) in *Xenopus laevis* embryos can be used as a model system to study cell migration, since during embryogenesis they actively migrate within the endoderm towards genital ridges. Transition to active cell migration is a highly regulated process important for the normal PGC development in many species.

This study is focused on molecular and cellular mechanisms involved in initiation of active PGC migration within the endoderm of *X. laevis* embryos. Analysis of cell shape fluctuations demonstrated that in comparison to pre-migratory neural stage, PGCs isolated from tailbud stage embryos are characterized by an increased cellular dynamics due to formation of bleb-like protrusions and migration via bleb-associated mechanism. Analysis of intracellular PIP3 distribution that depends on the function of kinesin xKIF13B suggests role of PIP3 enrichment in the bleb-like protrusions for PGC polarisation prior to migration, but not for cellular motility during active phase of migration. In addition, cellular adhesion of PGCs to surrounding somatic cells and fibronectin is decreased at the migratory stages, and is not required for the migration *in vitro*. Whole transcriptome analysis of PGCs and somatic endodermal cells isolated from the neurula and tailbud stages revealed downregulation of several adhesion molecules in migratory PGCs. Downregulated expression of Claudin 6.1, Gap junction protein beta 1 and E-cadherin was confirmed by quantitative RT-PCR analysis with isolated cells.

---

**LIST OF FIGURES**

<b>Fig. 1</b>	<b>Primordial germ cell development in different model organisms</b>	<b>17</b>
<b>Fig. 2</b>	<b>Molecular regulation of active PGC migration in <i>Drosophila</i>, zebrafish and mice</b>	<b>26</b>
<b>Fig. 3</b>	<b>PGC motility and morphology during different developmental stages of <i>X.laevis</i> embryos</b>	<b>32</b>
<b>Fig. 4</b>	<b>The life cycle of a bleb</b>	<b>33</b>
<b>Fig. 5</b>	<b>PGC polarization and migration on fibronectin towards the dorsal extract source</b>	<b>35</b>
<b>Fig. 6</b>	<b>Models of bleb-associated motility</b>	<b>38</b>
<b>Fig. 7</b>	<b>Labeling and isolation of <i>X. laevis</i> PGCs</b>	<b>61</b>
<b>Fig. 8</b>	<b>Cultivation of isolated PGCs within the endodermal cell mass did not facilitate active migration</b>	<b>62</b>
<b>Fig. 9</b>	<b>Isolated PGCs cultivated on mammalian cell substrate formed bleb-like protrusions, but did not exhibit migratory behavior</b>	<b>63</b>
<b>Fig. 10</b>	<b>Isolated PGCs cultivated in extracellular matrix had high cellular dynamics, but did not initiate active migration</b>	<b>64</b>
<b>Fig. 11</b>	<b>PGCs embedded in the agarose gel showed migratory behavior, but could not initiate migration</b>	<b>65</b>
<b>Fig. 12</b>	<b><i>X. laevis</i> PGC can migrate <i>in vitro</i> in the under-agarose migration</b>	<b>66</b>
<b>Fig. 13</b>	<b>Surrounding cells can ‘anchor’ PGCs and prevent their migration <i>in vitro</i> in the under-agarose migration</b>	<b>67</b>

---

<b>Fig. 14</b>	<b>Actin is not enriched in the leading edge of <i>X. laevis</i> PGCs during their migration <i>in vitro</i></b>	<b>68</b>
<b>Fig. 15</b>	<b>PIP3 enrichment is not observed in the leading edge of PGCs migrating <i>in vitro</i></b>	<b>69</b>
<b>Fig. 16</b>	<b>Motility of PGCs isolated from the tailbud stage embryos is increased in comparison to the neurula stage</b>	<b>70</b>
<b>Fig. 17</b>	<b>PGCs isolated from tailbud stage embryos show high cellular motility</b>	<b>72</b>
<b>Fig. 18</b>	<b>High cellular dynamics of PGCs isolated from tailbud stage embryos correlates with increased cell blebbing</b>	<b>73</b>
<b>Fig. 19</b>	<b>Formation and retraction of the bleb-like protrusions in isolated <i>X. laevis</i> PGCs correlates with disruption and re-polymerization of actin cortex on the plasma membrane</b>	<b>74</b>
<b>Fig. 20</b>	<b>PGCs reduce overall cell-cell adhesion activity after transition to the active migration state</b>	<b>75</b>
<b>Fig. 21</b>	<b>Pre-migratory PGCs show high affinity to fibronectin.</b>	<b>77</b>
<b>Fig. 22</b>	<b>Next generation sequencing analysis confirms identity of the used cell populations and reveals novel PGC-specific candidate genes</b>	<b>80</b>
<b>Fig. 23</b>	<b>Whole mount in situ hybridization analysis of novel PGC-specific transcripts</b>	<b>82</b>
<b>Fig. 24</b>	<b>Comparative whole transcriptom analysis led to identification of several candidate adhesion molecules differentially regulated between neurula and tailbud stage PGCs</b>	<b>83</b>
<b>Fig. 25</b>	<b>Expression of Claudin 6.1, E-cadherin and gap junction protein beta 1 is downregulated specifically in PGC at tailbud stage</b>	<b>85</b>

- 
- Fig. 26** *xKIF13B* is expressed in the PGCs at neurula and early tailbud stages of embryonic development 87
- Fig. 27** *xKIF13B* knockdown does not affect germ plasm localization in *X. laevis* embryos at blastula stage 88
- Fig. 28** Knock-down of *xKIF13B* leads to the reduction of PGC number after transition of PGCs to the active migration 89
- Fig. 29** Reduction of the total PGC number in *xKIF13B* morphants is not caused by apoptosis 90
- Fig. 30** *xCentaurin- $\alpha$ 1* is expressed in *X. laevis* embryos during gastrula, neurula and tailbud stages outside the endoderm 91
- Fig. 31** Syntabulin is expressed in *X. laevis* PGCs up to tailbud stage 92
- Fig. 32** *xSyntabulin* is not localized in bleb-like protrusions formed by isolated PGCs of *X. laevis* tailbud stage embryos 93
- Fig. 33** Morpholino knock-down of *xSyntabulin* results in a defect in the neural tube development, but has little impact on PGC number and localization in tailbud stage embryos 94

---

**LIST OF TABLES**

<b>Table 1</b>	<b>Expression constructs</b>	<b>43</b>
<b>Table 2</b>	<b>Candidate PGC specific genes</b>	<b>44</b>
<b>Table 3</b>	<b>Primer list</b>	<b>44</b>
<b>Table 4</b>	<b>Antisense Morpholino oligonucleotides</b>	<b>45</b>
<b>Table 5</b>	<b>Thresholds to identify defferentially expressed genes in PGCs</b>	<b>51</b>
<b>Table 6</b>	<b>Rehydration of embryos</b>	<b>52</b>
<b>Table 7</b>	<b>Proteinase K treatment procedure</b>	<b>53</b>
<b>Table 8</b>	<b>Acetylation of <i>Xenopus</i> embryos</b>	<b>53</b>
<b>Table 9</b>	<b>Washing and RNAse treatment of <i>Xenopus</i> embryos</b>	<b>54</b>
<b>Table 10</b>	<b>Blocking and antibody incubation</b>	<b>54</b>
<b>Table 11</b>	<b>Alkaline phosphatase staining reaction</b>	<b>55</b>
<b>Table 12</b>	<b>Bleaching of pigmented <i>Xenopus</i> embryos</b>	<b>55</b>

## 1. INTRODUCTION

All sexually reproducing organisms arise from gametes, a specialized cell population that is capable of generating entire new organism. Gametes in turn are differentiated from a small stem cell population known as germ cells. Primordial germ cells (PGCs) are progenitors to the germ cells during early stages of embryogenesis in many animal species including *Xenopus*. Together with somatic cells they contribute to the formation of gonads and emerge early during embryogenesis (Wylie, 1999). In many species, the site of gonad formation is different from the region of germ cell specification. Thus, during embryogenesis PGCs have to migrate in a directional manner from the region of their specification to the site of gonad formation. This makes PGCs an attractive model to study the general mechanisms underlying cell migration (Molyneaux and Wylie, 2004; Raz, 2004). Directional cell migration is a key developmental event, crucial for embryo- and organogenesis. Aberrant cell migration can cause developmental defects and impair wound healing and immune response affecting the body's ability to respond to injury. It is also associated with a number of human diseases such as chronic inflammation and cancer (Franz et al., 2002; Webb et al., 2005). Therefore, understanding of the cellular and molecular mechanisms underlying cell migration is not only important for a number of fundamental developmental processes, but can also be applied in the medical practice.

### 1.1 Specification of PGCs

There are at least two strategies of germ line specification in animals (Extavour and Akam, 2003). In some species, including mammals and urodeles, germ line cells are formed *de novo*. This type of PGC specification may be the most widespread (and ancestral) among metazoans. Specification in this case occurs in response to the inductive signals from surrounding tissue. In mouse, specification of PGCs occurs due to the induction of proximal epiblast cells by the surrounding extraembryonic cells. Several of these inductive signals belong to the bone morphogenetic protein (BMP) family, such as Bmp2, Bmp4 and Bmp8b (Lawson et al., 1999; Ying et al., 2000, Ying and Zhao, 2001). In a subset of mouse proximal epiblast cells there is also an up-regulated expression of genes *fragilis* and *stella*, which makes these cells competent to respond to BMP signals and differentiate into PGCs (Saitou et al., 2002). However, other cell populations with no *fragilis* and *stella* expression can differentiate into PGCs if transplanted next to the source of the inductive signals (Tam and Zhou, 1996).

The second type of PGC specification is common among the prominent experimental model organisms in developmental biology, including *Drosophila*, *Caenorhabditis elegans*, zebrafish and *Xenopus*. Specification of germ cells in these species occurs very early in embryogenesis due to the inheritance of specific maternal determinants, consisting of proteins and RNAs. These factors are localized in the germ plasm, a cytoplasmic region with a discrete morphological constitution. It contains cisterns of the endoplasmic reticulum (ER), mitochondria, and electron-dense granules with complex structure that are termed germinal

granules in *Xenopus*, polar granules in *Drosophila*, and P-bodies in *C. elegans* (Klock et al., 2004). Only those cells that inherit germ plasm can differentiate into germ cells in these species.

In *Xenopus laevis*, maternally supplied factors of the germ plasm are localized to the vegetal pole of fertilized eggs (Ikenishi et al., 1984). Localization of these factors to the vegetal pole and the formation of the germ plasm occur already during oogenesis. In *Xenopus* oocytes, germ plasm is formed out of the mitochondrial cloud (MC), a macroscopic structure containing granular/fibrous material, mitochondria, ER, maternal RNA and proteins (Heasman et al., 1984). At the earliest stages of oogenesis, the MC is formed near the nucleus in the vegetal hemisphere of the oocyte. At stages I/II of oogenesis, the MC starts to migrate towards the vegetal pole. At stages II/III, the MC disintegrates at the vegetal pole of the oocyte and adopts a conical shape. By the end of oogenesis, the MC components are spread along the vegetal cortex.

Since development and specification of PGCs during embryogenesis is dependent on the maternal RNAs, a very important process in the organization of germ plasm is the delivery or localization of specific RNA molecules. There are two main pathways involved in the localization of these RNAs (Kloc and Etkin, 1995). One relies on the transport of specific RNAs to the vegetal pole via the MC and is known as the early transport/localization or the message transport organizer (METRO) pathway. In the very early stages of oogenesis, RNAs migrating via this pathway, such as *Xcat2*, *Xdazl*, *Xlsirts*, *Xpat*, *Xwnt11*, *Germes* and *DEADSouth*, are homogeneously distributed in the oocyte cytoplasm. At stage I/II of the oogenesis they become localized in the MC and migrate along with it to the vegetal pole of the oocyte (Kloc et al., 1996; King et al., 2005). An alternative mechanism to localize specific RNAs to the vegetal pole of *Xenopus* oocytes is known as the late RNA transport/localization pathway. It operates at stages III/IV of the oogenesis (Yisraeli et al., 1990; Kloc and Etkin, 1995). Examples of the RNAs being localized by this pathway are *Vg1* and *VegT*. At oogenesis stages I and II, *Vg1* and *VegT* mRNAs are still homogeneously distributed throughout the oocyte cytoplasm, but excluded from the MC. At stages III/IV, *Vg1* and *VegT* RNAs move to the vegetal hemisphere, where they concentrate around the disintegrating MC and then occupy the vegetal cortex (King et al., 2005).

The specific localization of maternal RNAs during oogenesis is dependent on the presence of *cis*-acting sequences. These sequences are known as localization elements (LE) and usually reside in 3' untranslated regions (UTRs) of the RNAs. Localization elements can be recognized by specific protein machinery, which leads to the assembly of RNP-complexes and localization of the RNAs. Apart from the localization, assembled RNP-complexes also regulate translation and stability of the respective RNAs (Kloc et al., 2002; King et al., 2005). Several germ plasm-specific RNAs were shown to be degraded in the somatic endodermal cells when the zygotic transcription starts after mid-blastula transition (MBT) (Koebernick et al., 2010). This degradation occurs via a microRNA-based mechanism that depends on the presence of microRNA target sites in the LEs of the corresponding RNAs. In PGCs, however,

recognition of the respective target site in the LEs by microRNAs is prevented by the protein complex that is bound to these LEs. This RNP-complex, therefore, masks the target site leading to the stabilization of the corresponding RNAs specifically in PGCs (Koebernick et al., 2010).

## 1.2 PGC development in different model organisms

Despite of the type of specification, PGCs in many organisms have to migrate to the region of gonad formation. This process is described for several model organisms and includes passive and/or active migration within the embryo. PGCs also have to remain undifferentiated and maintain their cell fate during this migration. Interestingly, the mechanisms promoting PGC fate and maintenance seem to be conserved and include transcriptional silencing, as well as post-transcriptional regulation of gene expression.

### 1.2.1 PGC development in *C. elegans*

In *C. elegans* separation of germ cell line takes place during the first four embryonic cleavages. The zygote divides asymmetrically to give rise to a large somatic blastomere and a smaller germ line blastomere. The latter subsequently undergoes three more unequal divisions resulting in three additional somatic blastomeres and a single germ line blastomere P<sub>4</sub>, which then divides symmetrically giving rise to two PGCs (Z2 and Z3). Unequal cell division is accompanied by unequal segregation of germinal granules, called P-bodies or P-granules. They are specifically inherited only by the germ line blastomeres. After two PGCs are formed, these cells stop cell division and are passively involuted inside of the embryo in close association with intestinal cells via gastrulation movements. In mid-embryogenesis PGCs are joined by two somatic gonad precursor cells, Z1 and Z4, resulting in the formation of the gonad primordium (Fig. 1A). Association between these four cells is required for proper gonad formation. After *C.elegans* larvae hatch and begin feeding (stage L1), PGCs resume cell division giving rise to more than 1000 germ cells (Kemphues and Strome, 1997; Schedl, 1997).

One of the specific features of the germ line blastomeres in *C. elegans* is transcriptional silencing. It is mediated by inheritance of maternal factor PIE-1 (*pharynx and intestine in excess*). Similar to P-granules, PIE-1 is specifically segregated only to the germ line blastomeres and accumulates in the nuclei of these cells. It functions as a general transcription repressor via inhibiting transcriptional elongation by RNA polymerase II. Absence of PIE-1 results in differentiation of the descendants of germ line blastomeres into other cell lineages indicating importance of transcriptional repression for PGC specification (Nakamura and Seydoux, 2008).

PIE-1 is degraded when the last germ line blastomere P<sub>4</sub> divides into the PGCs. However, selective transcriptional repression is still required for proper development and differentiation of germ cells. This is achieved by chromatin remodeling of the PGCs that follows directly the PIE-1 degradation. At this point 'active' chromatin modifications (like H3meK4 and H4ack8) and histone linker H1.1 (*his-24*) disappear, and PGCs become arrested



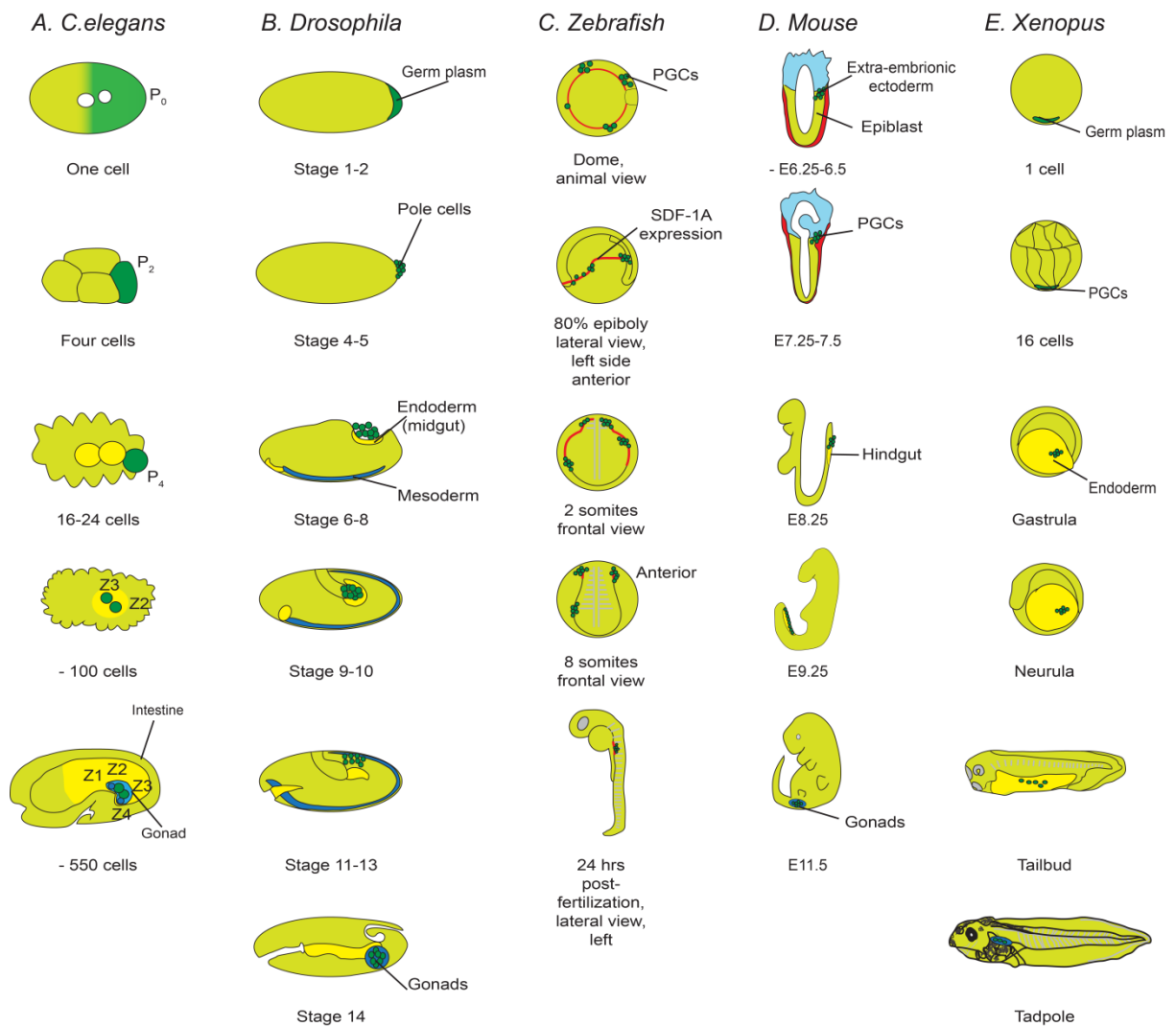


**Fig. 1. Primordial germ cell development in different model organisms. (A)** Germ plasm (green) in *C. elegans* after fertilisation is redistributed in the embryo towards posterior site. During cleavage stages of embryonic development it is asymmetrically inherited by germ line blastomeres P1-P4. At ~100 cell stage equal division of the last germ line blastomere P4 gives rise to two primordial germ cells (PGCs), Z2 and Z3. Together with intestinal cells (yellow), they move inside the embryo, where they are joined by somatic gonad precursor cells, Z1 and Z4. **(B)** In *Drosophila*, germ plasm (green) is assembled at the posterior pole of the oocyte. After fertilisation, germ plasm is inherited by the PGC precursors, known as pole cells. These cells are carried inside of the embryo during germ band extension in association with midgut epithelium cells. Later, PGCs pass through the midgut, migrate towards the mesoderm (blue), and then coalesce with somatic gonadal cells to generate embryonic gonads. **(C)** After the specification in four random locations, PGCs in zebrafish migrate to the dorsal side. During gastrulation, they follow the expression of chemoattractant SDF-1 $\alpha$  (red). Later, they move anteriorly towards somites 1-3, and finally to the somites 8-10, where they coalesce with somatic cells of the gonads. **(D)** During stage E6.25-6.5 of mouse embryonic development, signals from extra-embryonic ectoderm (blue) promote several epiblast cells to differentiate in to PGCs (green). Specification is followed by the migration of these cells to the extra-embryonic mesoderm (red) posterior to the primitive streak. After stage E7.5, PGCs migrate from the primitive streak back to the embryo and along the endoderm (yellow), and by stage E11.5 they reach genital ridges and together with somatic cell form embryonic gonads (blue). **(E)** During oogenesis in *Xenopus*, germ plasm (green) is assembled at the vegetal pole and after fertilization is unequally segregated between the blastomeres during the cleavage stages. Three to seven cells, that inherit germ plasm, differentiate into PGCs and during gastrulation become involuted inside the embryo together with somatic endodermal cells. They form a cluster during neurula stages of development. At the tailbud stage (stages 24-44) actively migrate dorsally and anteriorly within the endoderm, and then through the dorsal mesentery to the genital ridges (blue) in the tadpole (according to Santos and Lehmann, 2004a; Kunwar et al., 2006; Seydoux, 2008; Nakamura et al., 2010).

in the G2 or early prophase of the cell cycle (Nakamura and Seydoux, 2008). Transcriptional repression in PGCs remains throughout embryogenesis and is released at the first larval stage (L1). Even after the PGCs resume cell division and generate germ cells, partial repression mediated by MES (*maternal effect sterile*) proteins still remains essential for proliferation and maintenance of totipotency in these cells (Nakamura and Seydoux, 2008; Furuhashi et al., 2010).

Mechanisms of transcriptional repression and epigenetic reprogramming in PGCs are not the only factors that influence gene expression. Post-transcriptional regulation plays an important role in PGC development not only in *C. elegans*, but is common in all species. It was shown by Merritt and co-workers (2008) that with the exception of genes expressed during spermatogenesis, promoters alone are not sufficient to provide germ line-specific gene expression in *C. elegans*. Regulation of gene expression in this case is mediated mainly by 3' UTRs of the corresponding mRNAs, which function post-transcriptionally to orchestrate spatio-temporal protein expression. Many of the important regulators of germ line development are RNA-binding proteins. In *C. elegans* translational regulators MEX-3 and GLD-1 were shown to regulate expression of several germ line-specific genes via 3' UTRs (Merritt et al., 2008). Simultaneous loss of MeX-3 and GLD-1 causes germ cells to over-proliferate and to adopt somatic cell fates, as if prematurely activating an embryonic-like program (Ciosk et al., 2006).

A good example for post-transcriptional expression control is the regulation of NOS-2, a *C. elegans* homologue of *nanos* family of germ cell regulators. Transcripts of the *nos-2* gene are inherited maternally, but its transcription starts only in PGC precursor P<sub>4</sub>. Inhibition of *nos-2* translation occurs already during oogenesis and depends on a short stem loop in the 3' UTR. Repression is dependent on OMA-1 and OMA-2, two closely related CCCH-finger proteins expressed only in the female germ line and enriched in oocytes. After fertilization, translational repression is maintained by two other RNA-bind proteins MEX-3 and SPN-4, while OMA-1 and OMA-2 get degraded. MEX-3 and SPN-4 interact with a second region in the *nos-2* 3' UTR and mediate translational repression in early germ-line blastomeres. In somatic blastomeres *nos-2* RNA is degraded by a process that is independent of translational repression and requires the CCCH finger proteins MEX-5 and MEX-6. Another maternal RNA-binding protein, POS-1, relieves suppression in P<sub>4</sub> by competing with SPN-4 for binding to *nos-2* RNA (D'Agostino et al., 2006; Jadhav et al., 2008). Moreover, PIE-1 is necessary for *nos-2* activation independent of its role in transcriptional silencing, and thus could act as a translational activator (Tenenhaus et al., 2001). Therefore, early germ cell specification and control may involve cascades of RNA regulation.

### **1.2.2 PGC development in *Drosophila***

Specification of germ line in *Drosophila* also starts during oogenesis. Assembly of the germ plasm occurs at the posterior pole of the oocyte. This cytoplasmic region contains large ribosome-rich structures, polar granules and is enriched in specific maternal RNAs and proteins (Santos and Lehmann, 2004a). One of the major factors essential for germ plasm

formation in *Drosophila* is Oskar protein. It was shown to be sufficient to induce ectopic germ plasm assembly and germ cell fate (Ephrussi and Lehmann, 1992). *Oskar* RNA is translocated by a direct movement along microtubules to the posterior pole of the oocyte, which results in the enrichment of the corresponding protein in this region. Localized Oskar expression is required for the subsequent recruitment and anchoring of other germ plasm-specific components (Mahowald, 2001; Tanaka and Nakamura, 2008).

After fertilization, early *Drosophila* embryos develop in a syncytium. Nuclei start to divide synchronously in the middle of the embryo without segregation to the individual cells, and at the seventh division all nuclei move to the periphery. PGC progenitors, also known as the pole cells, are the first cells to be formed by budding of the nuclei together with germ plasm from the posterior pole of the embryo. At this point nuclei of the pole cells stop synchronous division, while somatic nuclei continue to do so before they become incorporated into cells. In contrast to the pole cells, somatic cells are formed not by budding of the nuclei, but rather by the ingrowth of a polarized membrane (Santos and Lehmann, 2004a). After cellularization is complete, PGCs remain tightly associated with each other and with the surrounding somatic cells. During gastrulation they are passively carried by tissue movement to the interior of the embryo into the forming posterior midgut pocket surrounded by midgut epithelium. Later, they first lose contact with somatic cells and then with each other, and subsequently start active migration as individual cells through the posterior midgut. After reaching the body cavity, PGCs reorient themselves on the basal surface of the midgut epithelium and start the migration towards the adjacent mesoderm. Within the mesoderm they separate into two bilateral clusters and align with somatic gonad precursor cells. During germ band retraction, PGCs and the associated somatic gonad precursors migrate anteriorly until two tissues coalesce to form a pair of embryonic gonads (Fig. 1B) (Santos and Lehmann, 2004a; Kunwar et al., 2006; Richardson and Lehmann, 2010).

From the moment of their specification, similar to *C. elegans*, PGCs in *Drosophila* become transcriptionally repressed. Three genes, *germ cell-less* (*gcl*), *nanos* (*nos*) and *polar granule component* (*pgc*), were shown to be involved in this process. All of these genes encode germ plasm specific RNAs. *Gcl* is a nuclear pore-associated protein. It is required for PGC formation and repression of transcription prior to pole cell cellularization. The exact mechanism of its function, however, is not clear. *Nanos* functions later during PGC development in the regulation of gene expression and maintaining PGC identity. Being a translational regulator, the function of *Nanos* in transcriptional repression is most likely indirect (Richardson and Lehmann, 2010). Similar to *PIE-1* in *C. elegans*, the mechanism of transcriptional silencing by *polar granule component* (*pgc*) also involves inhibition of transcriptional elongation by RNA polymerase II. *Pgc* encodes a small protein which is conserved only among *Drosophila* species. Pole cells can be formed even in the embryos lacking *pgc*, but its absence leads to the somatic gene expression in the pole cells and degeneration of these cells during gastrulation. On the other hand, ectopic *pgc* expression is sufficient to down-regulate RNA polymerase II-dependent transcription in the somatic cells (Hanyu-Nakamura et al., 2008; Nakamura et al., 2010).

Chromatin remodeling also contributes to the transcriptional silencing in *Drosophila* PGCs. 'Active' chromatin modifications like H3meK4 are removed during pole cell formation, while the 'silent' chromatin modification H3meK9 shows a different pattern of distribution in comparison to the somatic nuclei. Despite the early appearance of this remodeling, its main function becomes evident when Pgc protein disappears from the pole cells during the gastrulation. Similar to the loss of PIE-1 in *C. elegans*, PGCs remain transcriptionally inactive due to the chromatin-based silencing (Nakamura and Seydoux, 2008). However, in contrast to *C. elegans*, PGCs in *Drosophila* have to undergo active migration to the site of gonad formation. The onset of active migration correlates with a release of transcriptional silencing that takes place in *C. elegans* only upon PGC differentiation into the germ cells.

An important role in the control of germ line specific gene expression belongs to the translational regulation. Due to transcriptional repression, regulation of translation is especially important for the spatial and temporal expression. For several germ line specific genes, including *gcl*, *pgc* and *nos*, it was shown that the 3' UTR of the corresponding RNAs is responsible for the repression or activation of translation at distinct stages of development. Moreover, sequences within the 3' UTR restrict and protect corresponding RNAs in the germ line (Rangan et al., 2009).

### **1.2.3 PGC development in zebrafish**

As in *C. elegans* and *Drosophila*, specification of PGCs in the zebrafish occurs due to the inheritance of maternal determinants localized in the germ plasm. However, in contrast to other model organisms, zebrafish PGCs are formed not at a single site of the embryo, but in four clusters randomly distributed in the early embryo. During their migration to the genital ridges from these clusters, PGCs migrate to several intermediate target sites within the embryo. This complex migration pathway is required for collecting cells from the four clusters to the two sites of gonad formation. PGCs initially migrate along the margin of an embryo toward the dorsal side avoiding the dorsal midline. Afterwards, they cluster in the anterior mesoderm between the head and trunk, or at the lateral border of the mesoderm. Subsequently, PGCs form two lateral clusters and move in the direction of the first somite that serves as an intermediate target. Finally, more anteriorly located PGCs migrate posteriorly, and trailing PGCs join the main PGC clusters at somite 8 in the region of the somatic gonad (Fig. 1C) (Kunwar et al., 2006).

Shortly after their specification, PGCs exhibit a simple, round cell morphology. This stage is followed by a phase when PGCs start the formation of large bleb-like protrusions, but are unable to migrate. Subsequently, cells acquire polarity and motility, loose contacts with each other and start active migration in the embryo (Blaser et al., 2005). Transition between these stages correlates with the regulation of transcription. Block of RNA polymerase II by  $\alpha$ -amanitin prevents PGCs from the initiation of active migration, but does not affect PGC survival (Blaser et al., 2005). Transition to active PGC migration also depends on the levels of translational regulator Dead end (Dnd). Similar to the inhibition of zygotic transcription via RNA polymerase II, knock-down of Dnd results in the block of PGC

polarization and migration. *Dnd* is a key factor involved in PGC survival and migration in the zebrafish (Weidinger et al., 2003). It functions by preventing microRNA-mediated degradation by miR-430 of several PGC-specific transcripts, such as *Nanos* and Tudor domain containing protein 7 (*Tdrd7*) (Kedde et al., 2007). This suggests posttranscriptional regulation to be crucial for the PGC development and migration in zebrafish as well.

#### **1.2.4 PGC development in mouse**

In contrast to the most other model organisms, PGC specification in mice occurs not due to the inheritance of specific maternal determinants, but via inductive mechanisms. In this case formation of the PGCs occurs as a result of BMP 4 and 8 signaling from extraembryonic ectoderm and BMP2 from visceral endoderm to the underlying pluripotent epiblast cells. In addition, the ability of the epiblast cells to respond to BMP signals is induced by Wnt and Nodal signaling, originating from the epiblast cells and visceral endoderm (Saitou and Yamaji, 2012). PGCs emerge as a group of approximately 40 cells at the interface between extraembryonic and embryonic tissues in the posterior region of the embryo, also known as posterior primitive streak. Formation of PGCs depends on the dosage of Smad-mediated BMP signaling. Spatial restriction of BMP, Wnt and Nodal signaling is achieved by their inhibition in the anterior epiblast via the expression of antagonist factors by the anterior visceral endoderm, such as *Lefty1* against Nodal, *Dkk1* against Wnt and *Cerberus-like* against BMP (Saitou, 2009; Saitou and Yamaji, 2010).

Shortly after PGCs are formed, they initiate active migration through the primitive streak into the adjacent posterior embryonic endoderm, extraembryonic endoderm and allantois (Anderson et al., 2000). PGCs continue their migration along the hindgut that is formed from posterior embryonic endoderm during its anterior extension (Kunwar et al., 2006). Finally, PGCs exit the gut, sort into two groups and migrate towards the gonadal ridges. After arriving there, they coalesce with somatic gonad precursors to form the gonads (Fig. 1D) (Molyneaux et al., 2001).

Despite differences in specification, mouse PGCs also show transcriptional repression shortly after their formation. However, in contrast to the PGCs that receive all factors necessary for the early development due to the inheritance of maternal determinants, PGCs formed by inductive mechanism need to produce all these factors by themselves. Therefore, newly formed mouse PGCs are characterized not only by transcriptional repression of somatic genes, but also by selective transcriptional activation of the genes involved in germ cell development (like *Dnd1* and *Nanos3*) and pluripotency (like *Sox2* and *Nanog*) (Nakamura and Seydoux, 2008). One of the key players in both of these processes is B-lymphocyte-induced maturation protein 1 (*Blimp1*, also known as *Prdm1*). This protein contains five zinc finger domains and a PR (PRDI-BF1 and RIZ) domain and is a potential transcriptional repressor. During early embryogenesis, it is expressed in a small number of proximal epiblast cells which are the precursors to the PGCs. Although it is not required for PGC specification, mutations in *Blimp1* lead to the loss of the PGCs later on and to an inability of these cells to populate the gonads (Ohinata et al., 2005; Vincent et al., 2005). *Blimp1* is responsible for the

transcriptional repression of genes downregulated in the early PGCs, but, as mentioned above, it does not globally repress mRNA transcription (Kurimoto et al., 2008). In early PGC development Blimp1 is not only responsible for the repression of somatic gene expression, but is also involved in the activation of approximately half of the genes upregulated in PGCs. These genes mostly encode factors involved in PGC development, survival and migration (Kurimoto et al., 2008; Saitou and Yamaji, 2010). Blimp1 levels were shown to be subject to posttranscriptional regulation by *let-7* microRNA. It was shown, that Lin28, a negative regulator of *let-7* microRNA, is critical for proper PGC specification. Since Blimp1 translation can be blocked by the binding of *let-7* to its 3' UTR, it was suggested that Lin28 releases this block by inhibiting maturation of the microRNA (Saitou and Yamaji, 2012).

Another activator of PGC gene expression in the early stages is Prdm14. Similar to Blimp1 it is also a PR domain-containing protein (Yamaji et al., 2008). Initial expression of Prdm14 in PGCs is independent of Blimp1, but its subsequent maintenance is strictly dependent on it. The main function of Prdm14 in PGCs is upregulation of the genes involved in maintenance of pluripotency and in epigenetic reprogramming (Saitou and Yamaji, 2012; Seervai and Wessel, 2013). The exact mechanism of function for both Blimp1 and Prdm14 is, however, not known.

In mouse PGCs, global transcriptional repression only occurs after PGCs start active migration to the somatic gonads. Similar to *C. elegans* and *Drosophila*, global repression is achieved via the inhibition of RNA polymerase II. In addition, migrating PGCs have been shown to undergo extensive epigenetic reprogramming, including genome-wide DNA demethylation, erasure of parental imprints, and re-activation of the inactive X-chromosome (Sasaki and Matsui, 2008; Saitou, 2009).

#### **1.2.5 PGC development in *Xenopus***

In *Xenopus*, specification of PGCs occurs on the basis of the inheritance of maternally supplied factors. These factors, mostly constituents of the germ plasm, become enriched at the vegetal cortex during oogenesis. After fertilization, they become asymmetrically segregated between daughter blastomeres. Cells in the vegetal part of the embryo inheriting the germ plasm will become primordial germ cells. At the blastula stage, the germ plasm is mostly found in three to seven cells located in between the vegetal pole and the floor of the blastocoel (Whittington and Dixon, 1975; Houston and King, 2000a). During gastrulation, PGCs, together with the surrounding endodermal cells, involute inside of the embryo. At this stage, PGCs are in tight contact with their neighboring cells and thereby seem to undergo passive migration (Whittington and Dixon, 1975; Houston and King, 2000a). After gastrulation, PGCs are located centrally within the endodermal cell mass. They remain associated with surrounding cells up to stage 23 (Nishiumi et al., 2005; Terayama et al., 2013). From stage 24 onwards, PGCs start active directional migration within the endoderm. They migrate as individual cells within a cohort of cells in the endodermal somatic cell mass, first laterally, then dorsally and anteriorly until they reach the dorsal crest of the endoderm (Houston and King, 2000a). Subsequent migration of the PGCs to the gonads takes place

through the dorsal mesentery, a thin stripe of connective tissue that links the dorsal body wall and the gut. The mesentery forms from two sheets of splanchnic mesoderm surrounding the gut. As these sheets converge at the dorsal crest of the endoderm, PGCs exit the endoderm and incorporate into the mesentery (stage 43/44). From the mesentery, PGCs then migrate laterally to the forming genital ridges, enter the gonads, and differentiate into germ line stem cells capable of forming the gametes (Fig. 1E) (Wylie and Heasman, 1976; 1993).

PGCs in *Xenopus* are also characterized by the delay of the zygotic gene transcription. Similar to all species described above, this is achieved by the inhibition of RNA polymerase II-dependent transcriptional elongation (Venkataraman et al., 2010). Repression is rescued at neurula stage of embryonic development. This is an intermediate stage for PGC development that occurs after passive involution within the embryo during gastrulation and before active migration during tailbud stages. Therefore, it is tempting to assume that, similar to *Drosophila* and zebrafish, transition to the active migration requires initiation of zygotic transcription. This correlation, however, is not quite clear at the moment.

In addition, transcriptional repression in PGCs at the early stages seems to be required to preserve pluripotency. During oogenesis, several maternally supplied factors, including specific mRNAs and proteins, are enriched at the vegetal pole of the oocyte. Some of these factors are required for the PGC development, while the others are involved in the patterning of the embryo and endoderm differentiation (see also section 1.1). PGCs inherit both groups of factors, but do not undergo differentiation to the somatic endodermal cells. One of the key determinants for endodermal differentiation is maternally supplied transcription factor VegT. It is inherited by vegetally localized cells, including PGCs. However, in contrast to somatic cells, downstream targets of VegT are not expressed in PGCs (Venkataraman et al., 2010).

Similar to other species in which PGCs are specified due to the inheritance of maternal determinants, development of PGCs strongly depends on the mechanisms of translational regulation. Nanos is an RNA-binding translational repressor, which is involved in the PGC proliferation, migration and survival. It is evolutionary conserved and functions in PGC development of *Drosophila*, *C. elegans*, zebrafish, mouse and *Xenopus* (Kobayashi et al., 1996; Forbes and Lehmann, 1998; Köprunner et al., 2001; Tsuda et al., 2003; Lai et al., 2011; 2012). In *Xenopus*, maternal *nanos* RNA is inherited by PGCs and can be detected in these cells together with a corresponding protein until PGCs leave the endoderm (Lai et al., 2011). Knock-down of Nanos resulted in trapping of PGCs in the endoderm and subsequent death of these cells by apoptosis. Loss of Nanos is coupled to the premature zygotic transcription in PGCs. Cells deficient in Nanos express somatic genes downstream of VegT that are required for endoderm specification. Therefore, Nanos1 was proposed to be required to preserve PGC identity by translationally repressing RNAs that normally promote the endoderm developmental program and apoptosis (Lai et al., 2012).

Several other RNA-binding proteins were reported to be involved in PGC development in *Xenopus*. One of them, *Xdazl* is encoded by maternal germ plasm mRNA. The *Xdazl* protein is a positive translational regulator which functions by direct recruitment of the poly(A) binding protein on *Xdazl* target mRNAs (Collier et al., 2005). Maternal depletion of *Xdazl* mRNA results in a loss of PGCs at the late tailbud stages, as well as in abnormal PGC migration earlier on. It was proposed to be required for early PGC differentiation and indirectly necessary for the migration of PGCs through the endoderm (Houston and King, 2000b).

Another RNA-binding protein, *Dead end*, is also encoded by a germ plasm-associated mRNA (Horvay et al., 2006). It was shown to counteract microRNA-mediated mRNA degradation in zebrafish and *Xenopus* PGCs (Kedde et al., 2007; Koebernick et al., 2010). Knock-down of *Dead end* in *Xenopus* embryos revealed a phenotype very similar to the one observed with *Xdazl* morphants. PGCs at stage 24-25 failed to start active migration and remained clustered in the endoderm that was followed by decrease of their number at stage 31-32 (Horvay et al., 2006). In somatic cells, germ plasm-specific mRNAs are degraded via a microRNA-dependent mechanism. It was proposed, that *Dead end* functions as a part of a protein complex, which also includes *Elr*-type proteins. This complex might bind to germ plasm-specific RNAs in PGCs and shield them from microRNAs that results in specific stabilization of these RNAs exclusively in PGCs (Koebernick et al., 2010).

In contrast to *C. elegans*, *Drosophila* and mouse, chromatin remodeling does not seem to play a role in transcriptional repression at the early stages of *Xenopus* PGC. Chromatin composition between PGCs and somatic cells does not show any significant differences. Analysis of 'active' and 'silent' chromatin modification showed that transcriptional repression in PGCs occurs in spite of a 'permissive' chromatin environment (Venkataraman et al., 2010).

### **1.3 Control of active PGC migration in *Drosophila*, zebrafish and mouse.**

#### **1.3.1 PGC migration in *Drosophila***

As mentioned in the section 1.1.2, *Drosophila* PGCs first undergo passive involution inside the embryo and after gastrulation can be found in the posterior midgut pocket surrounded by midgut epithelium. During these stages of embryonic development, PGCs are tightly associated with each other and with somatic cells. Several data suggest that PGCs have migratory ability shortly after their formation, but adhesion might prevent active PGC migration (Santos and Lehmann, 2004a; Kunwar et al., 2006). When PGCs arrive in the posterior midgut, they form tight cluster with each other, but form little contact with the surrounding epithelium. In this cluster cells become organized in a radial manner and are polarized with a leading edge facing outwards. One of the key regulators involved in PGC polarization is *Trapped in endoderm 1* (*TRE1*). The corresponding mRNA is maternally supplied and encodes a G-protein coupled receptor which belongs to the rhodopsin family. Most likely, it acts through the small GTPase *Rho1*, but the exact molecular mechanism of



TRE1 function in PGCs is not known (Richardson and Lehmann, 2010). Since TRE1 is provided maternally, an unknown ligand coming from the surrounding tissues was suggested to initiate PGC polarization and subsequent migration (Kunwar et al., 2006). Polarization by a TRE1-dependent mechanism could cause redistribution of the G $\beta$  subunit of the heterotrimeric G-protein, Rho1 and adherent junction components (E-cadherin and catenins) from the periphery to the cell rear, facing the inside of the PGC cluster. Polarized PGCs start to extend cellular protrusions at the leading edge towards the surrounding midgut epithelium. Transition to active migration is associated with a loss of contacts between the PGCs. They begin to disperse from the cluster and migrate as individual cells through the posterior midgut (Fig. 2a1) (Richardson and Lehmann, 2010). Epithelium cells of the posterior midgut also undergo reorganization. They lose apical junctions that results in the formation of the gaps between the cells. This process was shown to be critical for the passage of the migrating PGCs (Jaglarz and Howard, 1994).

Once PGCs pass through the midgut, they reorient on its surface and migrate dorsally along the epithelium. Later they leave the midgut and migrate towards the posterior mesoderm. This migration depends on surrounding tissues and is regulated by two related proteins with redundant functions, Wunen (Wun) and Wunen2 (Wun2). Wun and Wun2 are expressed in most ventral regions of posterior midgut and other tissues that PGCs normally avoid during their migration. Knock-down of the Wunens causes loss of directionality during PGC migration, while their overexpression in mesoderm prevents PGC migration towards this region (Kunwar et al., 2006). Both *wun* and *wun2* genes encode homologs of mammalian lipid phosphate phosphatases (LPPs), transmembrane exoenzymes that have catalytic phosphatase domain on the cell surface. Although *in vitro* experiments helped to identify several phospholipid substrates for LPPs and Wunens, *in vivo* targets for both classes of proteins remain unknown (Fig. 2a2) (Richardson and Lehmann, 2010). It has been shown that LPPs and Wunens are not only responsible for the hydrolysis of the phospholipids, but also facilitate uptake of dephosphorylated lipids by Wunen- or LPP-expressing cells (Roberts and Morris, 2000). The exact mechanism of Wunens' function in PGC migration remains unclear, but two possible models were suggested. According to one model, Wun and Wun2 expressing cells produce PGC repellent, that facilitates migration of PGCs away from Wun/Wun2-positive cells. The alternative model suggests that PGC migration and/or survival might depend on certain extracellular factor that can be processed by Wun/Wun2 expressing cells. According to the second model, somatic Wun/Wun2-producing cells locally deplete a putative attraction factors creating an inverse gradient and forcing PGCs to migrate away from this region (Richardson and Lehmann, 2010).

Migration of *Drosophila* PGCs to the somatic gonad precursors in the mesoderm is also regulated by the 3-hydroxy-3-methylglutaryl coenzyme A reductase (HMGC $\text{CoAR}$ , also known as Columbus) pathway. Expression of HMGC $\text{CoAR}$  in the mesoderm is required for directional PGC migration towards this tissue and association of PGCs with somatic gonad precursors. In addition, ectopic expression of HMGC $\text{CoAR}$  in ectoderm or nervous tissue causes abnormal PGC migration towards these regions (Van Doren et al., 1998). This

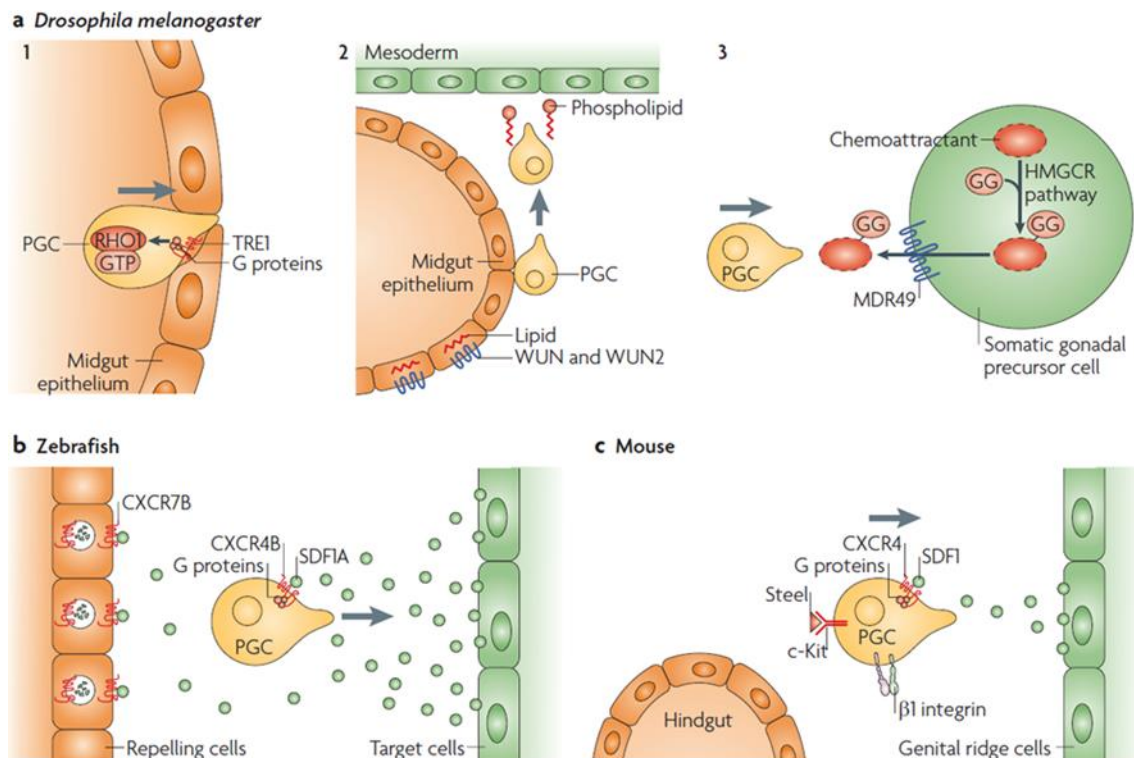


**Fig. 2. Molecular regulation of active PGC migration in *Drosophila*, zebrafish and mice.** (a) Initiation and transepithelial migration of *Drosophila* PGCs through the midgut is controlled by the G-protein coupled receptor (GPCR) TRE-1. Upon polarization of PGCs, there is redistribution of Rho1 to the cell rear, which can act as downstream target of TRE-1. Wun and Wun2 are expressed at sites that PGCs avoid, like ventral midgut. They may participate in PGC repulsion, or hydrolyse putative phospholipid attractant or survival factor to create a gradient for PGC migration. Migration of PGCs to the somatic gonads depends on the isoprenylation branch of HMGR pathway. It may act in the attachment of geranyl-geranyl (GG) group to a putative chemoattractant, or factors necessary for its secretion, such as MDR49. (b) In zebrafish, PGCs are guided by a gradient of the chemoattractant SDF-1 $\alpha$ . They express the receptor CXCR4b that also belongs to the GPCR family. Another somatically expressed GPCR, CXCR7B, promotes the internalization and degradation of SDF-1 $\alpha$  that might lead to proper gradient formation and precise targeting of PGCs. (c) In mice, PGC migration to the genital ridges is also controlled by CXCR4 and SDF1. SDF1 is expressed by the somatic cells of the genital ridge and PGCs express CXCR4. Integrin  $\beta$ 1 is also required for this step. PGC motility and survival requires the receptor tyrosine kinase c-Kit and its ligand Steel. Steel is expressed by somatic cells surrounding PGCs throughout migration (taken from Richardson and Lehmann, 2010).

suggests that the HMGR pathway is involved in the production of yet unidentified signal necessary and sufficient to attract PGCs. HMGR regulates several pathways within animal cells, mainly cholesterol synthesis and protein isoprenylation. However, genes necessary for cholesterol synthesis are not present in *Drosophila* genome and this pathway is not active in these species. On the other hand, mutation in other genes involved in the isoprenylation pathway revealed a requirement of this pathway for *Drosophila* PGC migration (Santos and Lehmann, 2004b). This suggests two possibilities how HMGR could contribute to directional PGC migration. According to one hypothesis, the isoprenylation pathway is directly involved in a modification of the hypothetical attractant guiding PGCs. Alternatively, the isoprenylation pathway could be rate limiting for expression or secretion of the attractant, for example by modifying small GTPases like Ras and Rabs (Fig. 2a3) (Kunwar et al., 2006).

In the final step of the active migration, *Drosophila* PGCs divide into two clusters within the mesoderm and associate with somatic gonadal precursors. PGCs initially associate with posterior gonadal precursor clusters and then move anteriorly during germ band retraction. At this point, PGCs round up, lose their motility and form tight contacts with each other and with somatic cells in a process known as coalescence (Jaglarz and Howard, 1994). This process correlates with the level of HMGCOR expression in somatic gonadal precursors, since ectopic expression of HMGCOR leads to an arrest of PGC migration in HMGCOR-expressing tissues (Van Doren et al., 1998). This can be explained by the highest concentration of potential attractant in this region. Interestingly, formation of cell clusters by somatic gonadal precursors could occur even in the absence of PGCs (Brookman et al., 1992). Formation of contacts between the cells requires expression of Fear of intimacy (Foi) and *Drosophila* E-cadherin (DE-cadherin, also known as Shotgun). Foi encodes a conserved transmembrane protein, which belongs to a family of putative zinc transporters. Based on the role of this family of proteins in cell migration, it has been proposed that Foi may be involved in the regulation of adhesion molecule expression, for example in the regulation of E-cadherin levels (Santos and Lehmann, 2004a). However, additional factors might mediate coalescence, since initial interactions between PGCs and somatic cells are not affected in *foi* or *DE-cadherin* mutants.

### 1.3.2 PGC migration in zebrafish

As discussed previously (see section 1.1.3), transition of zebrafish PGCs to the active migration state correlates with zygotic transcription and depends on Dead end expression (Blaser et al., 2005). Dnd is essential for PGC motility, since knock-down of this protein leads to inability of the cells to generate protrusions and migrate (Weidinger et al., 2003). This phenotype could be rescued by simultaneous induction of myosin contractility using MLCK, decrease of E-cadherin mediated adhesion and decrease of cortical rigidity, revealing that proper regulation of these features is sufficient for restoring cell migration of PGCs in Dead end morphant zebrafish embryos (Goudarzi et al., 2012).

A major role in polarization of PGCs in zebrafish was assigned to calcium signaling. Calcium levels are elevated at the leading edge of migrating cells that leads to phosphorylation and activation of myosin by Myosin light-chain kinase (MLCK) (Blaser et al., 2006). Myosin-dependent contraction near the leading edge serves as a driving force for the motility of zebrafish PGCs (Kardash et al., 2010; Goudarzi et al., 2012).

PGC transition to active migration in zebrafish correlates with a slight reduction of E-cadherin levels. Since they migrate as individual cells, downregulation of E-cadherin was suggested to allow the detachment of PGCs from neighboring cells (Blaser et al., 2005). Control of E-cadherin expression is mediated by the transcriptional repressor Zeb1 (also known as ZFH1). *Zeb1* mRNA is itself a subject for the microRNA miR-430 dependent degradation, but expression of Zeb1 can be stabilized by Dnd (Goudarzi et al., 2012). A certain level of E-cadherin is still required for the proper PGC migration to generate a traction force. Migrating cells form actin-rich brushes at the cell front in a Rac1-dependent

manner. These structures are coupled to the E-cadherin molecules, which in turn mediate adhesion to the neighboring cells. Together with RhoA-dependent retrograde flow of the brushes, this adhesion generates a traction force for cellular translocation. When the cell advances forward, brushes disassemble, while new ones appear at the newly formed leading edge (Kardash et al., 2010).

During their migration to the gonads, PGCs in the zebrafish embryo pass through several intermediate target sites. This requires a tight regulation of the directionality during migration. Guidance of PGCs is mediated by the chemoattractant Stromal-derived factor 1 $\alpha$  (SDF-1 $\alpha$ , also known as Chemokine C-X-C motif ligand 12 (CXCL12)) and its G protein coupled receptor in PGCs CXCR4b (chemokine C-X-C motif receptor 4b) (Doitsidou et al., 2002; Knaut et al., 2003). PGCs respond to the SDF-1 $\alpha$  gradient and can be attracted to ectopic position if SDF-1 $\alpha$  is expressed elsewhere. Interestingly, PGCs are capable of migration even in the absence of SDF-1 $\alpha$  signaling, since knock-down of both SDF-1 $\alpha$  and CXCR4b does not disrupt motility of PGCs, but rather leads to the random migration within the embryo (Reichman-Fried et al., 2004). SDF-1 $\alpha$  in the zebrafish embryo is expressed in a dynamic spatio-temporal manner. Patterns of highest SDF-1 $\alpha$  expression in the embryo correlate with intermediate target sites of PGC migration. Once PGCs reach a target site, SDF-1 $\alpha$  expression in this region goes down and becomes elevated in the next target site. This goes on until PGCs reach the genital ridges (Reichman-Fried et al., 2004). In order to migrate directionally from one site to another, a new gradient of chemoattractant has to be established that goes along with fast removal of the former gradient from the system. This is achieved with the help of somatic cells that can bind, internalize and degrade SDF-1 $\alpha$ . Somatic cells express CXCR7, receptor of GPCR family that, similar to CXCR4b, can bind to SDF-1 $\alpha$ . However, in contrast to CXCR4b, CXCR7, upon binding to SDF-1 $\alpha$ , does not initiate signaling via G-proteins, but together with SDF-1 $\alpha$  undergoes endocytosis that leads to lysosomal degradation in the somatic cell. Knock-down of CXCR7 results in a loss of PGC polarity and decreases the speed of migration. Somatic cells, therefore, via CXCR7 provide continuous clearance of SDF-1 $\alpha$  from intercellular environment and facilitate the migration of PGCs by shaping the distribution of the chemokine in the environment (Fig. 2b) (Boldajipour et al., 2008; Mahabaleshwar et al., 2008). In addition, expression of both SDF-1 $\alpha$  and CXCR7 is regulated by microRNA miR-430. Regulation at the level of the mRNA facilitates dynamic expression of SDF-1 $\alpha$  by clearing its mRNA from previous expression domains, modulates the levels of the decoy receptor CXCR7 to avoid excessive depletion of SDF-1 $\alpha$  and buffers against variation in gene dosage of chemokine signaling components to ensure accurate PGC migration (Staton et al., 2011).

The SDF-1 $\alpha$  gradient that acts through CXCR4b, polarizes PGCs and instructs them about the directionality of migration. Being a G-protein coupled receptor (GPCR), CXCR4b transduces the signal through heterotrimeric G proteins that consist of a guanine-nucleotide-binding  $\alpha$  subunit of the G $\alpha$ i subfamily and a dimer consisting of  $\beta$  and  $\gamma$  subunits (Luther and Cyster, 2001; Thelen, 2001). It has been shown that signaling through the G $\beta\gamma$  subunit is required to regulate cell polarization. The downstream target of this subunit in the process of zebrafish PGC polarization and migration is a small GTPase Rac1 (Xu et al., 2012).

As discussed above, localization of Rac1 at the leading edge is required to generate actin brushes involved in PGC migration (Kardash et al., 2010). In addition, disruption of G $\beta$ y localization to the leading edge prevents enrichment of calcium that results in the absence of PGC polarization (Mulligan et al., 2010). Similar to *Drosophila*, isoprenylation branch of the HMGC $\alpha$ R pathway is also involved in PGC migration in zebrafish, since inhibition of HMGC $\alpha$ R or geranylgeranyl transferase disrupts PGC migration (Thorpe et al., 2004). In PGCs, this pathway is required for geranylation, membrane localization of G $\gamma$  subunit and its ability to participate in signal transduction (Mulligan et al., 2010). It is not known, however, whether geranylation also affects the guidance of germ cells by the soma, similar to what has been observed in *Drosophila*.

### 1.3.3 PGC migration in mouse

Active migration of mouse PGCs starts shortly after their specification in the primitive streak. Cells become polarized and form cytoplasmic extensions and pseudopodia (Anderson et al., 2000). During the initial step of migration, PGCs disperse in the primitive streak and invade as individual cells the adjacent posterior embryonic endoderm that differentiates into hindgut. The molecular mechanism involved in the initiation of PGC migration is not well understood. It was thought to be regulated by interferon-induced transmembrane protein 1 (IFITM1) that is involved in several cellular processes including cell adhesion. Knock-down of this protein by RNAi resulted in a failure of PGCs to invade the endoderm (Tanaka et al., 2005). In the knock-out experiments, however, no defects in PGC migration were observed (Lange et al., 2008). The same was shown for another member of this protein family, IFITM3 that was thought to be involved in the latter stages of PGC migration. Another adhesion molecule, E-cadherin that is downregulated in *Drosophila* and zebrafish PGCs upon initiation of the active migration, is expressed in the hindgut, but not in the PGCs at this stage of development (Bendel-Stenzel et al., 2000; Gu et al., 2009). Dead end (Dnd) that is a key initiation factor for PGC migration in the zebrafish, was also found in mice, but it functions in PGC survival, rather than active migration (Youngren et al., 2005).

One of the key regulators during active PGC migration in the mouse is the Steel factor (also known as stem cell factor, kit ligand or mast cell growth factor) and its receptor c-Kit. Although the initiation of active PGC migration occurs even in its absence, Steel factor is essential for the regulation of PGC motility, proliferation and survival (Gu et al., 2009). It has been reported that Steel factor can attract PGCs *in vitro* (Farini et al., 2007), but according to *in vivo* studies, the direction of movement is not randomized in the absence of Steel factor (Gu et al., 2009). C-Kit is a tyrosine kinase receptor of the PDGFRB superfamily and is expressed in PGCs throughout migration (Yabuta et al., 2006). Steel protein is present in the mouse embryo in two isoforms generated by alternative splicing. The membrane-bound form lacks an extracellular domain containing a proteolytic cleavage site that normally causes release of the extracellular region of the protein (Flanagan et al., 1991; Huang et al., 1992). From the moment of their specification and throughout the migration, PGCs are surrounded by cells expressing the Steel factor. Moreover, similar to SDF-1 expression in zebrafish, the Steel factor expression pattern is changed during PGC migration in a way that

that PGCs are constantly surrounded by Steel-expressing cells. This creates a 'spatio-temporal niche' for PGC migration that controls their survival, motility, and proliferation (Gu et al., 2009). Two splice variants of the Steel factor contribute to different aspects during PGC migration. The membrane-bound isoform creates a higher local concentration of Steel factor. It controls germ cell motility and cells expressing this isoform accompany PGCs during their migration to the gonads. The expression pattern of membrane-bound Steel factor, therefore, creates a 'motility niche' for the PGCs. An escape from this niche causes cessation of motility and death by apoptosis of the ectopic germ cells. Soluble Steel factor is sufficient for PGC survival and can also contribute to the motility (Gu et al., 2011). A possible role of this isoform is to maintain PGCs that migrated slightly out of the 'motility niche', but can still reach the gonad region.

After the hindgut is formed, PGCs incorporate into the hindgut epithelium. Subsequently, they migrate from the dorsal side of the hindgut, separate into left and right streams of individual cells, and migrate laterally across the dorsal body wall towards the genital ridges (Kunwar et al., 2006). Similar to the zebrafish, directionality of this migration is controlled by SDF-1 and its receptor CXCR4. SDF-1 is expressed in mesenchyme and genital ridges, while expression of CXCR4 can be found in PGCs. Ectopic SDF-1 expression results in the attraction of PGCs to ectopic locations, while removal of SDF-1 or CXCR4 leads to the arrival of only few PGCs at the genital ridges (Fig. 2c) (Ara et al., 2003; Molyneaux et al., 2003).

In the final step, PGCs continue to migrate close to the genital ridges, and then enter the genital ridges to form the primary sex cords by coalescence with somatic gonad precursors. PGCs remaining in the midline structures die by apoptosis (Molyneaux et al., 2001). As in *Drosophila*, interaction with somatic cells requires E-cadherin. It is also needed for the PGC-PGC interaction during migration (Bendel-Stenzel et al., 2000). In addition, adhesion via integrin- $\beta$ 1 is required for the colonization of the gonads (Anderson et al., 1999).

## 1.4 PGC migration in *Xenopus*

### 1.4.1 Labeling and identification of PGCs in *Xenopus* embryos

One of the biggest problems in the study of PGC migration in *Xenopus* is visualization of PGCs. Active migration of these cells occurs mainly within the endoderm, which is not transparent in *Xenopus* embryos due to high yolk content. Over the years, a variety of different techniques has been employed for the identification and tracking of individual PGCs. Initially, PGCs were distinguished from somatic cells via the presence of microscopically identifiable cytoplasmic inclusions, referred to as germ plasm (Blackler, 1965; Whittington and Dixon, 1975). When methods to analyze the molecular composition of the germ plasm became available, whole mount in situ hybridization (WMISH) using anti-sense RNAs complementary to germ-cell specific mRNAs, such as Xpat, was introduced in order to visualize PGCs in the fixed embryos (Hudson and Woodland, 1998; Houston and

King, 2000a). Alternatively, antibodies for germ plasm specific proteins, such as XVLG1 (*Xenopus vasa-like gene*), were employed (Komiya et al., 1994). With the availability of fluorescent microscopy techniques, *in vivo* observation of PGCs became possible. Due to the high amount of mitochondria in germ plasm, PGCs can be labeled by DiOC6(3) (3,3'-dihexyloxacarbocyanine). If embryos at the early stages are treated with this fluorescent dye, it accumulates on hyperpolarized membranes, such as mitochondria, and is translocated into the lipid bilayer (Venkataraman et al., 2004). The drawback of this method is potential toxicity and dilution of the dye during development, making it difficult to distinguish PGCs from the surrounding cells after neurula stages. Another approach was to inject chimeric mRNAs, containing ORFs encoding different fluorescent proteins fused to 3'-UTR of germ plasm-specific mRNAs. It was shown, that such 3' UTRs mediate PGC-specific stabilization by protection against miRNA-mediated RNA degradation after the MBT (Kataoka et al., 2006; Koebernick et al., 2010). Fusion of these 3' UTRs to other ORFs developed into a very powerful tool in promoting PGC-specific overexpression of proteins for their functional analysis (Morichika et al., 2010; Takeuchi et al., 2010; Tarbashevich et al., 2011). More recently, using the same principal approach, a novel transgenic *Xenopus laevis* line with fluorescently labeled mitochondria was generated, which can now be used for germ plasm and PGC visualization *in vivo* (Taguchi et al., 2012).

Lack of transparency makes it hard to investigate PGC migration in *Xenopus* at the cellular level. It has been shown that PGCs isolated from tailbud stage embryos can migrate *in vitro* on the fibronectin-coated surfaces (Fig. 3) (Tarbashevich et al., 2011; Terayama et al., 2013). However, the efficiency of this migration was quite low and improvement of the *in vitro* assays is still desirable.

#### **1.4.2 Blebbing-associated motility as a basis for PGC migration in the endoderm**

In *Xenopus*, PGCs initiate active migration at developmental stage 24, when they disperse from the cluster that they had formed in the endoderm (Nishiumi et al., 2005). Similar to *Drosophila* and zebrafish, active migration of *Xenopus* PGCs within the endoderm is coupled to changes of their locomotive activity. Prior to migration (stage 18 and 24), isolated PGCs show little protrusion formation and exhibit mainly a spherical round morphology, similar to somatic endodermal cells. Upon dispersal at stage 28, isolated PGCs acquire an elongated shape, correlating with the onset of migratory activity. At stage 33/34, PGCs exhibit a high level of cellular dynamics that is characterized by the formation of numerous bleb-like protrusions and migratory activity. In these stages, PGCs alternate between locomotive and pausing phases (Fig. 3). At stage 41, isolated PGCs exhibit a reduced tendency to form bleb-like protrusions and locomotive activity (Terayama et al., 2013).

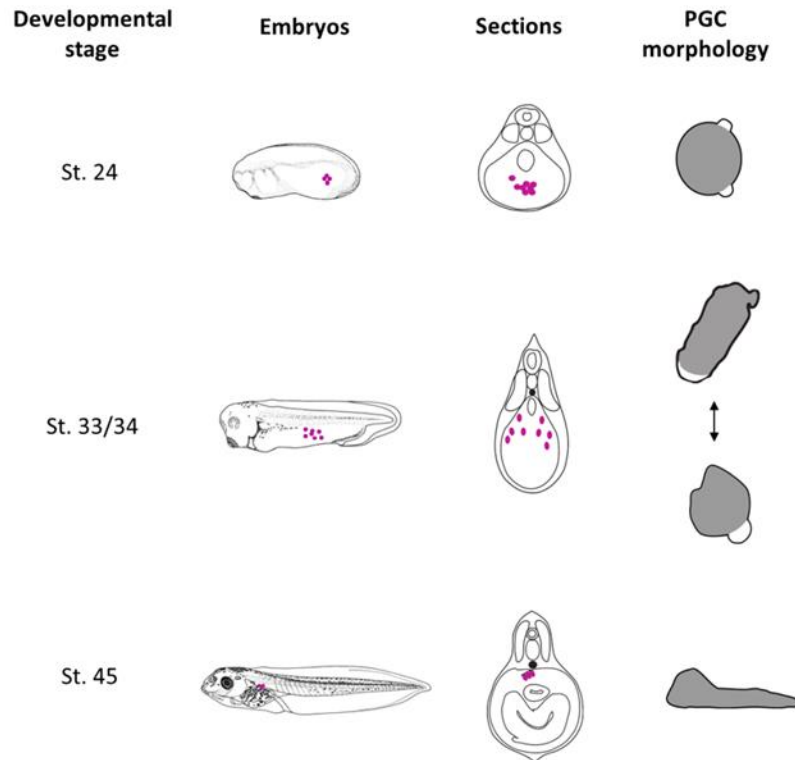


**Fig. 3. PGC motility and morphology during different developmental stages of *X.laevis* embryos.** At stage 24 PGCs initiate active migration from the cluster they formed in the endoderm. At this stage isolated PGCs have mostly round morphology and form bleb-like protrusions. During tailbud stage (St. 24-44), they migrate anteriorly and dorsally around the gut. Isolated PGCs at these stages alternate between migratory elongated shape and round shape with bleb-like protrusions. During the migration via dorsal mesentery (St. 45), isolated PGCs form filopodia-like protrusions. Embryos are drawn after Nieuwkoop and Faber, 1994. Vertical sections perpendicular to the anterior-posterior with the positions of PGCs (pink dots) in the embryo are indicated. The morphology of isolated PGCs is indicated according to Terayama et al., 2013; Heasman and Wylie, 1978.

Migration of zebrafish and *Xenopus* PGCs within the endoderm occurs via a blebbing-associated mechanism (Tarbashevich et al., 2011; Terayama et al., 2013). Blebs are pressure-driven plasma membrane protrusions formed by the cells. In majority of the animal cells plasma membrane is tightly bound to the underlying cortex formed from actin, myosin, cortex-membrane linker ERM (ezrin, radixin and moesin) proteins and some other associated proteins. Myosin motors constantly keep the cortex under tension, applying a pressure on the cytoplasm. If disruption occurs either in the cortex or at the interface between cortex and plasma membrane, the internal pressure of the cell generated by acto-myosin contraction drives the cytoplasm to flow into this space. As a result, a spherical, cellular bleb-like protrusion is formed (Fig. 4a). It is not clear what causes these events. Most likely, in nonpolarized cells bleb initiation occurs randomly throughout the plasma membrane, but it also can be caused by some external triggers (Charras and Paluch, 2008; Fackler and Grosse, 2008). In nonpolarized cells the expansion of the bleb lasts 5-30 seconds (Fig. 4b). In these cells, the acto-myosin cortex reassembles on the plasma membrane (Fig. 4c) and the bleb retracts to the initial position (Fig. 4d). In migratory polarized cells, formation of the blebs occurs preferentially at the leading edge. In these cells, cortex re-polymerization on the surface of the bleb is followed by a new disruption of cortex-plasma membrane interactions



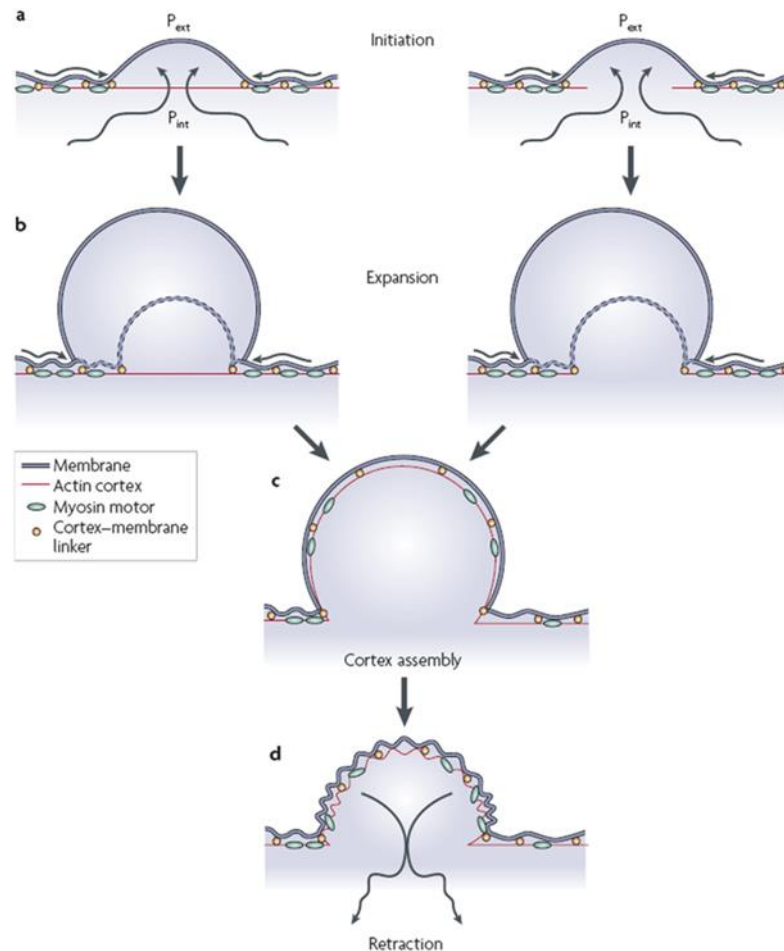


**Fig. 4. The life cycle of a bleb.** (a) The initiation of the bleb formation can be the result of a local detachment of the cortex from the membrane (left) or from a local rupture of the cortex (right). (b) The expansion of the bleb is supported by the flow of the cytoplasm into the bleb, caused by the intracellular hydrostatic pressure through the remaining cortex (left) or through the cortex hole (right). The bleb base can be increased by detaching the cortex from the plasma membrane. (c) At the end of the bleb expansion stage, the cortex starts its reassembly under the plasma membrane of the bleb. (d) Retraction of the bleb, dependent on the Rho-ROCK-myosin II machinery, restores the initial shape of the cell (taken from Charras and Paluch, 2008).

before the bleb is retracted. This results in the formation of a new bleb at the leading edge before the retraction of a former bleb occurs. The position of the bleb at the leading edge can also be stabilized by newly formed interactions with extracellular substrates. In both of these cases, the plasma membrane of the bleb is not retracted to its initial position, and the cell translocates to a new position with the help of acto-myosin cortex contraction in the rear (Charras and Paluch, 2008).

Lipid bilayer composition is also important for the rigidity of the cortex-membrane interaction. It has been shown, that phosphatidylinositol (4,5)-biphosphate (PIP<sub>2</sub>) increases the level of cortex-membrane adhesion, while the sequestering of PIP<sub>2</sub> results in the decrease of the adhesion energy (Raucher et al., 2000). PIP<sub>2</sub> has many structural and anchoring functions and serve as a precursor for the second messengers inositol (1,4,5)-trisphosphate (IP<sub>3</sub>), calcium, and diacylglycerol (DAG) that may act in parallel with PIP<sub>2</sub> in regulating cytoskeletal structure. The presence of PIP<sub>2</sub> facilitates actin polymerization in

multiple ways (Sechi and Wehland, 2000; Yin and Janmey, 2003), while generation of IP3 and DAG, following phospholipase C (PLC)-mediated hydrolysis of PIP2, lead to solubilization of the actin network (Meberg, 2000; McGough et al., 2003). In addition, PIP2 induces conformational changes in vinculin, talin and ERM family proteins to promote anchoring of the actin cytoskeleton to the plasma membrane (Sechi and Wehland, 2000). PLC-mediated hydrolysis of PIP2 and the downstream activation of Ca<sup>2+</sup>/CaM (calmodulin) and protein kinase C (PKC) also influence actin-myosin based contractility. Ca<sup>2+</sup>/CaM activates myosin regulatory light chain kinase (MLCK), leading to phosphorylation of the myosin regulatory light chain (MLC) (Iwasaki et al., 2001). Similarly, PKC has been shown to phosphorylate and activate MLC (Naka et al., 1988; Varlamova et al., 2001). Moreover, PIP2 is a substrate for phosphatidylinositol-3-OH kinase (PI3K) to generate phosphatidylinositol (3,4,5)-trisphosphate (PIP3), an effector of different downstream targets of PI3K signaling cascades (Katso et al., 2001).

Therefore, PIP2 concentration could be directly involved in the regulation of membrane-cortex interactions reducing or increasing local interactions between the cytoskeleton and the plasma membrane. Alternatively, PIP2 can also indirectly regulate adhesion by modulating signaling cascades that alter the cortical cytoskeleton structure.

Actin polymerization and myosin activity are required for the locomotion and protrusion formation of *Xenopus* PGCs. In isolated non-migrating PGCs, actin filaments are localized to the periphery of the cell, forming a cortex underlying the plasma membrane, while in the migratory PGCs actin filaments can be found in the rear, but not at the leading edge of the cell (Terayama et al., 2012). Interestingly, in contrast to the migration of *Xenopus* PGCs *in vitro*, formation of actin brushes at the leading edge is required for PGC migration in the zebrafish *in vivo* (Kardash et al., 2010; discussed in chapter 1.3.2). Similar to the zebrafish, however, inhibition of actin polymerization and myosin activity by chemical inhibitors in *Xenopus* PGCs results in a loss of protrusion formation and cell locomotion (Terayama et al., 2013). In the same study, similar results were obtained by inhibition of RhoA/ROCK signaling, which regulates bleb formation by phosphorylating myosin light chain (MLC), as described by Fackler and Grosse, 2008.

#### **1.4.3 Signaling pathways involved in PGC migration in *Xenopus***

In order to migrate directionally, blebs should form primarily on the leading edge of the cell. Most of the cells that migrate via bleb-associated mechanisms are guided by chemoattractants. For the amoeba *Dictyostelium discoideum* such attractants are nutrients and cAMP, for neutrophils – complement factor C5a, platelet-activating factor (PAF) and formylated Met-Leu-Phe (fMLP) (Charras and Paluch, 2008; Fackler and Grosse, 2008). As discussed above, PGCs derived from zebrafish, chicken and mouse are guided by a system consisting of the chemoattractant stem cell derived factor 1 (SDF-1), also known as Chemokine C-X-C motif ligand 12 (CXCL12), and its receptor C-X-C chemokine receptor type 4 (CXCR4) (Doitsidou et al., 2002; Molyneaux et al., 2003; Stebler et al., 2004).

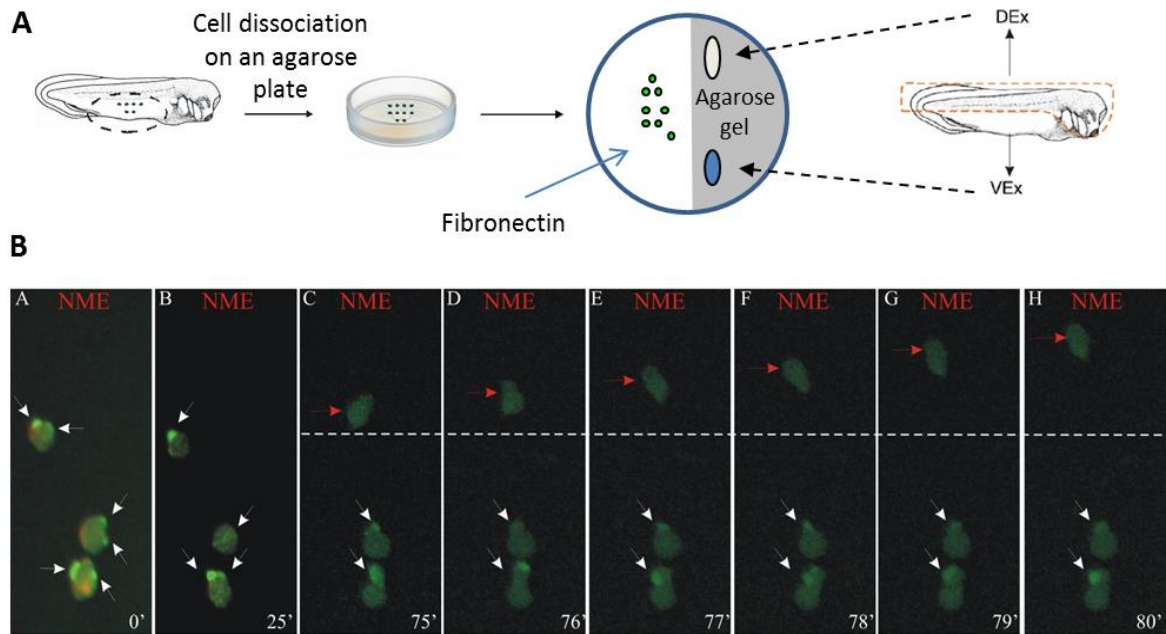


**Fig. 5. PGC polarization and migration on fibronectin towards the dorsal extract source.** (A) PGCs were isolated from tailbud stage embryos injected at the two-cell stage with *EGFP\_GRPI\_PH\_DE* mRNA. This chimeric RNA encodes PIP3 sensor fused GFP, and also contains Dead end localization element to target expression specifically in PGCs. Isolated cells were transferred on fibronectin-coated Petri dish in DFA buffer. One sector of the dish was covered with agarose gel. Tailbud stage embryos were dissected to obtain homogenized dorsal (DEx) and ventral (VEx) extracts. These extracts were injected into the opposite corners of the agarose sector. (B) Snapshots from the time-lapse movie illustrating polarization and migration of PGCs on the fibronectin towards the dorsal protein extract (neuro-mesodermal extract, NME) source in the DFA-medium. White arrows depict PIP3-enriched bleb-like protrusions formed by the cells. The red arrow indicates the PGC migrating towards the chemoattractant source (according to Tarbashevich et al, 2011).

In the case of *Xenopus* PGCs, cell migration is guided by chemoattractants, originating from the dorsal part of the embryo. Isolated *Xenopus laevis* PGCs can be polarized and migrate towards extracts prepared from stage 30-31 embryos lacking endoderm (Fig. 5) (Tarbashevich et al., 2011). Interestingly, expression of chemoattractant SDF-1 in *X. laevis* embryos at the tailbud stage can be observed in dorsal and anterior structures: mid- and hindbrain, otic vesicles and eyes, the dorsal fin, and the posterior heart anlage (Braun et al., 2002). Expression of the receptor CXCR4 can be observed in PGCs at tailbud stages 24-40 (Nishiumi et al., 2005). Overexpression of SDF-1 in the embryos upon knock-down of its repressor IRX5 leads to mislocalization of PGCs due to a loss of directionality in their migration within the endodermal cell mass (Bonnard et al., 2012). In addition, interference with endogenous SDF-1 or CXCR4 expression results in a decreased number of PGCs arriving at the genital ridges (Takeuchi et al., 2010). Thus, even though it seems highly likely that this signaling system has a role in PGC polarization and migration, an exact guidance mechanism for *Xenopus* PGCs remains to be determined.

CXCR4, as well as other receptors involved in chemotaxis, belongs to G-protein coupled receptor (GPCR) family. In the context of cell migration, activated heterotrimeric G-proteins activate various downstream pathways, including calcium flux (Dutt et al., 1998; Blaser et al., 2006), Phospholipase C (PLC) and Phosphatidylinositol 3-kinase (PI3-kinase)

(Wang et al., 2000). Activation of PI3-kinases was reported to be one of the major events for polarization of many migratory cells (Chung et al., 2001; Iijima et al., 2002). PI3-kinases generate inositol phospholipids that bind to a subset of PH domain-containing molecules thus recruiting them to the membrane. There are three classes of enzymes in PI3-kinase family (Katso et al., 2001). Class I PI3-kinases catalyze the phosphorylation of the 3' hydroxyl subunit of PIP2 converting it into PIP3. This class of enzymes was shown to be involved in the regulation of cellular polarization by the localization of PIP3 to the leading edge of the cell (Meili et al., 1999; Haugh et al., 2000; Servant et al., 2000; Merlot and Firtel, 2003; Dumsteri et al., 2004). Asymmetrical localization of PIP2 and PIP3 in the cell facilitates the recruitment of PIP3-specific PH domain-containing proteins, primary effectors of PI3-kinase signaling pathway, to the leading edge. The restriction of PIP3 to the leading edge of the cell is also influenced by the function of PI3K antagonist PTEN (phosphatase and tensin homolog), a phosphoinositide 3'-specific phosphatase that dephosphorylates PIP3 to PIP2 (Maehama and Dixon, 1998). Studies in *Dictyostelium* have revealed that, in resting cells, PTEN is localized to the plasma membrane and is uniformly distributed all over the cell (Funamoto et al., 2002; Iijima and Devreotes, 2002). In chemotaxing cells, PTEN is downregulated at the leading edge, but persists at the sides and the rear of the cell. Thus, PTEN prevents the accumulation of PIP3 exclusively at these places, resulting in cellular polarization. In addition, distribution of PIP2 and PIP3 can influence formation of the bleb-like protrusions, as discussed above (see section 1.4.2).

*In vitro* migration of murine PGCs was reported to be activated by the Kit ligand (KL) as a guiding cue, and also described to depend on the PI3-kinase pathway (Farini et al., 2007). In the zebrafish model system, the *in vivo* motility of PGCs depends on appropriate PIP3 levels, but a polarized distribution of PIP3 was not observed. It was proposed that PI3K activity might be linked to substrate adhesion, rather than to polarization (Dumstrei et al., 2004). Polarization of *Xenopus* PGCs correlates with asymmetries in respect to the intracellular PIP3 distribution (Tarbashevich et al., 2011). PIP3 is found to be enriched in the bleb-like protrusions formed by isolated PGCs at migratory stage. Downregulation of endogenous PIP3 levels leads to a decrease in PGC number and to abnormal PGC migration. Loss of endogenous PIP3 is also coupled to a loss of plasma membrane blebbing. One of the molecules involved in generating PIP3 asymmetries in *Xenopus* PGCs is the kinesin KIF13B. The corresponding maternal mRNA localizes to the germ plasma and can be later detected in PGCs at the tailbud stages of development. Knock-down of KIF13B leads to the loss of PIP3 enrichment and inhibits formation of bleb-like protrusions in PGCs isolated from stage 30-32 embryos. In contrast, KIF13B overexpression leads to increased plasma membrane blebbing and PIP3 enrichment throughout the plasma membrane (Tarbashevich et al., 2011). Thus, similar to what is observed upon reducing the cellular levels of PIP3, knock down of KIF13B results in a decrease of PGC number and abnormal PGC migration. In good correlation, KIF13B was previously shown to be involved in the polarization of hippocampal neurons prior to axonal growth. It was suggested that KIF13B might contribute to the local enrichment of PIP3 at the tip of growing neurites by directional transport of PIP3-containing

vesicles, mediated by the interaction with a PIP3-binding protein (PIP3BP or Centaurin- $\alpha$ 1) (Venkateswarlu et al., 2005; Horiguchi et al., 2006). However, the exact molecular mechanism by which KIF13B influences the PIP3 distribution in *Xenopus* PGCs remains to be determined.

As outlined above, PIP3 polarization was described to be relevant for a number of different cells migrating via a bleb-associated mechanism, including *Dictyostelium* amoeba and vertebrate neutrophils (Franca-Koh et al., 2006; Franca-Koh et al., 2007; Yoo et al., 2010). In the case of *Dictyostelium*, however, multiple parallel pathways appear to be involved in chemotaxis, with each individual one, such as the PI3K pathway, being dispensable (Hoeller and Kay, 2007; King and Insall, 2008; Van Haastert and Veltman, 2007). Several observations suggest that multiple pathways might also be involved in regulating the directional migration of *Xenopus* PGCs. One of these comes from experiments characterizing the *Xenopus* glutamate receptor interacting protein 2 (XGRIP2). Similar to KIF13B, XGRIP2 is also encoded by germ plasm specific maternal mRNA. GRIP multi-PDZ domain family proteins usually serve as adaptor proteins and they are involved in various processes, including cell-matrix interactions during embryogenesis in mammals and control of directional migration of embryonic muscle cells in *Drosophila* (Takamiya et al., 2004; Swan et al., 2004). Knock-down of XGRIP2 resulted in decelerated PGC migration at tailbud stages and a decrease in the average number of PGCs. PGCs in XGRIP2 morphants were mislocalized to more posterior positions at stage 33/34 (Tarbashevich et al., 2007). These observations on PGC migration in XGRIP2 morphant embryos were confirmed in a second, independent study, also revealing that the ability of the PGCs to enter dorsal mesentery was also significantly impaired (Kirilenko et al., 2008).

Another pathway involved in regulation of PGC migration in *Xenopus* is the one depending on Notch/Suppressor of Hairless [Su(H)]. The Notch receptor and its ligands Delta and Serrate are single-pass transmembrane proteins. When Notch binds to one of these ligands, the Notch intracellular domain (NICD) is released and translocates into the nucleus, where it forms a complex together with Su(H) and regulates gene expression (Lai, 2004). Suppression or activation of this pathway in the endoderm of *Xenopus* embryos starting from stage 18, as well as PGC-specific activation, resulted in defects in PGC migration in the endoderm. In this case PGCs failed to reach the dorsal mesentery by stage 41 and were found ectopically in the endoderm. Similar results were observed upon knock-down of X-Delta-2, one of the ligands of Notch (Morichika et al., 2010). Activation of the Notch pathway leads to the induction of the expression of HES and HES-related genes that encode basic helix-loop-helix type transcriptional repressors (Iso et al., 2003). Activation of such genes in the PGCs, as well as in somatic endodermal cells was observed upon activation of Notch signaling in the endoderm of *Xenopus* embryos. Altogether these data suggest that proper levels of Notch/Su(H) activity in the endoderm are required for normal PGC migration. Perturbation of this pathway may affect directionality, motility and/or adhesion of PGCs (Morichika et al., 2010).

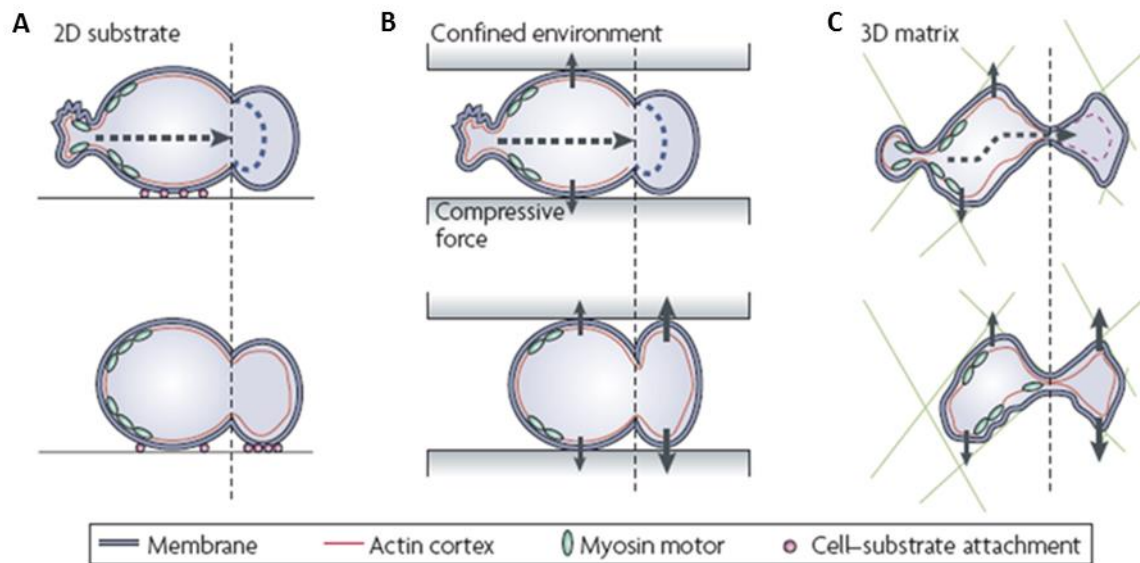


**Fig. 6. Models of bleb-associated motility.** (A) In two-dimensional (2D) cultures, in order to translate polarized blebbing into movement, the cell must adhere to the substrate. When a new bleb is formed and comes in contact with the substrate, new cell–substrate adhesions are formed and the cell mass can stream forward. The pink dots indicate cell–substrate attachment points. (B) When the cell is in a confined environment (for example, between two glass coverslips or in a thin microfluidic channel), it can move in the absence of cell–substrate adhesions. Instead, the cell exerts forces perpendicularly to the substrate and can squeeze itself forward. (C) When the cell is migrating in an extracellular matrix (ECM) gel (three-dimensional (3D) matrix), it can move by a combination of the mechanisms described. The fluid nature of growing blebs enables the cell to squeeze through the ECM network mesh. The dashed line indicates the position of the leading edge before bleb nucleation, arrows indicate the forces that are exerted by the cells on the extracellular environment and dashed arrows indicate the streaming of cytoplasm (taken from Charras and Paluch, 2008).

#### 1.4.4 Role of cell adhesion in *Xenopus* PGC migration

For the translocation of the cell body, directionally migrating cells need to interact with their environment. Unlike lamellipodia-based migration, where cells rely on adhesion to generate traction force (Giannone et al., 2007; Le Clainche and Carlier, 2008), cells migrating via bleb-associated mechanism are usually characterized by a decrease in adhesive activity (Fackler and Grosse, 2008). Interaction with a substrate can be achieved through weak adhesion to the surrounding cells or to the extra-cellular matrix (Fig. 6A). Conversely, blebbing cells can exert forces on the surrounding environment perpendicular to the direction of movement (Fig. 6B). In this latter case, a cell can squeeze itself forward without or with little adhesion to the substrate (Charras and Paluch, 2008). Interestingly, some cell types, like lymphocytes and cancer cells, can switch between lamellipodia-based migration and bleb-associated motility depending on the extracellular environment. Migration via lamellipodia that relies on the adhesion to the substrate and actin polymerization at the leading edge to generate traction force, is more efficient for the migration along the rigid environment, like basal membrane, or extracellular matrix filaments. In contrast, migration via a blebbing-associated mechanism is beneficial when cell has to pass through a randomly oriented 3D environment and cannot form specific adhesion contacts (Charras and Paluch, 2008; Fackler and Grosse, 2008).

As mentioned above, active PGC migration in *Xenopus* starts after stage 24, when the cluster, formed by these cells at earlier stages, starts to disperse. In addition, PGCs also change their morphology, from a spherical and poorly blebbing to a motile elongated form (Fig. 3) (Nishiumi et al., 2005; Terayama et al., 2012). In normal *Xenopus* embryos, although PGCs migrate as a cohort, they do not form direct contacts with one another. Analysis of sectioned tailbud (stage 28-36) and early tadpole (stage 42-45) stage embryos showed that the area of contact between PGCs and somatic cells is relatively small, leaving gaps between these cells. In contrast, somatic cells surrounding PGCs, both *in vivo* and *in vitro*, exhibit a high degree of cell-cell contact formation (Heasman and Wylie, 1978; Kamimura et al., 1976; 1980).

Independent observations coming from the analysis of different germ plasm associated RNAs have suggested that regulation of cell adhesion is involved in PGC development in *Xenopus* embryos. The Germes protein, encoded by one of these RNAs, contains two leucine zipper motifs and putative calcium binding EF-hand domain, but doesn't show substantial homology to other known proteins (Berekelya et al., 2003). It co-localizes with two dynein light chains (dlc8a and dlc8b) and is suggested to regulate germ plasm formation and development. Overexpression of Germes results in a decrease of the average number of PGCs at the tailbud stage (stage 33/34). Furthermore, the remaining PGCs failed to migrate laterally and were found deep in the endoderm. This phenotype might either be a direct result of Germes-mediated effect on cytoskeletal motor complexes in the PGCs, or an indirect one through alterations in germ plasm organization (Berekelya et al., 2007).

Clustering in the endoderm and subsequent loss of the PGCs was also observed upon knock-down of Dead end (Dnd) and Xdazl. These RNA-binding proteins are also encoded by maternal germ plasm specific mRNAs, and their function in PGC development was discussed previously (see section 1.2.5). The role of Dnd in the initiation of PGC migration was already described in zebrafish (see section 1.3.2). However, the molecular mechanisms that might link Xdazl, Germes and Dnd functions in the context of PGC migration in fish and frogs remains to be defined.

After they reach the dorsal body wall, PGCs leave the endoderm and migrate to the gonads via the dorsal mesentery, a thin stripe of connective tissue that links the dorsal body wall and the gut. From the mesentery, PGCs then migrate laterally to the forming genital ridges, enter the gonads, and differentiate into germ line stem cells capable of forming the gametes (Wylie and Heasman, 1976; 1993). Similar to the cells migrating within the endoderm, PGCs isolated from *Xenopus laevis* embryos at stage 42-45 show plasma membrane blebbing on artificial substrates (Wylie and Roos, 1976; Heasman et al., 1977). When seeded on a monolayer of amphibian mesentery cells, such spherical PGCs attach to the substrate and form filopodia-like protrusions (Fig. 3). Similar to bleb-associated migration, translocation is mediated by the contraction of the cell body and cytoplasm being pushed forward, resulting in an elongation of the cell. Following detachment of the rear,

---

cells return to a spherical shape upon arrival in the new position. Similar cell shapes of PGCs were observed in sectioned embryos (Heasman et al., 1977; Heasman and Wylie, 1978). Adhesion of PGCs to somatic mesentery cells was discovered to be mediated by fibronectin, a large extracellular protein that can bind to extracellular matrix components and membrane-spanning receptor proteins called integrins (Heasman et al., 1981; Pankov and Yamada, 2002). Mesentery cells produce large amounts of fibronectin both *in vivo* and *in vitro*. Isolated PGCs, in contrast, do not secrete detectable quantities of fibronectin *in vitro*, but are able to adhere to fibronectin and also fibronectin-producing cells, regaining migratory and invasive ability (Heasman et al., 1981; Wylie and Heasman, 1982; Brustis et al., 1984). Interestingly, fibrils of fibronectin formed by mesentery cells *in vitro* were demonstrated to be often co-linear with microfilament bundles within the cells (Heasman et al., 1981; Wylie and Heasman, 1982). As PGCs frequently formed filopodia-like protrusions and were elongated in the same direction as underlying cells, it was suggested that somatic cells might influence directionality of PGC migration through the dorsal mesentery. For the future, it remains a major challenge to define the regulation of these events on a molecular level and to tie them to the function of the regulators of PGC development and migration in *Xenopus*, in particular the set of RNA binding proteins that are already known to play a major role in this context.



## 2. MATERIALS AND METHODS

### 2.1 Model Organism

The African clawed frog *Xenopus laevis* (*X. laevis*) was used as a model organism during this study. Adult frogs were purchased from Nasco (Ft. Atkinson, USA).

### 2.2 Bacteria

For the cloning procedure *E. coli* strain XL-1 was used in this study: RecA1, endA1, gyrA96, thi-1, hsdR17, supE44, relA1, lac[F'proAB, lacIqΔM15, Tn10(Tetr)]<sup>c</sup> (Stratagene).

### 2.3 Cell line

For cultivation of PGCs cell line HEK293 (human embryonic kidney cells immortalized by adenovirus transfection) was used. ATCC<sup>R</sup> number CRL-1573TM.

### 2.4 Buffers and media

**Alkaline phosphatase buffer (APB):** 100 mM Tris-HCl (pH 9.5), 50 mM MgCl<sub>2</sub>, 100 mM NaCl, 0.1% Tween20

**Danylchik's for Amy (DFA) medium:** 53 mM NaCl, 5 mM Na<sub>2</sub>CO<sub>3</sub>, potassium gluconate 4.5 mM, sodium gluconate 32 mM, MgSO<sub>4</sub> 1 mM, CaCl<sub>2</sub> 1 mM, BSA 0.1%

**Dejelly solution:** 1.5-2% (w/v) L-cysteine hydrochloride in 0.1X MBS, pH 8.0

**Hybridization mix (Hyb-mix):** 50% (v/v) Formamid, 5xSSC, 1 mg/ml Torula RNA (Sigma), 100 μg/ml Heparin, 1x Denhards, 0.1% (v/v) Tween20, 0.1% (w/v) CHAPS (Sigma)

**Injection buffer:** 1% (w/v) FICOLL in 1X MBS

**IPP145 buffer:** (10mM Tris pH=8,0, 145mM NaCl, 0.1% NP-40, 5% (v/v) Glycerol, Inhibitor tablets (Roche) according to the manufacturer's instructions)

**Laemmli running buffer (10x):** 250 mM Tris-base, 2.5 M Glycine, 0.1% SDS

**Laemmli loading buffer (6x):** 350 mM Tris-HCl pH 6.8, 9.3% Dithiotreit, 30% (v/v) Glycerol, 10% SDS, 0.02% Bromphenolblue

**Luria-Bertani (LB)-Medium:** 1% (w/v) Bacto-Trypton (DIFCO), 0.5% (w/v) yeast extract (DIFCO), 1% (w/v) NaCl, pH 7.5

**LB-Agar:** 1.5% (w/v) agar (DIFCO) in liquid LB-medium

**MAB:** 100 mM Maleinic acid; 150 mM NaCl, pH 7.5

**MBSH (5x):** 50 mM HEPES pH 7.4, 440 mM NaCl, 10 mM KCl, 10 mM MgSO<sub>4</sub>, 25 mM NaHCO<sub>3</sub>, 2.05mM CaCl<sub>2</sub>, 1.65 mM Ca(NO<sub>3</sub>)<sub>2</sub>

**MEM:** 100 mM MOPS, 2 mM EGTA, 1 mM MgSO<sub>4</sub>

**MEMFA:** 1x MEM with 3.7% (v/v) Formaldehyde

**Nile blue staining:** 0.01% (w/v) Nile Blue chloride, 89.6 mM Na<sub>2</sub>HPO<sub>4</sub>, 10.4 mM NaH<sub>2</sub>PO<sub>4</sub>, pH~7.8;

**PBS (10x):** 8% (w/v) NaCl, 2% (w/v) KCl, 65 mM Na<sub>2</sub>HPO<sub>4</sub>, 18 mM KH<sub>2</sub>PO<sub>4</sub>, pH 7.4

**PTw buffer:** 1xPBS with 0.1% Tween20

**SSC:** 150 mM NaCl, 15 mM Sodium citrate, pH 7.4

**TAE (Tris/Acetate/EDTA):** 40 mM Tris-Acetate (pH 8.5), 2 mM EDTA

**TBST:** 10mM 1M Tris pH=8,0, 150mM NaCl, 0.1% (v/v) Tween-20

**TE-Buffer:** 10 mM Tris-HCl pH 8.0, 1 mM EDTA

**Tris-HCl (pH 6.8, 7.5, 8.2, 8.8, or 9.5):** 1 M Tris-HCl, pH adjusted with 37% HCl

**Western blotting buffer:** 3.03 g Tris-base, 14.4g Glycine, 200 ml methanol, 800 ml H<sub>2</sub>O

## 2.5 DNA constructs, vectors and oligonucleotides

### 2.5.1 Vectors

**pCS2+:** an expression vector, which can be used in the *Xenopus* model system. It contains a strong promoter/enhancer region (simian CMV IE94), polylinker and SV40 viral polyadenylation signal. The SP6 viral promoter allows in vitro transcription of sense polyadenylated mRNA for microinjections. The T7 viral promoter allows in vitro transcription of antisense RNA for in situ hybridization (Rupp et al. 1994).

**pCS2+HA:** PCS2+ with hemagglutinin tag was generated from the pCS2+ vector by the insertion of the hemagglutinin tag (HA) via the XbaI site for the expression of tagged proteins (Damianitsch et al., 2009).

**pCS2+DELE:** pCS2+ with Dead end localization element was generated from the pCS2+ vector by insertion of XDead end localization element cDNA via XhoI/ SnaBI sites for PGC-specific expression (Horvay et al., 2006).

**pCS2+gfpDELE:** pCS2+ containing the EGFP ORF cloned via BamHI site and the XDeadend localization element cDNA cloned into XhoI/ SnaBI sites was generated for labelling of PGCs, PGC-specific expression and visualization of intracellular distribution of molecules.

**2.5.2 Expression constructs****Table 1. Expression constructs**

Construct name	Insert	Vector	Reference/Comments
GFP_DELE		pCS2+gfpDELE	Transcribed directly from the vector
LifeAct-GFP_DELE	LifeAct-GFP	pCS2+DELE	Cloned via Clal/XhoI, amplified from LifeAct-GFP in pCS2+, kindly provided by A. Borchers
GFP_GRIP_PH_DELE	GFP_GRPI_PH	pCS2+DELE	Tarbashevich et al., 2011
GFP-Syntabulin_DELE	xSyntabulin ORF	pCS2+gfpDELE	Cloned via Clal/XhoI; amplified from oocyte cDNA kindly provided by M. Clausen
5'UTR_xSybu ORF_HA	5'UTR_xSyntabulin ORF	pCS2+HA	Cloned via Clal/XhoI; amplified from oocyte cDNA kindly provided by M. Clausen
xCentaurin ORF_HA	xCentaurin- $\alpha$ 1 ORF	pCS2+HA	Cloned via Clal/XhoI; amplified from oocyte cDNA kindly provided by M. Clausen

**2.5.3 Marker constructs**

1. The **MyoD** antisense RNA probe was generated by BamHI digestion of the plasmid pSP73XMyoD (Hopwood et al., 1989) and Sp6 transcription;
2. The **Xpat** antisense RNA probe was generated by EcoRI digestion of the pBKXpat plasmid (Hudson and Woodland, 1998) and T7 transcription;

### 2.5.4 Candidate PGC specific genes

WMISH probes were generated from the IMAGE cDNA clones, obtained from Open Biosystems/Thermo Scientific

**Table 2. Candidate PGC specific genes**

Gene name	IMAGE clone reference
AHA1	IMAGE:5073823
Histone cluster 1, H2aa	IMAGE:4031854
Heat shock protein 90kDa alpha	IMAGE:4970292
LEPROTL1	IMAGE:6956998
Similar to rras2	IMAGE:8328337
Transcribed locus (Xl.11269)	IMAGE:3301095

### 2.5.5 Sequencing and cloning primers

The oligonucleotides (primers) were purchased from Sigma-Aldrich Chemie

**Table 3. Primer list**

Primer name	Primer sequence 5'-3'
Sp6	TTAGGTGACACTATAGAATAC
T3	AATTAACCCTCACTAAAGGG
xSybulin RT F	TAAGCGAGTTGGCGTCGGTA
xSybulin RT R	TCCGGCACAGCACTGAGAAT
ODC-F	GCCATTGTGAAGACTCTCTCCATTC
ODC-R	TTCGGGTGATTCCTTGCCAC
Clal_5'UTR_xSybu	CCATCGATGGAGGTTGTTCTCACAGGAG
xSybulin_End_XhoI	CCGCTCGAGCGGGATGCGGGTGGTGC GGAT
Clal_LOC495044_Start (for xCentaurin)	CCATCGATGGATGTCTGGGGAGCATAACTG
LOC495044_XhoI_Stop (for xCentaurin)	CCGCTCGAGCGGTTAGGACCTTGCTTAAACTGTGC
GAPDH-UP	CTCCGCCCCCTCAGCAGATG

---

GAPGH-LOW	GCAGGCGGCAGGTCAGAT
Xpat_RT_F	AGCTCCAACACTACGAGCCACA
Xpat_RT_R	ACATCGGACACAGCAAACCA
E-cadherin_RT_F	GGTACAGATGCCTGGAATGC
E-cadherin_RT_R	TCCTGTGCGGTATAGGTAGC
Actb_RT_F	TATTGTGGGTCGCCAAGAC
Actb_RT_R	TGTGAGCAGCACTGGGTGTT

---

### 2.5.6 Morpholino oligonucleotides

Antisense Morpholino oligonucleotides (Morpholinos, MO) were purchased from Gene Tools, LLC (Philomath, USA). Morpholinos were dissolved in RNase-free water to a 1 $\mu$ M concentration.

**Table 4. Antisense Morpholino oligonucleotides**

Oligo name	Sequence 5'-3'
xKIF13B MO	ATCTTGACAGCGAGCTCCCCTAAC
Control MO	CCTCTTACCTCAGTTACAATTTATA
xSybu MO	TGCAGGTAAGTGA CTCTTCTG

---

## 2.6 DNA-methods

### 2.6.1 DNA isolation and purification

Isolation of plasmid DNA in analytical amounts (miniprep) was done using illustra<sup>TM</sup> plasmidPrep MiniSpin Kit (GE Healthcare) according to manufacturer's protocol. Isolation of plasmid DNA in preparative amounts (midiprep) was done by Plasmid Midi Kit (Qiagen) according to the manufacturer's protocol.

### 2.6.2 DNA restriction digest

For the analytical digest 0.2-0.5  $\mu$ g of DNA was incubated with 5 U or an appropriate enzyme in the corresponding enzyme buffer in the 10  $\mu$ l total reaction volume for 1 hour at 37<sup>o</sup>C. For the preparative digest up to 3  $\mu$ g of DNA was incubated with 10 U or an appropriate enzyme in the corresponding enzyme buffer in the 50  $\mu$ l total reaction volume for 4-5 hours at 37<sup>o</sup>C.

### **2.6.3 Agarose-gel electrophoresis (Sharp et al., 1973)**

DNA or RNA fragments were separated by size in the horizontal electrical field being embedded into the agarose-matrix. Depending on the expected sizes of DNA/RNA fragments, 0.5 to 2 % (w/v) agarose gels in TBE buffer were prepared. Gels always contained 0.5 µg/ml ethidium bromide to visualize nucleic acids later on. Before loading into gel slots, nucleic acids were mixed with the DNA-loading dye. The electrophoresis was run in the standard TBE-running buffer at 90-120 V in the house made horizontal electrophoresis chamber. After the run, DNA/RNA bands were visualized with UV-transilluminator (Herolab) and documented with ChemiDoc video documentation system (EASY view). Sizing of experimental bands was determined according to the standard DNA ladder run in parallel (High, Middle or Low Range, Fermentas)

### **2.6.4 Standard Polymerase chain reaction (PCR) (Mullis et al., 1986)**

To amplify a wanted DNA fragment a standard PCR reaction was used, containing the following components:

- 1x PCR buffer;
- 0.2 mM each dNTPs;
- 0.2 mM each primer;
- 100-500 ng DNA template;
- 0.5-1 U Taq polymerase;

All denaturation steps were performed at 94°C, all elongation steps – at 72°C, annealing temperatures depended on the GC-content of the amplifying fragment and primers used in the given reaction. In majority of cases, the 56-60°C annealing temperature was chosen.

### **2.6.5 DNA-sequencing and sequence analysis**

Dye-termination sequencing method, which is the modification of Sanger chain-termination sequencing, was used (Sanger et al. 1977). The Big Dye™ Terminator Kit (Applied Biosystems) was used for preparation of the sequencing PCR according to the manufacturer's instructions.

#### **The sequencing PCR mixture:**

DNA matrix – 200-400 ng

Seq mix – 1.5 µl

Seq buffer – 1.5 µl

Primer – 8 pmole

HPLC water – up to 10 µl

### **The sequencing PCR**

26 cycles:

96 °C, 30 sec

56°C, 30 sec

60°C, 4 min

To purify the sequencing reaction the following components were added to the PCR mixture: 1 µl of 125 mM EDTA (pH 8.0), 1µl of 3 M sodium acetate (pH 5.4) and 50 µl 100% ethanol. The sample was incubated 5 min at room temperature, then centrifuged 15 min at 14000 rpm. The pellet was washed with 70 µl of 70% ethanol, dried and diluted in 15 µl of HiDi™ buffer (Applied Biosystems).

The automated sequencing was performed by in-house sequencing lab using the ABI 3100 Automated Capillary DNA Sequencer (Applied Biosystems).

#### **2.6.6 Purification of DNA fragments**

To purify preparative PCR-amplified DNA fragments or linearized plasmids illustra™ GTFTM PCR DNA and Gel Band Purification Kit (GE Healthcare) was used according to manufacturer's protocol. DNA was eluted with 20-50 µl HPLC-water. Concentrations were measured using the ND-1000 Spectrophotometer, Coleman Technologies Inc.

#### **2.6.7 Ligation of DNA fragments**

T4 DNA ligase (Fermentas) was used according to manufacturer's instructions. The total amount of vector DNA was 100 ng, insert in excess. For 20 µl of a single reaction mixture 2 µl of T4 DNA ligase (5 U/µl) was used. The ligation was performed 1 hour at room temperature or O/N at 4 °C.

#### **2.6.8 Transformation**

100 µl of house-made chemically competent cells were tough on ice, mixed with 1-2 µl of a ligation mix, incubated for 20 min on ice, heat-shocked for 90 sec at 42 °C, left for 1 more min on ice, incubated at 37 °C for 60 min with 1 ml of LB-medium and plated on LB-agar-plates with the appropriate selectivity antibiotic. Colonies were grown ON at 37°C (Mandel and Higar, 1970).

#### **2.6.9 Verification of the integration of a DNA fragment of interest**

To verify the integration of the insert DNA fragment into a vector of interest a PCR with the colony material as a DNA template was used (colony-PCR). An insert specific pair of primers was selected for the amplification. Alternatively to the colony-PCR, plasmid isolation in analytical quantities followed by restriction digest was performed.

## 2.7 RNA-methods

### 2.7.1 *in vitro* transcription of labelled RNA probe for *in situ* hybridization

For the synthesis of a digoxigenin-labelled antisense RNA probe for *in situ* hybridization the following reaction mix was set up:

5  $\mu$ l of a 5x transcription buffer,  
1  $\mu$ l each 10 mM rATP, rCTP, rGTP  
0.64  $\mu$ l 10 mM rUTP,  
0.36  $\mu$ l digoxigenin-rUTP (Boehringer),  
1  $\mu$ l 0.75 M DTT,  
0.5  $\mu$ l RNaseout,  
200 ng linearized plasmid (the DNA template),  
1  $\mu$ l corresponding polymerase (T3, T7 or Sp6),  
DEPC-water to the final volume of 25  $\mu$ l

This reaction was incubated minimum 2 hours at 37°C, then 0.5  $\mu$ l of TurboDNase (Ambion) was added to destroy the template (15 min, 37°C) followed by the RNA purification.

### 2.7.2 *in vitro* transcription of capped-mRNA for microinjections

The synthesis of sense capped-mRNA for microinjections was done with Sp6 mMESSEGE mMACHINE Kits (Ambion) according to manufacturer's protocol. For 10  $\mu$ l reaction 200-500 linear template DNA was used. Reactions were incubated 3.5 hours at 37°C, then 0.5  $\mu$ l of TurboDNase (Ambion) was added to destroy the template (15 min, 37°C) followed by the RNA purification.

### 2.7.3 Purification of synthetic RNAs

The purification of *in vitro* synthesised RNAs was performed using illustra™ RNA spin MiniRNA Isolation Kit from GE Healthcare according to the company's protocol. Elution was done in 30  $\mu$ l of DEPC-water. Purity of the RNA obtained was controlled photometrically by OD260/OD280 ratio and on a 2% agarose gel.

### 2.7.4 Isolation of total RNA

500  $\mu$ l of Trizol-mix was added to 5-10 *Xenopus* embryos frozen in liquid nitrogen. After toughing embryos were homogenised with a 1 ml insulin-syringe and let stand for 5 min at RT. The homogenate was mixed by shaking with 0.1 ml of chloroform for 15 sec, let stand for 2-3 min at RT and centrifuged for 15 min at 10000 rpm, 4°C. The upper phase was transferred into a new eppendorf, mixed with 0.25 ml of isopropanol, incubated for 10 min



at RT and centrifuged for 10 min at 10000 rpm, 4°C. The upper phase was discarded and the pellet washed with 75% ethanol in DEPC-water. After the centrifugation step (9000 rpm, 5 min, 4°C), ethanol solution was decanted, pellet air dried and subjected for the DNase digest (1 U DNaseI, 1x DNaseI buffer, DEPC-water to the final volume of 10 µl) for minimum 1 hour at 37°C. The reaction was stopped by adding 1 µl of 25 mM EDTA and heat inactivation for 10 min at 65°C. to precipitate RNA after the DNA digest 10µl of 10 M ammonium acetate and 250 µl of 100% ethanol in 100 µl of DEPC-water were added and incubated ON at -20°C or for 3 hours at -80°C. After the centrifugation step (9000 rpm, 5 min, 4°C), the supernatant was discarded and the pellet washed twice with 75% ethanol in DEPC-water, air dried and dissolved in 30 µl of DEPC-water.

### **2.7.5 Semiquantitative Reverse-Transcription PCR (RT-PCR)**

The RT-PCR with RNA extracted from different embryonic stages and tissues was performed using an RT-PCR Kit (Perkin Elmer). For the reverse transcription the following reaction mix was prepared:

1 µl 10x PCR Buffer without MgCl<sub>2</sub>,

2 µl 25 mM MgCl<sub>2</sub>,

2 µl each 10 mM desoxynucleotide solutions (dATP, dCTP, dGTP, dTTP),

0.5 µl RNaseout,

0.5 µl random hexamers (50 µM)

0.2 µl reverse transcriptase,

50-100 ng RNA,

DEPC-water to the final volume of 10 µl

The synthesis of cDNA was performed in three steps: 10 min 22°C (annealing), 50 min 42°C (reverse transcription) and 5 min 99 °C (heat inactivation of the reverse transcriptase). 5 µl of the obtained cDNA was subjected for the standard Taq-PCR with gene specific primers.

### **2.7.6 Quantitative RT-PCR analysis**

PGCs and somatic endodermal cells were isolated from stage 17-19 and stage 28-30 embryos as described above. 30 cells from each cell population were used for the preparation of cDNA using SuperScript III CellsDirect cDNA Synthesis System (Invitrogen, Carlsbad) according to the manufacturer's protocol. As a negative control, reverse transcriptase was replaced by the addition of the equal amount of water (RT-) during cDNA preparation from the unsorted group of endodermal cells. This control was included in every

cDNA preparation from the corresponding stage. Obtained cDNA was purified using Agencourt AMPure XP paramagnetic beads (Beckman Coulter) according to the manufacturer's protocol and eluted in 16-50  $\mu$ L of purification buffer (10 mM Tris-Cl, pH 8.5). Amplification of *Xpat* as a PGC-specific gene (Hudson and Woodland, 1998) and  *$\beta$ -actin* as a positive control were used to monitor quality and contamination of analyzed cell populations using DreamTaq DNA Polymerase (Thermo Fisher Scientific Inc.). Relative size of the amplified products was determined by comparison to the FastRuler Low Range DNA Ladder (Fermentas). Quantitative PCR was done using iQ SYBR Green Supermix (Bio-Rad) on CFX96 Real-Time System according to manufacturer's protocol. 1/18 of purified cDNA was used for one PCR reaction. The experiment was done with three independent cDNA preparations. For every cDNA preparation, two technical replicates were performed. 'RT-' from the corresponding stage was used as a template for negative control. Analysis of the gene expression was done by  $\Delta$ Ct method with  $\beta$ -actin (*Actb*) as a reference gene ( $Ct_{Actb} - Ct_{gene}$ , where Ct is a threshold cycle). Comparison of the expression level between cells isolated from stage 17-19 and stage 28-30 embryos was done by  $\Delta\Delta$ Ct method ( $\Delta C_{t_{gene, St. 28-30}} - \Delta C_{t_{gene, St. 17-19}}$ ) (Livak and Schmittgen, 2001).

### 2.7.7 Whole transcriptome analysis

PGCs and somatic endodermal cells were isolated from stage 17-19 (PGC 17; Som 17) and stage 28-30 (PGC 28; Som 28) embryos as described above. 30 cells from each cell population were used for the preparation of amplified cDNA with SMARTer<sup>®</sup> Ultra Low RNA Kit for Illumina<sup>®</sup> Sequencing (Clontech) according to manufacturer's protocol. Integrity of the samples was analyzed by High Sensitivity DNA assay with BioAnalyzer (Agilent Technologies). Amplified full-length cDNA was subjected to controlled DNA shearing with the Covaris AFA system to generate 200-500 bp fragments. Illumina Sequencing Library was generated with the Illumina Paired-End DNA Sample Prep Kit (Illumina Cat. Nos. PE-102-1001 & PE-102-1002) according to manufacturer's protocol and analyzed with Illumina HiSeq2000 platform. Mapping of the obtained short sequences (reads) was done to the *X. tropicalis* database available at that moment (Gilchrist and Pollet, 2012). Gene expression in each cell population was represented as normalized number of aligned reads (NR), obtained by Reads Per Kilobase per Million mapped reads (RPKM) normalization (Mortazavi et al., 2008). In short, in this method gene counts (number of aligned reads for specific gene in one cell population) are normalized to the total number of mapped reads associated with corresponding cell population and normalized to the length of the transcript. To identify genes differentially expressed in PGCs, NR for genes in PGC population isolated from stage 28-30 was divided to NR for corresponding genes in PGC population isolated from stage 17-19. This gives fold change difference in expression ( $FC_{PGC28/17}$ ). Same analysis was done for somatic endodermal cells ( $FC_{Som28/17}$ ). To eliminate genes that are co-upregulated or co-downregulated in PGCs and somatic cells,  $FC_{PGC28/17}$  was divided to  $FC_{Som28/17}$  ( $FC_{PGC/Som}$ ). Thresholds were applied:

**Table 5. Thresholds to identify differentially expressed genes in PGCs**

	Downregulated	Upregulated
NR	>100 (for PGC17)	>100 (for PGC28)
FC <sub>PGC28/17</sub>	≤0.5	≥2
FC <sub>PGC/Som</sub>	<0.5	>2

## 2.8 Protein methods

### 2.8.1 *In vitro* translation of the proteins and immunoprecipitation

In vitro translation of the proteins was done using the TNT SP6 Coupled Reticulocyte Lysate System (Promega) according to the manufacturer's instructions. To test for MO specificity, the reaction was carried out in a volume of 12.5  $\mu$ l with either xSybu MO, xKIF13B MO or Control MO. For immunoprecipitation, proteins after *in vitro* translation were mixed (1:1) and incubated at RT for 30-60 minutes. 2-3  $\mu$ l of each *in vitro* translation mixture were taken for the input control. After incubation, protein mixtures were diluted in IPP145 buffer and incubated for 1 hour at 4 °C with anti-Myc antibodies (9E10, Sigma) immobilized on  $\gamma$ -sepharose beads. Protein complexes were precipitated by low-speed centrifugation (400 g). Sepharose beads were washed three times with IPP145 buffer, boiled in Laemmli sample buffer and analyzed by western blotting.

### 2.8.2 Western blotting

Proteins were separated by 8 or 10% SDS-PAGE (Laemmli, 1970) and transferred onto a nitrocellulose membrane (0.45  $\mu$ m, Schleicher & Schuell) using the semi-dry blotting method (Sambrook J., 1989). The membrane was blocked by 5% (w/v) milk powder in TBST for 1 hour at room temperature or overnight in a cold room. The membrane was incubated with a primary antibody solution (5% (w/v) milk powder, 1:1000 dilution of mouse anti-HA (Convance) in TBST) ON in a cold room, then washed three times for 10 min in TBST and incubated with a secondary antibody solution (5% (w/v) milk powder, 1:5000 dilution of goat anti-mouse (Santa Cruz) HRP-coupled antibody in TBST) for 1 hour at room temperature. After three 10 min washes in TBST, the ECL Direct™ labeling and detection system (Amersham) was used to visualize proteins.

## 2.9 Preparation and manipulation of *Xenopus laevis* embryos

### 2.9.1 Preparation of *Xenopus laevis* testis

Both testes was taken out from a narcotized decapitated male frog, washed with and stored in the 1x MBSH buffer at 4°C.

### 2.9.2 Embryo injections and culture

Embryos were obtained from *Xenopus laevis* female frogs by HCG (5000 U/mL human chorionic gonadotropin; Sigma-Aldrich) induced egg-laying (800 - 1000 U HCG approximately 12 hours before egg-laying). Spawns were *in vitro* fertilized with minced testis in 0.1X MBSH, dejellied with 1.5-2% cystein hydrochloride (pH 7.5) and cultured in 0.1 X MBSH at 12.5°C. Albino embryos were stained with Nile Blue for 10 min at RT prior to injections to distinguish better between animal and vegetal poles. Injections were performed in the injection buffer on a cold plate (12.5°C) vegetally into both blastomeres of the two-cell stage. 1-4nl of mRNA or morpholino oligonucleotides dilutions per blastomere were injected. Injected embryos were kept for at least 1 hour in the injection buffer at 12.5°C and then transferred into 0.1x MBSH.

### 2.9.3 Whole-mount *in situ* hybridization (WMISH)

Whole-mount *in situ* hybridization (WMISH) was performed as described (Harland 1991). All the steps were performed at room temperature with mild agitation.

#### WMISH day 1

#### Rehydration of embryos

Prior to WISH embryos were rehydrated, as it is described in the Table 6

**Table 6. Rehydration of embryos**

Step Number	Solution	Incubation time
1	100% ethanol	3 min
2	75% ethanol in water	3 min
3	50% ethanol in water	3 min
4	25% ethanol in PTw	3 min
5	PTw	3 min

#### Proteinase K treatment

To make the embryos after developmental stage 8 accessible for RNA probes, they were treated with proteinase K (10 µg/ml) in PTw. The proteinase K incubation time was chosen depending on the embryo stage (Table 7).

**Table 7. Proteinase K treatment procedure**

Developmental stage of <i>Xenopus</i> embryos	Incubation time (min)	Temperature
8 - 10.5	6 - 8	room temperature
14 - 16	8 - 10	room temperature
20 - 25	15 - 18	room temperature
36	22 - 25	room temperature
40	17 - 20	37°C
42 - 43	27 - 30	37°C
46	32 - 35	37°C

**Acetylation and refixation**

Acetylation of embryos was performed as described in the Table 8.

**Table 8. Acetylation of *Xenopus* embryos**

Step Number	Buffer	Incubation time
1	1M Triethanolamine chlorid, pH 7.0 (TEA)	2x 5min
2	1M TEA with 0.3% acetic anhydride	5 min
3	1M TEA with 0.6% acetic anhydride	5 min
4	PTw	5 min

Upon acetylation, embryos were fixed for 20 min in PTw containing 4% (v/v) formaldehyde and washed 5 times with PTw buffer.

**Hybridization**

After the last washing step approximately 1 ml of PTw was left in the tubes and 250  $\mu$ l Hyb-Mix was added. The solution was replaced immediately by 500  $\mu$ l of fresh Hyb-Mix and incubated for 10 minutes at 60°C. Hyb-Mix was exchanged again and embryos were incubated 4 - 5h at 60°C. The Hyb-Mix was replaced with the desired labeled RNA probe, diluted in Hyb-Mix solution. The hybridization took place overnight at 60°C.

**WISH day 2**

### Washing and RNase treatment

To remove unbound RNA probes, the samples were washed and digested with RNase A (10 µg/ml) and RNase T1 (10 U/ml) as described in the Table 9.

**Table 9. Washing and RNase treatment of *Xenopus* embryos**

Step Number	Solution	Incubation temperature and time
1	Hyb Mix	60°C, 10 min
2	2x SSC	60°C, 3x 15 min
3	RNases in 2x SSC	37°C, 60 min
4	2x SSC	room temperature, 5 min
5	0.2x SSC	60°C, 2x 30 min
6	MAB	room temperature, 2x 15 min

### Blocking and antibody reaction

Embryos were blocked with MAB buffer, containing the Boehringer Mannheim Blocking Reagent (BMB) and horse serum, and incubated with Sheep Alkaline phosphatase-coupled anti-Dig antibody (Sigma) according to the Table 10.

**Table 10. Blocking and antibody incubation**

Step Number	Solution	Incubation temperature and time
1	MAB/2% BMB	room temperature, 10 min
2	MAB/2% BMB/20% Horse serum	room temperature, 30 min
3	MAB/2% BMB/20% Horse serum 1:5000 α-DIG antibodies	room temperature, 4 hours
4	MAB	room temperature, 3x 10 min
5	MAB	4°C, overnight

**WISH day 3****Staining reaction**

The alkaline phosphatase staining reaction was performed as described in Table 11.

**Table 11. Alkaline phosphatase staining reaction**

Step Number	Solution	Incubation time
1	MAB	5x 5 min, room temperature
2	APB	3x 5min, room temperature
3	APB with 80 µg/ml NBT, 175 µg/ml BCIP	Up to three days, 4°C

Upon the staining, albino embryos were fixed in MEMFA, washed with PTw, documented and stored in 100% ethanol. Pigmented embryos were bleached as described in section 2.10.3 to remove the pigment, which can interfere with the specific WISH signal.

**2.9.4 Bleaching**

The bleaching of pigmented embryos was performed as described in Table 12.

**Table 12. Bleaching of pigmented *Xenopus* embryos**

Step Number	Solution	Incubation time
1	2x SSC	3x 5 min
2	2x SSC with 50% formamide, 1% H <sub>2</sub> O <sub>2</sub> ,	Until embryos loose pigment
3	MEMFA	30 min
4	PTw	3x 5 min

Bleached embryos were documented and stored in 100% ethanol.

**2.9.5 Clearing of the endoderm**

To visualize staining in the endoderm, embryos after WMISH were wased 3x with methanol (10 min) and trnsfered into the in-house made glass well. Methanol was exchanged with Benzyl Benzoate and Benzyl Alcohol mixture (BB:BA) (2:1). After

documentation, embryos were washed 3x with methanol, transferred back into glass vials and stored at -20°C.

### **2.9.6 TUNEL-staining**

The TdT-mediated dUTP digoxigenin nick end-labeling (TUNEL) staining technique was modified from Hensey and Gautier (1997) (Hensey and Gautier, 1997). Embryos were rehydrated with the MeOH series to PBS. After one wash in PBS for 10 min, the solution was exchanged twice with PTw, 15 min each. Embryos were washed twice in PBS for 20 min before they were incubated for 1 hour in TdT buffer. During this pre-incubation step and the following overnight incubation vials were standing upright. End-labeling was carried out overnight at RT in TdT buffer containing 0.5 mM digoxigenin-dUTP and 150 U/ml terminal deoxynucleotidyl transferase (Invitrogene). Embryos were washed twice for 2 hours with PBS/EDTA at 65°C in a water bath. After washing embryos four times for 1 hour in PBS, it was exchanged with PBT and incubated for 20 min. Embryos were blocked for 1 hour by incubation in PBT containing 20% heat-treated horse serum. Embryos were placed in the antibody solution and incubated overnight at 4°C. To remove unbound antibody, embryos were washed 8 times in PBT and then washed overnight in PBT at 4°C. The chromogenic reaction was performed as described for WMISH.

## **2.10 PGC cultivation**

### **2.10.1 Labelling and isolation of PGCs and somatic endodermal cells**

Embryos were injected vegetally into both blastomeres at 2-cell stage with 300-400pg of the synthetic mRNA encoding for a GFP ORF fused Dead end localisation Element (*GFP\_DELE*). They were cultivated until stage 17-19 or stage 28-30 (Nieuwkoop and Faber, 1994), and dissected into dorsal (mainly brain and spinal cord) and ventral (mainly endoderm) parts. Ventral explants were placed in a 30 mm Petri-dish coated with 0.7% agarose, dissolved in the accutase solution (Sigma-Aldrich) and washed with 0.8x MBSH. GFP-positive PGCs and GFP-negative somatic endodermal cells were manually sorted using an in-house made eyebrow hair tool under LumarV.12 fluorescence stereomicroscope (Zeiss) (GFPA filter), AxioCam camera and AxioPlan software (Zeiss) (Fig. 7).

### **2.10.2 Cultivation of PGCs on a layer of HEK 293**

HEK 293 cells were cultured in DMEM medium (Biochrom) supplemented with 10% fetal calf serum (FCS), 100 units/μl penicillin and 100 μg/ml streptomycin (full DMEM) at 37°C, 95 % humidity, 5 % CO<sub>2</sub>. For subculture, the cells in 75 cm<sup>2</sup> flask were rinsed with 1x PBS and incubated with 2 - 3 ml of 0.25% (w/v) trypsin 10 - 20 min at 37°C until the cell layer was dispersed. The reaction was stopped with 5 ml of DMEM medium. The appropriate number of cells was transferred into a fresh 75 cm<sup>2</sup> flask or 30 mm Petri dish containing 15 ml of fresh full DMEM medium. Dissociated endodermal explants from *GFP\_DELE*-injected embryos were transferred on top of HEK 293 monolayer in 30mm Petri dish. For some experiments, dorsal extract, prepared by homogenization of dissected dorsal part of the embryo in the presence of 0.2mM PMSF to prevent protein degradation, was applied



ectopically. Time-lapse images were recorded and analyzed with Axio Imager 2 (Zeiss), AxioCam camera and AxioPlan software (Zeiss).

### **2.10.3 Cultivation of PGCs in between two layers of endodermal cells**

Endodermal explants were dissected from uninjected tailbud stage embryos (stage 28-34) and dissociated by accutase solution (Sigma-Aldrich). Dissociated cells were washed with 0.8x MBSH and transferred on top of 30mm Petri dish or glass cover slip pre-coated overnight with concentrated fibronectin solution (50  $\mu\text{g}/\text{ml}$  in 1x PBS; F1141-5MG, Sigma-Aldrich). Dissociated endodermal explants with labeled PGCs isolated from stage 30-32 embryos were transferred on top of the 30mm Petri dish covered with endodermal cells. After that, explanted cells were covered with endodermal cell-containing glass cover slip. Cultivation was done in 0.8xMBSH. For some experiments, dorsal extract, prepared by homogenization of dissected dorsal part of the embryo in the presence of 0.2mM PMSF, was applied ectopically. Time-lapse images were recorded and analyzed with Axio Imager 2 (Zeiss), AxioCam camera and AxioPlan software (Zeiss).

### **2.10.4 Cultivation of PGCs in extracellular matrix**

One sector of a 30mm Petri-dish was filled with 2% agarose. Dissociated endodermal explants from *GFP\_DELE*-injected embryos were either premixed or applied on top of polymerized extracellular matrix (ECM, Sigma-Aldrich). Cells were cultivated in 0.8xMBSH, DMEM or DFA buffers. For some experiments, dorsal extract, prepared by homogenization of dissected dorsal part of the embryo in the presence of 0.2mM PMSF, was injected in the agarose gel. Time-lapse images were recorded and analyzed with Axio Imager 2 or LumarV.12 fluorescence stereomicroscope (Zeiss), AxioCam camera and AxioPlan software (Zeiss).

### **2.10.5 Cultivation of PGC imbedded in agarose gel**

One sector of a 30mm Petri-dish was filled with 2% agarose, while the rest of the Petri dish was coated with 0.1-0.5% agarose gel. Dissociated endodermal explants from *GFP\_DELE*-injected embryos were transferred on top of the agarose-coated Petri dish. Precooled 0.1-0.3% agarose, shortly before polymerization, was applied on top of the explanted cells. After agarose gel polymerized, 0.8x MBSH was added on top to cover the agarose gel. For some experiments, dorsal extract, prepared by homogenization of dissected dorsal part of the embryo in the presence of 0.2mM PMSF, was injected in the 2% agarose gel. Time-lapse images were recorded and analyzed with Axio Imager 2 or LumarV.12 fluorescence stereomicroscope (Zeiss), AxioCam camera and AxioPlan software (Zeiss).

### **2.10.6 Under-agarose migration assay**

30 mm Petri dishes were incubated overnight with 2 ml of either fibronectin (20  $\mu\text{g}/\text{ml}$  in 1x PBS; F1141-5MG, Sigma-Aldrich), 5% (w/v, 1x PBS) bovine serum albumine (BSA or Albumin Fraction V, Carl Roth GmbH) or left untreated. After incubation, Petri dishes were washed three times with 1x PBS and then covered with agarose (0.5% (w/v) in 0.8x MBSH). After the gel polymerized, 0.8x MBSH was added on top to cover the agarose gel. Cells, isolated as described above, were transferred with a pipette under the agarose layer,

between the BSA-covered bottom of the Petri dish and the agarose gel. Cells were monitored by time-lapse imaging using a LumarV.12 fluorescence stereomicroscope (Zeiss) and the AxioPlan software (Zeiss). Tracking was made using Fiji MTrackJ plug-in and analyzed using ImageJ Chemotaxis Tool plug-in.

## 2.11 Biophysical methods

### 2.11.1 Electric cell-substrate impedance sensing

Analysis of cellular dynamics was performed by electric cell-substrate impedance sensing system (Applied Biophysics). Isolated individual PGCs or somatic endodermal cells obtained either from stage 17-19 or stage 28-30 embryos injected with *GFP\_DELE* were transferred on top ultra-small gold electrodes with a diameter of 250  $\mu\text{m}$ . Cells were cultured in 0.8x MBSH. The impedance at a frequency of 10 kHz was recorded over time. The recorded time traces of the impedance  $|Z|$  were detrended by applying a continuous sliding window of 250 data points and subtracting its arithmetical mean from the central point of the window. This was done to compensate the effect of thermal drifts. Calculation of variances of the detrended impedance fluctuations of a 30 min time regime was performed to monitor the dynamic behaviour of the different cell populations. Inhibition of cellular dynamics was done by ectopic application of cytochalasin B (Sigma-Aldrich) to a final concentration of 100  $\mu\text{M}$ . Detrended fluctuation analysis (DFA) was carried out according to Peng et al. (Peng et al., 1994) using a self-written MatLab script.

**Note:** measurements, data analysis and text preparation was done in collaboration with D. Schneider.

### 2.11.2 Time-lapse image analysis

PGCs were isolated as described above from *GFP\_DELE* injected embryos and monitored with Axio Imager 2 (Zeiss) and AxioCam camera and AxioPlan software (Zeiss). Fluorescence microscopy images of migratory and pre-migratory GFP-labeled PGCs were recorded every 15 s for about 15 min. These images were dissected with a self-written picture analysis program based on Matlab. Original fluorescence images were converted into black and white using individual threshold values for black and white discrimination. Difference image was generated by a subtraction of one image from the prior one. This resulted in the detection of changes in cellular shape over time and allowed to distinguish between contracting and expanding areas of the cells. The occurring alterations in area are normalized to the overall cell area at each time point and plotted in percentages. Cellular motility is quantified by calculating the variances of the detected temporal shape fluctuations.

**Note:** Matlab analysis and text preparation was done in collaboration with D. Schneider.

### 2.11.3 Single-cell force spectroscopy

PGCs and somatic endodermal cells were isolated from stage 17-19 or stage 28-30 embryos injected with *GFP\_DELE* as described above. All measurements were performed with a Cellhesion200 setup (JPK Instruments) placed on an Olympus IX81 microscope (Olympus). Cells were picked by poly-D-lysine coated cantilevers with a nominal spring constant of 0.03 N/m. Thermal noise method (Hutter and Bechhoefer, 1993) was used to determine the spring constant of each cantilever before the measurements (Hutter and Bechhoefer, 1993). Cantilevers were washed twice with isopropanol and ultra-pure water, cleaned in argon plasma for 1min and incubated in a 10 µg/ml poly-D-lysine solution (in 1x PBS) for 15 min. To attach either a primordial germ cell or a somatic endodermal cell to the cantilever, a setpoint of 500 pN and a contact time of 30 s before retraction were chosen. To investigate the interaction of either somatic or primordial germ cells with different substrate coatings, Petri dishes were separated into three parts by Liquid-repellent Slide Marker Pen (Super PAP Pen Liquid Blocker, mini; Daito Sangyo Co., Ltd, Osaka, Japan). Each third was coated with either bovine serum albumin (BSA) (5% (w/v) in 1xPBS; Albumin Fraction V, Carl Roth GmbH), fibronectin (50 µg/ml in 1x PBS; F1141-5MG, Sigma-Aldrich) or collagen I (50 µg/ml in 0.02 M Acetic acid and 1x PBS; Gibco). Incubation was done overnight, followed by 3x washing with 1x PBS. At least 10 force curves were recorded on each substrate using the same cell on the cantilever. At least three cells were investigated per cell population.

For quantification of cell-cell interactions, dissociated endodermal explants were transferred on top of the Petri dishes separated into two parts by Liquid-repellent Slide Marker Pen (Super PAP Pen Liquid Blocker, mini; Daito Sangyo Co., Ltd, Osaka, Japan). One part was incubated with fibronectin solution (50 µg/ml in 1x PBS; F1141-5MG, Sigma-Aldrich), whereas the second part was saturated by employing BSA (5% (w/v) in 1xPBS; Albumin Fraction V, Carl Roth GmbH) to avoid cell spreading and therefore facilitate picking of the cells. Incubation was done overnight, followed by three times washing with 1x PBS.

Adhesion experiments were carried out with a contact time of 5sec, an approach/retraction velocity of 3 µm/s and a contact force of 500 pN between the cells attached to the cantilever and the substrate. As a substrate, either a spread cell or one of the different surface coatings mentioned above, was employed.

**Note:** measurements, data analysis and text preparation was done in collaboration with D. Schneider.

;

### 3. RESULTS

#### 3.1 Isolated *X. laevis* PGCs can migrate *in vitro* in the confined environment via bleb-associated mechanism without specific adhesion to the substrate

In *X. laevis*, active PGC migration in the endoderm occurs starting from early up to late tailbud stages of embryonic development (stages 24-44 according to Nieuwkoop and Faber, 1994) and starts at developmental stage 24 (Houston and King, 2000a; Nishiumi et al., 2005; Terayama et al., 2013; discussed in section 1.2.5). At this stage of development, however, endoderm is not transparent due to the high yolk content in the endodermal cells. This phenomenon makes it difficult to study PGC migration on the cellular level *in vivo*.

PGCs can be labelled by vegetal injection of chimeric mRNA *GFP\_DELE*, consisting of the GFP open reading frame (ORF) and the Dead end localization element (LE). Vegetal injection into the germ plasm region ensured enrichment of the mRNA in the germ plasm, while presence of the Dead end LE mediated degradation of the transcript in somatic endodermal cells (Koebernick et al., 2010; reviewed in sections 1.1 and 1.4.1). After injected embryos reach desired developmental stage, PGCs can be isolated by the dissociation of dissected endodermal explant, and identified as GFP-positive cells (Fig 7).

In the previous studies, we managed to establish conditions for cultivation and migration of PGCs *in vitro*. In short, PGCs isolated from tailbud stage embryos were able to polarize and in some cases directionally migrate on the fibronectin-coated Petri dish towards crude extract, prepared from homogenized dorsal part of the embryo (Tarbashevich et al., 2011; Fig 5). In this assay, although polarization towards dorsal extract was observed for most of the PGCs, only few cells were able to initiate the migration. In the context of this project, several conditions, including cultivation of PGCs on artificial and cellular substrates, were analyzed to improve the efficiency of PGC migration *in vitro*.

##### 3.1.1 Cultivation of *X. laevis* PGCs on the cellular substrates

Migration of many cell types, including zebrafish PGCs, requires adhesion to the surrounding cells or extracellular matrix (Kardash et al., 2010). It has been shown, that during migration of *X. laevis* PGCs in the dorsal mesentery, somatic cells secrete fibronectin, and PGCs can migrate *in vitro* on the layer of these cells (Heasman et al., 1977; Heasman and Wylie, 1978; discussed in chapter 1.4.4). To test whether presence of somatic endodermal cells is required for PGC migration in *X. laevis* at tailbud stage of development, isolated PGCs were cultivated in the endodermal explants. To recreate an environment similar to the *in vivo* situation, PGCs were placed between two layers of endodermal cells that in turn were attached to a fibronectin-coated Petri dish and glass cover slip (Fig 8A). Cells were cultivated up to 24 hours, but did not initiate active migration (Fig. 8B). Since no gradient for the directional cell migration was applied in this case, cultivated cells were not polarized but formed cellular protrusions in random directions. Ectopic addition of homogenized dorsal

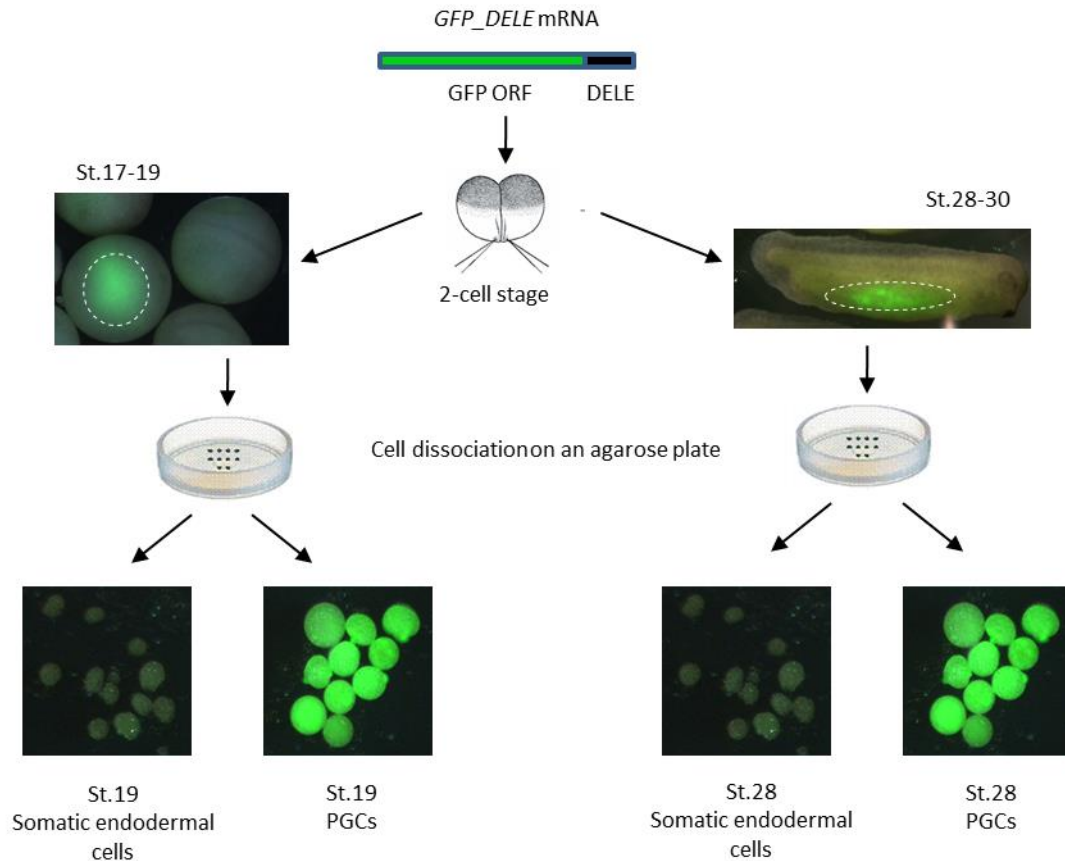


**Fig. 7. Labeling and isolation of *X. laevis* PGCs.** *X. laevis* embryos at 2-cell stage were injected with *in vitro* transcribed *GFP\_DELE* mRNA, consisting of green fluorescence protein (GFP) open reading frame (ORF) fused to Dead end localization element (DELE). Injections were performed in the vegetal side of both blastomeres. Schematic representation of 2-cell stage embryo corresponds to a lateral view; animal pigmented side is up, vegetal is down. Embryos were cultivated till neurula (St.17-19; ventral (left) and dorsal (right) view, anterior side is to the right) or tailbud (St.28-30; lateral view, anterior side is to the right) stages of embryonic development. Endodermal explants, highlighted by the white dashed line, containing PGCs and somatic endodermal cells were dissected from the embryos and dissociated on the agarose-coated Petri dish by enzymatic treatment with mild protease (accutase). Dissociated cells can be distinguished as GFP-positive PGCs and GFP-negative somatic endodermal cells.

extract that was sufficient to polarize PGCs *in vitro* and could induce their motility (Tarbashevich et al., 2011), resulted in a more intensive protrusion formation, but no migrating cells were observed.

Since explanted dissociated endodermal cells used in the previous approach did not form a uniform cell layer, cultivation of PGCs on a monolayer of a mammalian cell line, HEK 293, was performed (Fig. 9A). Under these conditions, cultivated PGCs formed bleb-like protrusions, but did not initiate migration (Fig 9B), and did not respond to ectopic application of the homogenized dorsal explant.

### 3.1.2 Cultivation of *X. laevis* PGCs on the artificial substrates

As discussed previously, migration of *X. laevis* PGCs during tailbud stage of embryonic development occurs via a bleb-associated mechanism. In order to migrate, cells need to interact with their environment to generate the traction force necessary for translocation.

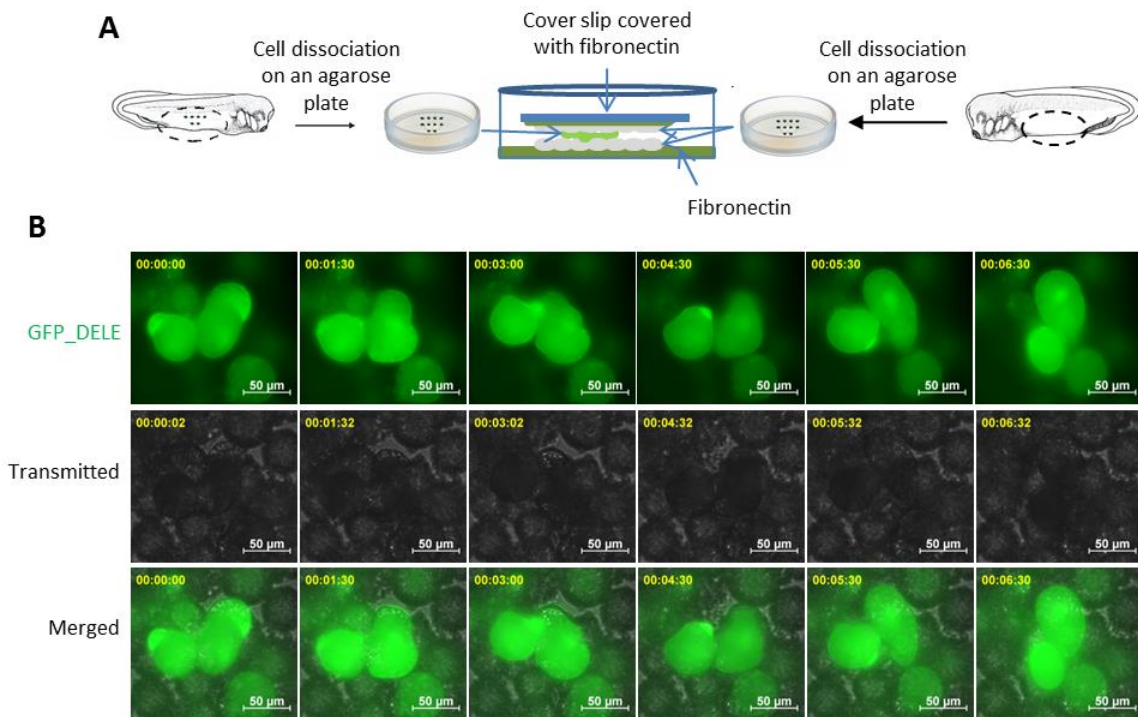


**Fig. 8. Cultivation of isolated PGCs within the endodermal cell mass did not facilitate active migration.** (A) Ventral explants were dissected from tailbud stage embryos injected with *GFP\_DELE* mRNA to label PGCs. Explants were dissociated via enzymatic treatment. Isolated PGCs (green) were transferred in between two layers of endodermal cells (grey). These layers were obtained by dissociation of endodermal explant from uninjected embryos; isolated cells were pre-cultivated on top of the fibronectin-coated culture dish, or fibronectin-coated glass cover slip. Fibronectin coating was used for the adhesion and spreading of the endodermal cells. (B) Representative time-lapse images of PGCs (green) recorded 1 hour after cultivation in the endodermal cell mass. The upper row represents images taken under UV light to identify GFP-positive PGCs. The middle row corresponds to the images taken at the same time under brightfield transmitted light. The lower panel represents merged images. Despite active cellular dynamics, migration of PGCs was not observed. Cells were cultivated up to 24 hours, but after several hours of cultivation cellular dynamics was significantly decreased. Relative time after the first recorded image (hours : minutes : seconds) is indicated in the upper left corner of the images, scale bar: 50  $\mu\text{m}$ .

There are two major models describing how plasma membrane bleb-like protrusions can contribute to directional migration. One model is based on the formation of specific contacts between the migrating cell and the substrate. In the alternative model, a traction force is generated by compressive forces applied by the cell on the substrate. In the latter case, adhesion is not required, but the cell should be surrounded by at least two resistant surfaces (Charras and Paluch, 2008; Fig. 6). To establish an *in vitro* migration assay on artificial substrates, both of these models were taken in consideration. Isolated PGCs, therefore, were either cultivated on top of, or embedded into the substrate.

First, PGCs isolated from tailbud stage embryos were cultivated in the presence of extracellular matrix (ECM) that contained mainly laminin, collagen type IV, heparan sulfate proteoglycan and entactin. Cells were either premixed with ECM, or applied on top of the polymerized substrate. Homogenized dorsal extract was added in the pocket made in the agarose gel on one side of the culture dish (Fig. 10). Cells were cultivated up to 24 hours.

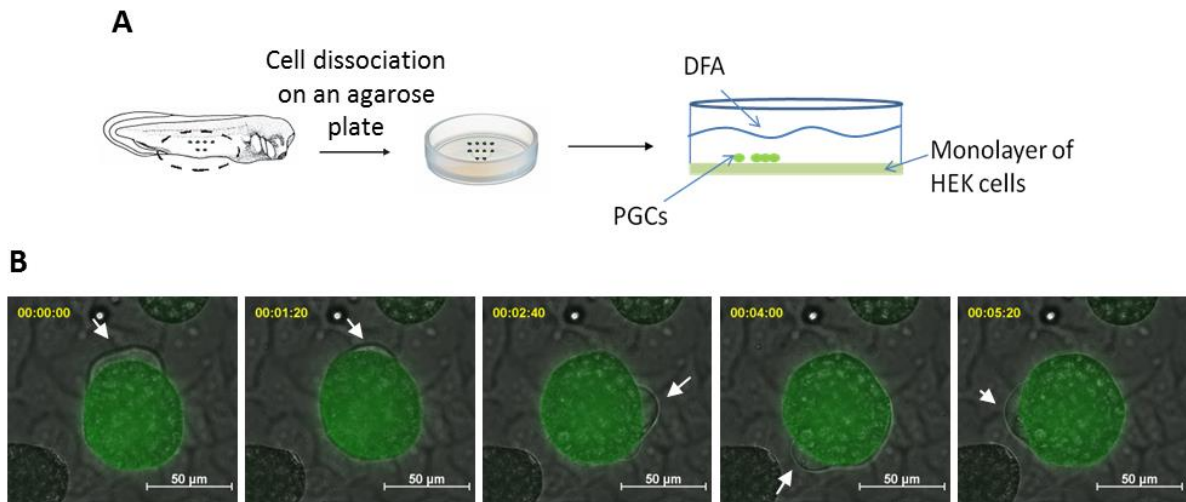


**Fig. 9. Isolated PGCs cultivated on mammalian cell substrate formed bleb-like protrusions, but did not exhibit migratory behavior.** (A) Ventral explants were dissected from tailbud stage embryos injected with *GFP\_DELE* mRNA to label PGCs. Explants were dissociated via enzymatic treatment. Isolated PGCs (green) were seeded on top of a monolayer of a mammalian cell line, HEK 293, and cultivated in DFA buffer up to 24 hours. (B) Representative time-lapse images of a PGC (GFP-positive, green) recorded approximately 1 hour after the cells were seeded on the surface of mammalian cells. PGC formed bleb-like protrusions (white arrows), but did not reveal high cellular dynamics and did not initiate migration. Merged images are generated from UV and normal transmitted light channels. Relative time after the first recorded image (hours : minutes : seconds) is indicated in the upper left corner of the images, scale bar: 50  $\mu\text{m}$ .

Within first few hours, PGCs formed bleb-like protrusions, and some of the cells started to contract from one side in order to migrate, but could not move from their point of origin (Fig. 10C). Later, formation of protrusions and overall cellular dynamics were decreased. Cultivation in different buffer conditions, including cultivation in DFA, DMEM and 0.8x MBSH, did not show any difference in PGC behavior. Similar results were obtained upon cultivation of PGCs in the agarose gel. PGCs were either cultivated on top, or covered with the second layer of the gel (Fig. 11). Variation in the concentration of agarose in the range from 0,1 to 0,5% (m/v) did not affect the results. However, if concentration of the covering agarose gel exceeded 0,5%, PGCs got smashed.

In a similar approach, known as under-agarose migration assay (Tranquillo et al., 1988), isolated PGCs were placed on the bottom of the culture dish underneath a layer of agarose gel. In this approach, few cells could initiate migration via the bleb-associated mechanism within first several hours (Fig. 12). Later, similar to the cultivation in the other tested conditions, PGCs decreased formation of the bleb-like protrusions and were unable to migrate. Application of homogenized dorsal extract did not lead to an increased motility of the cells. Although in this assay many PGCs showed migratory behavior, characterized by elongated shape and polarized waves of the cell body contraction, only few cells could initiate active migration. This can be explained by the 'stickiness' of the plastic surface of the culture dish that 'anchored' the cells and prevented translocation of the cell body. To improve efficiency of migration, culture dishes were coated with either fibronectin, or bovine serum albumin (BSA). Coating with fibronectin did not alter the efficiency of

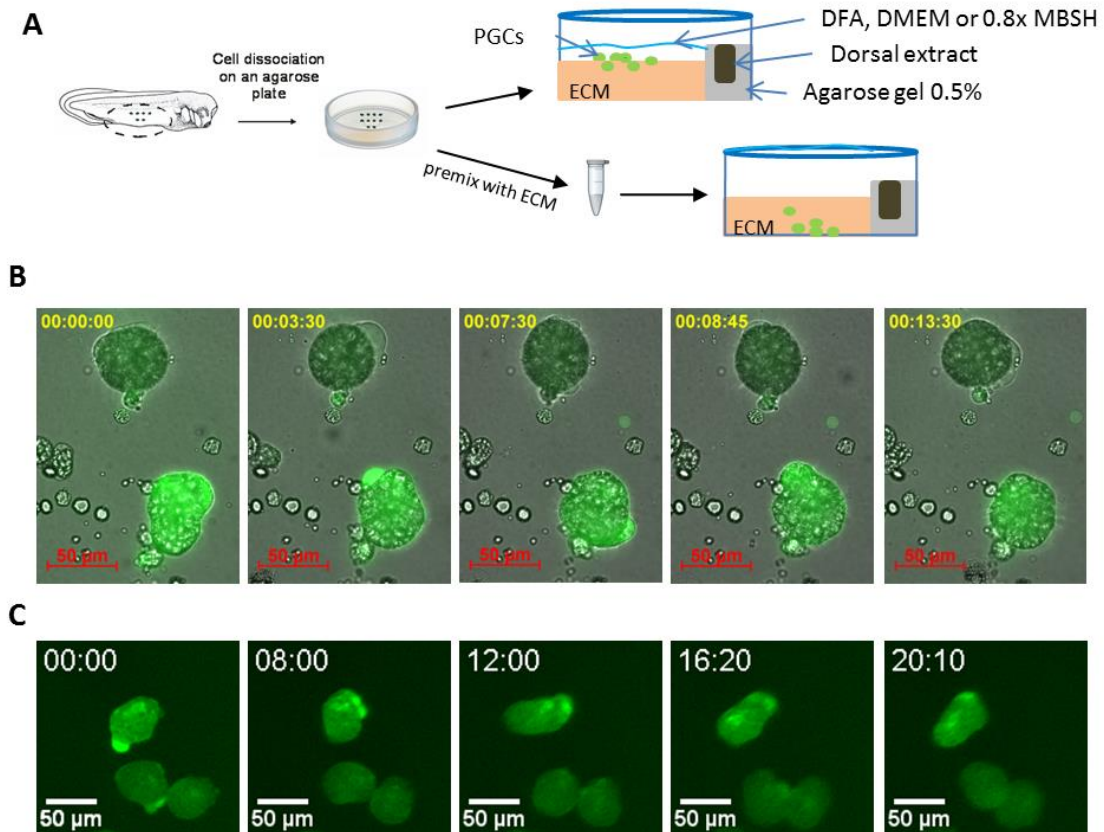


**Fig. 10. Isolated PGCs cultivated in extracellular matrix had high cellular dynamics, but did not initiate active migration.** (A) Ventral explants were dissected from tailbud stage embryos injected with *GFP\_DELE* mRNA to label PGCs. Explants were dissociated via enzymatic treatment. Isolated cells were either transferred on top of polymerized extracellular matrix (ECM), or premixed with ECM prior to polymerization. One sector of the culture dish was covered with 0,5% (m/v) agarose. Dorsal extract was added in a pocket made in the agarose gel to induce polarization of PGCs. Cells were cultivated in DFA, DMEM or 0.8x MBSH buffer conditions. (B) Representative time-lapse images of two PGCs (GFP-positive, green) cultivated on top of ECM. Images were recorded approximately 30 minutes after cell seeding. Cells formed bleb-like protrusions and had high cellular dynamics, but did not initiate migration. Merged images are generated from UV and normal transmitted light channels. Relative time after the first recorded image (hours : minutes : seconds) is indicated in the upper left corner of the images; scale bar – 50 μm; agarose gel with dorsal extract is towards upper side (C) Representative fluorescent time-lapse images of PGCs (GFP-positive, green) imbedded in the ECM. Despite high cellular dynamics, cells failed to initiate migration. Cells were cultivated up to 24 hours, but after several hours of cultivation cellular dynamics and formation of bleb-like protrusions were significantly decreased. Relative time after the first recorded image (minutes : seconds) is indicated in the upper left corner of the images; scale bar – 50 μm; agarose gel with dorsal extract is towards upper side .

migration, while on BSA-coated culture dishes migration was increased from 1-2 cells per experiment to almost 10% of the analyzed PGCs (Fig. 16A).

### 3.1.3 Bleb-associated motility of PGCs in the under-agarose migration assay

In the assay described above, BSA prevents nonspecific binding of the cells to the plastic surface of the Petri dish, while an agarose gel creates a second resistant surface. Migration of PGCs in this assay suggests that they do not require specific cell-cell or extracellular matrix adhesion for motility. This is very much in line with the assumptions of the second model of bleb-associated motility that suggests the traction force for cell



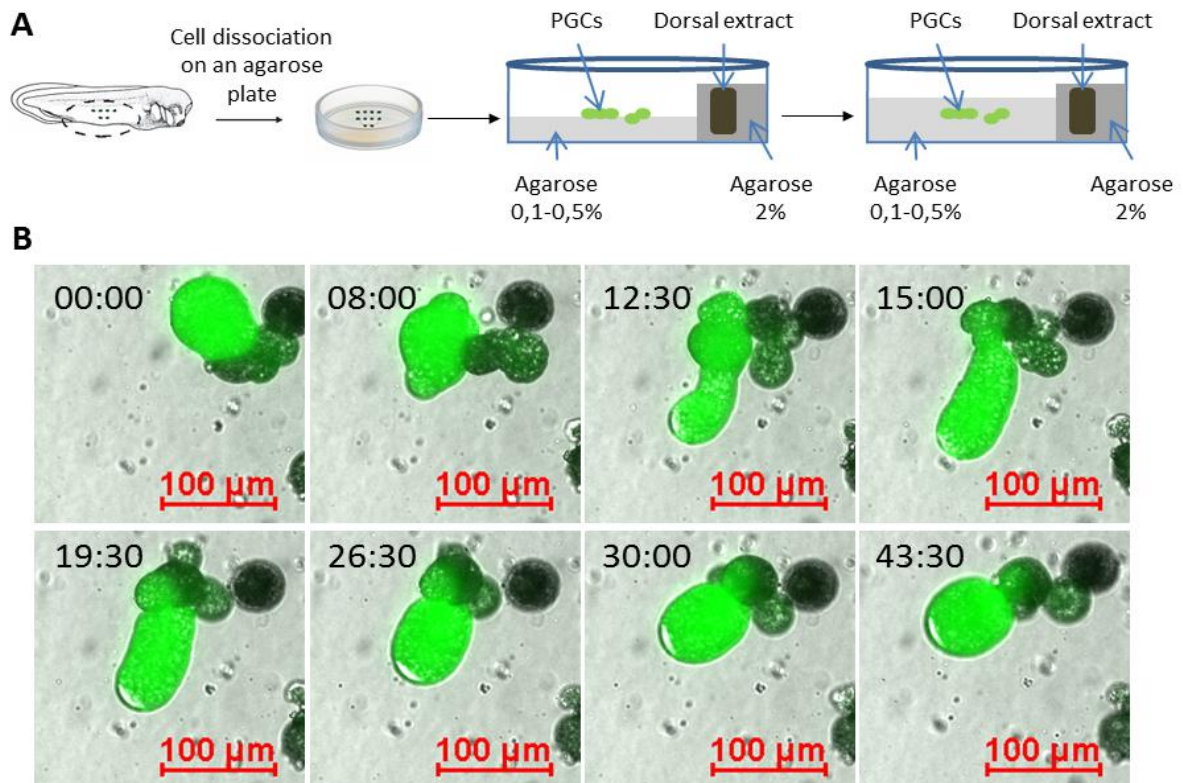


**Fig. 11. PGCs embedded in the agarose gel showed migratory behavior, but could not initiate migration.** (A) Ventral explants were dissected from tailbud stage embryos injected with *GFP\_DELE* mRNA to label PGCs. Explants were dissociated via enzymatic treatment. Isolated PGCs (green) were transferred on top of a polymerized 0,1-0,5% (m/v) agarose gel and coated with another layer of the gel. One sector of the culture dish was covered with 2% (m/v) agarose. Dorsal extract was added in a pocket made in the 2% agarose gel to induce polarization of PGCs. (B) Representative time-lapse images of a PGC (GFP-positive, green) recorded after approximately 20 minutes of cultivation. Cultivated PGCs had high cellular dynamics and exhibited migratory-like behavior, but could not initiate migration. After several hours of cultivation cells obtained stationary round morphology. Merged images are generated from UV and normal transmitted light channels. Relative time after the first recorded image (minutes : seconds) is indicated in the upper left corner of the images; scale bar: 100  $\mu\text{m}$ ; agarose gel with dorsal extract is towards upper side .

migration to be independent of specific adhesion (Charras and Paluch, 2008; Fig. 5). Moreover, when migrating PGCs get into contact with another cell, new interactions form that 'anchor' PGCs and prevent them from moving despite persisting cellular dynamics to resume or start migration (Fig. 13).

In contrast to the migration via lamellipodia, cells migrating via a bleb-associated mechanism do not exhibit constant actin polymerization at the leading edge (Charras and Paluch, 2008; Fackler and Grosse, 2008). To investigate actin filament distribution in migrating *X. laevis* PGCs, cells were isolated from tailbud stage embryos injected at 2-cell stage with chimeric mRNA *LifeAct-GFP\_DELE*, consisting of actin sensor, LifeAct, fused to GFP ORF and Dead end LE. As described in section 3.3.2, in non-migrating PGCs actin cortex reassembles on the plasma membrane of the bleb, which is followed by the retraction of the protrusion. In PGCs that initiate active migration, re-polymerization of the actin filaments was not observed and retraction of the bleb-like protrusions did not occur. Instead, during *in*

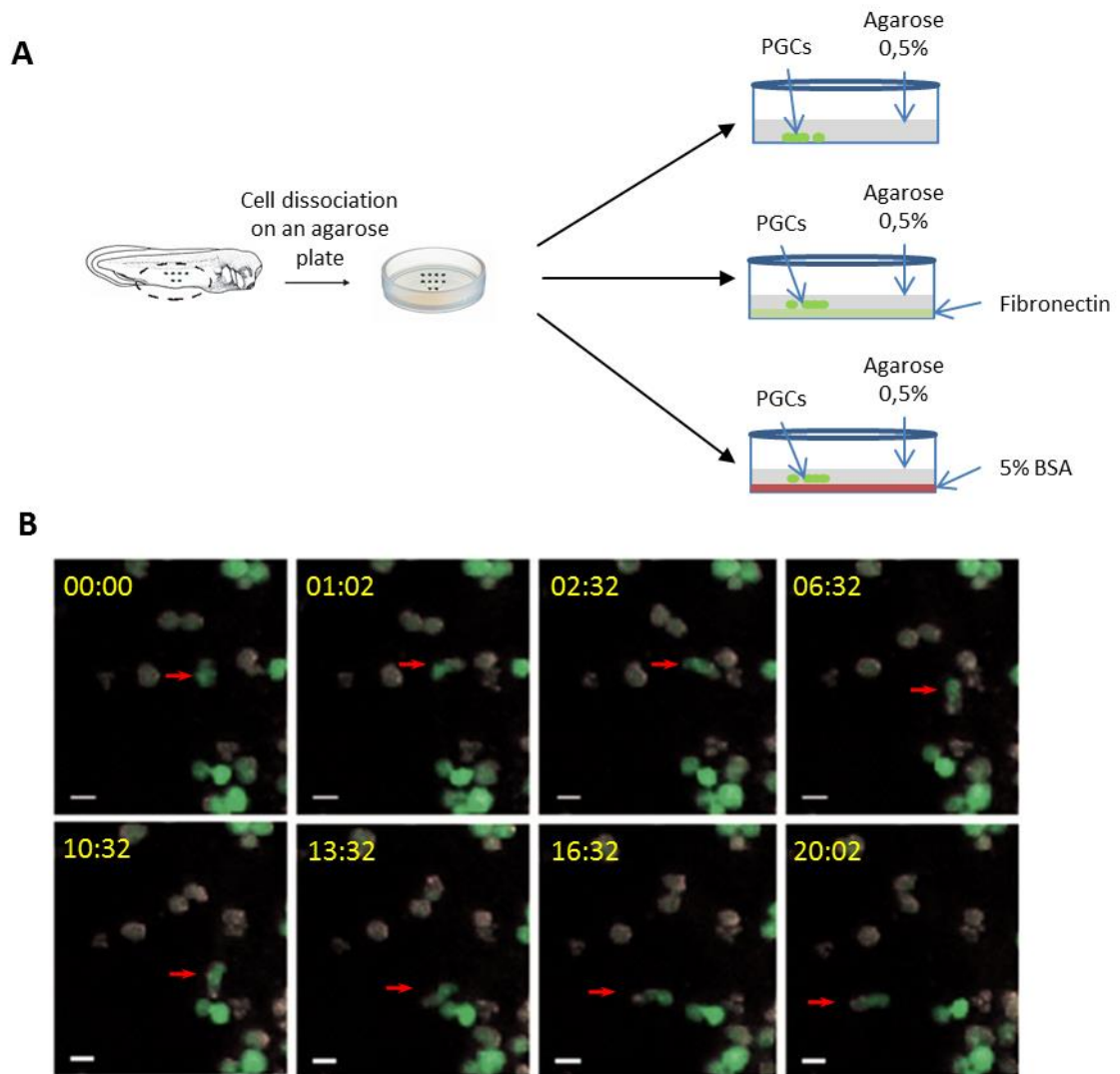


**Fig. 12. *X. laevis* PGC can migrate *in vitro* in the under-agarose migration.** (A) Ventral explants were dissected from tailbud stage embryos injected with *GFP\_DELE* mRNA to label PGCs. Explants were dissociated via enzymatic treatment. Dissociated cells, including PGCs (green), were transferred between 0.5% (m/v) polymerized agarose gel and the bottom of a Petri dish. Prior to addition of agarose gel, in some experiments, the Petri dish was pre-coated with fibronectin or 5% (m/v) bovine serum albumin (BSA). (B) Time-lapse images of an under-agarose migration assay with a BSA-coated Petri dish. PGCs can be identified as GFP-positive (green) in contrast to the GFP-negative somatic cells. Red arrows indicate migrating PGC. Merged images are generated from UV and normal transmitted light channels. Relative time after the first recorded image (minutes : seconds) is indicated in the upper left corner of the images, scale bar: 20  $\mu\text{m}$ .

*in vitro* PGC migration in the under-agarose assay, actin filaments were enriched in the rear and the sides of the cell, but not in the leading edge (Fig 14). This confirms that *X. laevis* PGCs migrate via bleb-associated amoeboid movement and not via lamellipodia-based actin-dependent mechanism.

Previous results from our lab showed that phosphatidylinositol (3,4,5)-trisphosphate (PIP3) is enriched in the bleb-like protrusions formed by isolated PGCs. Interference with endogenous PIP3 levels led to a decrease or absence of cell blebbing. It also resulted in the mislocalization during migration and loss of PGCs *in vivo* (Tarbashevich 2007; Tarbashevich

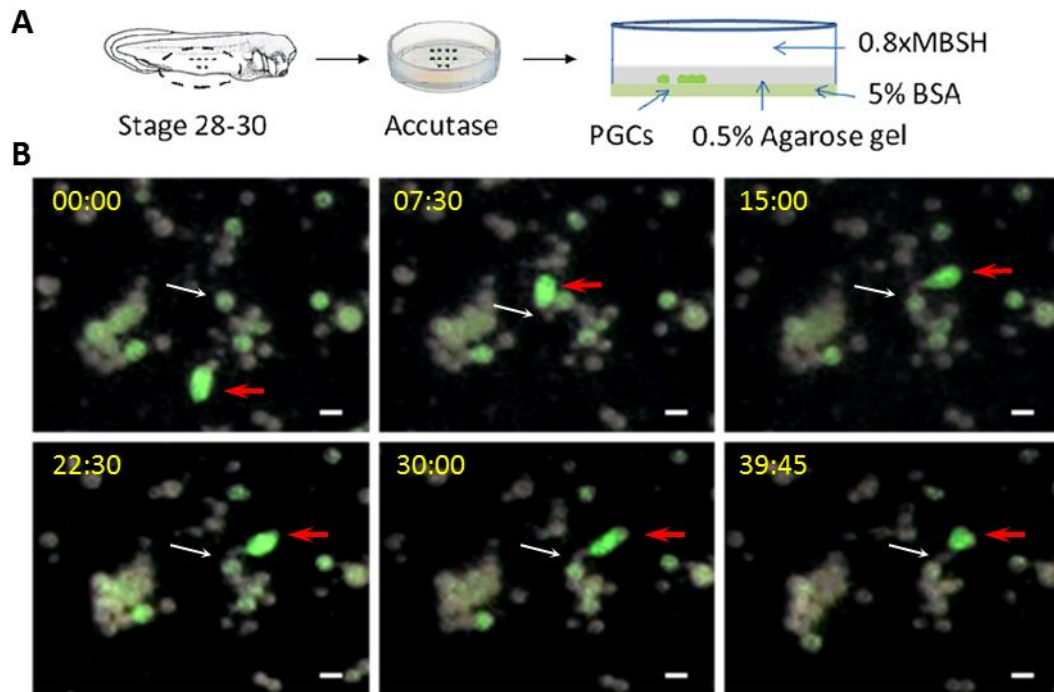


**Fig. 13. Surrounding cells can ‘anchor’ PGCs and prevent their migration *in vitro* in the under-agarose migration.** (A) Ventral explants were dissected from tailbud stage embryos injected with *GFP\_DELE* mRNA to label PGCs. Explants were dissociated via enzymatic treatment. Dissociated cells, including PGCs (green), were transferred between 0.5% (m/v) polymerized agarose gel and a 5% BSA-coated Petri dish in 0.8x MBSH buffer. (B) Time-lapse images of an under-agarose migration assay depicting an anchoring of migrating PGC (red arrow) by another cell (white arrow). Merged images are generated from UV and normal transmitted light channels. Relative time after the first recorded image (minutes : seconds) is indicated in the upper left corner of the images, scale bar: 20  $\mu\text{m}$ .

et al., 2011). To visualize PIP3 distribution in migrating PGCs, cells were isolated from the embryos injected with chimeric mRNA *GFP\_GRPI\_PH\_DELE*, consisting of pleckstrin homology (PH) domain of GRPI protein, used as a PIP3 sensor, fused to GFP ORF and Dead end LE. As a control, *GFP\_GRPI\_PH\_DELE*-injected embryos were also co-injected with mRNA encoding membrane red fluorescent protein (mRFP) to visualize cell membrane. Distribution of mRFP served as a control to monitor the intracellular distribution of PIP3. Although PIP3 was enriched in the protrusions formed by non-migrating cells, no specific enrichment was observed during active migration (Fig. 15). This suggests that PIP3 enrichment in the bleb-like protrusions is required for polarization, but is not maintained during PGC migration.

### 3.2 PGCs isolated form neurula stage can migrate in the under-agarose migration assay, but migration efficiency is increased at the tailbud stage

Active migration of *X. laevis* PGCs *in vivo* starts at stage 24 of embryonic development (Nishiumi et al., 2005; Terayama et al., 2013; discussed in chapter 1.2.5). The under-agarose migration assay described above was used to test *in vitro* migratory abilities of PGCs isolated from neurula stage embryos (developmental stage 17-19) compared to PGCs isolated from tailbud stage embryos (developmental stage 28-30) (Fig. 7). Time-lapse microscopy was used to monitor the behavior of PGCs. For quantification, PGCs were assigned to one of three

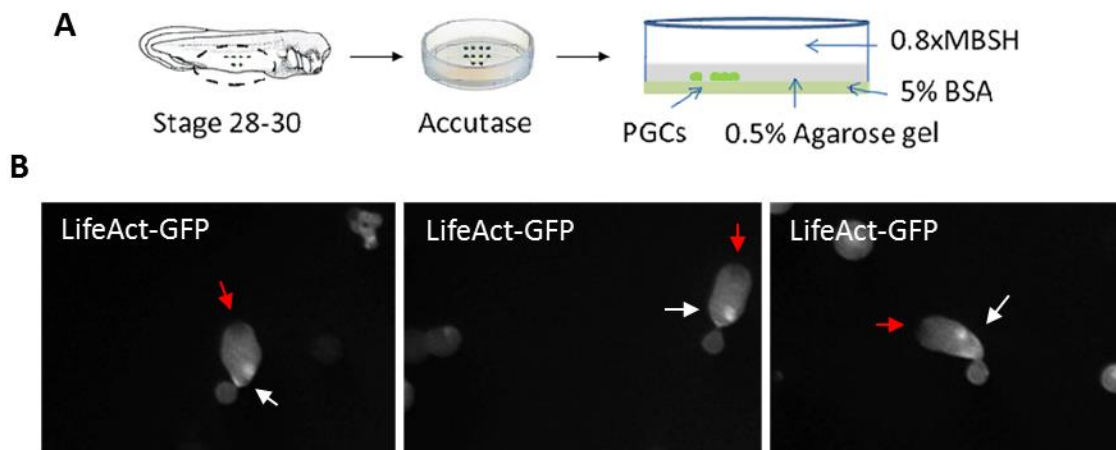


**Fig. 14. Actin is not enriched in the leading edge of *X. laevis* PGCs during their migration *in vitro*.** (A) Ventral explants were dissected from tailbud stage embryos injected with LifeAct-GFP<sub>DELE</sub> mRNA to visualize actin distribution in PGCs. Explants were dissociated via enzymatic treatment. Dissociated cells, including PGCs (green), were transferred between 0.5% (m/v) polymerized agarose gel and a 5% BSA-coated Petri dish in 0.8x MBSH buffer. (B) Representative fluorescent time-lapse images of an under-agarose migration assay depicting migrating PGC. Actin is enriched in the rear and the sides of the cell (white arrow), but not in the leading edge (red arrow).

groups according to their morphology. The first group consisted of non-migratory cells, spherical shaped and with random bleb-like protrusions formed. In the second group, termed migrating PGCs, cells were polarized, had an elongated shape, showed high cellular dynamics resembling waves of cell body contraction, and could migrate via a bleb-associated mechanism. PGCs assigned to the third group, termed migratory PGCs, had morphology similar to the migrating PGCs, but failed to translocate the cell body. These cells also acquired an elongated polarized morphology and showed high cellular dynamics, but could not migrate, for example, due to an ‘anchoring’ by surrounding cells.

Approximately half of the PGCs isolated from tailbud stage embryos showed migratory behavior, and about 10% of the total cells population could actively migrate in the under-agarose migration assay (Fig. 16A). Although most of the PGCs (about 80%) from the neurula stage had a non-polarized morphology, some of the PGCs also showed migratory behavior, and even could initiate migration. To test for the possible differences in the migration of PGCs isolated from neurula and tailbud stages, tracking analysis of PGC migration was performed (Fig. 16B-E). Since no gradient was applied to the system, migration of both groups of PGCs occurred in random directions. During migration, cells alternated between trembling at one position and active migration phases (Fig. 16B, C). No differences in morphology of the cells, as well as in mean and maximum velocity or traveled distance were observed (Fig. 16D, E). This suggests that already at the neurula stage PGCs can perform active migration, but they do so more avidly at the tailbud stage.

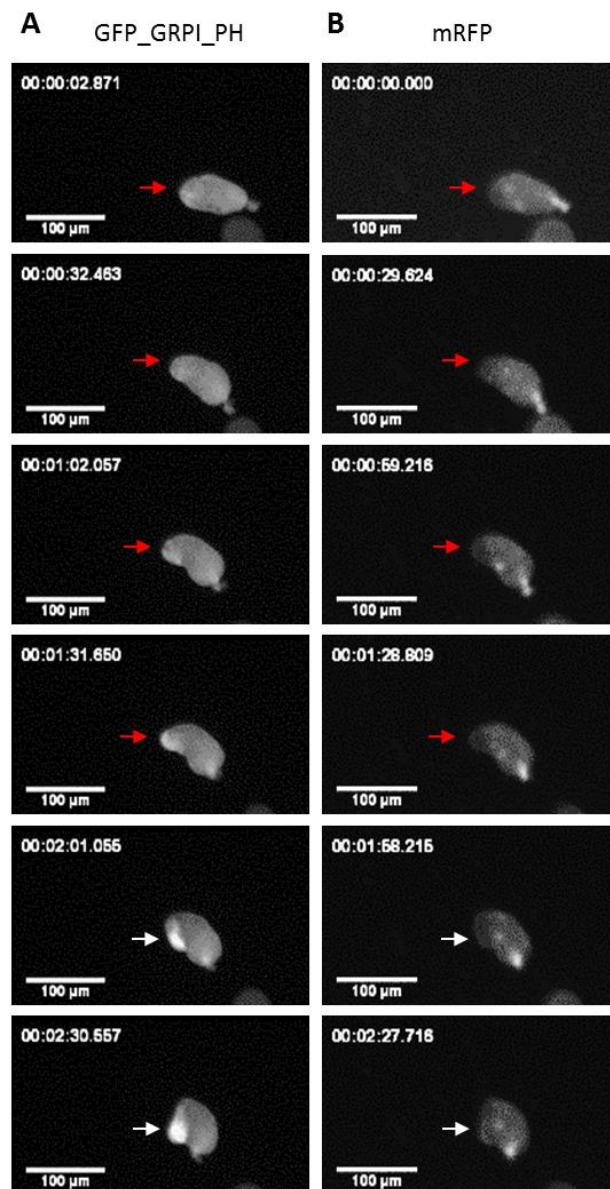


**Fig. 15. PIP3 enrichment is not observed in the leading edge of PGCs migrating *in vitro*.** Representative time-lapse images of a PGC in the under-agarose migration assay, isolated from the embryos injected with *GFP\_GRPI\_PH\_DELE*, and co-injected with *mRFP ORF* mRNAs. Membrane RFP (mRFP) was used to visualize plasma membrane, while pleckstrin homology (PH) domain of GRPI protein fused to GFP (*GFP\_GRPI\_PH*) serves as a sensor for PIP3 distribution. Images in column (A) correspond to fluorescent signal coming from *GFP\_GRPI\_PH*. It was equally distributed in the migrating PGCs (red arrows indicate the leading edge), but was enriched in the large bleb-like protrusions formed by the cell when it ceased the migration (white arrow). Images in the panel (B) show distribution of mRFP and were taken at the same time as corresponding images from panel (A). Some enrichment of mRFP can be observed in the rear of the cell, but, in contrast to *GFP\_GRPI\_PH*, no difference in the enrichment at the leading edge was present. Relative time after the first recorded image (minutes : seconds) is indicated in the upper left corner of all images, scale bar: 100  $\mu\text{m}$ .

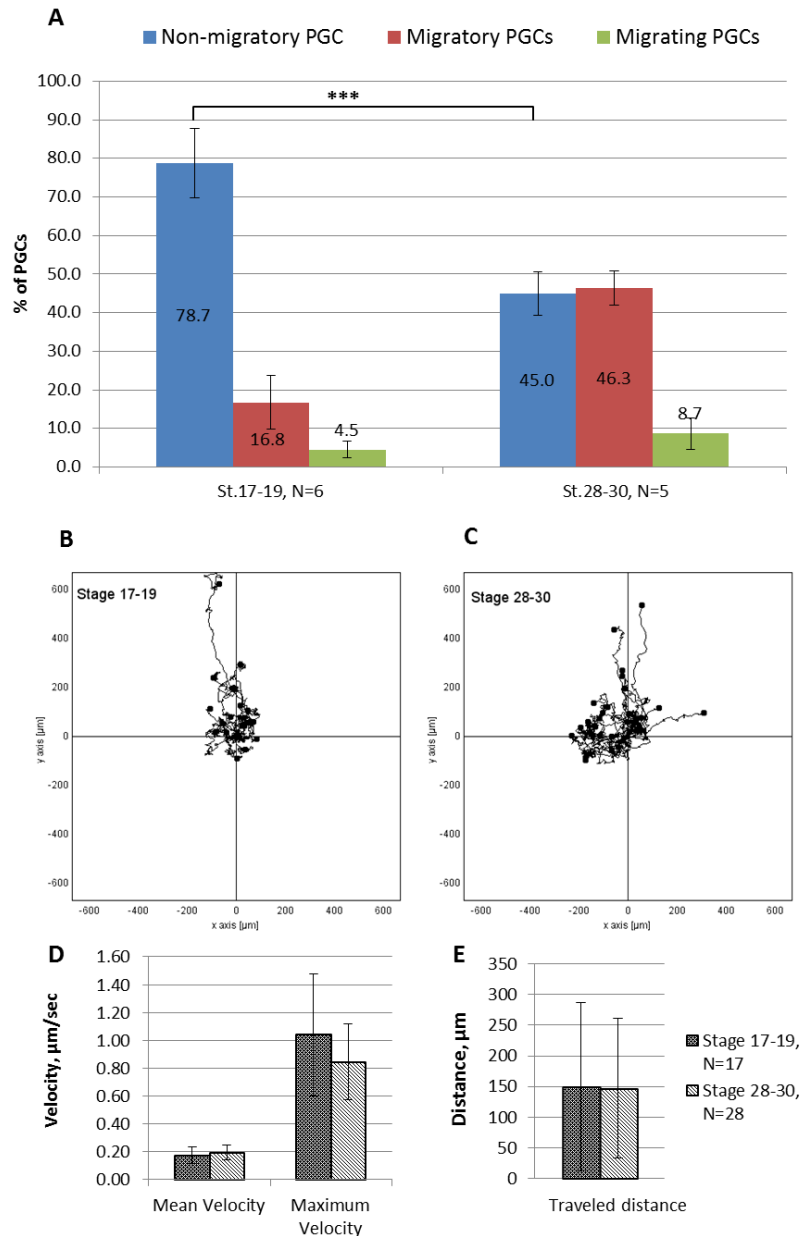


**Fig. 16. Motility of PGCs isolated from the tailbud stage embryos is increased in comparison to the neurula stage.** The time-lapse microscopy was used to monitor the behavior of PGCs in the under-agarose migration assay. Cells were isolated from neurula (St.17-19), or tailbud (St.28-30) embryos. (A) Depending on the migratory behavior, PGCs were assigned to one of three groups. Round non-migrating cells were termed as ‘Non-migratory PGCs’; cells which had high cellular dynamics and elongated shape, but could not initiate migration, were termed as ‘Migratory PGCs’; finally, the cells that migrated via bleb-associated mechanism were termed ‘Migrating PGCs’. Relative amount of the three morphological groups in the total amount of PGCs was calculated for each experiment. *N* – number of experiments. Error bars represent standard deviation. \*\*\*-  $p < 0.001$ . Tacking analysis of migrating PGCs was performed (B, C) Plotted migratory paths of PGCs isolated from neurula (St.17-19, B) and tailbud (St.28-30, C) stages. Since no gradient was applied during migration of the cells in the under-agarose migration assay, directionality of migration is plotted randomly. Black dots represent individual cells. Scale in y and x axis is given in  $\mu\text{m}$ . Diagrams (D, E) represent mean and maximum velocity of the cells (D), as well as distance travelled by migrating PGCs from the start (E). Error bars represent standard deviation, *N* – number of analysed cells.

### 3.3 PGCs isolated from tailbud stage *Xenopus laevis* embryos show higher plasma membrane dynamics in comparison to neurula stage due to increased formation of bleb-like protrusions

At tailbud stage of development, primordial germ cells actively migrate in *X. laevis* embryos within the endoderm (see section 1.2.5). Previous findings from our lab (Tarbashevich et al., 2011), as well as recently published results by Terayama et al. (2013), showed that PGCs, isolated from tailbud stage embryos, form bleb-like protrusions and can migrate *in vitro* via a bleb-associated mechanism (see section 1.4.2). In many migratory cells, including PGCs in *Drosophila*, zebrafish and mouse, increased formation of cellular protrusions and high cellular dynamics are coupled to the initiation of active migration (reviewed in section 1.3). To analyse whether these events also take place during the transition of *X. laevis* PGCs to the active migration, cellular dynamics of the pre-migratory cells isolated from neurula stage embryos (stage 17-19) was compared to the migratory cells isolated from tailbud stage embryos (stage 28-30). PGCs were labelled by vegetal injection of chimeric mRNA *GFP\_DELE* and isolated by the dissociation of dissected endodermal explant. (Fig 7). To quantify cellular dynamics of pre-migratory and migratory PGCs, Electric Cell-substrate Impedance Sensing (ECIS) (Wegener et al., 2000), in conjunction with time-lapse image analysis, was performed.

#### 3.3.1 Analysis of cellular dynamics by electric cell-substrate impedance sensing

For the ECIS measurements, single cells from the dissociated explant were manually isolated and transferred on top of the small electrode (Fig. 17A). Changes in the fluctuation amplitude of the detected impedance signal reflect the movement of the cell on the electrode including bleb formation and retraction. This movement is commonly referred to as micromotion. The uncovered electrode, as a negative control, was used for the normalization. In comparison to the pre-migratory cells isolated from neurula stage (stage 17-19), the amplitude of fluctuation was increased in case of migratory PGCs, isolated from tailbud stage embryos (stage 28-30) (Fig. 17B, C). This is reflected in variance values being about 1.8-fold higher. Upon addition of Cytochalasin B, an actin-depolymerizing agent and consequently an inhibitor of cellular motility, a strong decline in the impedance noise was detectable, finally reaching values comparable to those of an uncovered electrode. This confirms that the observed fluctuations and differences in the amplitude were associated with increased cellular dynamics. In addition, in contrast to PGCs, somatic endodermal cells isolated from both neurula and tailbud stages did not cause any significant fluctuations, and the values were similar to the uncovered electrode (Fig. 17C). Besides changes in fluctuation amplitude captured by the variance, correlation analysis (DFA: detrended fluctuation analysis) reveals a considerable shift to higher time correlation (long memory) in case of PGCs at migratory stage. Long memory is mirrored in the so called Hurst coefficient that amounts up to 0.7 in the case of migratory PGCs while PGCs isolated from neurula stage display only a value of 0.2. Hurst coefficient in the range between 0.5 and 1 mean that a high value in the series will probably be followed by another high value (or vice versa) and that

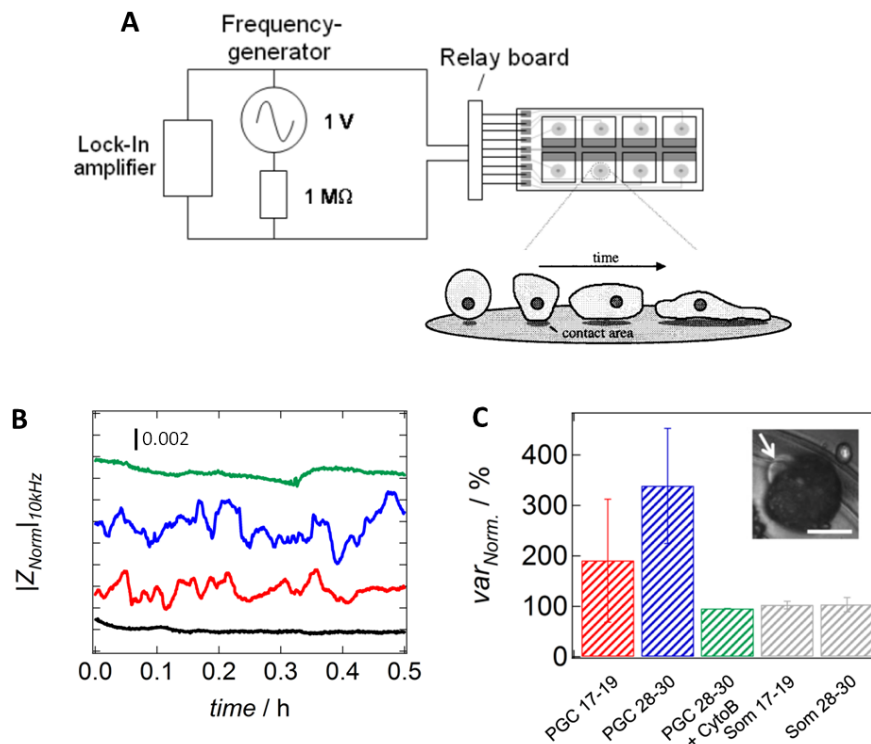


**Fig. 17. PGCs isolated from tailbud stage embryos show high cellular motility.** (A) Schematic representation of experimental setup for Electric cell-substrate impedance sensing (ECIS) measurements. Cells are seeded on the surface of small and planar gold-film electrodes that are deposited on the bottom of a cell culture well. The AC impedance of the cell-covered electrode is then measured at one or several frequencies as a function of time. Due to the insulating properties of their membranes, the cells behave like dielectric particles in away that with increasing coverage of the electrode increases impedance. If cell shape changes occur, the current pathways through and around the cell bodies change as well, leading to a corresponding increase or decrease of impedance (modified from Wegener et al., 2000). (B) Time-resolved, normalized and detrended impedance data of an uncovered electrode (*black line*), a single pre-migratory primordial germ cell (PGC stage 17-19, *red line*), a single migratory primordial germ cell (PGC stage 28-30, *blue line*) and a migratory primordial germ cell treated with 100 μM cytochalasin B (PGC stage 28-30, *green line*). All measurements were recorded at an excitation frequency of 10 kHz. The curves are arbitrarily shifted in the y-direction for better visibility. (C) Calculated variances obtained from time-resolved impedance data (B) for single pre-migratory primordial germ cell (PGC stage 17-19,  $N = 5$ , *red*), single migratory primordial germ cell (PGC stage 28-30,  $N = 3$ , *blue*) and single migratory primordial germ cell treated with 100 μM cytochalasin B (PGC stage 28-30, *green*). Additionally, normalized variances of somatic endodermal cells from both stages of embryonic development (stage 17-19 and stage 28-30, both with  $N = 3$ ) are shown in grey. Values are given in percentages and normalized to the variance of the time-trace of an uncovered electrode (100%).  $N$  depicts the number of investigated cells per category. Error bars represent standard deviation. Inlay: single migratory PGC (stage 28-30) showing a strong formation of blebs (indicated by white arrow). Scale bar: 20 μm. All measurements, data analysis and preparation of images were done in collaboration with D. Schneider.

this correlation will be maintained in the future. Hurst coefficient in the range between 0 and 0.5 mean that in a time series values tend to switch sign, for example high value will be most probably followed by a low value, but the next one will be high again. This correlation also lasts a long time into the future. For comparison, Brownian motion would show a Hurst coefficient of 0.5 (Peng et al., 1994; Schneider et al., 2011).



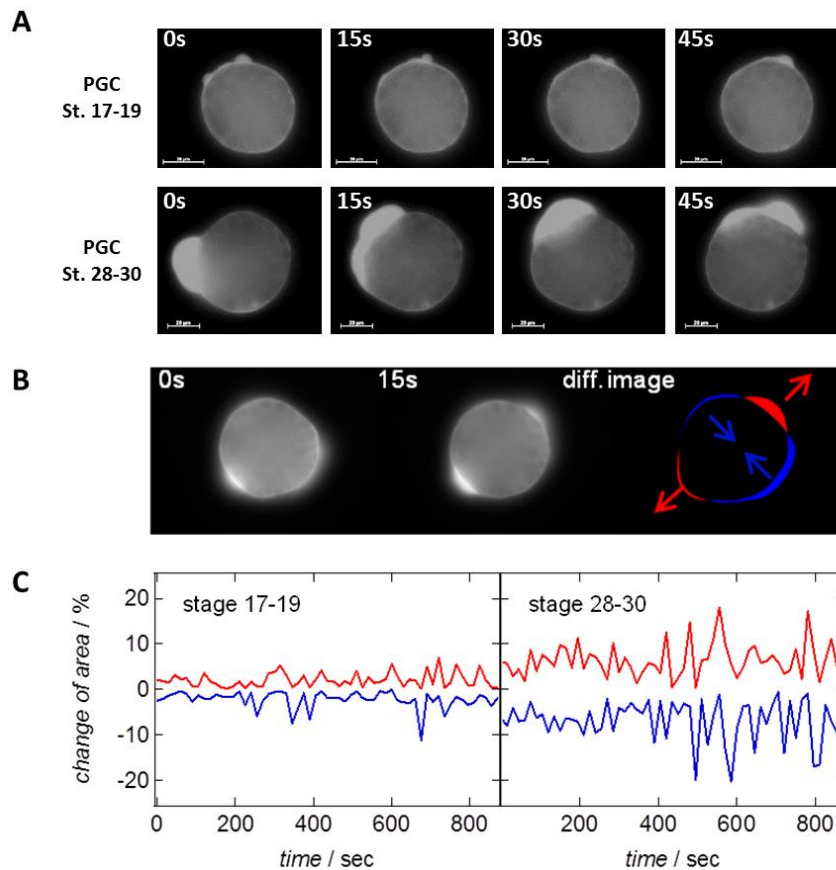


**Fig. 18. High cellular dynamics of PGCs isolated from tailbud stage embryos correlates with increased cell blebbing.** (A) Time-lapse fluorescence images of GFP-labeled pre-migratory (St. 17-19) and migratory (St. 28-30) PGCs were taken with a time interval of 15s. Cells isolated from both developmental stages showed formation of bleb-like protrusions. Scale bar: 20  $\mu\text{m}$ . (B) Subtracting two successive images from each other results in a difference image showing the expanding (red) and contracting (blue) regions of the cell over time. Arrows underscore the direction of expansion/contraction. (C) Time traces of the contracting (blue) and expanding (red) area of PGCs from the pre-migratory (stage 17-19) and the migratory (stage 28-30). Values are normalized to the current cell area at every time point and given in percentages. Time-lapse analysis and preparation of the images was done in collaboration with D. Schneider.

### 3.3.2 Time-lapse image analysis of isolated PGCs

To better understand what causes the difference in cellular dynamics, a time-lapse image analysis of isolated PGCs was performed. PGCs from both neurula and tailbud stages formed bleb-like protrusions and showed significant shape fluctuations (Fig. 18A). Cellular dynamics was analysed as a fluctuation of the cell shape over time, including areas of plasma membrane expansion and retraction (Fig 18B, C). Calculated variances of the temporal shape fluctuations revealed a 2.4-fold increase upon onset of migration. Interestingly, areas of expansion are in most cases neighboured by contracting areas, reflecting that the overall area remains quite constant and therefore, no additional lipid material needs to be incorporated into the cellular membrane.

To confirm that protrusions formed by isolated PGCs are indeed bleb-like protrusions formed by other cell types (Charras and Paluch, 2008; Fackler and Grosse, 2008; see chapter

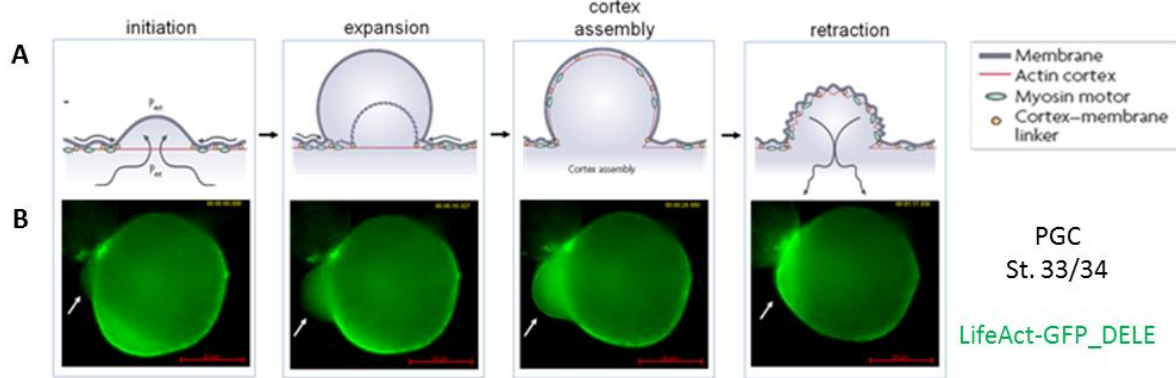


**Fig. 19. Formation and retraction of the bleb-like protrusions in isolated *X. laevis* PGCs correlates with disruption and re-polymerization of actin cortex on the plasma membrane.** (A) Actin dynamics in *X. laevis* PGCs is compared to actin distribution in bleb-like protrusions described by Charras and Paluch, 2008. (B) PGCs were isolated from tailbud stage embryos (St. 33/34), which were injected with *in vitro* transcribed *LifeAct-GFP\_DELE* mRNA to visualize distribution of actin filaments. Time-lapse fluorescent images of isolated PGCs were taken to visualize distribution of actin filaments during different stages in the formation of the bleb-like protrusions (white arrow). Scale bar: 20  $\mu\text{m}$ .

1.4.2), the distribution of actin filaments in these protrusions was monitored over time. To visualize actin filaments in PGCs, cells were isolated from the embryos injected with chimeric mRNA *LifeAct-GFP\_DELE*, consisting of actin filament sensor, LifeAct, fused to GFP ORF and Dead end LE. Similar to other cell types, the actin cortex surrounds the cell periphery, but is excluded from the forming bleb-like protrusions. After bleb expansion, actin cortex reassembly on the plasma membrane of the bleb was observed, which was immediately followed by the retraction of the bleb. These events are in a good correlation with the data obtained from the other cell types (reviewed by Charras and Paluch, 2008), suggesting that increased cellular dynamics of migratory *X. laevis* PGC occurs due to the increased formation of bleb-like protrusions (Fig. 19).

In summary, both ECIS and time-lapse analysis reveal similar changes in calculated variances, underscoring that the dynamic properties of PGCs change significantly during development. In case of somatic cells, no altered cellular dynamics was detectable independent of the embryonic stage of development.

**Note:** work described in section 3.3 was done in the collaboration with Prof. A. Janshoff and D. Schneider. ECIS measurements and cellular shape analysis was done by D. Schneider. Preparation of the text and figures was done with the help of D. Schneider and A. Janshoff.

### 3.4 Adhesion of PGCs to surrounding somatic endodermal cells and fibronectin decreases at the tailbud stage of embryonic development

In addition to the increased cellular dynamics, regulation of cellular adhesion is also known to play an important role in the context of germ cell migration in different animal species (Richardson and Lehmann, 2010; see section 1.3). To find out whether cell adhesion is changed during the transition of *X. laevis* PGCs to active migration, Single-Cell Force Spectroscopy (SCFS) studies using isolated cells were performed. SCFS is a modification of

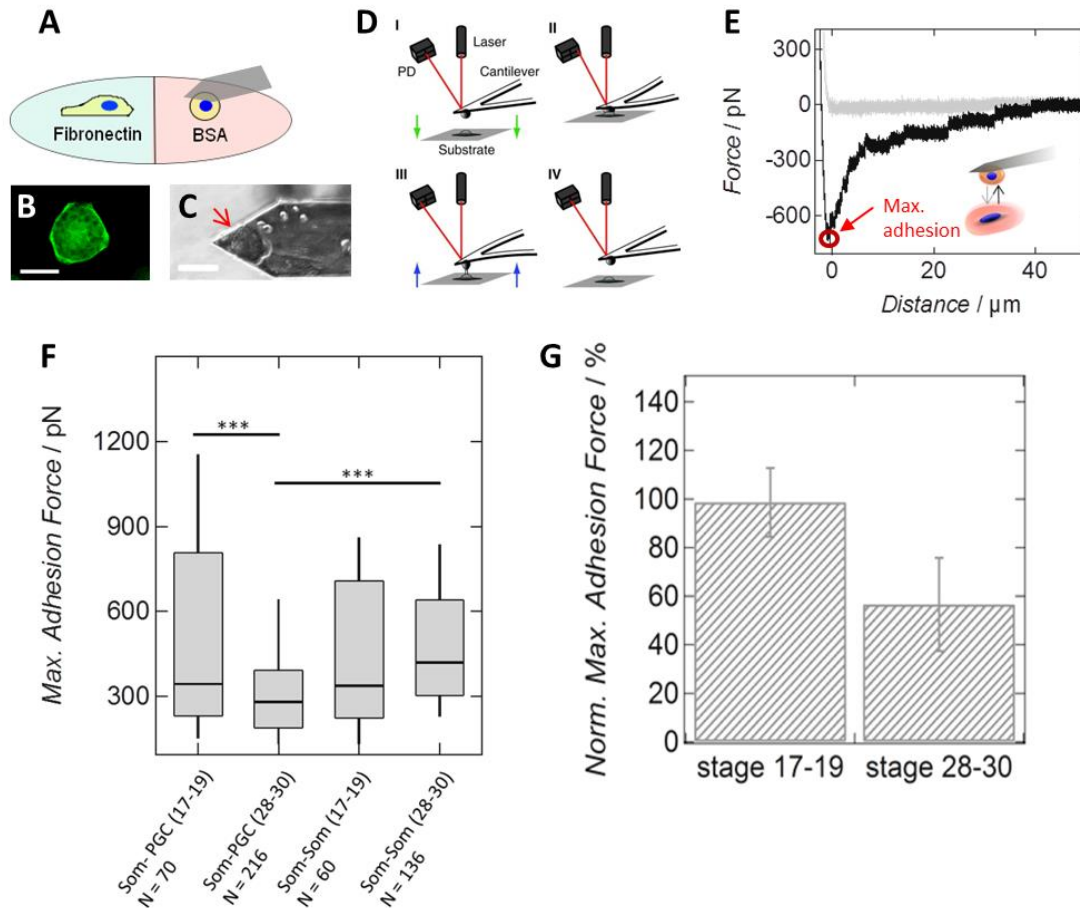


**Fig. 20. PGCs reduce overall cell-cell adhesion activity after transition to the active migration state.** (A) Cells were isolated from *GFP\_DELE* mRNA-injected embryos and transferred to the Petri dish, half coated with fibronectin (blue) and half coated with bovine serum albumin (BSA, pink). Weakly adhering cells from BSA-coated region were attached to an atomic force microscope cantilever. Subsequently, the attached cell was brought into contact with a cell spread on the fibronectin-coated part of the Petri dish. (B) Fluorescence image of a labeled primordial germ cell spread on a fibronectin-coated Petri dish. (C) Bright-field image of a migratory PGC attached to a poly-D-lysine coated cantilever. Scale bars: 50  $\mu\text{m}$ . (D) During single-cell force spectroscopy (SCFS) measurements, the cell and the substrate are brought into contact. The position on a photodiode (PD) of a laser beam (red line) that is reflected off the back of the cantilever measures the deflection of the cantilever and thus the force that acts on the cantilever. During the approach (denoted by green arrows), the cell (probe) is pressed onto the substrate (I-II). After 30 seconds of contact time, the cell is retracted from the substrate (III, marked by blue arrows) until cantilever reaches initial position (IV), and a force-distance curve is recorded (Helenius et al., 2008). (E) Example of a force-distance curve of two somatic cells from the same developmental stage. The approach curve (grey), as well as the retraction curve (black) are shown. (F) Maximum adhesion force either between PGCs and somatic endodermal cells (PGC-Som) or between two somatic endodermal cells (Som-Som) isolated from embryos at stages 17-19 (pre-migratory PGCs) or stages 28-30 (migratory PGCs). N corresponds to the number of curves that have been analyzed per category. \*\*\* corresponds to p-values < 0.001 (Wilcoxon rank sum test). The number in brackets describes the stage of PGC development: 17-19 for pre-migratory PGCs and 28-30 for migratory PGCs. (F) Mean maximum adhesion force of either pre-migratory (stage 17-19,  $N = 4$ ) or migratory (stage 28-30,  $N = 7$ ) PGCs after contact with a somatic cell from the corresponding stage. For each PGC-somatic cell interaction, values are normalized to the interaction between the same somatic cell and a second somatic cell. All measurements, data analysis and preparation of images were done in collaboration with D. Schneider.

Atomic Force Microscopy (AFM). In AFM, a laser beam is applied on top of a small elastic cantilever and is reflected to a photodetector. Fluctuations of the cantilever can be detected by a change in the reflection of the beam. For SCFS studies, a single cell can be attached to the cantilever and used as a probe to measure the interaction force with another cell or substrate. The attached cell is brought into contact with a substrate, followed by a retraction of the attached cell. During the retraction, the deflection of the cantilever correlates with the level of the adhesion forces generated between attached cell and the substrate (Helenius et al., 2008) (Fig. 20D).

#### **3.4.1 Measurement of cell-cell adhesion forces**

Isolated PGCs and somatic endodermal cell from neurula (stage 17-19) and tailbud stages (stage 28-30) were used for SCFS measurements. As described in previous section, cells were isolated from *GFP\_DELE* mRNA-injected embryos to distinguish between GFP-negative somatic endodermal cells and GFP-positive PGCs. By using single-cell force spectroscopy, interactions of PGCs with either somatic endodermal cells or with extracellular matrix components were quantified. As a measure of dynamic strength, force-distance curves were recorded and the maximum adhesion force upon retraction of the cantilever was determined (Fig 20E).

Interaction forces between migratory PGCs and somatic cells isolated from tailbud stage were significantly decreased, as compared to the interactions of PGCs and somatic cells earlier in development (Fig 20F). By normalizing the maximum adhesion force recorded during interaction of a PGC with a somatic cell to the maximum adhesion force obtained during attachment of the same somatic cell with a second somatic one, the effect becomes even more obvious (Fig 20G). This way of representing data was chosen to avoid effects that can occur due to differences between individual PGCs. These experiments reveal that PGCs reduce their adhesiveness to the surrounding somatic cells during development. Interestingly, the adhesive strength between pre-migratory PGCs and somatic cells is similar to that of somatic cells with each other. In addition, the maximum adhesion force between two somatic cells from either the early or the late stage showed no significant differences in absolute values (Fig 20F). Therefore, it seems likely that within the endodermal cell mass, alterations concerning adhesive properties are restricted to primordial germ cells.

#### **3.4.2 Measurement of cell adhesion to fibronectin and collagen I**

The influence of the extracellular matrix on PGC migration in *X. laevis* has been described for the migration of these cells in the dorsal mesentery (Heasman et al., 1981; see section 1.4.4). Previous studies also showed that PGCs at tailbud stages can interact with fibronectin (Tarbashevich et al., 2011; Terayma et al., 2013). To investigate whether changes in the adhesion to the extracellular matrix contribute to the transition of PGCs to the active migration, a quantitative study concerning the interaction strength was performed. PGCs and somatic endodermal cells were isolated from neurula (stage 17-19) and tailbud stage embryos (stage 28-30). Attachment of these cells to extracellular matrix components, collagen I and fibronectin, was investigated using single-cell force spectroscopy. Additionally,

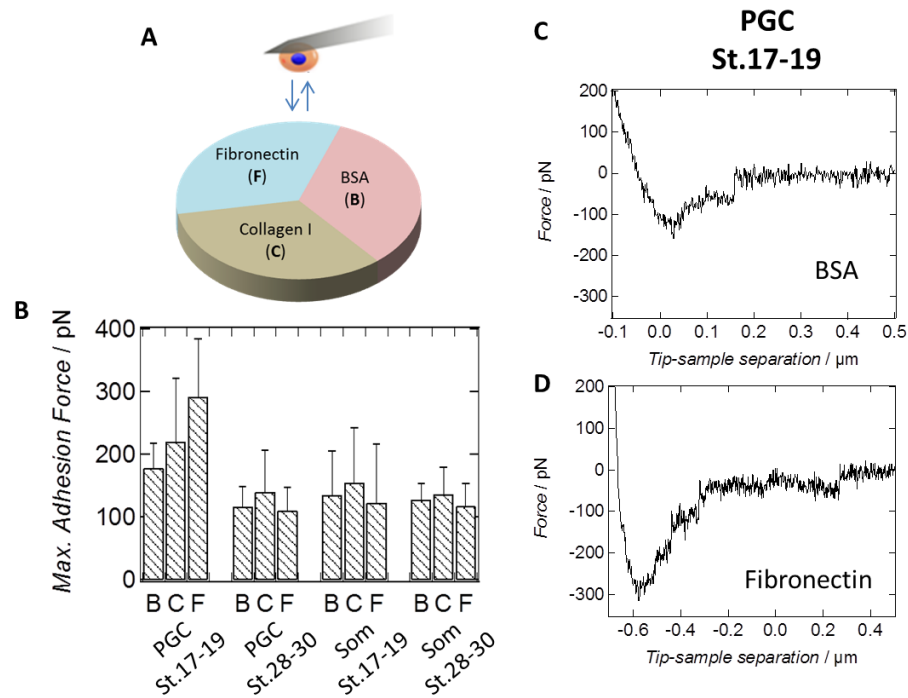


**Fig. 21. Pre-migratory PGCs show high affinity to fibronectin.** (A) Schematic drawing of a Petri dish being divided into three sectors coated either with fibronectin (blue sector), collagen I (grey sector) or bovine serum albumin (BSA, pink sector). Either PGCs or somatic cells from both neurula and tailbud stages were brought into contact with the different substrates using single-cell force spectroscopy. (B) Maximum adhesion forces of either PGCs or somatic cells (Som) isolated from *GFP\_DELE* mRNA injected embryos at developmental stage 17-19 (pre-migratory PGCs) or stage 28-30 (migratory PGCs) during interaction with BSA (B), collagen I (C) or fibronectin (F) coated surfaces. Values are obtained from AFM force-distance curves. Negative forces correspond to positive adhesion forces. (C, D) Typical AFM force-distance curves monitoring the interaction of a pre-migratory primordial germ cell with a (C) BSA-coated and a (D) fibronectin-coated part of the Petri dish. All measurements, data analysis and preparation of images were done in collaboration with D. Schneider.

application of bovine serum albumine (BSA) was used as a negative control, resulting in a saturation of nonspecific binding sites on the surface of the culture dish (Fig 21A). AFM retraction curves revealed a higher adhesiveness of early PGCs to fibronectin as compared to collagen I and BSA that is evident from higher values of the maximum adhesion force (Fig 21B). Six hours after cell seeding, pre-migratory PGCs isolated from neurala stage embryos started to adhere to the fibronectin-coated part of the Petri dish, whereas cells seeded on collagen I and BSA remained only loosely attached. Interestingly, in case of pre-migratory PGCs, values of the maximum adhesion force are generally higher than those for other cell types (Fig 21B). This finding is independent of the investigated substrate, suggesting *per se* a higher adhesiveness of primordial germ cells before their transition to the state of active migration. Pre-migratory PGCs show a nearly 3-fold stronger attachment to fibronectin than PGCs from the tailbud stage or somatic cells, as well as an almost 1.5-fold and 1.4-fold higher maximum adhesion force in case of collagen I and BSA, respectively. Assuming that the interaction between PGCs and the bovine serum albumin coated surface serves as a useful negative reference, the strength of interaction to the fibronectin-coated part of the Petri dish is about 2-fold higher for pre-migratory PGCs than for migratory PGCs. For somatic cells

and migratory PGCs, no differences in the adhesive behavior, neither to collagen I nor to fibronectin, were detectable in comparison to BSA. Furthermore, no significant increase in adhesive strength between PGCs isolated from neurula stage embryos and collagen I was detected (Fig 21B).

It can be concluded that the overall adhesiveness of pre-migratory PGCs is higher compared to PGCs within the active migratory state. Pre-migratory PGCs also show higher specific binding to fibronectin, but no specific interaction with collagen I was detected.

**Note:** work described in section 3.4 was done in the collaboration with Prof. A. Janshoff and D. Schneider. SCFS measurements and analysis was done by D. Schneider. Preparation of the text and figures was done with the help of D. Schneider and A. Janshoff.

### **3.5 Differential transcriptome analysis of PGCs and somatic endodermal cells isolated from tailbud and neurula stage embryos**

As discussed in section 1.1, zygotic transcription in PGCs is delayed in many species, including *X. laevis*. Moreover, initiation of zygotic transcription in mouse and zebrafish PGCs correlates with the initiation of the active migration within the embryo (Blaser et al., 2005; Nakamura and Seydoux, 2008). To understand the molecular basis of *X. laevis* primordial germ cell transition to the motile state, next generation sequencing analysis to compare expression profiles of pre-migratory (stage 17-19, neurula) and migratory (stage 28-30, tailbud) PGCs was performed. Somatic endodermal cells from the corresponding stages were also included in the analysis to identify genes that are differentially regulated specifically in PGCs. In addition, comparison between PGCs and somatic cells can be used to identify novel PGC-specific transcripts.

#### **3.5.1 Strategy used for the whole transcriptome analysis of PGCs and somatic endodermal cells**

Labeling and isolation of PGCs was done by injection of *GFP\_DELE* mRNA, as described in section 3.1 (Fig. 7). To avoid any bias coming from differences between individual frogs, all four cell populations were isolated from the same batch of embryos, which were cultivated in the same buffer, upon equal temperature conditions. Furthermore, PGCs and somatic cells from one stage were obtained from the same embryos. In the dissociated endodermal explants from these embryos, PGCs were identified as GFP-positive cells and somatic endodermal cells as GFP-negative. There are two major draw-backs of this method. First, there is a high back-ground GFP signal in the somatic cells, especially in the early stages. Presence of the Dead end localization elements targets the degradation of the transcript by microRNA-mediated decay. This degradation, however, is only initiated during gastrulation and is incomplete at neurula stage. Second, manual injection of the mRNA into the embryos leads to the uneven distribution of signal intensity in the PGCs. For example, the back-ground signal in somatic cells from one embryo can be similar in intensity to the signal in PGCs obtained from another embryo. These events make automated sorting, for

example Fluorescence-activated cell sorting (FACS), not suitable for the isolation of individual cell populations. Possible solutions for this problem might be employment of a transgenic frog line, or alternative labeling of PGCs by the antibody. However, no transgenic line with specific PGC labeling was available at that moment, and generation of such a line could take several years. Furthermore, no PGC-specific extracellular markers that can be used for labeling of the cells by antibody, were identified. Therefore, as it was not possible to perform automated sorting of PGCs and somatic cells, only 30 cells from each population were manually selected for the downstream analysis.

Limitations in the amount of the initial cellular material cause difficulties for the transcriptome analysis by all high throughput platforms available. Most of the methods require at least 100 ng of RNA, while the estimated amount of total RNA in a single cell is around 10-50 pg, with only 1-5% of the it being actually mRNA. To overcome this issue, amplification of the starting material was required prior to the sequencing. Amplified cDNA was sheared to generate 100-300 base pair (bp) fragments and used for the next generation sequencing by the illumina technology.

### **3.5.2 Evaluation of the sequencing results**

Short sequences (reads), obtained after transcriptome sequencing of the four cell populations, were first aligned to the existing *Xenopus laevis* database. However, since *X.laevis* is pseudotetraploid and its genome is not sequenced, the database is poorly annotated. Many mapped regions are described as ‘hypothetical protein’ or ‘transcribed locus’. These sequences usually cover only 3’ parts of the mRNAs, since most of the information is coming from cDNA library preparation. Moreover, there is a big redundancy in the database, meaning that several transcribed regions can represent the same gene. Therefore, a database of a closely related species, *Xenopus tropicalis*, was used for the alignment. In contrast to *X. laevis*, *X. tropicalis* is diploid, its genome has already been sequenced and database is much better annotated. Alignment to *X. tropicalis* database helped to reduce redundancy and the amount of non-annotated coding regions that was important for the further analysis.

To verify that the experiment worked and was designed properly, expression of several control genes was compared between different cell populations. The first group of genes consisted of known PGC-specific transcripts: *Pat* (Hudson and Woodland, 1998), *DeadEnd* (Horvay et al., 2006), *Dazl* (Houston and King, 2000b), *Nanos* (Lai et al., 2011), *DeadSouth*, *KIF13B* (Tarbashevich et al., 2011), *Syntabulin* (current study, see section 3.8.2), and *GRIP2* (Tarbashevich et al., 2007; Kirilenko et al., 2008). The second group included genes, usually used as a house-keeping reference in many studies: *ODC*, *GAPDH*, *Tubulin alpha*, *Tubulin beta*, *Actin beta*, *Actin gamma* (Stürzenbaum and Kille, 2001). The third group consisted of known neuronal and mesodermal markers: *Xbra3* (Hayata et al., 1999), *BMP2 inducible kinase* (Hoffmann and Gross, 2001), *NCAM* (Levi et al., 1987), *Twist* (Hopwood et al., 1989) and *Snail* (Essex et al., 1993). Comparison of gene expression between different cell populations revealed, as expected, increased expression of known PGC-specific

Gene Description	PGC St.17-19	Som St.17-19	PGC St.28-30	Som St.28-30	FC PGC/Som
Transcribed locus	1301	58	915	1	37.56
CPEB 1	514	37	518	1	27.16
Pat	2042	165	2171	8	24.35
GRIP2	1081	85	814	0	22.29
Histone cluster 1, H2aa	712	66	692	6	19.50
DeadSouth (ddx25)	4614	602	7093	5	19.29
Dazl	3082	400	4543	0	19.06
Nanos1	1287	142	1354	0	18.60
Similar to rras2	2127	248	3292	65	17.31
Syntabulin (Sybu)	413	37	313	6	16.88
DeadEnd (dnd1)	93	12	138	3	15.40
Heat shock protein 90kDa alpha	4234	781	10570	312	13.54
LEPROTL1	340	68	723	20	12.08
AHA1, activator of heat shock 90kDa protein ATPase homolog 1	1090	168	1907	144	9.61
KIF13B	201	40	111	3	7.26
phosphoglycerate mutase (Velo7)	594	166	534	33	5.67
GAPDH	454	240	2438	364	4.79
ODC1	1008	758	558	507	1.24
Tubulin beta (tubb3)	2454	1717	2168	3325	0.92
Tubulin alpha (tuba8)	3821	2667	4001	6734	0.83
Tubulin alpha (tuba1c)	5447	3819	5141	9361	0.80
Tubulin alpha (tuba4a)	1038	652	811	1678	0.79
Tubulin alpha (tuba1a)	1453	1019	1042	2912	0.63
Actin gamma (actg1)	2141	2803	2101	3929	0.63
Actin beta (actb)	5328	7151	5543	10233	0.63
Xbra3	0	0	2	2	
BMP2 inducible kinase	4	65	7	12	
NCAM1	21	19	23	5	
Twist1	47	10	47	16	
Snail homolog 1	68	13	9	3	
Snail homolog 2	36	12	20	26	

Heat map: > 4000 4000-1000 1000-300 300-100 < 100

Candidate PGC specific genes -  PGC specific -

Mesoderm and neurall maker -  House keeping -

**Fig. 22. Next generation sequencing analysis confirms identity of the used cell populations and reveals novel PGC-specific candidate genes.** Expression of known PGC specific (green), candidate PGCs specific (blue), house keeping (purple) and mesoderm or neuronal marker (pink) genes in PGCs and somatic endodermal cells (Som) isolated from neurula (St.17-19) and tailbud (St.28-30) stage embryos. Normalized relative expression was determined by next generation sequencing analysis and presented in form of a heat map for better visualization. The level of enrichment in PGCs was specified as a fold change (FC) difference in expression between PGC (St.17-19 + St.28-30) and somatic cells (St.17-19 + St.28-30). In the table, genes are arranged according to their enrichment in PGCs, with highest on top and lowest to the bottom. Mesoderm and neuronal marker genes were excluded from the analysis, since the values of expression are too low and, most probably, correspond to the back-ground.

transcripts specifically in primordial germ cells if compared to the somatic endodermal cells (Fig. 22). In relatively low amounts PGC-specific transcripts were also present in somatic cells isolated from stage 17-19 embryos that might be explained by incomplete degradation of maternal transcripts at these stages of development. Since there was no data available about the level of gene expression in PGCs or somatic endodermal cells at neurula and tailbud stages of *X. laevis* development, expression of standard house-keeping genes, commonly used in many cell types for normalization of gene expression, was was used as a control (Stürzenbaum and Kille, 2001). Despite the fact that the expression level was not



absolutely eqy equal for each cell population, this group of genes, in contrast to the known PGC-specific transcripts, showed no specific enrichment in PGCs or somatic cells. In addition, no significant amounts of neuronal and mesodermal markers were detected in all analyzed cell populations (Fig. 22). This indicates that there was no contamination by neuronal or mesodermal cells that could bias the results.

### **3.5.3 Analysis of candidate PGC-specific transcripts by WMISH**

To verify bioinformatical analysis of next generation sequencing experimentally, several candidate PGC-specific genes were selected for whole mount *in situ* hybridization (WMISH) analysis. Selected genes had different level of expression, but all of them showed enrichment in PGCs comparable to the known PGC-specific transcripts, as was evident from the next generation sequencing analysis (Fig. 22).

Spatio-temporal expression analysis by whole mount *in situ* hybridization (WMISH) demonstrated that all tested genes were expressed in distinct cells in the endodermal region of tailbud stage embryos (stage 28-30). For approximately half of them, weak expression was also observed in neurula stage embryos (stage 17-19) (Fig. 23). This pattern of expression in the endoderm was very similar to the known PGC-specific transcripts, for example *Pat* (Hudson and Woodland, 1998, Fig. 26D-F). In addition, expression of all tested genes, excluding CPEB1 and Similar to *rras2*, was observed in regions other than endoderm. High level of expression of these genes in other tissues may explain relatively weak signal observed in individual cells in the endoderm.

## **3.6 Expression of several adhesion molecules is downregulated during PGC transition to the active migration**

### **3.6.1 Transcriptom analysis to identify differential gene expression in pre-migratory and migratory PGCs**

In the context of this project, main interest was to determine genes involved in the transition of PGCs to active migration in the endoderm. For this purpose, next generation sequencing analysis results were used to look for differential expression of the genes between pre-migratory PGCs isolated from neurula stage embryos (stage 17-19) and migratory PGCs isolated from tailbud embryos (stage 28-30). Candidate genes were selected by several criteria. First, difference in gene expression between two PGC populations should be more than two folds. Second, gene expression in migratory PGCs for upregulated genes and pre-migratory PGCs for downregulated genes should be above certain threshold. This criterium was used to eliminate false positive expression of the genes coming from the measurement error. Third, expression in somatic endodermal cells, isolated from both neurula and tailbud stages, was also analyzed to identify genes, expression of which changes specifically in PGCs (see section 2.7.7). Application of these criteria led to identification of 449 genes differentially regulated specifically in pre-migratory (stage 17-19) versus migratory (stage 28-30) PGCs. Among these genes, 187 were downregulated, while 262 were

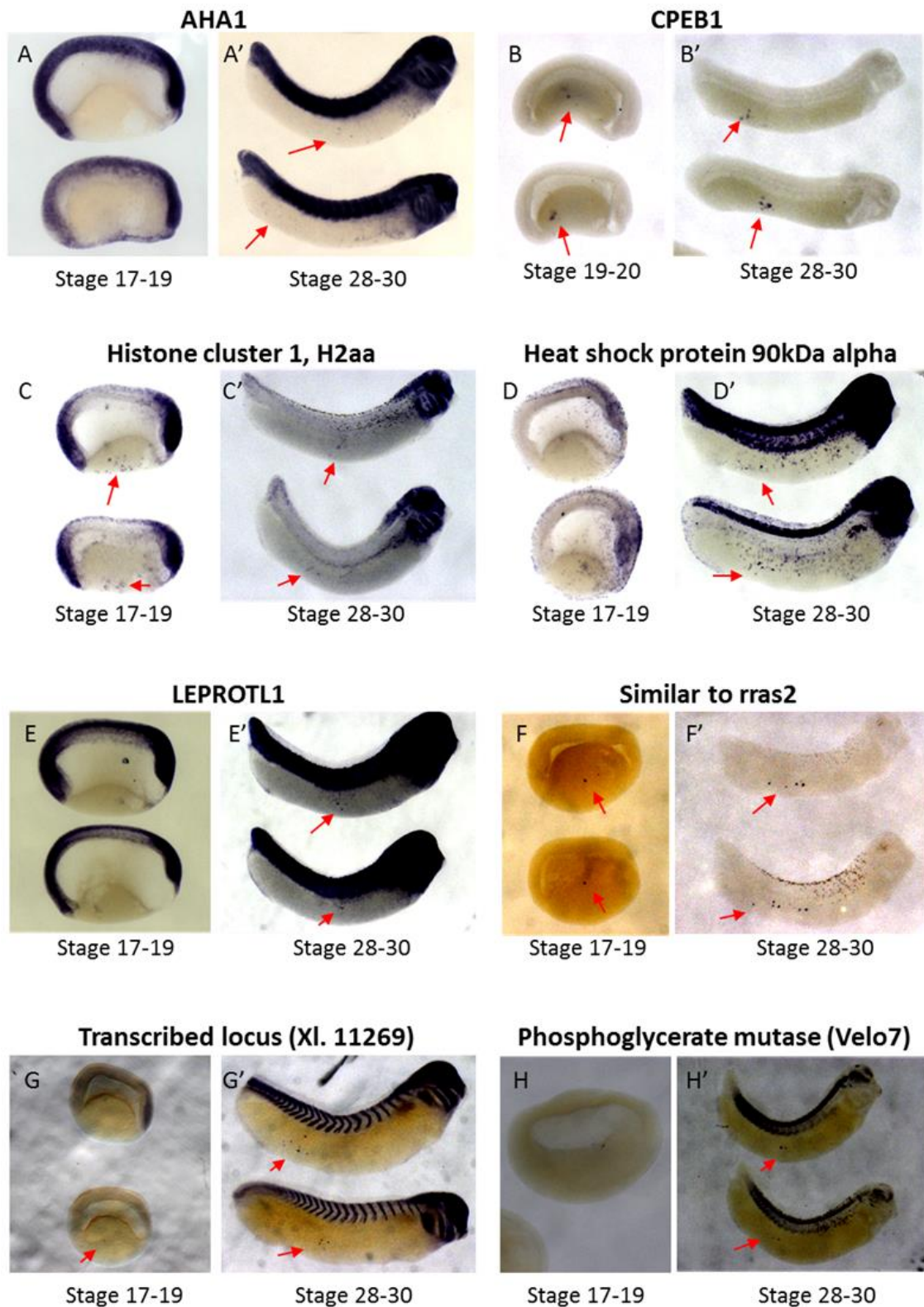


**Fig. 23. Whole mount in situ hybridization analysis of novel PGC-specific transcripts.** *X. laevis* embryos were fixed in MEMFA at stage 17-19 (A-H) and 28-30 (A'-H') and subjected to the whole mount in situ hybridization (WMISH). Antisense riboprobes of candidate PGC-specific genes (Fig. Q, blue) were produced by the standard *in vitro* transcription from linearized plasmids in the presence of digoxigenin-coupled rUTP. After WMISH, embryos were dehydrated in methanol and cleared in BB:BA clearing agent. Dorsal side is up, anterior side is to the right. Red arrows indicate PGC-like expression in the endoderm.

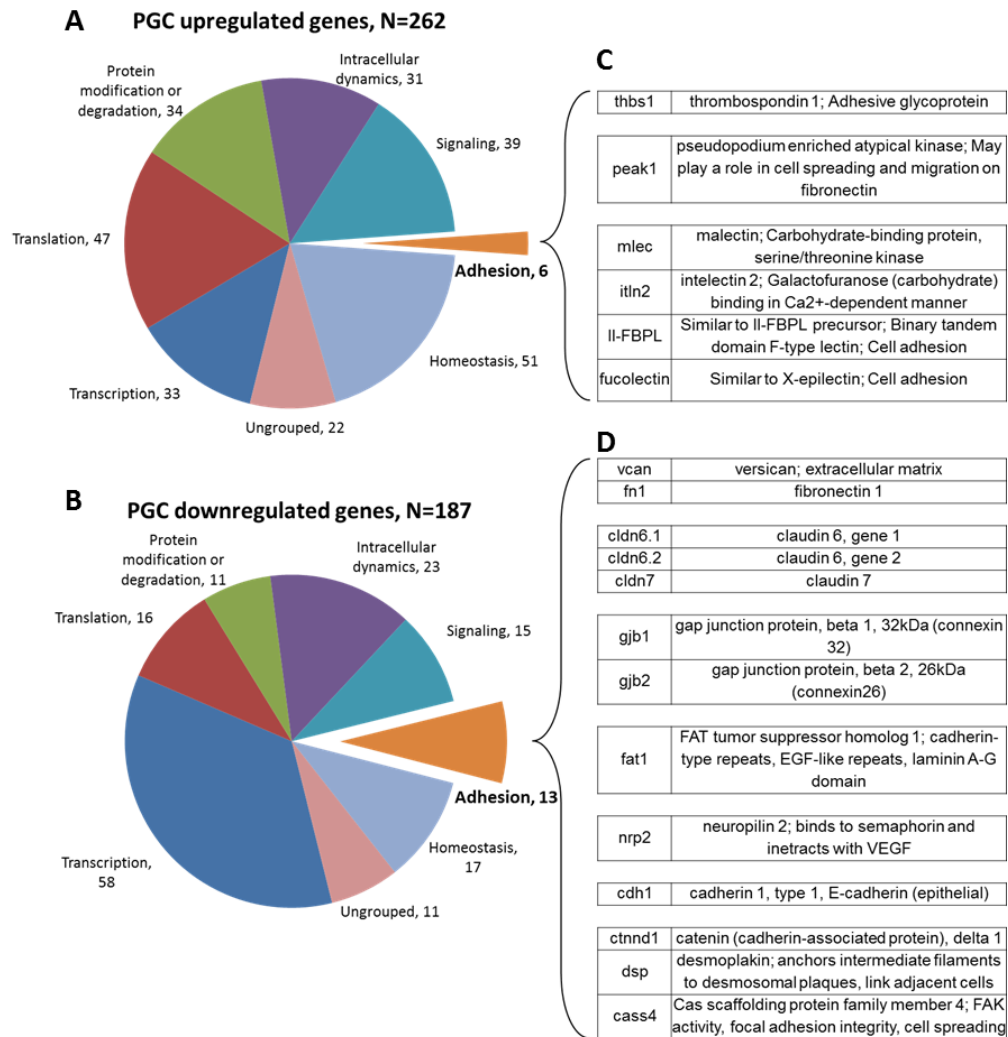


**Fig. 24. Comparative whole transcriptom analysis led to identification of several candidate adhesion molecules differentially regulated between neurula and tailbud stage PGCs.** Data obtained after next generation sequencing analysis were used to identify differentially expressed genes, upregulated (A) or downregulated (B) in migratory (tailbud, stage 28-30) versus pre-migratory (neurula, stage 17-19) PGCs. N represents the amount of identified genes for each category. Differentially expressed genes were grouped according to the function in the cell. Relative amount of genes in each group in the total amount of up- (A) or downregulated (B) genes is represented by pie chart. Number after the group name corresponds to the number of genes in the group. List of candidate up- (C) and downregulated (D) adhesion molecules indicates gene symbol (left column) and a short description (right column).

upregulated. Depending on the function of gene product in the cells, both up- and downregulated genes were assigned to one of the several groups (Fig. 24A, B; Suppl. Fig. 1).

Since our previous findings showed a decline in cell adhesion properties of PGCs isolated from tailbud stage embryos (see chapter 3.2), differential expression of adhesion molecules was of a special interest (Fig. 24C, D). Downregulated adhesion molecules (Fig. 24C) included proteins involved in the cell adhesion to the extracellular matrix (fibronectin and versican) and surrounding cells. Some of the downregulated adhesion molecules (Cldn6.1, Cldn6.2 and Cldn7), belong to claudin family of proteins, that mediates cell-cell

adhesion via tight junctions (Findley and Koval, 2009). Another group, consisting of gap junction proteins Gjb1 and Gjb2, mediates cell-cell adhesion via formation of gap junctions between adjacent cells (Giepmans, 2004). Several downregulated molecules participate in the formation of adherens junctions, including direct mediators of cell-cell adhesion E-cadherin (Cdh1) and cadherin Fat1, as well as cadherin-associated catenin delta (ctnnd1) (Harris and Tepass, 2010; Nishikawa et al., 2011). Other downregulated adhesion molecules were shown to participate in the formation of focal adhesions (Cass4) and desmosomal plaques (Dsp), or indirectly regulate cell adhesion (Nrp2) (Bornslaeger et al., 1996; Singh et al., 2008; Jia et al., 2010).

Most of the upregulated adhesion genes (Fig. 24D) encoded carbohydrate-binding proteins, known as lectins (*mlec*, *itln2*, *II-FBPL*, *fuclectin*), which can mediate protein-carbohydrate cell adhesion (Kaltner and Stierstorfer, 1998; Singh and Sarathi, 2012). Thrombospondin 1 (Thbs1) is an adhesive glycoprotein that mediates cell-to-cell and cell-to-matrix interactions (Li et al., 2002; Narizhneva et al., 2005). Another upregulated molecule, pseudopodium-enriched atypical kinase 1 (PEAK1), controls focal adhesion assembly and disassembly in a dynamic pathway (Bristow et al., 2013).

### **3.6.2 Quantitative RT-PCR analysis of candidate adhesion molecules expression in PGCs**

To validate differential expression of adhesion molecules in pre-migratory (neurula, stage 17-19) and migratory (tailbud, stage 28-30) PGCs, quantitative RT-PCR analysis was performed. Expression in the somatic endodermal cells isolated from both embryonic stages was used as a control. Corresponding cDNA was prepared from 30 cells isolated from *GFP\_DELE*-injected embryos. Expression in each cell population was normalized to  $\beta$ -actin (Actb), since next generation sequencing analysis suggests that it is expressed in comparable levels in both neurula and tailbud stage PGCs, and only slightly differs in expression between two populations of somatic cells. Prior to the quantitative RT-PCR (qRT-PCR), cDNA prepared from all cell populations was analyzed for the expression of  $\beta$ -actin as a positive control, and PGC-specific gene *xPat* (Fig. 25A). Similar to next generation sequencing data, qRT-PCR analysis demonstrated downregulation of adhesion molecules Claudin 6.1 (Cldn 6.1), Claudin 7 (Cldn 7), E-cadherin, and gap junction protein beta 1 (Gjb1). In comparison to somatic endodermal cells, downregulation of Cldn6.1, E-cadherin and Gjb1 occurred specifically in PGCs. However, downregulation of Cldn7 was not PGC-specific and was detected also in somatic endodermal cells. Downregulation of gap junction protein beta 2 (Gjb2) and Fibronectin (Fn), as well as upregulation of Malectin (*mlec*) was not observed (Fig. 25). Expression of other candidate upregulated adhesion molecules identified by next generation sequencing analysis, including Thbs1, PEAK1, Itln2 and fuclectin, was either too low or not detected by qRT-PCR. Expression of other candidate downregulated adhesion molecules was not analysed.

In conclusion, these results demonstrate that several adhesion molecules, including Cldn 6.1, E-cadherin and Gjb1, are downregulated specifically in PGCs during the transition of PGCs to the active migration, but not in the surrounding somatic endodermal cells.

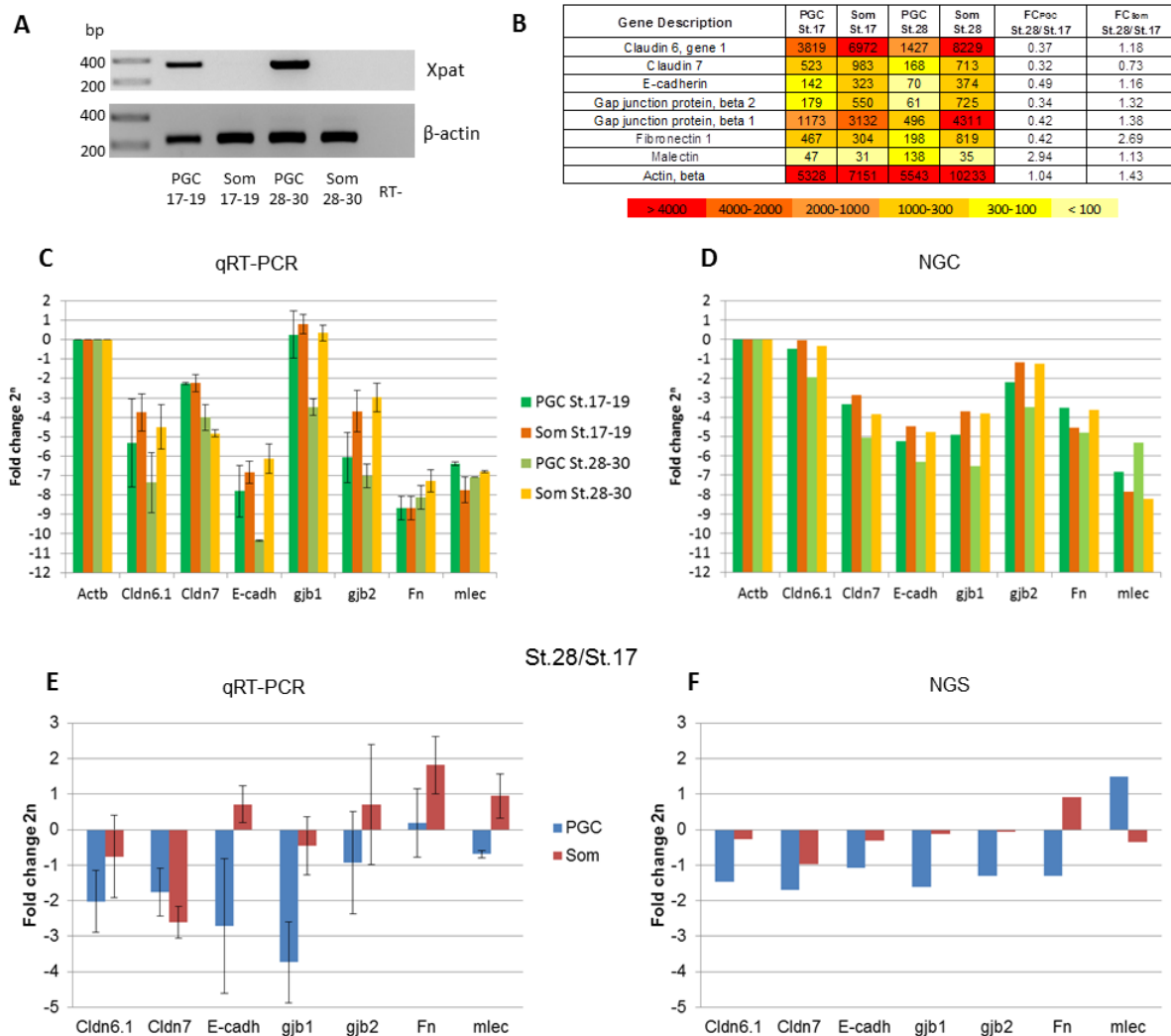


**Fig. 25. Expression of Claudin 6.1, E-cadherin and gap junction protein beta 1 is downregulated specifically in PGC at tailbud stage.** Expression of adhesion molecules Claudin 6.1 (Cldn6.1), Claudin7 (Cldn7), E-cadherin (E-cadh), gap junction protein beta 1 (gjb1), gap junction protein beta 2 (gjb2), Fibronectin (Fn) and Malectin (mlec) was analyzed by quantitative RT-PCR (qRT-PCR) (**C**, **E**) and compared to the data obtained from whole transcriptome analysis (WTA) (**B**, **D**, **F**). Primordial germ cells (PGC) and somatic endodermal cells (Som) were isolated from neurula (St.17-19) or tailbud (St.28-30) embryos and used for the preparation of cDNA. (**A**) Agarose gel electrophoresis of PCR quality control for cDNA used in qRT-PCR analysis. In contrast to somatic cells, PGC-specific cDNA contains *Xpat* transcript. Amplification of  $\beta$ -actin is used as a positive control; a sample obtained from reverse transcription of endodermal cells without adding reverse transcriptase (RT-) was used as a negative control. Marker lane on the left side of the gel indicates the relative size of amplified products in base pairs (bp). (**B**) Data on the expression of corresponding adhesion molecules obtained by WTA. Normalized relative expression in each cell population is represented in a form of a heat map for the better visualization. Fold change (FC) difference in gene expression between tailbud (St.28) and neurula (St.17) is indicated for PGCs (FC<sub>PGC</sub>) and somatic endodermal cells (FC<sub>Som</sub>). (**C**) Relative expression of adhesion molecules in different cell populations was analyzed by qRT-PCR and normalized to expression of  $\beta$ -actin (Actb) by  $\Delta$ Ct method (Livak and Schmittgen, 2001). One scale unit corresponds to 2-fold difference in expression, error bars represent standard deviation. At least three independent experiments were performed for analysis of each gene. (**D**) Data obtained by qRT-PCR (**C**) can be compared to the data from NGS (**B**), normalized to  $\beta$ -actin in the same manner. (**E**, **F**) Gene expression in tailbud (St.28) PGCs and somatic endodermal cells (Som) was normalized to the expression in neurula stage (St.17) by  $\Delta\Delta$ Ct method (Livak and Schmittgen, 2001). One scale unit corresponds to 2-fold difference in expression, error bars represent standard deviation.

### **3.7 *xKIF13B* mRNA is present in germ plasm and PGCs up to tailbud stages, but its translation is not required for PGC development before active migration**

Previous results from our lab demonstrated that kinesin *xKIF13B*, encoded by maternally supplied germ plasm specific mRNA (Horvay et al., 2006), is required for the proper PGC migration and survival. Knock-down mediated by the injection of antisense morpholino oligonucleotides (MOs), or PGC-specific overexpression via injection of *xKIF13B* mRNA fused to Dead end LE, resulted in a decreased number and mislocalization of PGCs in *X. laevis* embryos at the tailbud stage. (Tarbashevich, 2007; Tarbashevich et al., 2011; see section 1.4.3). It was not clear, however, whether these effects are a direct result of abnormal expression of *xKIF13B* in PGCs at the tailbud stage, or PGC development is disrupted due to *xKIF13B* malfunction at the earlier stages.

As has been shown previously, *xKIF13B* mRNA is vegetally localized during oogenesis and can be found in the germ plasm up to gastrula stage of embryonic development. It is also expressed in PGCs during their migration in the endoderm at stage 30-34 (Horvay et al., 2006; Tarbashevich, 2007; Tarbashevich et al., 2011). To test whether *xKIF13B* is expressed in pre-migratory PGCs between gastrula and tailbud stages, whole mount *in situ* hybridization (WMISH) analysis was performed with following embryonic stages: neurula (stage 17-19), early tailbud prior to active PGC migration (stage 22-23) and early tailbud upon initiation of active PGC migration *in vivo* (stage 24-25). Expression of *xKIF13B* could be detected in PGC at all tested stages. No significant difference in the level of expression was observed (Fig. 26).

The observed effects of *xKIF13B* knock-down in PGCs at the tailbud stages might be secondary to the earlier defects in germ plasm aggregation. To investigate, whether *xKIF13B* knock-down by specific morpholino oligonucleotides (*xKIF13B* MO) affects germ plasm morphology and localization at the early developmental stages, *xKIF13B* MO-injected embryos were tested for the expression of *Pat*, a specific germ plasm marker. Uninjected embryos from the same frog, and embryos injected with unspecific control morpholino (Control MO) were used as a negative reference. Knock-down of *xKIF13B* did not reveal any significant effects of the treatment in respect to germ plasm aggregation or intracellular localization (Fig. 27).

In order to address the question at what stage of development phenotypic effects of *xKIF13B* knock-down first occur, the analysis of average PGC number in control (Control MO) versus *xKIF13B* (*xKIF13B* MO) morpholino-injected embryos at different developmental stages was performed (Fig. 28). It turned out that a significant reduction in PGC number can only be detected after stage 24/25, i.e. after the transition from passive to active PGC migration. Similar to the previous observations, number of mislocalized PGCs in the tailbud stage embryos (stage 31-32) injected with *KIF13B* MO was significantly increased in comparison to the control. No difference in the relative position of PGCs was observed at the

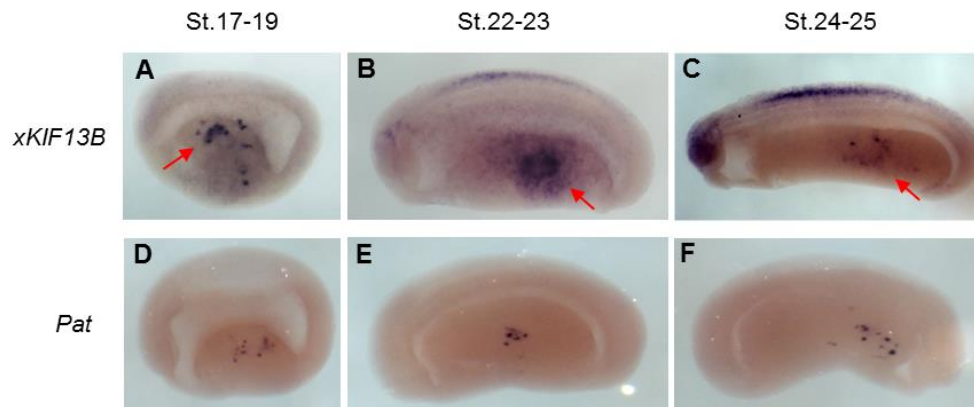


**Fig. 26. *xKIF13B* is expressed in the PGCs at neurula and early tailbud stages of embryonic development.** *X. laevis* embryos were fixed in MEMFA at stage 17-19 (A), stage 22-23 (B) and stage 24-25 (C), and subjected to the whole mount in situ hybridization (WMISH). Antisense riboprobes were produced by the standard *in vitro* transcription from linearized plasmids in the presence of digoxigenin-coupled rUTP. To amplify the signal, the complex probe composed of several antisense RNAs covering the entire ORF of *xKIF13B* was used (A-C). Staining with PGC-specific marker *Pat* was used as a control (D-F). After WMISH, embryos were dehydrated in methanol and cleared in BB:BA clearing agent. PGC-like pattern of *xKIF13B* expression was observed in the endoderm of all tested embryos (red arrows). Expression of *xKIF13B* was also observed in the nervous system. Dorsal side is up, anterior side is to the left.

earlier stages. A decreased PGC number observed in the *xKIF13B* knock-down morphants could be a result of apoptosis. To address the issue of altered cell survival as the basis for reduced numbers of PGCs upon *xKIF13B* MO injection, TUNEL staining was performed. Similar to previous observations (Hensey and Gautier, 1998), apoptotic cells in neurula (stage 17) and tailbud (stage 24-25 and stage 31-32) embryos were mainly detected in the epithelium and nervous system. However, no indication of the increased number of apoptotic cells in the endoderm was observed (Fig. 29).

### 3.8 *Xenopus* homologues of Centaurin- $\alpha$ 1 and Syntabulin are not likely to be involved to be involved in the interaction with *xKIF13B* in PGCs

#### 3.8.1 Known interaction partner of *xKIF13B*, Centaurin- $\alpha$ 1, is not expressed in *X. laevis* PGCs

Our previous studies showed that interference with endogenous levels of kinesin *xKIF13B* resulted in defects during directional PGC migration. These effects were connected to the distribution of PIP3 and polarization of PGCs (Tarbashevich, 2007; Tarbashevich et al., 2011). For the *Drosophila* and mammalian homologues of *KIF13B*, two main bind partners were identified: the membrane-associated guanylate kinase (MAGUK) homologue scaffolding protein hDlg/SAP97, and Centaurin- $\alpha$ 1, also known as PIP3-binding protein (PIP3BP). Both proteins were implicated in the establishment of cell polarity and in the cell adhesion (Asaba et al., 2003; Venkateswarlu et al., 2005; Horiguchi et al., 2006). Interaction with Centaurin- $\alpha$ 1 was particularly interesting, since it connected *xKIF13B* to the intracellular distribution of PIP3.

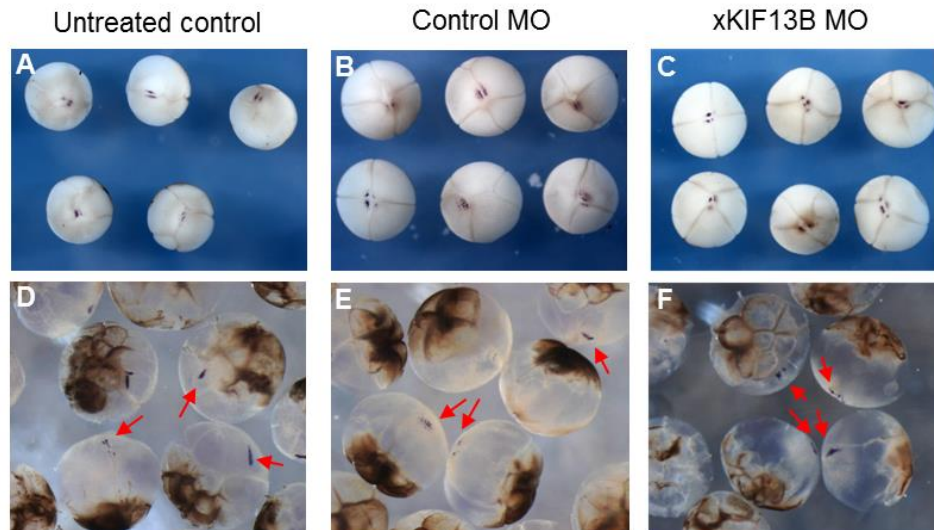


**Fig. 27. *xKIF13B* knockdown does not affect germ plasm localization in *X. laevis* embryos at blastula stage.** Embryos were injected vegetally into both blastomeres at 2-cell stage with the control morpholino (Control MO) (B, E), *xKIF13B* morpholino (*xKIF13B* MO) (C, F), or left untreated (A, D). All embryos were fixed at stage 4-5 and subjected to WMISH. To visualize germ plasm, WMISH was performed using Dig-labeled antisense *Pat* RNA as specific germ plasm marker (Hudson and Woodland, 1998). *Pat* mRNA was observed in the vegetal pole of all tested types of embryos in the region corresponding to germ plasm (purple) (A-C, vegetal pole view). To visualize distribution of the germ plasm with the blastomeres, embryos were dehydrated in methanol and cleared in BB:BA clearing agent (D-F, pigmented side corresponds to the animal pole). No differences in germ plasm localization (purple, highlighted by red arrows) between tested groups of embryos were observed.

To test expression of Centaurin- $\alpha$ 1 in *Xenopus* RT-PCR analysis and whole mount in situ hybridization were performed (Fig. 30). Shortly after fertilization *xCentaurin- $\alpha$ 1* mRNA was not detected (Fig. 30B). During midblastula transition (stage 8-9), expression of *xCentaurin- $\alpha$ 1* can be observed in the animal half of the embryo (Fig. 30C). Later during embryogenesis *xCentaurin- $\alpha$ 1* was expressed in the developing nervous system (Fig. 30D-J), with the strongest expression at stages 20-21 (Fig. 30F). However, no expression in the endoderm was detected, suggesting that the transcript of this gene is not associated with germ plasm or PGCs. Whole transcriptom analysis of PGCs and somatic endodermal cells (see section 3.5) also did not show any expression of *xCentaurin- $\alpha$ 1* in these cell populations.

### 3.8.2 *xSyntabulin* as a potential binding partner of *xKIF13B* in PGCs

Syntabulin (or Syntaxin-1-binding protein) is a microtubule associated protein, which was initially identified in developing hippocampal neurons. It acts as a KIF5B motor adaptor and mediates anterograde transport of presynaptic cargoes and mitochondria, presynaptic assembly, and activity-induced plasticity (Su et al., 2004; Cai et al., 2005; 2007). Syntabulin is not specific for neuronal cells, as it was also found in tissue homogenates from rat heart, liver, kidney and testis (Su et al., 2004). Apart from its role in the nervous system, Syntabulin is also known to regulate the microtubule-dependent transport of the dorsal determinants (DDs) in zebrafish embryos that plays an important role in formation of dorsoventral (DV) and anteroposterior (AP) body axes. It was suggested that in zebrafish, Syntabulin links DDs to the maternally expressed kinesin I heavy chain (KIF5B). This complex can mediate initial



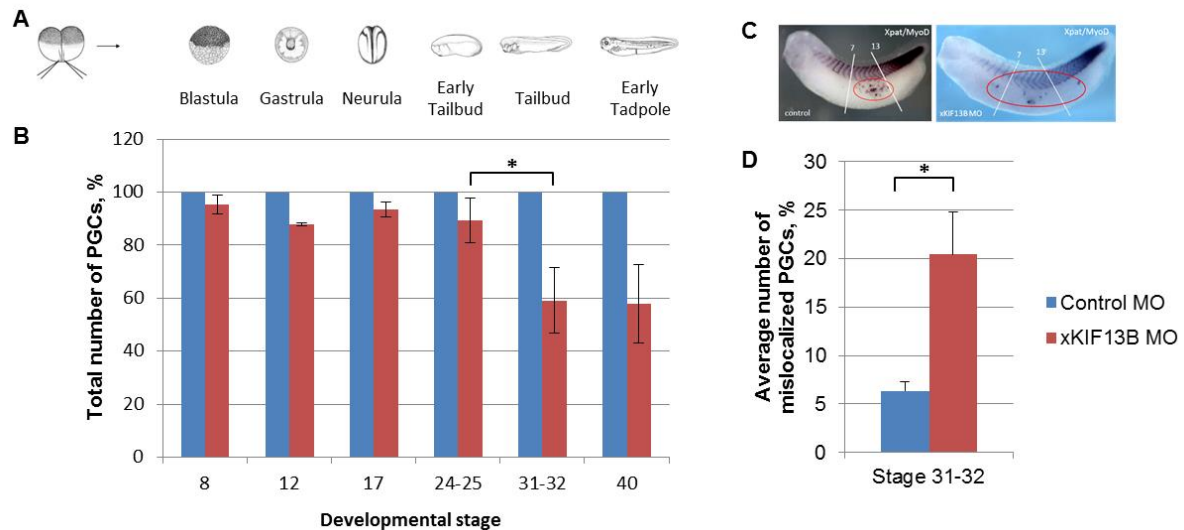


**Fig. 28. Knock-down of xKIF13B leads to the reduction of PGC number after transition of PGCs to the active migration.** (A) Embryos obtained from the same frog were injected vegetally into both blastomeres at 2-cell stage with the control (Control MO) or xKIF13B antisense morpholino oligonucleotide (xKIF13B MO). Injected embryos were fixed at blastula (developmental stage 8), gastrula (stage 12), neurula (stage 17), early tailbud (stage 24-25), tailbud (stage 31-32), or early tadpole (stage 40). To visualize PGCs, WMISH was performed using Dig-labeled antisense *Pat* RNA as a specific PGC marker. Embryos were dehydrated in methanol and cleared in BB:BA clearing agent before PGC counting. (B) The number of PGCs in the Control MO-injected embryos (blue) was set to 100%. In each experiment, total number of PGCs in the xKIF13B MO-injected embryos (red) was normalized to the number of PGCs in the embryos injected with Control MO. (C) Representative examples of xKIF13B MO and Control MO-injected embryos, fixed at 31-32 stage and subjected to WMISH with Dig-labeled antisense *Pat* and *MyoD* labeled riboprobes. *MyoD* expression was used as a somite marker to analyze relative localization of PGCs in the embryo (red ellipse). Majority of PGCs in the control embryos are localized between the seventh and the thirteenth somites. PGCs in other regions of the embryo were considered mislocalized. (D) Amount of mislocalized PGCs in Control MO (blue) and xKIF13B MO-injected embryos (red) was normalized to the total amount of PGCs per embryo at the stage 31-32. Graph represents average number of mislocalized PGCs in the embryo. Numbers in (B) and (D) were averaged from three independent experiments. Error bars represent the standard deviation, \* -  $p < 0.05$ .

vegetal pole localisation and subsequent transport of DDs to the prospective dorsal side, thereby linking oocyte AV polarity to embryonic DV polarity (Nojima et al., 2010). Similar to kinesin xKIF13B, *Xenopus* homologue of Synatbulin (xSybu) was identified as a novel vegetally localizing mRNA in *Xenopus laevis* oocytes (Horvay et al., 2006). Therefore, we wanted to test possible role of xSybu in PGC development as a potential mediator of xKIF13B.

Expression analysis using RT-PCR and whole mount in situ hybridization (WMISH) was performed to test the expression of xSybu in PGCs. Shortly after fertilization, *xSyntabulin* mRNA was detected at vegetal pole in the germ plasm region (Fig. 31A). During blastula and gastrula stages it remains to be associated with germ plasm (Fig. 31B, C). Although no specific signal was detected in PGCs at the neurula stage (Fig. 31D), WMISH with tailbud stage embryos demonstrated weak staining of several cells in the endoderm in the PGC-like

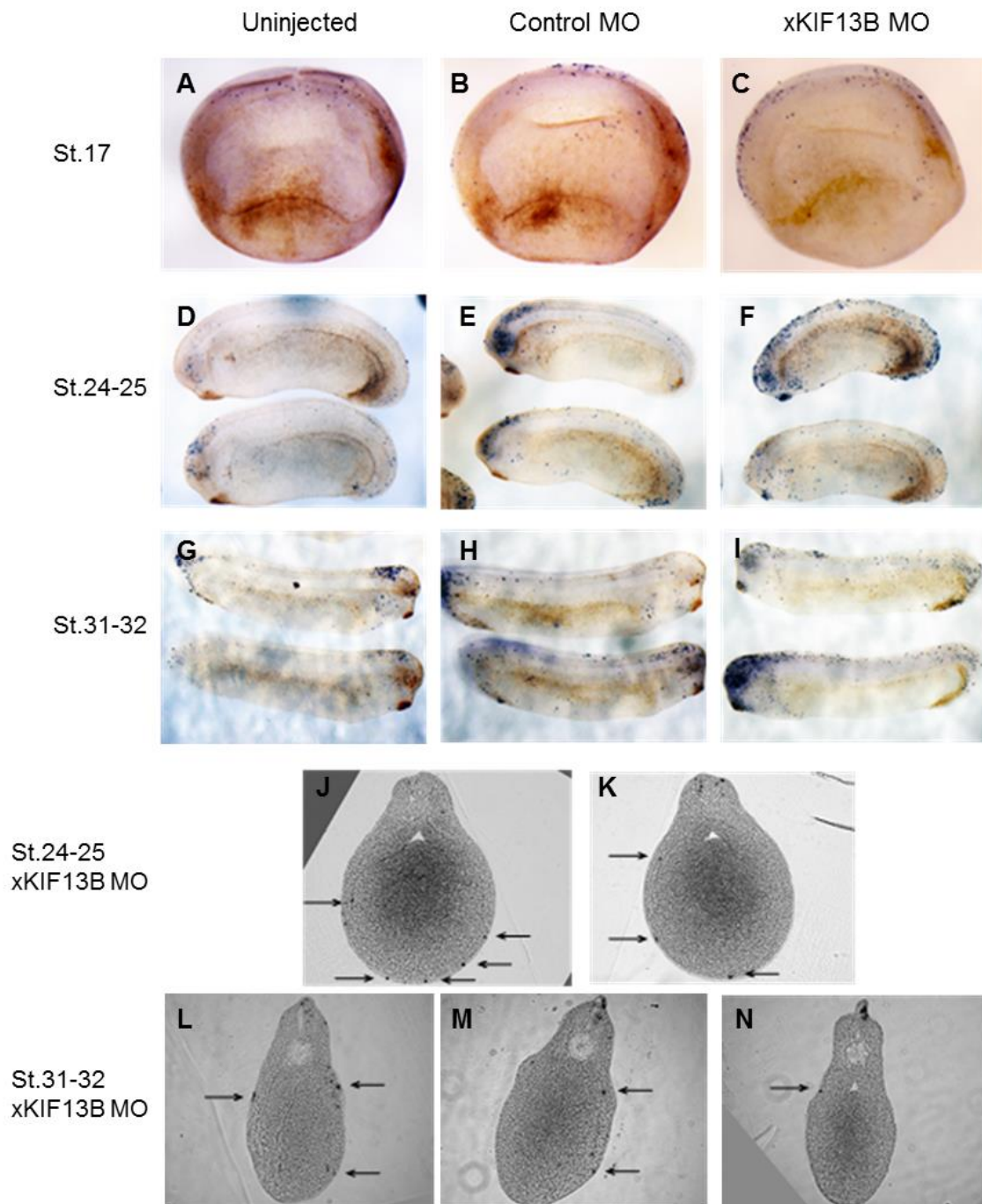


**Fig. 29. Reduction of the total PGC number in xKIF13B morphants is not caused by apoptosis.** (A) Embryos were injected vegetally into both blastomeres at 2-cell stage with the control (Control MO) or xKIF13B antisense morpholino oligonucleotide (xKIF13B MO), or left untreated (Uninjected). At developmental stages 17 (A-C), 24-25 (D-F) and 31-32 (G-I) embryos were fixed and subjected to TUNEL staining performed as described by Hensey and Gautier, 1998. After staining, embryos were dehydrated in methanol and cleared in BB:BA clearing agent. Purple staining corresponds to the apoptotic cells. (J-N) Representative sections along the anterior-posterior axis from xKIF13B MO-injected embryos at stage 24-25 (J, K) and stage 31-32 (L-N); dorsal is up. Arrows indicate apoptotic cells, which are generally found in the epidermis but not in the endoderm.

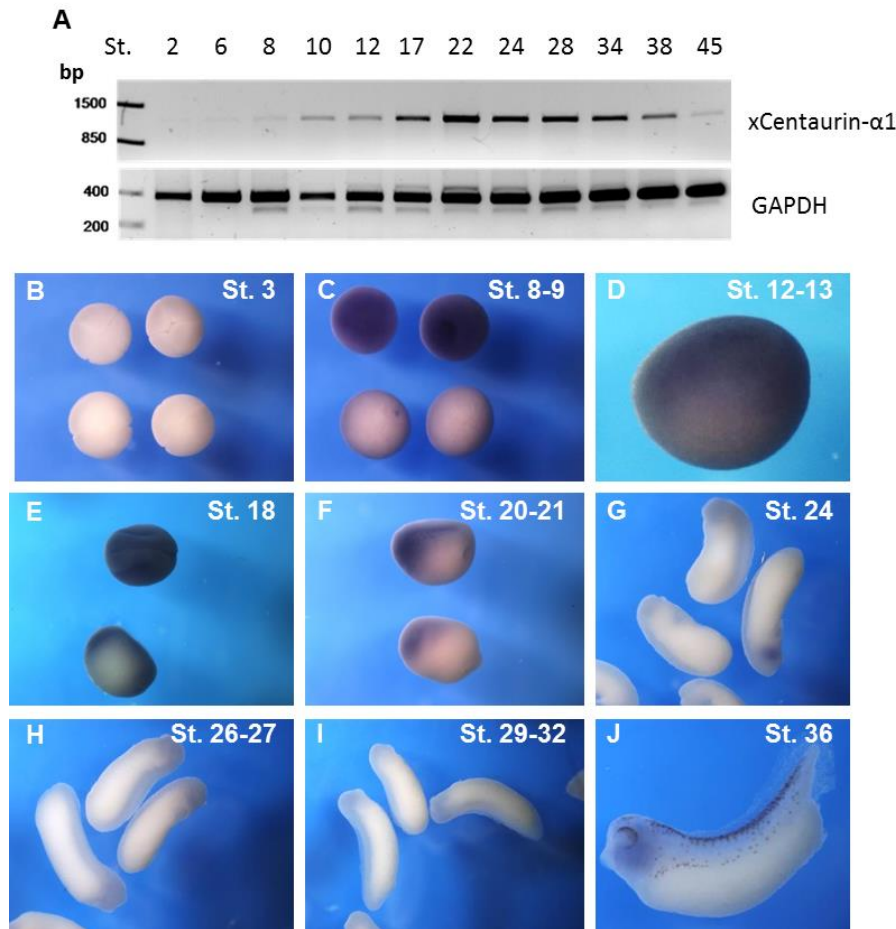


**Fig. 30. xCentaurin- $\alpha$ 1 is expressed in *X. laevis* embryos during gastrula, neurula and tailbud stages outside the endoderm.** (A) RT-PCR analysis of xCentaurin- $\alpha$ 1 expression during different stages (St.) of *X. laevis* development. Total RNA isolated from the whole embryo was used for cDNA preparation. RT-PCR of the housekeeping gene glyceraldehyde-3-phosphate dehydrogenase (GAPDH) was used as a positive control. Marker lane on the left side of the gel indicates the relative size of amplified products in base pairs (bp). (B-J) Whole mount in situ hybridization analysis of xCentaurin- $\alpha$ 1 expression (purple) during different stages of *X. laevis* development. xCentaurin- $\alpha$ 1 mRNA was detected using *in vitro* transcribed dioxygenin-labeled antisense riboprobe. (B, C) Animal pole (upper embryos) and vegetal pole view (lower embryos) of 4-cell stage (St. 3) (B) and blastula (St. 8-9) (C) embryos. (D) Lateral view of late gastrula stage (St.12-13). Anterior is to the right. (E) Dorsal (upper embryo, anterior is to the left) and lateral view (lower embryo, anterior is to the upper left corner) of neurula stage (St. 18) embryos. (F) Lateral (upper embryo) and ventral (lower embryo) view of early tailbud stage embryos (St. 20-21). Anterior is to the left. (G-I) Lateral view of tailbud stage embryos (St.24, 26-27 and 29-32). (J) Lateral view of late tailbud stage embryo (St. 36). Dorsal side is up anterior is to the left.

pattern (Fig. 33E-G). In addition, PGC-specific expression of xSyntabulin was also confirmed by whole transcriptome analysis of PGCs and somatic endodermal cells isolated from stage stage 17-19 and stage 28-30 embryos (Fig. 22). Apart from the endoderm, expression of xSyntabulin is also observed in the nervous system starting from the neurula stage, with the highest expression level at stage 37-38. To have a closer look on the xSyntabulin expression at neurula and tailbud stages, RT-PCR analysis was performed. To distinguish between xSyntabulin expression in endoderm and nervous system, either ventral or dorsal parts of the embryos were used for the cDNA preparation, correspondingly (Fig. 31H). RT-PCR analysis showed the presence of 2 potential isoforms of xSyntabulin gene that differed in

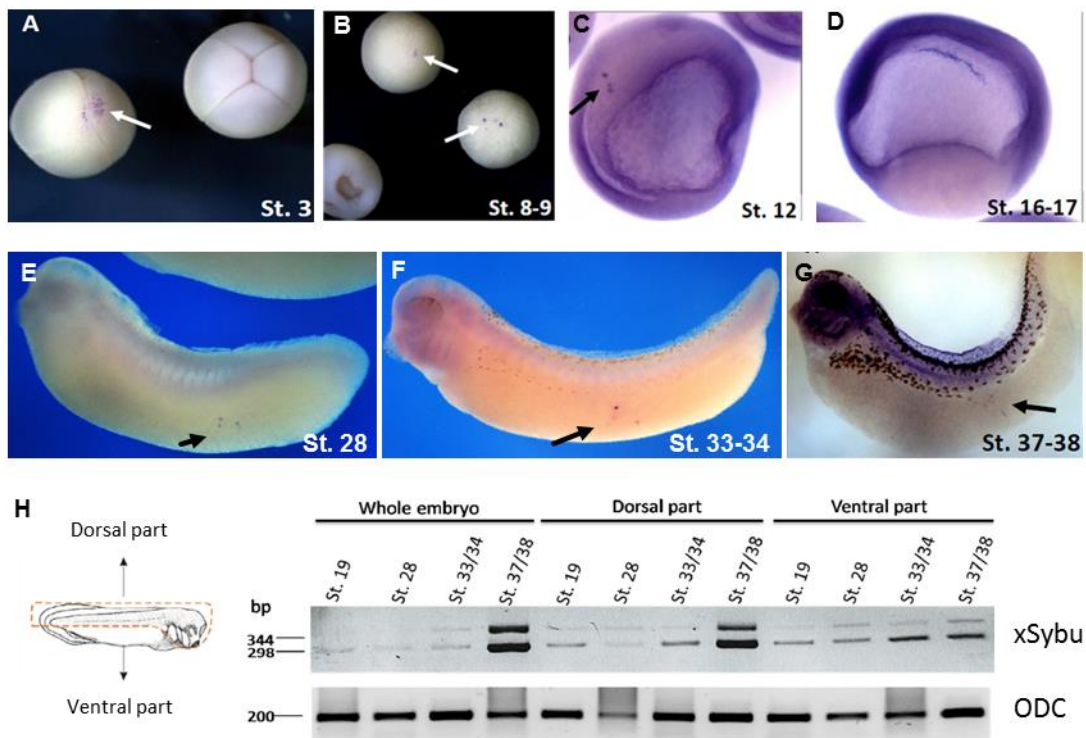


**Fig. 31. Syntabulin is expressed in *X. laevis* PGCs up to tailbud stage.** (A-G) Whole mount in situ hybridization analysis of xSyntabulin expression (purple) during different stages of *X. laevis* development. xSybulin mRNA was detected using *in vitro* transcribed dioxygenin-labeled antisense riboprobe. Arrows indicate expression of xSybulin in germ plasm and PGCs. (A) Vegetal (left) and animal (right) pole view of the 4-cell stage embryos (St. 3). (B) Vegetal (top and middle embryos) and animal (embryo at the bottom) pole view of blastula stage embryo (St. 8-9). (C) Lateral view of gastrula stage embryo (St. 12) cleared with BB:BA agent. Animal is to the right, blastopore is to the upper left corner. (D) Lateral view of neurula stage (St. 16-17) embryo. Dorsal side is up, anterior - to the left. (E-G) Lateral view of tailbud stage (St. 28, St. 33-34 and St. 37-38) embryos. Dorsal side is up, anterior - to the left. (H) RT-PCR analysis of xSyntabulin (xSybu) expression level at neural (St. 19), and tailbud (St. 28, St. 33/34 and St. 37/38) stages of *X. laevis* embryos. cDNA was prepared from the whole embryo or from the dissected dorsal and ventral parts of an embryo. Expression of the housekeeping gene ornithine decarboxylase (ODC) was used as a positive control.

size of approximately 50 base pairs. Both isoforms were detected in ventral and dorsal parts with the highest expression of both at stage 37/38. This increase of expression was stronger in the dorsal part, if compared to the ventral part. It correlates with the observations from WMISH analysis. Expression level of the longer isoform is lower in comparison to the shorter isoform. Increase of the longer isoform expression level in the endoderm was observed only after stage 19.

To visualize intracellular distribution of xSyntabulin in PGCs, embryos were injected with chimeric mRNA, consisting of xSyntabulin ORF fused to GFP and Dead end localization element (xSybu-GFP\_DELE). As a control, embryos from the same frog were injected with GFP\_DELE and PIP3 sensor GFP\_GRPI\_PH\_DELE (Fig. 32). In comparison to ubiquitous distribution of GFP in the isolated PGCs (Fig. 32B), xSyntabulin was localized in a specific

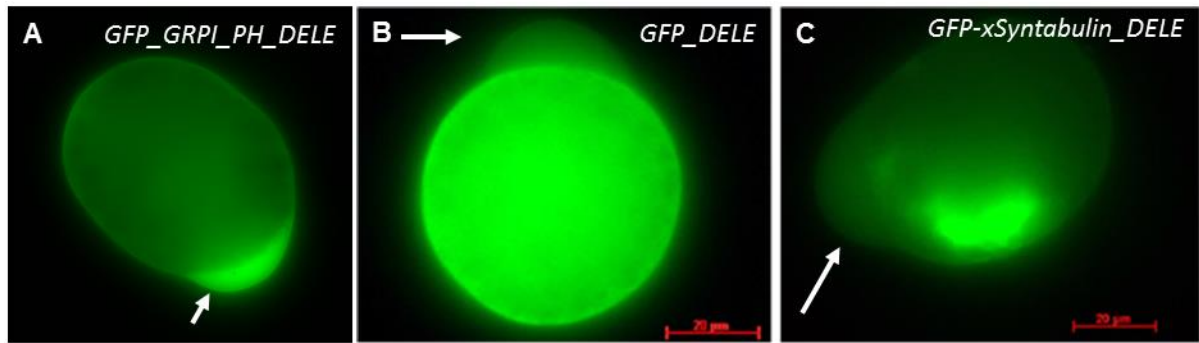


**Fig. 32. xSyntabulin is not localized in bleb-like protrusions formed by isolated PGCs of *X. laevis* tailbud stage embryos.** Embryos at 2-cell stage were vegetally injected with *GFP\_GRPI\_PH\_DELE* (A), *GFP\_DELE* (B) or *GFP-xSyntabulin\_DELE* (C) mRNA and were cultivated till stage 30-31. Individual PGCs were isolated from the endoderm and transferred to agarose-covered Petri dishes. Fluorescent images correspond to intracellular distribution GFP (A), PIP3 (B) and xSyntabulin (C). Arrows indicate bleb-like protrusions formed by isolated PGCs. Scale bar - 20 μm.

region, which might correspond to the Golgi apparatus (Fig. 32C). In the previous studies, localization of xKIF13B was observed at the plasma membrane of bleb-like protrusions formed by isolated PGCs (Dzementsei, 2009). However, in contrast to PIP3 (Fig. 32A), no localization of xSyntabulin at the plasma membrane or bleb-like protrusions formed by isolated PGCs was observed.

To investigate whether xSyntabulin is involved in the PGC development and migration, antisense morpholino oligonucleotides (xSybu MO) were designed to block the initiation of *xSyntabulin* mRNA translation. The activity and specificity of the xSybu MO was tested *in vitro* (Suppl. Fig. 2). After the injection of xSybu MO, embryos at the neurula stage showed defects in the neural tube closer and axis formation (Fig. 33A-C). Amount of the defective embryos increased with an increase in the xSybu MO concentration, suggesting the specificity of the observed phenotype (Fig. 33G). Embryos that passed neurulation, were subjected to WMISH with PGC-specific marker *Pat*. In addition, antisense *MyoD* probe was used to visualize relative position of the PGCs in relation to the somites (Fig. 33D-F). Although in case of xSybu MO-injected embryos slight decrease in the total number of PGCs was observed, the difference is not significant in comparison to the uninjected embryos. No difference in PGC localization within the embryo was detected.

In conclusion, although *xSyntabulin* mRNA can be detected in the germ plasm and PGCs, it most likely functions at the early stages of development. Similar to zebrafish, it may be involved in the axis formation and in embryonic patterning. Knock-down of xSyntabulin does not lead to the defects in PGC migration and survival at tailbud stage, and in contrast to xKIF13B, it is not localized to the membrane of bleb-like protrusion formed by isolated tailbud PGCs. Altogether, these findings suggest that xSyntabulin is not likely to be an interaction partner for xKIF13B in PGCs.

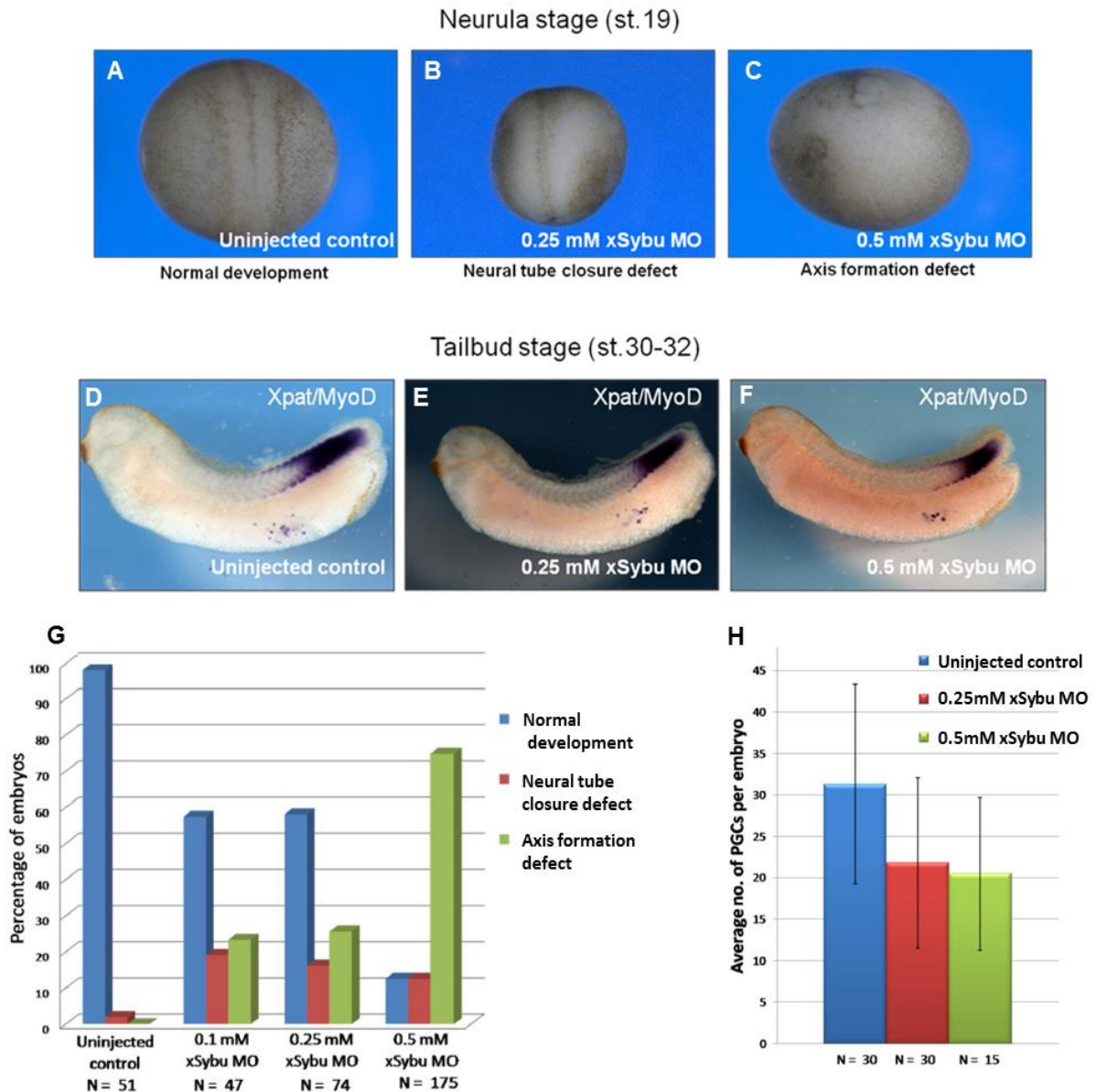


**Fig. 33. Morpholino knock-down of xSyntabulin results in a defect in the neural tube development, but has little impact on PGC number and localization in tailbud stage embryos.** Embryos at 2-cell stage were injected vegetally with xSyntabulin antisense morpholino oligonucleotides (xSybu MO) at different concentrations (0.25 mM and 0.5 mM) and cultivated till stage 19 (B, C) or 30-32 (E, F). Uninjected embryos were used as a control (A, D). (A-C) Defect in the neural tube development and axis formation is seen during neurulation in stage 17-19 *X. laevis* embryos. (A) Dorsal view of an uninjected embryo with normal development. Anterior side is up. (B) Dorsal view of a representative xSybu MO-injected embryo with neural tube closer defect. Anterior side is up. (C) Representative xSybu MO-injected embryo with axis formation defect. (D-F) Embryos, which survived neurulation, at the tailbud stage were subjected to WMISH using Dig-labeled riboprobes for *Xpat* (PGC-specific marker) and *MyoD* (somite marker). (G) Histogram depicting the percentage of neurula stage (St. 19) embryos which developed normally and those which had neural tube closer or axis formation defects after injections of xSybu MO at different concentrations (0.1 mM, 0.25mM and 0.5 mM). Uninjected embryos were used as a control; N corresponds to the total number of embryos. (H) Average number of PGCs in the tailbud stage (St. 30-32) that survived neurulation. Embryos were injected with 0.25 or 0.5 mM of xSybu MO; uninjected embryos were used as a control. Error bars represent the standard deviation of the mean. Experiments and images were prepared with a help of A. Shukla.

## 4. DISCUSSION

In animals, active cell migration plays a major role in many developmental processes, including gastrulation, formation of embryonic tissues and organogenesis. In addition, it is also important for the maintenance and function of mature organisms. For example, wound healing is associated with migration of epidermal cells, while immune response involves directional migration of lymphocytes towards the sites of infection. Precise control of the cell migration is, therefore, very important for the proper development and function of an organism. Aberrations in the regulation of active cell migration may lead to many pathological events, including defects during development, abnormal immune response and formation of metastasis by migrating cancer cells. Hence, understanding of the cellular and molecular mechanisms underlying cell migration is crucial not only for the fundamental studies, but also for the clinical applications (Franz et al., 2002; Webb et al., 2005).

Initiation of active migration is a highly regulated process in many cell types. Investigation of mechanisms underlying transition of cells to active migration is important to understand many developmental and pathological processes. To investigate molecular mechanisms regulating transition to active migration, we used *X. laevis* primordial germ cells (PGCs) as a model system. PGCs are embryonic precursors to the germ cells that are required for maintenance of genomic information in sexually reproducing organisms. In many species, including *Xenopus*, germ line cells are specified in the region distinct to the site of the gonad formation. Therefore, to reach their destination point, PGCs have to be translocated during embryogenesis (Wylie, 1999). In *C. elegans*, this translocation occurs via gastrulation movements, when PGCs are passively involuted inside the embryo in association with surrounding tissue (Chihara and Nance, 2012). However, in many species, including *Drosophila*, zebrafish, *Xenopus* and mouse, passive migration during gastrulation is followed by active migration of individual PGCs at the later stages (Richardson and Lehmann, 2010). This makes PGCs an attractive model to study cell migration.

### 4.1 Polarization and directional migration of *X. laevis* PGCs *in vitro*

#### 4.1.1 *In vitro* PGC migration in the presence of different substrates

Active migration of *X. laevis* PGCs starts after developmental stage 24 and at tailbud stage embryos (stages 24-44) takes place within the endoderm (Nishiumi et al., 2005; Terayama et al., 2013). Due to a high content of the yolk in endodermal cells, it is hard to study cellular and molecular mechanisms underlying active PGC migration. This issue can be solved by the establishment of an *in vitro* migration assay. In our previous studies, active migration of PGCs isolated from tailbud stage embryos was observed on the fibronectin-coated surface (Tarbashevich et al., 2011; Fig. 5). In the same study, it has also been shown that PGCs can be polarized towards crude extract prepared by homogenization of the dorsal part of tailbud stage embryos. However, the number of cells able to migrate in these conditions was very low. To improve migration efficiency, in the context of this study PGCs

were cultivated in the presence of different cellular and artificial substrates (see section 3.1). These experiments demonstrated that PGCs migrate most efficiently in the so called under-agarose migration assay on top of the culture dish pre-coated with bovine serum albumin (BSA) (Fig. 12; section 3.1.2). In this case, PGCs were placed in between surface of the culture dish and polymerized agarose gel. Pre-coating of the culture dish with bovine serum albumin (BSA) was performed to saturate unspecific binding sites. In the under-agarose migration assay, PGCs migrate via bleb-associated mechanism (section 3.1.3). Migrating cells have elongated polarized morphology and can be characterized by waves of cell body contraction perpendicular to the leading edge–cell rear axis. Since no enrichment of actin filaments was observed at the leading edge of migrating cells (Fig. 14), traction force required for cell motility is most likely generated by contractions of the cell body that pushes the cell forward due to compressive forces applied on the agarose gel and surface of the culture dish. Similar morphology, but inability of PGCs to migrate in the assays with less rigid environment (extracellular matrix, embedding in the agarose gel and cultivation in the endodermal cells) favours this assumption (Fig. 8, 10, 11).

Studies in *Drosophila*, zebrafish and mouse demonstrated that surrounding somatic cells contribute to the establishment of directionality and survival of PGCs during active migration (see section 1.3). In *Drosophila* and zebrafish, somatic cells are involved in the shaping of the chemoattractant gradient required for directional migration (Boldajipour et al., 2008; Mahabaleshwar et al., 2008; Richardson and Lehmann, 2010). In addition, E-cadherin-mediated interaction of PGCs with somatic cells in zebrafish is required for PGC motility (Kardash et al., 2010). In mouse, survival and motility of PGCs depends on the Steel factor, expressed by surrounding somatic cells. Steel factor-expressing cells create a ‘motility niche’ and accompany PGCs all the way through their migration to the gonads (Gu et al., 2009). Role of somatic cells was also demonstrated for PGC migration through dorsal mesentery in *X. laevis* embryos. It was suggested, that distribution of fibronectin filaments produced by mesentery cells can guide PGC migration at the early tadpole stage of *X. laevis* development (Heasman et al., 1981; Wylie and Heasman, 1982; Brustis et al., 1984). In addition, PGCs, seeded on the layer of isolated fibronectin-producing mesentery cells, could form filopodia-like protrusions and translocate the cell body (Wylie and Roos, 1976; Heasman et al., 1977). To test possible requirement of somatic cells for active migration of PGCs during tailbud stage of *X. laevis* development, isolated PGCs were cultured in the surrounding of pre-cultivated somatic endodermal cells (Fig. 8; section 3.1.1). During the first several hours of cultivation, PGCs revealed increased cellular dynamics, but could not translocate the cell body. Although cultivation of PGCs in these conditions was performed up to 24 hours, decrease of cellular dynamics after the first few hours, also observed during cultivation of PGCs in the presence of artificial substrates, indicates that somatic endodermal cells do not produce factors required for PGC motility. This can also be confirmed by our previous experiments with isolated PGCs cultivated in the presence of dorsal and ventral homogenized extracts. PGCs cultivated on top of fibronectin-coated Petri dish can be polarized towards crude homogenized extract prepared from the dorsal part of tailbud stage



embryos, but did not respond to the extract prepared from the ventral part, which consists mostly from endodermal cells (Tarbashevich et al., 2011; Fig. 5)

Active migration of PGCs in zebrafish and mouse depends on the gradient of chemoattractant SDF-1 (Doitsidou et al., 2002; Ara et al., 2003; Molyneaux et al., 2003). In these species, polarization of PGCs towards somatic cells expressing SDF-1 is followed by directional migration within the embryo (Kunwar et al., 2006). Since PGC migration takes place during active tissue- and organogenesis, migrating cells must quickly respond to the changes in chemoattractant gradient. In the under-agarose migration assay (described in sections 3.1.3 and 3.2) migrating *X. laevis* PGCs alternated between migratory 'run' phase, characterized by an elongated polarized cell morphology and active migration, and 'tumbling' phase, characterized by a loss of cell polarity and formation of large bleb-like protrusions in random directions. An alternation between 'run' and 'tumbling' phases was also described for zebrafish PGCs (Reichman-Fried et al., 2004), and was recently reported for *X. laevis* PGC migration on fibronectin-coated surface (Terayama et al., 2013). It was suggested that 'tumbling' phase is required to re-establish cell polarity in the environment with dynamically changing gradient of chemoattractant. As it was shown previously, *X. laevis* PGCs can be polarized *in vitro* by a homogenized extract, prepared from the dorsal part of the tailbud stage embryos (Tarbashevich et al., 2011; Fig. 5). Interestingly, in the under-agarose migration assay, PGCs could initiate active migration even in the absence of any gradient (Fig. 12). This suggests that expression of putative chemoattractant(s) in the dorsal part of *X. laevis* embryos is important for PGC polarization, but is not required for PGCs migration. On the other hand, PGCs cultivated in different environmental conditions lost polarization and strongly decreased cellular dynamics several hours after dissociation from the endodermal explant. In the same time, ectopic addition of dorsal extract to the PGCs cultivated in the presence of endodermal cells resulted in a more intensive protrusion formation (Fig. 8; section 3.1.1). These observations can be explained by induction of PGC migration by some factors from the dorsal part of *X. laevis* embryos, and by a remaining potential of PGCs to migrate within few hours after removal of these factors. In the under-agarose migration assay, no increase in the efficiency of PGC migration upon application of dorsal extract can be explained by a poor diffusion of potential factors in the agarose gel.

#### **4.1.2 Role of PIP3 in PGC polarization**

Studies in *Drosophila*, zebrafish and mouse revealed that directionality of PGC migration, similar to chemotaxis in many other cell types, is mediated by G-protein coupled receptors (GPCR) (see section 1.3). In *Drosophila*, polarization and initiation of PGC migration depends on the expression of GPCR, known as Trapped in endoderm 1 (TRE1) (Richardson and Lehmann, 2010). In zebrafish and mouse, SDF-1 gradient is recognized by chemokine C-X-C motif receptor 4 (CXCR4) expressed in PGCs (Knaut et al., 2003; Molyneaux et al., 2003). Interaction of GPCRs with their ligands activates dissociation of heterotrimeric G-proteins. This, in turn, triggers activation of several downstream signaling cascades, including calcium flux, activation of phospholipase C (PLC) and phosphatidylinositol 3-kinase (PI3K) (Dutt et

al., 1998; Wang et al., 2000; Blaser et al., 2006). In *Drosophila* PGCs, activation of TRE1 was suggested to activate the small GTPase Rho1 and cause redistribution of adherent junctions and Rho1 to the cell rear (Kunwar et al., 2006). In zebrafish, activation of CXCR4b in PGCs leads to activation of the other small GTPase, Rac1, required for formation of the actin brushes at the leading edge of migrating cells (Xu et al., 2012). In addition, it also mediates enrichment of  $\text{Ca}^{2+}$  at the leading edge that is required for PGC polarization in zebrafish (Blaser et al., 2006).

Although it is not clear what kind of molecules serves as guiding cue for PGC migration in *X. laevis*, several signaling pathways were described to be involved in proliferation and directional migration of PGCs at the tailbud stage (discussed in section 1.4.3). Similar to zebrafish and mouse, *X. laevis* PGCs at the tailbud stage of embryonic development express CXCR4 that is required for the directionality of PGC migration within the endoderm (Nishiumi et al., 2005; Takeuchi et al., 2010). In the previous studies from our lab, it was shown that formation of bleb-like protrusions and directional migration of *X. laevis* PGCs depends on intracellular distribution of phosphatidylinositol (3,4,5)-trisphosphate (PIP3) (Tarbashevich et al., 2011). Aberrations in intracellular PIP3 levels, mediated by the modulation of endogenous activity of PI3K or PTEN, led to the defects in directionality of migration and loss of PGCs. In isolated PGCs, PIP3 is localized at the plasma membrane and is enriched in the bleb-like protrusions formed by these cells (Fig. 32A). This localization depends on the function of kinesin, xKIF13B, is encoded by the germ plasm-specific mRNA. PGC-specific overexpression of xKIF13B results in the enrichment of PIP3 throughout the plasma membrane and increased formation of bleb-like protrusions, while knock-down leads to the loss of PIP3 localization at the membrane and decreased protrusion formation. Both phenotypes cause defects in directionality of migration and loss of PGCs, similar to the aberrations in intracellular PIP3 levels (Tarbashevich et al., 2011).

In the present study, PGC-specific expression of pleckstrin homology (PH) domain of GRPI protein that served as a PIP3 sensor, was used to monitor endogenous PIP3 distribution in isolated *X. laevis* PGCs during active migration in the under-agarose assay. During the migratory 'run' phase, no enrichment of PIP3 at the leading edge of PGCs was observed. However, enrichment of PIP3 was restored in the bleb-like protrusions formed by PGCs at the 'tumbling' phase (Fig. 15). This suggests PIP3 to be involved in polarization of the cell prior to active migration; however, maintenance of polarized PIP3 distribution during active phase of migration is not required. Interestingly, loss of polarized PIP3 distribution in PGCs, caused by knock-down and overexpression of xKIF13B, or by modulating endogenous activity of PI3K and PTEN, resulted in migration of these cells to ectopic locations in tailbud stage *X. laevis* embryos (Tarbashevich et al., 2011). Similar PGC distribution was reported in *X. laevis* embryos with upregulated expression of SDF-1 (Bonnard et al., 2012). This phenotype is different in comparison to the clustering of PGCs in the endoderm observed in *Dnd* and *Xdazl* knock-down (Houston and King, 2000b; Horvay et al., 2006). Ectopic localization of PGCs was also observed in zebrafish and mouse embryos upon knock-down of SDF-1 and its

receptor CXCR4 (Ara et al., 2003; Molyneaux et al., 2003; Reichman-Fried et al., 2004). Altogether, these observations suggest that polarized PIP3 distribution in *X. laevis* PGCs is required for cell polarization and directionality of migration at the tailbud stage, but not for cellular motility.

## 4.2 Role of cellular dynamics in the transition to active migration

Transition to the active migration in many cell types, including *Drosophila*, zebrafish and mouse PGCs, correlates with increased cellular dynamics (discussed in section 1.3). To investigate this phenomenon in *X. laevis* PGCs, cells were isolated from embryonic stages before and after PGC transition to active migration *in vivo* (Fig. 7). Since active migration of *X. laevis* PGCs is initiated after developmental stage 24, PGCs were isolated from stage 17-19 (neurula) and stage 28-30 (tailbud) embryos to obtain pre-migratory and migratory cells, correspondingly. Electric Cell-substrate Impedance Sensing (ECIS) measurements, as well as time-lapse image analysis, demonstrated increased cellular dynamics of PGCs isolated after the transition to active migration in comparison to the pre-migratory cells (Fig. 17). Somatic endodermal cells, isolated at the same developmental stages, showed almost no cellular dynamics in comparison to both pre-migratory and migratory PGCs. Main contribution to the increased cellular dynamics observed in PGCs belongs to the formation of bleb-like protrusions. These protrusions are formed randomly by the isolated PGCs, and, similar to other cell types, depend on the assembly and disassembly of actin cortex. Actin cortex was detected at the periphery of the isolated PGCs underneath cell membrane, but was excluded from the plasma membrane of bleb-like protrusions. Re-polymerisation of actin underneath the plasma membrane of bleb-like protrusions caused retraction of cell membrane to its initial position. In addition, inhibition of actin polymerization by Cytochalasin B resulted in the loss of cellular dynamics. According to the detrended fluctuation analysis of ECIS measurements, increased fluctuations of the cell shape observed in PGCs isolated after the transition to active migration was characterized by a long term memory. In contrast to tailbud stage PGCs, long-term behaviour of PGCs isolated from the neurula stage was not characterized by persistent cellular movement (section 3.3.1). In summary, these results demonstrate that in comparison to pre-migratory PGCs and somatic endodermal cells, migratory PGCs are characterized by increased and persistent cellular dynamics, and that this dynamics depends on the formation of bleb-like protrusions.

Analysis of PGC migration *in vitro* also confirms contribution of increased cellular dynamics to the initiation of active migration. Most of the pre-migratory PGCs isolated from the neurula stage were characterized by low cellular dynamics, absence of polarization and did not initiate active migration. In contrast, more than a half of PGCs isolated from the tailbud stage were characterized by increased cellular dynamics and elongated migratory morphology. Some PGCs isolated from the neurula stage, however, could migrate *in vitro* in the same manner as PGCs isolated from tailbud stage embryos, suggesting that increased cellular dynamics is not the only process regulating initiation of active PGC migration in *X. laevis* embryos (Fig. 16).

Altogether, these findings nicely correlate with recently published results by Terayama et al. (2013). In their work, authors analysed relative amount of different morphological subtypes of isolated PGCs at different stages of *X. laevis* development. They demonstrated that before stage 25 most of *X. laevis* PGCs have stationary, round morphology with low amount of bleb-like protrusions. After transition to the active migration, most of the isolated cells were characterized by increased plasma membrane blebbing or elongated migratory morphology. In addition, inhibition of actin polymerization and myosin activity led to the abolishment of cellular dynamics.

### 4.3 Cell-cell and cell-extracellular matrix adhesion in active migration

#### 4.3.1 Role of adhesion during PGC migration

In addition to cellular dynamics, regulation of cellular adhesion is also one of the key mechanisms that govern transition to active migration. Relatively weak cell adhesion was observed in many cells migrating via bleb-associated mechanism (Charras and Paluch, 2008; Fackler and Grosse, 2008). Downregulation of cell adhesion was shown to be required for initiation of migration in many cell types, including *Drosophila*, zebrafish and mouse PGCs (Richardson and Lehmann, 2010). However, for several other cell types, especially those migrating via lamellipodia-based mechanism, adhesion to the substrate is required to generate traction force for the migration (Giannone et al., 2007; Le Clainche and Carlier, 2008). In this context, regulation of cellular adhesion during PGC migration in zebrafish is especially interesting. Downregulation of E-cadherin is required to initiate PGC migration in zebrafish, but certain level of E-cadherin expression is still required to generate traction force for translocation of the cell body (Blaser et al., 2005; Kardash et al., 2010). Moreover, some cell types, like lymphocytes and cancer cells, can switch between bleb-associated and lamellipodia-based motility depending on the environment (Charras and Paluch, 2008). Several observations also indicated that regulation of cellular adhesion might be involved in the development of *X. laevis* PGC. In these studies, knock-down of *Germes*, *Xdazl* and *Dnd*, encoded by germ plasm-associated transcripts, resulted in the clustering and subsequent loss of PGCs in the endoderm of tailbud stage embryos (Houston and King, 2000b; Horvay et al., 2006; Lai et al., 2012).

Interestingly, migration of *X. laevis* PGCs in the under-agarose migration assay on top of BSA-coated culture dish demonstrated that specific cell adhesion is not required for active migration of these cells *in vitro* (Fig. 12). Furthermore, surrounding cells were able to 'anchor' PGCs in the under-agarose migration assay and prevent their motility (Fig. 13). Similar observations were done during cultivation of PGCs in the presence of cellular and artificial substrates (Fig. 8, 10, 11). Adhesive contacts between PGCs and cellular or artificial substrates, including surrounding endodermal cells, fibronectin and uncoated surface of the culture dish, were observed not at the leading edge, but rather at the cell rear. Instead of facilitating PGC migration, these contacts were quite stable and often prevented motility of PGCs. These findings differ from the observations of zebrafish PGC migration *in vivo*. In zebrafish, complete loss of E-cadherin-mediated cell adhesion between PGCs and

surrounding somatic cells resulted in the loss of PGC motility (Kardash et al., 2010). Since migration of both *X. laevis* and zebrafish PGCs occurs via bleb-associated mechanism, it is possible that cells can compensate a lack of substrate rigidity *in vivo* by weak adhesion to the substrate. It is also possible that presence of some extracellular factors, like chemoattractants, might alter mechanism of active migration.

Another interesting observation from the under-agarose migration assay is the ability of some PGCs isolated neurula stage embryos to migrate in the same manner as PGCs isolated from the tailbud stage. This suggests that although specific cell adhesion is not required for PGC migration via bleb-associated mechanism *in vitro*, it might be involved in the regulation of the transition to active PGC migration in *X. laevis* embryos.

#### **4.3.2 Quantification of cell-cell and cell-extracellular matrix adhesion of PGCs**

To investigate role of cellular adhesion in the transition to active PGC migration, adhesive properties of pre-migratory (neurula) and migratory (tailbud) PGCs were determined by Single-Cell Force Spectroscopy (SCFS). Quantitative analysis of interactions formed between PGCs and extracellular matrix components, fibronectin and Collagen I, as well as between PGCs and surrounding somatic endodermal cells, was performed (Fig. 21). Interaction with extracellular matrix components revealed stronger attachment of pre-migratory PGCs to fibronectin. This was similar to mouse PGCs that decreased adhesion to fibronectin during initiation of active migration (Ffrench-Constant et al., 1991). In the previous studies in our lab (Tarbashevich et al., 2011), as well as in the recently published results by Terayama et al. (2013), PGCs isolated from tailbud stage *X. laevis* embryos could migrate *in vitro* on top of the fibronectin-coated surfaces. However, motility of isolated PGCs on BSA-coated culture dish in the under-agarose migration assay, described in the present study, demonstrates that these cells do not require fibronectin for migration. PGC-specific downregulation of fibronectin was also detected by whole transcriptome analysis, but this observation was not confirmed by quantitative RT-PCR (Fig. 24, 25). Role of fibronectin was also addressed during PGC migration through dorsal mesentery in early tadpole stage of *X. laevis* embryos. PGCs isolated from this stage could regain migratory and invasive activity if cultured on top of fibronectin-producing mesentery somatic cells. It was suggested that distribution of fibronectin filaments could be involved in polarization of PGCs. However, exact role of fibronectin during active PGC migration in *X. laevis* remains to be clarified.

In addition to the decreased adhesion of migratory PGCs to fibronectin, their adhesion to surrounding endodermal cells was also decreased in comparison to pre-migratory PGCs (Fig. 20). In contrast, no significant difference in the adhesion of two somatic endodermal cells isolated from the neurula stage in comparison to the adhesion strength between two somatic endodermal cells isolated from tailbud stage embryos has been noted. Interestingly, strength of adhesion between somatic cells was comparable to the adhesion of somatic cells and pre-migratory PGCs, but was significantly reduced between somatic cells and migratory PGCs.

These results nicely correlate with the whole transcriptome analysis of PGCs and somatic endodermal cells isolated from the neurula and tailbud stages. Next generation sequencing analysis was performed to identify candidate genes involved in the transition to active PGC migration (Fig. 24). It revealed differential expression of several candidate adhesion molecules. Quantitative RT-PCR with PGCs and somatic endodermal cells isolated from the neurula and tailbud stages was performed to validate results of next generation sequencing analysis (Fig. 25). Expression of several adhesion molecules, including Claudin 6.1 (Cldn6.1), E-cadherin and gap junction protein beta 1 (Gjb1), was specifically downregulated in the migratory PGCs. These molecules represent different types of cell junctions. Claudins mediate cell-cell adhesion in the tight junctions that are often involved in formation of diffusion barriers (Koval, 2006); gap junction proteins are involved in the formation of hydrophilic channels between cells in the gap junctions (Evans and Martin, 2002); cadherins in the adherent junctions form dimers in  $\text{Ca}^{2+}$ -dependent manner with other cadherins on adjacent cells (Harris and Tepass, 2010). Both tight and gap junctions mediate very strong adhesion between the cells, and has to be removed during transition to the active migration in many cell types. Adherent junctions are not that potent and usually are highly regulated in migratory cells.

Role of E-cadherin in PGC migration was demonstrated for other model organisms. In *C. elegans*, E-cadherin is postranscriptionally upregulated to mediate attachment of PGCs to endodermal cells for the internalisation during gastrulation (Lai, 2004). In *Drosophila*, E-cadherin is also required for the internalisation of PGCs. However, prior to cell dispersal and initiation of active migration, E-cadherin is redistributed to the rear of polarized cells (Richardson and Lehmann, 2010). Later, E-cadherin is required for coalescence of PGCs with somatic gonadal precursors (Santos and Lehmann, 2004a). This suggests complex regulation of E-cadherin expression during PGC development in *Drosophila*. In zebrafish, downregulation of E-cadherin is required to initiate PGC migration (Blaser et al., 2005). However, certain level of E-cadherin is required for the attachment of migrating zebrafish PGCs to surrounding cells in order to generate traction force (Kardash et al., 2010). In mouse, similar to *Drosophila*, expression of E-cadherin in PGCs is required for the coalescence of these cells with somatic gonadal precursors (Bendel-Stenzel et al., 2000).

Downregulation of several adhesion molecules involved in formation of different types of cell junctions was not previously reported for PGCs. Since many adhesion proteins are regulated post-translationally, further analysis is required to confirm that downregulation of these molecules is indeed required for the transition of PGCs to active migration.

#### 4.4 Differential gene expression in PGCs

##### 4.4.1 Regulation of gene expression in PGCs among different species

Regulation of gene expression is a key mechanism involved in the PGC development in many species. Tight regulation of gene expression is required to maintain pluripotency of

the germ line and avoid differentiation into the somatic cells. As discussed in section 1.1, there are two main alternative mechanisms of germ line specification. In most of the prominent model organisms in developmental biology, including *C. elegans*, *Drosophila*, zebrafish and *Xenopus*, specification of the germ line depends on the inheritance of maternal determinants, often organized in the specific structure or region during oogenesis, known as germ plasm (Klock et al., 2004). The second mechanism involves induction of the germ line specification by signals coming from surrounding embryonic tissue. Although specification via inheritance of maternal determinants is observed in many species, more detailed analysis revealed that specification via inductive mechanism is more common and seems to be ancestral for metazoans (Extavour and Akam, 2003). Furthermore, some species use a combination of both and can compensate depletion of maternal determinants by the induction of germ line fate. In addition, even among the same class of animals, for example among amphibians or among insects, there is no conservation of germ line specification mechanism among species (Seervai and Wessel, 2013). This suggests that transition from inductive mechanism to specification by maternal determinants occurred multiple times during evolution. This is reflected in the differences in the molecular mechanisms underlying germ line specification and development. However, most of these differences occur during the specification of germ line. It is remarkable that many events during germ cell development are conserved, or at least similar, in different species (discussed in the Introduction). After specification, molecular mechanisms gradually become more and more similar among species during germ cell line development. One of the key features of germ line cells in all species is a complex regulation of gene expression during development. Zygotic transcription in germ line cells is inhibited right after the specification, independent of the specification mechanism (Nakamura and Seydoux, 2008). This inhibition involves repression of transcription, chromatin remodeling and translational regulation. However, several important differences depending on the type of specification can be outlined. In addition to the repression of somatic gene expression, in case of specification via inductive mechanism, for example in mice, to acquire germ line fate cells have to induce transcription of several genes required for pluripotency and germ cell development (Nakamura and Seydoux, 2008). In contrast, species that inherit maternal determinants for germ line specification, globally repress transcription, since most of the factors required for pluripotency and germ line differentiation are maternally supplied. Although molecular factors involved in transcriptional repression are not conserved among species, mechanisms of global transcriptional repression are strikingly similar and evolve block of transcriptional elongation by RNA polymerase II and chromatin remodeling (Nakamura and Seydoux, 2008). Since in these species transcription is globally repressed, a key role in the regulation of early primordial germ cell development belongs to the post-transcriptional regulation, specifically to the translational regulators, including Dead end, Nanos and Vasa, which are highly conserved among species. Moreover, function of these factors is also required in almost all investigated species, including those with inductive mechanism of germ line specification, during germ cell proliferation in gonads (discussed in the Introduction). In zebrafish and *Xenopus*, function of translational regulators was demonstrated to be important for the

active PGC migration. Remarkably, transition to the active migration in *Drosophila*, zebrafish and *Xenopus* is highly correlated with the release of transcriptional silencing and initiation of zygotic expression in PGCs. Since translational regulators are expressed throughout the PGC development, most likely they play an indirect role in the PGC migration by post-transcriptional regulation of stability and/or expression of the specific genes. However, exact molecular mechanisms of this regulation remain unclear. It is also not clear what triggers zygotic gene expression and PGC transition to active migration. One possibility is that induction of zygotic transcription and initiation of PGC migration is mediated by chemoattractant or other extracellular factors. However, knock-down of SDF-1 $\alpha$  and CXCR4b in zebrafish did not influence motility of PGCs, but resulted in loss of directionality during migration (Reichman-Fried et al., 2004). Another possibility is time-dependent degradation of maternally supplied factors involved in the repression of transcription in PGCs.

#### **4.4.2 Strategy for the next generation sequencing analysis**

In *Xenopus*, zygotic transcription in somatic cell starts during midblastula transition at stage 8-9 of development. In PGCs, however, transcription is repressed up to the late neurula stage (Venkatarama et al., 2010). Although exact development stage is not known, initiation of PGC zygotic transcription at the late neurula stage correlates with PGC transition to active migration shortly after at the early tailbud stage 24 (Nishiumi et al., 2005; Terayama et al., 2013). To identify factor involved in the transition of PGCs to the active migration, whole transcriptome analysis of PGCs isolated from neurula (stage 17-19) and tailbud stage (28-30) of *X. laevis* development was performed. In addition, somatic endodermal cells isolated from corresponding stages were included in the analysis. Analysis of gene expression in somatic cells was used to identify genes specifically up- or downregulated in PGCs. In addition, comparison of gene expression in PGCs and somatic cells can be used to identify novel PGC-specific transcripts. Labeling of PGCs was done by the injection of *in vitro* transcribed chimeric mRNA, consisting of GFP ORF fused to the Dead end localization element (Fig. 7). Several draw-backs of this method, including relatively high background signal in somatic cells and different signal intensity in PGCs, made it not possible to use automated sorting techniques for the isolation of specific cell populations. This issue was solved by the manual isolation of 30 PGCs and 30 somatic cells from the corresponding developmental stage and subsequent amplification of the starting material prior to the analysis (discussed in section 3.5.1). In the context of developmental biology, differences between individual organisms, as well as differences in the environmental conditions during cultivation, might significantly influence the outcome of the analysis. To reduce bias that can be caused by these differences, all four populations of cells used for whole transcriptome analysis were isolated from the same batch of embryos, cultivated in the same environment.

Analysis of gene expression in the small population of cells (up to single cell) is an interesting emerging concept. In most of the previous studies, this analysis has been done using quantitative or semi-quantitative RT-PCR and microarrays. However, sensitivity of most high throughput platforms is not sufficient and additional amplification steps are



required prior to the analysis. Application of the next generation sequencing techniques requires several additional steps in the preparation of the material for the analysis. Since sequencing can be done only with DNA sample, generation of cDNA from the mRNA is required. In addition, DNA fragments used for the analysis must be relatively short (100-300 bp) and flanked by the specific sequences. All these steps can lead to the bias in the results, for example due to the preferential amplification of one transcript in comparison to the other. In addition, contamination of the starting material, for example presence of somatic cells in the PGC population, can be amplified and influence the results. Therefore, outcome of the analysis must be validated using alternative methods.

#### **4.4.3 Annotation of the next generation sequencing results**

For the annotation, short sequences (reads) generated by the next generation sequencing platforms should be normalized and aligned to the database representing genome or transcriptome of the corresponding model organism. However, annotation of *X.laevis* database is quite poor due to the fact that *X. laevis* genome has not been sequenced. In addition, this species is pseudotetraploid that results in the presence of several alleles for the certain genes. To overcome this issue, alignment has been done using database of *Xenopus tropicalis*. In contrast to *X. laevis*, *X. tropicalis* is diploid and its genome has been sequenced and much better annotated. Although both of these species belong to the same genus, possible differences in the sequence could influence the outcome of the analysis. This should be kept in mind for the interpretation of the results. For example, one gene in *X. tropicalis* might have multiple isoforms in *X. laevis*.

In the context of this study, to compare differences in the expression between several cell populations, expression level of the genes in one population was normalized to the total amount of sequences (reads) obtained for this population. This eliminates bias of the detection and differences in the total amount of material used for the analysis between different cell populations, keeping the ratio of gene expression in the specific population unaffected. Since the longer genes generate more fragments during the preparation of the material for the analysis, to compare gene expression within one cell population, expression was normalized to the size of the gene (see section 2.7.7).

#### **4.4.4 Analysis of the differential gene expression**

As it was mentioned above, many events during preparation of the material for next generation sequencing could trigger bias in the results. In the context of this study, whole transcriptome analysis was used to identify differentially regulated candidate molecules between pre-migratory and migratory PGCs. However, no information was available concerning differential gene expression in the endoderm between stage 17-19 and stage 28-30. Therefore, results of the next generation sequencing analysis were compared to the previous observations concerning differential gene expression in embryonic tissues and PGCs (Fig. 22). As evident from the analysis, expression of previously identified PGC-specific genes, including *Pat* (Hudson and Woodland, 1998), *DeadEnd* (Horvay et al., 2006), *Dazl* (Houston and King, 2000b), *Nanos* (Lai et al., 2011), *DeadSouth*, *KIF13B* (Tarbashevich et al., 2011),

*Syntabulin* (current study, see section 3.8.2) and *GRIP2* (Tarbashevich et al., 2007; Kirilenko et al., 2008), was increased in the PGC populations in comparison to the somatic cell populations. However, expression of these genes in somatic cells isolated from the neurula stage (stage 17-19) was higher in comparison to the somatic cells isolated from the tailbud stage (stage 28-30). One of the explanations for this observation is a contamination of somatic cell population with PGCs. The other possibility is an incomplete degradation of the maternal transcripts inherited by somatic cells. Degradation of PGC-specific transcripts in somatic cells is mediated by microRNA-dependent mechanism. This degradation takes place at the gastrula stage, and could be incomplete at the neurula in comparison to the tailbud stage. Several observations favour the second assumption. According to the first one, presence of *Pat* was detected by quantitative and semi-quantitative RT-PCR in several experiments in non-amplified cDNA sample obtained from the neurula stage somatic endodermal cells in comparison to the somatic cells from the tailbud stage. In these experiments, expression of *Pat* in PGCs was significantly higher (data not shown). The second observation is a high background of the GFP signal in the somatic cells at the neurula stage in comparison to the tailbud stage in the embryos injected with *GFP\_DELE* mRNA. Injection of *GFP\_DELE* mRNA to label PGCs can be the actual reason for the incomplete degradation of maternal PGC-specific transcripts in somatic cells at the neurula stage, since labelling of PGCs by this mechanism also relies on the degradation of *GFP\_DELE* in somatic cells by microRNA-mediated mechanisms. *GFP\_DELE* can, therefore, serve as a competitor for the endogenous transcripts. Cells used for both RT-PCR and next generation sequencing were isolated from *GFP\_DELE*-injected embryos.

Expression of the previously identified PGC-specific transcripts was also compared to the expression of the genes commonly used for normalization of gene expression in other cell types (Stürzenbaum and Kille, 2001). In comparison to increased expression of PGC-specific genes in PGC populations used for next generation sequencing, expression of *ODC*, *GAPDH*, *Tubulin alpha*, *Tubulin beta*, *Actin beta*, *Actin gamma* did not reveal any specific enrichment. Some differences in the expression of these genes between cell populations could be expected, since no information about expression of these genes in the endoderm was available. As a negative control, expression of the mesoderm and neural markers was relatively low in the PGC and somatic cell populations, corresponding to the errors of the analysis.

To validate the next generation sequencing analysis experimentally, spatio-temporal expression analysis of several candidate PGC-specific genes was performed by whole mount in situ hybridisation (WMISH). For the analysis, genes with different expression level, but with the enrichment in PGCs similar to the PGC-specific genes were selected. As expected, expression of these genes in the endoderm was observed in the individual cells, resembling PGC-like expression pattern (Fig. 23). Expression of some genes was also observed in other tissues. With the exception of *CPEB1* and *Velo7*, generated antisense Dig-labelled riboprobes for the WMISH were complementary to 3' end of the mRNA, which could include poly(A) site

and 3'UTR. This could explain poor signal for many transcripts, and absence of the signal in the endoderm of the neurula stage (stage 17-19). In addition, high expression outside the endoderm for some genes was observed that also could reduce staining intensity in the individual cell in the endoderm.

In conclusion, whole transcriptom analysis by next generation sequencing revealed expected expression pattern of the previously identified genes, and could be validate experimentally. Expression analysis of candidate PGC-specific genes with WMISH demonstrated that results from the next generation sequencing data can be used for the identification of novel PGC-specific transcripts. However, since in the context of this project main focus was on the transition of PGCs to the active migration, no further analysis in this direction was performed.

#### **4.4.5 Differential gene expression in migratory and pre-migratory PGCs**

To identify candidate genes differentially regulated during the transition to active PGC migration, several thresholds to the data were applied (discussed in section 2.7.7 and 3.6.1). Since zygotic expression in *X. laevis* PGCs starts already at the neurula stage, relatively low, two fold, threshold for the difference in the expression was used. Since the lowest values of normalized expression for previously identified PGC-specific genes started at around 100, this value was used as a threshold to eliminate the measurement error. To limit analysis for the differences in gene expression specifically to PGC, all genes that were co-upregulated or co-downregulated in somatic endodermal cells were excluded. In this case differences in the gene expression between PGCs had to stay above two fold after normalization to the difference in somatic endodermal cells.

This approach resulted in identification of 449 candidate genes differentially regulated specifically in PGCs during the transition of these cells to active migration. Among them, 262 genes were upregulated and 187 were downregulated. Genes were arbitrary grouped according to the available information about their function in the cell. Groups were chosen in order to reflect main events that could be connected to initiation of active migration (Fig. 24). Many genes were involved in the regulation of transcription and translation. As it was mentioned above, activation of transcription correlates with initiation of PGC migration in several species. Translational control is also involved in the regulation of active PGC migration. In the group of transcription, genes encoded different transcription factors, chromatin modifiers and cell cycle regulators. Among downregulated genes, relative amount of the genes involved in transcription was higher in comparison to the genes involved in translation. Interestingly, the situation was opposite in the group of upregulated genes. Large amount of upregulated genes encoded ribosomal proteins that suggests activation of translation.

Comparison between up- and downregulated genes involved in protein modification and degradation reveals upregulation of genes involved in folding (shaperons),

ubiquitination and protein degradation. In the same time, several protease inhibitors, a2m and serpine2, are downregulated.

Some genes, both up- and downregulated, were involved in intracellular dynamics, including regulation of cytoskeleton and vesicular traffic. Another group of differentially expressed genes was involved in cell signaling. However, it is hard to make any conclusions about regulation of specific signaling pathways.

Interestingly, many differentially expressed genes were involved in homeostasis. Both up- and downregulated genes encoded membrane channels, metabolic genes, regulators of iron and calcium levels. Upregulation was observed for the genes involved in lipid metabolism.

Adhesion molecules were grouped separately, since our previous finding described in the present study demonstrated decrease of the cell adhesion during transition to active migration (see section 3.4.1). Downregulation of several adhesion molecules was confirmed by quantitative RT-PCR (qRT-PCR). Remarkably, results from next generation sequencing analysis and qRT-PCR demonstrated correlation in relative expression of some of these genes in comparison between different cell populations. Interestingly, several candidate adhesion molecules were found to be upregulated, but this could not be confirmed by quantitative RT-PCR. Several genes could not be assigned to any group due to the lack of information about their function.

Although it is tempting to analyse these groups of genes in order to find specific pathways or correlations, results of this analysis cannot be used to make conclusive statements. Analysis was performed only one time, and may contain many bias effects. However, as demonstrated in section 3.5.3, it can be used to identify candidate molecules for the further functional analysis.

## **4.5 Role of xKIF13B in the active PGC migration**

### **4.5.1 xKIF13B in the early stages of *X. laevis* embryogenesis**

Several germ plasm-associated transcripts, including Dnd, Xdazl, Nanos1, Fatvg, Germes, XGRIP2, and xKIF13B, were shown to be involved in the directional migration and survival of *X. laevis* PGCs at the tailbud stage (discussed in sections 1.2.5 and 1.4). Some of them, like Dnd, Xdazl and Nanos1, are translational regulators and influence PGC migration indirectly (Houston and King, 2000b; Horvay et al., 2006; Lai et al., 2012). Fatvg mediates vegetal localization of germ plasm-associated and other vegetally localized transcripts and is important for germ plasm assembly and embryonic patterning (Chan et al., 2007). Most likely, Germes is also indirectly involved in the regulation of PGC migration through organization of germ plasm (Berekelya et al., 2007). Since members of GRIP family are PDZ domain-containing adaptor proteins, XGRIP2 was suggested to be directly involved in the regulation of PGC migration similar to its homologues in other species (Tarbashevich et al., 2007; Kirilenko et al., 2008). In our previous studies, xKIF13B was shown to be involved in

the regulation of endogenous PIP3 distribution in PGC and, therefore, PGC polarization (Tarbashevich et al., 2011). However, it was not clear, whether effect of xKIF13B knock-down and overexpression directly effects PGC migration and survival at the tailbud stage, or is a consequence of its function earlier in the development. For example, similar to *Fatvg*, it could regulate assembly of the germ plasm. As it had been shown previously, xKIF13B transcripts are localized in the germ plasm during oogenesis and remain to be associated with the germ up to the gastrula stage. Later, xKIF13B expression could have been detected in the PGCs and nervous tissue at the tailbud stage (Tarbashevich, 2007). However, expression of xKIF13B in neurula and early tailbud stages had not been detected. It can be explained by the low expression level of xKIF13B that is also evident from the whole transcriptome analysis with isolated PGCs (Fig. 22). Moreover, in contrast to the midblastula transition to zygotic gene expression in somatic cells, transition to the zygotic transcription in PGCs occurs at the neurula stage of embryogenesis (Venkatarama et al., 2010).

To investigate xKIF13 expression during transition to active PGC migration, spatio-temporal expression of xKIF13B in *X. laevis* embryos at the neurula stage (stage 17-19), early tailbud stage prior to active migration (stage 22-23) and early tailbud shortly after the transition (stage 24-25) was analyzed by whole mount in situ hybridization (WMISH) (Fig. 26). To increase the sensitivity of WMISH, hybridization was performed with a complex digoxigenin-labeled antisense riboprobe that, unlike the probe used in the previous studies, covered several regions in the xKIF13B mRNA. This modification revealed PGCs-like pattern of xKIF13B expression in the endoderm at all analyzed embryonic stages. This pattern was very similar to the expression pattern of PGC marker *Pat*. Besides, similar to the previous observations, expression of xKIF13B was also detected in the developing nervous system. Human homologue of KIF13B, also known as GAKIN, was described to be involved in the polarization of hippocampal neurons prior to the axonal growth. Expression of xKIF13B in developing nervous system, therefore, could suggest similar function in *X. laevis* embryos.

To test whether xKIF13B functions before the transition to active PGC migration, knock-down of xKIF13B was performed by the injection of antisense morpholino nucleotides (xKIF13B MO) in the germ plasm region of 2-cell stage embryos. Germ plasm and PGC distribution at different stages of *X. laevis* development was analyzed by WMISH with antisense probe against a known marker gene, *Pat*. Germ plasm distribution and localization shortly after xKIF13B MO injections were not affected in comparison to the injection of control unspecific morpholino oligonucleotides (Control MO) and uninjected control (Fig. 27). Interestingly, the number of PGCs in the xKIF13B-deficient embryos before the transition to active PGC migration was similar to the control, but was significantly reduced at the tailbud stage (Fig. 28). Similar to the previous observations, many PGCs at the tailbud stage were mislocalized. As it was demonstrated previously, PGCs in tailbud stage embryos (stage 31-32) are normally distributed within the endoderm between the 7<sup>th</sup> and the 13<sup>th</sup> somites (Tarbashevich, 2007; Dzementsei, 2009). In the xKIF13B knock-down morphants, however, many PGCs are found outside this region. No difference in the distribution and

relative location of PGCs in *X. laevis* embryos before the transition to active migration was observed (data not shown). In addition, TUNEL staining demonstrated that the decrease in PGC number at the tailbud stage in KIF13B MO-injected embryos was not caused by the apoptosis (Fig. 29). Interestingly, it was shown that motor domain of KIF13B can bind to the stalk domain of the same molecule (Yamada et al., 2007). It was suggested, that in the absence of cargo, KIF13B is auto-inhibited by the intermolecular interaction. Binding of cargo to the stalk domain would then activate the translocation of the motor-cargo complex (Yamada et al., 2007). Therefore, it can be assumed that xKIF13B is not functional in PGCs before the tailbud stage, but can be activated during the transition to active PGC migration by some intracellular factors.

Unfortunately, it was not possible to detect endogenous levels of xKIF13B protein. In the previous studies, a polyclonal antibody for xKIF13B has been raised. However, obtained level of sensitivity was not sufficient to visualize the endogenous protein. Nevertheless, the antibody was successfully employed to detect xKIF13B in embryos injected with the corresponding mRNA. xKIF13B MO was demonstrated to block protein expression of the injected xKIF13B mRNA containing 5' UTR (Tarbashevich, 2007; Tarbashevich et al., 2011).

Despite of the similarity in the reduction of PGC number at the tailbud stage, knock-down of xKIF13B differs in several aspects from knock-down of translational regulators Dnd, Xdazl and Nanos1. In contrast to the xKIF13B MO phenotype, PGC deficient in these translational regulators cluster in the endoderm at the early tailbud stage and fail to leave the endoderm later on (Houston and King, 2000b; Horvay et al., 2006; Lai et al., 2012). Nanos1-depleted PGCs inappropriately express somatic endodermal genes downstream VegT and initiated zygotic transcription already at the midblastula transition. Furthermore, Nanos1-deficient PGCs appear to undergo apoptosis rather than convert to normal endoderm (Lai et al., 2012).

In conclusion, in the context of PGC migration, function of xKIF13B is required after the transition of PGCs to active migration. In contrast to the factors involved in germ plasm assembly and PGC-specific translational regulators, xKIF13B seems to be directly involved in the active PGC migration by establishing polarity of PGC through intracellular distribution of PIP3.

#### **4.5.2 xCentaurin- $\alpha$ 1 as a candidate interaction partner for xKIF13B**

Role of KIF13B in the PIP3 distribution was originally described in hippocampal neurons. It was suggested that KIF13B mediates traffic of PIP3 coated vesicles to the axonal cone (Horiguchi et al., 2006). Polarized PIP3 distribution is required for polarization of neurons prior to axonal growth. Interaction with PIP3 was shown to be mediated by direct interaction of KIF13B, Centaurin- $\alpha$ 1, also known as PIP3 binding protein (PIP3BP) (Venkateswarlu et al., 2005). KIF13B, similar to other motor proteins, consists of motor and stalk domains. Motor domain is conserved in motor proteins and is responsible for microtubule-dependent translocation. Stalk domain is much less conserved and contains

binding sites for the interaction with adaptor or cargo molecules (Hanada et al., 2000; Asaba et al., 2003). Mapping of the functional domains of xKIF13B revealed that overexpression of N-terminal part of the stalk domain mimic the phenotype of xKIF13B knock-down. It was suggested, that this part may act as a dominant negative for xKIF13B (Dzementsei, 2009). Interestingly, this part contained binding site for Centaurin- $\alpha$ 1. To test possible role of the *Xenopus* homologue of Centaurin- $\alpha$ 1 in PGCs as an adaptor for the kinesin xKIF13B, expression analysis by RT-PCR, as well as WMISH, were performed (Fig. 30). Expression of xCentaurin- $\alpha$ 1 in *X. laevis* embryos was not observed before midblastula transition, suggesting that in contrast to xKIF13B it is not maternally inherited. After midblastula transition, expression of xCentaurin- $\alpha$ 1 was first gradually increased up to stage 22, and then gradually decreased before it almost completely disappearing at the early tadpole stage. Distribution of xCentaurin- $\alpha$ 1 expression was restricted to the developing nervous system and could not be detected in the endoderm. Spatio-temporal expression of xCentaurin- $\alpha$ 1 suggests that in *X. laevis* embryos it might also be involved in the maturation and polarization of neurons. It may also interact with xKIF13B in developing neurons, since xKIF13B is also expressed in the nervous system. However, no expression in the endoderm, confirmed by the whole transcriptome analysis of isolated PGCs and somatic endodermal cells, suggests that xCentaurin- $\alpha$ 1 is not involved in the interaction with xKIF13B in *X. laevis* PGCs.

#### **4.5.3 xSyntabulin as a candidate interaction partner for xKIF13B**

Similar to xKIF13B, xSyntabulin (xSybu) mRNA was also found to be localized to the vegetal pole of *Xenopus* oocytes (Horvay et al., 2006). Syntabulin (or Syntaxin-1-binding protein) is a microtubule associated protein that serves as an adaptor for conventional kinesin-1 heavy chain (KHC), or KIF5B. In the neurons, this association mediates transport of mitochondria and vesicles containing syntaxin-1 along neuronal axons to the presynaptic membrane in order to form there SNARE core complex (Su et al., 2004; Cai et al., 2005). Furthermore, the Syntabulin-KIF5B interaction was also shown to mediate the axonal transport of active zone (AZ) precursors generated in the trans-Golgi network to the nascent synapses that is required for presynaptic assembly (Cai et al., 2007). Apart from its role in the nervous system, Syntabulin is also known to regulate the microtubule-dependent transport of the dorsal determinants (DDs) in zebrafish embryos. It is suggested that in zebrafish, Syntabulin links DDs to the maternally expressed kinesin I heavy chain (KIF5B) and mediates their initial vegetal pole localisation and subsequent transport to the prospective dorsal side. This process could link anteroposterior (AP) polarity in oocytes to embryonic dorsoventral (DV) polarity (Nojima et al., 2010).

Since xSybu is vegetally localized in *X. laevis* oocytes and serves as an adaptor for kinesin motors, its role was analyzed in the context of PGC development and possible interaction with xKIF13B. xSybu mRNA was found to be associated with germ plasm and PGC up to the early tadpole stage, with the exception of the neurula (stage 16-17) (Fig. 31). Furthermore, expression of xSybu was detected in the dorsal region, probably due its

function in the nervous system, as described for mammalian neurons. Weak expression in the neurula at stage 19 was also observed in the RT-PCR analysis, but no differences between neurula and the tailbud stage 28 were detected in the whole transcriptome analysis. This can be either due to poor handling of the embryos, or a result of a degradation of maternal transcripts prior to the zygotic expression in PGCs. Highest expression of xSybu was observed at stage 37/38. This was mainly mediated by the increased expression in the dorsal region that correlates with the function of xSybu in mature neurons. In contrast, expression of xCentaurin- $\alpha$ 1 in the developing neurons was observed to be highest at stage 22 (Fig. 30). RT-PCR analysis revealed presence of two isoforms of xSybu transcript in the embryo, both in dorsal and ventral parts. These isoforms varied in length in approximately 50 base pairs (Fig. 31). The shorter isoform was more uniformly expressed compared to the longer one that was enriched in the ventral part of *X. laevis* embryos. Expression of xSyntabulin in the PGCs revealed predominant intracellular localization to the specific region of the cell. Similar localization was observed for farnesylated fluorescent proteins, like mRFP, and most likely corresponds to the localization in Golgi apparatus (GA). Function of Syntabulin in the transport of active zone (AZ) precursors generated in the trans-Golgi network to nascent synapses in the neurons supports this assumption (Cai et al., 2007). It was previously demonstrated, that xKIF13B is localized close to the plasma membrane of bleb-like protrusion formed by isolated PGCs (Dzementsei, 2009). However, in contrast to xKIF13B, xSybu was not observed to be localized in this region (Fig. 32). This suggests that xSybu is not involved in the formation of xKIF13B-mediated PIP3 gradient. However, further experiments have to be performed to confirm this statement. To address this issue, co-immunoprecipitation experiments with *in vivo* and *in vitro* expressed xKIF13B and xSybu were performed. It seemed that there was no interaction between xKIF13B and xSyntabulin, but the data were inconclusive due to the poor expression of both xKIF13B and xSyntabulin. In these experiments interaction with the smaller isoform of xSybu was analyzed (data not shown).

Analysis of xSyntabulin function in the PGCs was addressed by morpholino-mediated knock down of xSybu (xSybu MO). Activity and specificity of xSybu MO was verified *in vitro* (Suppl. Fig. 2). Injections of different concentrations of xSybu MO resulted in the defects in neural tube closer in axis formation at the neurula stage in a concentration-dependent manner (Fig. 33). These effects can be explained by the role of xSybu in the transport of dorsal determinant during anterior-posterior axis formation at the early stages of development, described in zebrafish (Nojima et al., 2010). To determine whether xSybu knock-down also affects proliferation or directional migration of PGCs, embryos that survived neurulation were subjected to WMISH with PGC marker *Pat* and somite marker *MyoD*. Although average number of PGCs in the xSybu MO-injected embryos was reduced, no significant difference in the number of PGCs was observed in comparison to the control.

From these observations, we conclude that role of xSyntabulin in *X. laevis* embryogenesis is mainly restricted to the early patterning events. Role of xSybu as a



---

potential interaction partner for xKIF13B in PGCs is very unlikely, although some additional experiments have to be performed to validate this. Expression in the nervous system also suggests possible role of xSybu in the mature or developing neurons, similar to the mammalian system. Presence of two isoforms detected by the RT-PCR should also be taken into account for the future investigation of xSybu function in *X. laevis*.

## 5. SUMMARY AND CONCLUSIONS

The main focus of this study was on the molecular and cellular mechanism underlying initiation of active primordial germ cell (PGC) migration in the endoderm of tailbud stage *Xenopus laevis* embryos.

Isolated PGCs randomly form bleb-like protrusions. Expansion and retraction of the bleb correlates with disassembly and re-polymerization of actin cortex on the plasma membrane, correspondingly. At the tailbud stage, actin-dependent cellular dynamics of PGCs is increased in comparison to the neurula stage. In addition, cell shape fluctuations become less random. This correlates with the transition of PGCs to active migration *in vivo*.

Cultivation of PGCs *in vitro* in the presence of cellular and artificial substrates demonstrates that at the tailbud stage PGCs migrate via bleb-associated mechanism. Specific adhesion to the substrate, as well as polymerization of actin filaments at the leading edge, is not required for generation of the traction force for cell migration. Instead, for the cell body translocation migrating PGCs need rigid confined environment and traction force is generated by polarized contractions of the cell body.

During the migration, PGCs alternate between active migratory 'run' phase and non-polarized 'tumbling' phase. At the 'tumbling' phase, enrichment of PIP3 in the bleb-like protrusions formed by PGCs is required for polarization, but in the polarized elongated cells at the 'run' phase enrichment of PIP3 is lost.

Function of kinesin motor, xKIF13B, that was shown to be associated with PIP3 enrichment in the bleb-like protrusions, is required for the directionality of PGC migration at the tailbud stage. Knock-down of xKIF13B does not cause any defects in PGC distribution *in vivo* prior to the tailbud stage, but leads to mislocalization and non-apoptotic reduction of PGC number during their migration in the endoderm. Potential interaction partners of xKIF13B, xCentaurin- $\alpha$ 1 and xSyntabulin, do not seem to be directly involved in the PGC development and migration in *X. laevis*.

Quantitative analysis of adhesion forces demonstrated that pre-migratory PGCs isolated from the neurula stage have higher affinity to fibronectin in comparison to migratory PGCs isolated from the tailbud stage. In addition, after the transition to active migration overall adhesion of PGCs to the surrounding somatic endodermal cells is decreased. Global differential gene expression analysis revealed several adhesion molecules, downregulated specifically in PGCs during the transition to active migration. Downregulated expression of Claudin 6.1, Gap junction protein beta 1 and E-cadherin was validated by quantitative RT-PCR with isolated cells.

It can be concluded that increased cellular dynamics and reduced cellular adhesion correlate with the transition of *X. laevis* PGCs to active migration, while PIP3 enrichment is required for PGC polarisation, but not cellular motility.

## 6. BIBLIOGRAPHY

### A

- Anderson R., Fässler R., Georges-Labouesse E., Hynes R.O., Bader B.L., Kreidberg J.A., Schaible K., Heasman J., Wylie C. (1999). Mouse primordial germ cells lacking beta1 integrins enter the germline but fail to migrate normally to the gonads. *Development* **126**, 1655-1664.
- Anderson R., Copeland T.K., Schöler H., Heasman J., Wylie C. (2000). The onset of germ cell migration in the mouse embryo. *Mech Dev.* **91**, 61-68.
- Ara T., Nakamura Y., Egawa T., Sugiyama T., Abe K., Kishimoto T., Matsui Y., Nagasawa T. (2003). Impaired colonization of the gonads by primordial germ cells in mice lacking a chemokine, stromal cell-derived factor-1 (SDF-1). *Proc Natl Acad Sci USA* **100**, 5319-5323.
- Asaba N., Hanada T., Takeuchi A., Chishti A.H. (2003). Direct interaction with a kinesin-related motor mediates transport of mammalian discs large tumor suppressor homologue in epithelial cells. *J. Biol. Chem.* **278**, 8395–8400.

### B

- Bendel-Stenzel M.R., Gomperts M., Anderson R., Heasman J., Wylie C. (2000). The role of cadherins during primordial germ cell migration and early gonad formation in the mouse. *Mech Dev.* **91**, 143-152.
- Berekelya L.A., Ponomarev M.B., Luchinskaya N.N., Belyavsky A.V. (2003). Xenopus Germes encodes a novel germ plasm-associated transcript. *Gene Expr Patterns.* **3**, 521-524.
- Berekelya L.A., Ponomarev M.B., Mikryukov A.A., Luchinskaya N.N., Belyavsky A.V. (2005). Molecular mechanisms of germ line cell determination in animals. *Mol Biol (Mosk).* **39**, 572-584.
- Berekelya L.A., Mikryukov A.A., Luchinskaya N.N., Ponomarev M.B., Woodland H.R., Belyavsky A.V. (2007). The protein encoded by the germ plasm RNA Germes associates with dynein light chains and functions in Xenopus germline development. *Differentiation* **75**, 546-558.
- Blackler A. W. (1965). The continuity of the germ-line in amphibians and mammals. *Annee Biol.* **4**, 627-635.
- Blaser H., Eisenbeiss S., Neumann M., Reichman-Fried M., Thisse B., Thisse C., Raz E. (2005). Transition from non-motile behaviour to directed migration during early PGC development in zebrafish. *J Cell Sci.* **118**, 4027-4038.
- Blaser H., Reichman-Fried M., Castanon I., Dumstrei K., Marlow F.L., Kawakami K., Solnica-Krezel L., Heisenberg C.P., Raz E. (2006). Migration of zebrafish primordial germ cells: a role for myosin contraction and cytoplasmic flow. *Dev Cell* **11**, 613-627.
- Boldajipour B., Mahabaleshwar H., Kardash E., Reichman-Fried M., Blaser H., Minina S., Wilson D., Xu Q., Raz E. (2008). Control of chemokine-guided cell migration by ligand sequestration. *Cell* **132**, 463-473.
- Bonnard C., Strobl A.C., Shboul M., Lee H., Merriman B., Nelson S.F., Ababneh O.H., Uz E., Güran T., Kayserili H., Hamamy H., Reversade B. (2012). Mutations in IRX5 impair craniofacial development and germ cell migration via SDF1. *Nat Genet.* **44**, 709-713.

- Bornslaeger E.A., Corcoran C.M., Stappenbeck T.S., Green K.J. (1996). Breaking the connection: displacement of the desmosomal plaque protein desmoplakin from cell-cell interfaces disrupts anchorage of intermediate filament bundles and alters intercellular junction assembly. *J Cell Biol.* **134**, 985-1001.
- Braun M., Wunderlin M., Spieth K., Knöchel W., Gierschik P., Moepps B. (2002). Xenopus laevis Stromal cell-derived factor 1: conservation of structure and function during vertebrate development. *J Immunol.* **168**, 2340-2347.
- Bristow J.M., Reno T.A., Jo M., Gonias S.L., Klemke R.L. (2013). Dynamic phosphorylation of tyrosine 665 in pseudopodium-enriched atypical kinase 1 (PEAK1) is essential for the regulation of cell migration and focal adhesion turnover. *J Biol Chem.* **288**, 123-131.
- Brookman J.J., Toosy A.T., Shashidhara L.S., White R.A. (1992). The 412 retrotransposon and the development of gonadal mesoderm in Drosophila. *Development* **116**, 1185-1192.
- Brustis J.J., Cathalot B., Peyret D., Gipouloux J.D. (1984). Evolution of Xenopus endodermal cells cultured on different extracellular matrix components. Identification of primordial germ cells. *Anat Embryol (Berl).* **170**, 187-96.
- C
- Cai Q., Gerwin C., Sheng Z.H. (2005). Syntabulin-mediated anterograde transport of mitochondria along neuronal processes. *J Cell Biol.* **170**, 959-69.
- Cai Q., Pan P.Y., Sheng Z.H. (2007). Syntabulin-kinesin-1 family member 5B-mediated axonal transport contributes to activity-dependent presynaptic assembly. *J Neurosci.* **27**, 7284-96.
- Chan A.P., Kloc M., Larabell C.A., LeGros M., Etkin L.D. (2007). The maternally localized RNA fatvg is required for cortical rotation and germ cell formation. *Mech Dev.* **124**, 350-363.
- Charras G., Paluch E. (2008). Blebs lead the way: how to migrate without lamellipodia. *Nat Rev Mol Cell Biol.* **9**, 730-736.
- Chihara D., Nance J. (2012). An E-cadherin-mediated hitchhiking mechanism for C. elegans germ cell internalization during gastrulation. *Development* **139**, 2547-2556.
- Chung C.Y., Funamoto S., Firtel R.A. (2001). Signaling pathways controlling cell polarity and chemotaxis. *Trends Biochem Sci.* **26**, 557-566.
- Ciosk R., DePalma M., Priess J. R. (2006). Translational regulators maintain totipotency in the Caenorhabditis elegans germline. *Science* **311**, 851 -853.
- Collier B., Gorgoni B., Loveridge C., Cooke H.J., Gray N.K. (2005). The DAZL family proteins are PABP-binding proteins that regulate translation in germ cells. *EMBO J.* **24**, 2656-2666.
- D
- D'Agostino .I, Merritt C., Chen P.L., Seydoux G., Subramaniam K. (2006). Translational repression restricts expression of the C. elegans Nanos homolog NOS-2 to the embryonic germline. *Dev Biol.* **292**, 244-252.
- Damianitsch K., Melchert J., Pieler T. (2009). XsFRP5 modulates endodermal organogenesis in Xenopus laevis. *Dev Biol* **329**, 327-337.

- Doitsidou M., Reichman-Fried M., Stebler J., Köprunner M., Dörries J., Meyer D., Esguerra C.V., Leung T., Raz E. (2002). Guidance of primordial germ cell migration by the chemokine SDF-1. *Cell* **111**, 647–659.
- Dumstrei K., Mennecke R., Raz E. (2004). Signaling pathways controlling primordial germ cell migration in zebrafish. *J Cell Sci.* **117**, 4787–4795.
- Dutt P., Wang J.F., Groopman J.E. (1998). Stromal cell-derived factor-1 alpha and stem cell factor/kit ligand share signaling pathways in hemopoietic progenitors: a potential mechanism for cooperative induction of chemotaxis. *J Immunol.* **161**, 3652–3658.
- Dzementsei A. (2009). Mapping of xKIF13B domains in the context of primordial germ cell migration in *Xenopus laevis* embryos. Master thesis, IMPRS/ Georg-August University of Goettingen.
- E
- Essex L.J., Mayor R., Sargent M.G. (1993). Expression of *Xenopus* snail in mesoderm and prospective neural fold ectoderm. *Dev Dyn.* **198**, 108–122.
- Ephrussi A., Lehmann R. (1992). Induction of germ cell formation by oskar. *Nature* **358**, 387–392.
- Evans W.H., Martin P.E. (2002). Gap junctions: structure and function (Review). *Mol Membr Biol.* **19**, 121–136.
- Extavour C.G., Akam M. (2003). Mechanisms of germ cell specification across the metazoans: epigenesis and preformation. *Development* **130**, 5869–84.
- F
- Fackler O.T., Grosse R. (2008). Cell motility through plasma membrane blebbing. *J Cell Biol.* **181**, 879–884.
- Farini D., La Sala G., Tedesco M., De Felici M. (2007). Chemoattractant action and molecular signaling pathways of Kit ligand on mouse primordial germ cells. *Dev. Biol.* **306**, 572–583.
- Findley M.K., Koval M. (2009). Regulation and roles for claudin-family tight junction proteins. *IUBMB Life* **61**, 431–437.
- Flanagan J.G., Chan D.C., Leder, P. (1991). Transmembrane form of the kit ligand growth factor is determined by alternative splicing and is missing in the *Sld* mutant. *Cell* **64**, 1025–1035.
- Forbes A., Lehmann R. (1998). Nanos and Pumilio have critical roles in the development and function of *Drosophila* germline stem cells. *Development* **125**, 679–690.
- Franca-Koh J., Kamimura Y., Devreotes P. (2006). Navigating signaling networks: chemotaxis in *Dictyostelium discoideum*. *Curr Opin Genet Dev.* **16**, 333–338.
- Franca-Koh J., Kamimura Y., Devreotes P.N. (2007). Leading-edge research: PtdIns(3,4,5)P<sub>3</sub> and directed migration. *Nat Cell Biol.* **9**, 15–17.
- Franz C.M., Jones, G.E., Ridley, A. J. (2002). Cell migration in development and disease. *Dev. Cell* **2**, 153–158.
- French-Constant C., Hollingsworth A., Heasman J. and Wylie C. C. (1991). Response to fibronectin of mouse primordial germ cells before, during and after migration. *Development* **113**, 1365–1373.
- Funamoto S., Meili R., Lee S., Parry L., Firtel R. A. (2002). Spatial and temporal regulation of 3-phosphoinositides by PI 3-kinase and PTEN mediates chemotaxis. *Cell* **109**, 611–623.

Furuhashi H., Takasaki T., Rechtsteiner A., Li T., Kimura H., Checchi P.M., Strome S., Kelly W.G. (2010). Trans-generational epigenetic regulation of *C. elegans* primordial germ cells. *Epigenetics Chromatin*. **3**:15.

## G

Giannone G., Dubin-Thaler B.J., Rossier O., Cai Y., Chaga O., Jiang G., Beaver W., Döbereiner H.G., Freund Y., Borisov G., Sheetz M.P. (2007). Lamellipodial actin mechanically links myosin activity with adhesion-site formation. *Cell* **128**, 561-575.

Giepmans B.N. (2004). Gap junctions and connexin-interacting proteins. *Cardiovasc Res*. **62**, 233-245.

Gilchrist M.J., Pollet N. (2012). Databases of gene expression in *Xenopus* development. *Methods Mol Biol*. **917**, 319-345.

Goudarzi M., Banisch T.U., Mobin M.B., Maghelli N., Tarbashevich K., Strate I., van den Berg J., Blaser H., Bandemer S., Paluch E., Bakkers J., Tolić-Nørrelykke I.M., Raz E. (2012). Identification and regulation of a molecular module for bleb-based cell motility. *Dev Cell* **23**, 210-218.

Gu Y., Runyan C., Shoemaker A., Surani A., Wylie C (2009). Steel factor controls primordial germ cell survival and motility from the time of their specification in the allantois, and provides a continuous niche throughout their migration. *Development* **136**, 1295–1303.

Gu Y., Runyan C., Shoemaker A., Surani M.A., Wylie C. (2011). Membrane-bound steel factor maintains a high local concentration for mouse primordial germ cell motility, and defines the region of their migration. *PLoS One* **6**(10), e25984.

## H

Hanada T., Lin L., Tibaldi E. V., Reinherz E. L., Chishti A. H. (2000). GAKIN, a novel kinesin-like protein associates with the human homologue of the *Drosophila* discs large tumor suppressor in T lymphocytes. *J Biol Chem*. **275**, 28774–28784.

Hanyu-Nakamura K., Sonobe-Nojima H., Tanigawa A., Lasko P., Nakamura A. (2009). *Drosophila* Pgc protein inhibits P-TEFb recruitment to chromatin in primordial germ cells. *Nature* **451**, 730-733.

Harris T.J., Tepass U. (2010). Adherens junctions: from molecules to morphogenesis. *Nat Rev Mol Cell Biol*. **11**, 502-514.

Haugh J.M., Codazzi F., Teruel M., Meyer T. (2000). Spatial sensing in fibroblasts mediated by 3' phosphoinositides. *J Cell Biol*. **151**, 1269–1280.

Hayata T., Eisaki A., Kuroda H., Asashima M. (1999). Expression of Brachyury-like T-box transcription factor, *Xbra3* in *Xenopus* embryo. *Dev Genes Evol*. **209**, 560-563.

Heasman J., Mohun T., Wylie C.C. (1977). Studies on the locomotion of primordial germ cells from *Xenopus laevis* in vitro. *J Embryol Exp Morphol*. **42**, 149-161.

Heasman J., Wylie C.C. (1978). Electron microscopic studies on the structure of motile primordial germ cells of *Xenopus laevis* in vitro. *J Embryol Exp Morphol*. **46**, 119-133.

Heasman J., Hynes R.O., Swan A.P., Thomas V., Wylie C.C. (1981). Primordial germ cells of *Xenopus* embryos: the role of fibronectin in their adhesion during migration. *Cell* **27**, 437-447.

- Heasman J., Quarmby J., Wylie C.C. (1984). The mitochondrial cloud of *Xenopus* oocytes: the source of germinal granule material. *Dev. Biol.* **105**, 458-469.
- Helenius J., Heisenberg C.P., Gaub H.E., Muller D.J. (2008). Single-cell force spectroscopy. *J Cell Sci.* **121**, 1785-91.
- Hensey C., Gautier J. (1998). Program cell death during *Xenopus* development: a spatio-temporal analysis. *Dev. Biol.* **203**, 36-48.
- Hoeller O., Kay R.R. (2007). Chemotaxis in the absence of PIP3 gradients. *Curr Biol.* **17**, 813-817.
- Hoffmann A., Gross G. (2001). BMP signaling pathways in cartilage and bone formation. *Crit Rev Eukaryot Gene Expr.* **11**, 23-45.
- Hollemann T., Chen Y., Grunz H., Pieler T. (1998). Regionalized metabolic activity establishes boundaries of retinoic acid signalling. *EMBO J.* **17**, 7361-7372.
- Hollemann T., Panitz F., Pieler T. (1999). In situ hybridization techniques with *Xenopus* embryos. In: Richter, J.D. (Ed.), *A Comparative Methods Approach to the Study of Oocytes and Embryos*. Oxford University Press Inc., Oxford, pp. 279-290.
- Hopwood N.D., Pluck A., Gurdon J.B. (1987). A *Xenopus* mRNA related to *Drosophila* twist is expressed in response to induction in the mesoderm and the neural crest. *Cell* **59**, 893-903.
- Hopwood N.D., Pluck A., Gurdon J.B. (1989). MyoD expression in the forming somites is an early response to mesoderm induction in *Xenopus* embryos. *Embo J* **8**, 3409-3417.
- Horvay K., Claussen M., Katzer M., Landgrebe J., Pieler T. (2006). *Xenopus* Dead end mRNA is a localized maternal determinant that serves a conserved function in germ cell development. *Dev Biol.* **291**, 1-11.
- Horiguchi K., Hanada T., Fukui Y., Chishti A.H. (2006). Transport of PIP3 by GAKIN, a kinesin-3 family protein, regulates neuronal cell polarity. *J Cell Biol.* **174**, 425-436.
- Houston D.W., King M.L. (2000a). Germ plasm and molecular determinants of germ cell fate. *Curr Top Dev Biol.* **50**, 155-181.
- Houston D.W., King M.L. (2000b). A critical role for *Xdazl*, a germ plasm-localized RNA, in the differentiation of primordial germ cells in *Xenopus*. *Development* **127**, 447-456.
- Huang E.J., Nocka K.H., Buck J., Besmer P. (1992). Differential expression and processing of two cell associated forms of the kit-ligand: KL-1 and KL-2. *Mol. Biol. Cell* **3**, 349-362.
- Hudson C., Woodland H.R. (1998). *Xpat*, a gene expressed specifically in germ plasm and primordial germ cells of *Xenopus laevis*. *Mech Dev.* **73**, 159-168.
- Hutter J.L., Bechhoefer J. (1993). Calibration of Atomic-Force Microscope Tips. *Review of Scientific Instruments* **64**, 1868-1873.
- I
- Iijima M., Devreotes P. (2002). Tumor suppressor PTEN mediates sensing of chemoattractant gradients. *Cell* **109**, 599-610.
- Iijima M., Huang Y. E., Devreotes P. (2002). Temporal and spatial regulation of chemotaxis. *Dev. Cell* **3**, 469-478.

Ikenishi K., Okuda T., Nakazato S. (1984). Differentiation of presumptive primordial germ cell (pPGC)-like cells in explants into PGCs in experimental tadpoles. *Dev Biol.* **103**, 258-62.

Iso T., Kedes L., Hamamori Y. (2003). HES and HERP families: multiple effectors of the Notch signaling pathway. *J Cell Physiol.* **194**, 237-255.

Iwasaki T., Murata-Hori M., Ishitobi S., Hosoya H. (2001) Diphosphorylated MRLC is required for organization of stress fibers in interphase cells and the contractile ring in dividing cells. *Cell Struct. Funct.* **26**, 677–683.

## J

Jadhav S., Rana M., Subramaniam K. (2008). Multiple maternal proteins coordinate to restrict the translation of *C. elegans* nanos-2 to primordial germ cells. *Development* **135**, 1803-1812.

Jaglarz M.K., Howard K.R. (1994). Primordial germ cell migration in *Drosophila melanogaster* is controlled by somatic tissue. *Development* **120**, 83-89.

Jia H., Cheng L., Tickner M., Bagherzadeh A., Selwood D., Zachary I. (2010). Neuropilin-1 antagonism in human carcinoma cells inhibits migration and enhances chemosensitivity. *Br. J. Cancer* **102**, 541–552.

## K

Kaltner H. Stierstorfer B. (1998). Animal lectins as cell adhesion molecules. *Acta Anat (Basel)* **161**, 162-179.

Kamimura M., Ikenishi K., Kotani M., Matsuno T. (1976). Observations on the migration and proliferation of gonocytes in *Xenopus laevis*. *J Embryol Exp Morphol.* **36**, 197-207.

Kamimura M., Kotani M., Yamagata K. (1980). The migration of presumptive primordial germ cells through the endodermal cell mass in *Xenopus laevis*: a light and electron microscopic study. *J Embryol Exp Morphol.* **59**, 1-17.

Kardash E., Reichman-Fried M., Maitre J.L., Boldajipour B., Papusheva E., Messerschmidt E.M., Heisenberg C.P., Raz, E. (2010). A role for Rho GTPases and cell-cell adhesion in single-cell motility in vivo. *Nature Cell Biology* **12**, 47-53.

Kataoka K., Yamaguchi T., Orii H., Tazaki A., Watanabe K., Mochii M. (2006). Visualization of the *Xenopus* primordial germ cells using a green fluorescent protein controlled by cis elements of the 3' untranslated region of the DEADSouth gene. *Mech Dev.* **123**, 746-760.

Katso R., Okkenhaug K., Ahmadi K., White S., Timms J., Waterfield M.D. (2001). Cellular function of phosphoinositide 3-kinases: implications for development, homeostasis, and cancer. *Annu Rev Cell Dev Biol.* **17**, 615-675.

Kedde M., Strasser M.J., Boldajipour B., Oude Vrielink J.A., Slanchev K., le Sage C., Nagel R., Voorhoeve P.M., van Duijse J., Ørom U.A., Lund A.H., Perrakis A., Raz E., Agami R. (2007). RNA-binding protein Dnd1 inhibits microRNA access to target mRNA. *Cell* **131**, 1273-1286.

Kemphues K. J., Strome S. (1997). Fertilization and establishment of polarity in the embryo. In *C. elegans II* (eds. D. L. Riddle, T. Blumenthal, B. Meyer and J. R. Priess), pp. 335-360. Cold Spring Harbor: Cold Spring Harbor Laboratory Press.

King M.L., Messitt T.J., Mowry K.L. (2005). Putting RNAs in the right place at the right time: RNA localization in the frog oocyte. *Biol Cell.* **97**, 19-33.



- King J.S., Insall R.H. (2008). Chemotaxis: TorC before you Akt. *Curr Biol.* **18**, R864-866.
- Kirilenko P., Weierud F.K., Zorn A.M., Woodland H.R. 2008. The efficiency of *Xenopus* primordial germ cell migration depends on the germplasm mRNA encoding the PDZ domain protein Grip2. *Differentiation* **76**, 392-403.
- Kloc M., Etkin L.D. (1995). Two distinct pathways for the localization of RNAs at the vegetal cortex in *Xenopus* oocytes. *Development* **121**, 287-297.
- Kloc M., Larabell C., Etkin L.D. (1996). Elaboration of the messenger transport organizer pathway for localization of RNA to the vegetal cortex of *Xenopus* oocytes. *Dev Biol.* **180**, 119-130.
- Kloc M., Zearfoss N.R., Etkin L.D. (2002). Mechanisms of subcellular mRNA localization. *Cell* **108**, 533-44.
- Kloc M., Bilinski S., Etkin L.D. (2004). The Balbiani body and germ cell determinants: 150 years later. *Curr Top Dev Biol.* **59**, 1-36.
- Knaut H., Werz C., Geisler R., Nüsslein-Volhard C.; Tübingen 2000 Screen Consortium. (2003). A zebrafish homologue of the chemokine receptor Cxcr4 is a germ-cell guidance receptor. *Nature* **421**, 279-282.
- Kobayashi S., Yamada M., Asaoka M., Kitamura T. (1996). Essential role of the posterior morphogen nanos for germline development in *Drosophila*. *Nature* **25**, 708-711.
- Koebnick K., Loeber J., Arthur P.K., Tarbashevich K., Pieler T. (2010). Elr-type proteins protect *Xenopus* Dead end mRNA from miR-18-mediated clearance in the soma. *Proc Natl Acad Sci USA.* **107**, 16148-16153.
- Komiya T., Itoh K., Ikenishi K., Furusawa M. (1994). Isolation and characterization of a novel gene of the DEAD box protein family which is specifically expressed in germ cells of *Xenopus laevis*. *Dev Biol.* **162**, 354-363.
- Köprunner M., Thisse C., Thisse B., Raz E. (2001). A zebrafish nanos-related gene is essential for development of primordial germ cells. *Genes Dev.* **15**, 2877-2885.
- Koval M. (2006). Claudins--key pieces in the tight junction puzzle. *Cell Commun Adhes.* **13**, 127-138.
- Kunwar P.S., Siekhaus D.E., Lehmann R. (2006). In vivo migration: a germ cell perspective. *Annu Rev Cell Dev Biol.* **22**, 237-265.
- Kurimoto K., Yabuta Y., Ohinata Y., Shigeta M., Yamanaka K., Saitou M. (2008). Complex genome-wide transcription dynamics orchestrated by Blimp1 for the specification of the germ cell lineage in mice. *Genes Dev.* **22**, 1617-1635.
- L
- Laemmli U. K. (1970). Cleavage of structural proteins during the assembly of the head of bacteriophage T4. *Nature* **227**, 680-685.
- Lai E.C. 2004. Notch signaling: control of cell communication and cell fate. *Development* **131**, 965-973.
- Lai F., Zhou Y., Luo X., Fox J., King M.L. (2011). Nanos1 functions as a translational repressor in the *Xenopus* germline. *Mech Dev.* **128**, 153-163.
- Lai F., Singh A., King M.L. (2012). *Xenopus* Nanos1 is required to prevent endoderm gene expression and apoptosis in primordial germ cells. *Development* **139**, 1476-1486.

- Lange U.C., Adams D.J., Lee C., Barton S., Schneider R., Bradley A., Surani M.A. (2008). Normal germ line establishment in mice carrying a deletion of the *Ifitm/Fragilis* gene family cluster. *Mol Cell Biol.* **28**, 4688-4696.
- Lawson K.A., Dunn N.R., Roelen B.A., Zeinstra L.M., Davis A.M., Wright C.V., Korving J.P., Hogan B.L. (1999). *Bmp4* is required for the generation of primordial germ cells in the mouse embryo. *Genes Dev.* **13**, 424-436.
- Le Clainche C., Carlier M.F. (2008). Regulation of actin assembly associated with protrusion and adhesion in cell migration. *Physiol Rev.* **88**, 489-513.
- Levi G., Crossin K.L., Edelman G.M. (1987). Expression sequences and distribution of two primary cell adhesion molecules during embryonic development of *Xenopus laevis*. *J Cell Biol.* **105**, 2359-2372.
- Li S.S., Ivanoff A., Bergström S.E., Sandström A., Christensson B., van Nerven J., Holgersson J., Hauzenberger D., Arencibia I., Sundqvist K.G. (2002). T lymphocyte expression of thrombospondin-1 and adhesion to extracellular matrix components. *Eur J Immunol.* **32**, 1069-1079.
- Livak, K.J., Schmittgen T.D. (2001). Analysis of relative gene expression data using real-time quantitative PCR and the 2(T)(-Delta Delta C) method. *Methods* **25**, 402-408.
- Luther S. A., Cyster J. G. (2001). Chemokines as regulators of T cell differentiation. *Nat. Immunol.* **2**, 102-107.
- M**
- Maehama T., Dixon J.E. (1998). The tumor suppressor, PTEN/MMAC1, dephosphorylates the lipid second messenger, phosphatidylinositol 3,4,5-trisphosphate. *J Biol Chem.* **273**, 13375-13378.
- Mahabaleswar H., Boldajipour B., Raz E. (2008). Killing the messenger: The role of CXCR7 in regulating primordial germ cell migration. *Cell Adh Migr.* **2**, 69-70.
- Mahowald A.P. (2001). Assembly of the *Drosophila* germ plasm. *Int Rev Cytol.* **203**, 187-213.
- McGough A.M., Staiger C.J., Min J.K., Simonetti K.D. (2003) The gelsolin family of actin regulatory proteins: modular structures, versatile functions. *FEBS Lett.* **552**, 75-81.
- Meberg P.J. (2000) Signal-regulated ADF/cofilin activity and growth cone motility. *Mol. Neurobiol.* **21**, 97-107.
- Meili R., Ellsworth C., Lee S., Reddy T.B., Ma H., Firtel R.A. (1999). Chemoattractant-mediated transient activation and membrane localization of Akt/PKB is required for efficient chemotaxis to cAMP in *Dictyostelium*. *EMBO J.* **18**, 2092-2105.
- Merlot S., Firtel R.A. (2003). Leading the way: Directional sensing through phosphatidylinositol 3-kinase and other signaling pathways. *J Cell Sci.* **116**, 3471-3478.
- Merritt C., Rosoloso D., Ko D., Seydoux G. (2008). 3' UTRs are the primary regulators of gene expression in the *C. elegans* germline. *Curr. Biol.* **18**, 1476-1482.
- Molyneaux K.A., Stallock J., Schaible K., Wylie C. (2001). Time-lapse analysis of living mouse germ cell migration. *Dev Biol.* **240**, 488-498.
- Molyneaux K.A., Zinszner H., Kunwar P.S., Schaible K., Stebler J., Sunshine M.J., O'Brien W., Raz E., Littman D., Wylie C., Lehmann R. (2003). The chemokine SDF1/CXCL12 and its receptor CXCR4 regulate mouse germ cell migration and survival. *Development* **130**, 4279-86.

- Molyneaux K., Wylie C. (2004). Primordial germ cell migration. *Int J Dev Biol* **48**, 537-44.
- Morichika K., Kataoka K., Terayama K., Tazaki A., Kinoshita T., Watanabe K., Mochii M. (2010). Perturbation of Notch/Suppressor of Hairless pathway disturbs migration of primordial germ cells in *Xenopus* embryo. *Dev Growth Differ.* **52**, 235-244.
- Mortazavi A., Williams B.A., McCue K., Schaeffer L., Wold B. (2008). Mapping and quantifying mammalian transcriptomes by RNA-seq. *Nat Methods* **5**, 621-628.
- Mulligan T., Blaser H., Raz E., Farber S.A. (2010). Prenylation-deficient G protein gamma subunits disrupt GPCR signaling in the zebrafish. *Cell Signal.* **22**, 221-233.
- Mullis K., Faloona F., Scharf S., Saiki R., Horn G., Erlich H. (1986). Specific enzymatic amplification of DNA in vitro: the polymerase chain reaction. *Cold Spring Harb Symp Quant Biol* **51**, 263-273.
- N**
- Naka M., Saitoh M., Hidaka H. (1988). Two phosphorylated forms of myosin in thrombin-stimulated platelets. *Arch. Biochem. Biophys.* **261**, 235-240.
- Nakamura A., Seydoux G. (2008). Less is more: specification of the germline by transcriptional repression. *Development* **135**, 3817-3827.
- Nakamura A., Shirae-Kurabayashi M., Hanyu-Nakamura K. (2010). Repression of early zygotic transcription in the germline. *Curr Opin Cell Biol.* **22**, 709-714.
- Narizhneva N.V., Razorenova O.V., Podrez E.A., Chen J., Chandrasekharan U.M., DiCorleto P.E., Plow E.F., Topol E.J., Byzova T.V. (2005). Thrombospondin-1 up-regulates expression of cell adhesion molecules and promotes monocyte binding to endothelium. *FASEB J.* **19**, 1158-1160.
- Nieuwkoop P.D., Faber J. (1994). Normal Table of *Xenopus laevis* (Daudin). *Garland Publishing Inc, New York* ISBN 0-8153-1896-0.
- Nishikawa Y., Miyazaki T., Nakashiro K., Yamagata H., Isokane M., Goda H., Tanaka H., Oka R., Hamakawa H. (2011). Human FAT1 cadherin controls cell migration and invasion of oral squamous cell carcinoma through the localization of  $\beta$ -catenin. *Oncol Rep.* **26**, 587-592.
- Nishiumi F., Komiya T., Ikenishi K. (2005). The mode and molecular mechanisms of the migration of presumptive PGC in the endoderm cell mass of *Xenopus* embryos. *Dev Growth Differ.* **47**, 37-48.
- Nojima H., Rothhämel S., Shimizu T., Kim C.H., Yonemura S., Marlow F.L., Hibi M. (2010). Syntabulin, a motor protein linker, controls dorsal determination. *Development* **137**, 923-933.
- O**
- Ohinata Y., Payer B., O'Carroll D., Ancelin K., Ono Y., Sano M., Barton S.C., Obukhanych T., Nussenzweig M., Tarakhovskiy A., Saitou M., Surani M.A. (2005). Blimp1 is a critical determinant of the germ cell lineage in mice. *Nature* **436**, 207-213.
- P**
- Pankov R., Yamada K.M. (2002). Fibronectin at a glance. *J Cell Sci.* **115**, 3861-3863.

Peng C. K., Buldyrev S. V., Havlin S., Simons M., Stanley H. E., Goldberger A. L. (1994). Mosaic organization of DNA nucleotides. *Phys Rev E Stat Phys Plasmas Fluids Relat Interdiscip Topics* **49**, 1685-1689.

## R

Rangan P., DeGennaro M., Jaime-Bustamante K., Coux R.X., Martinho R.G., Lehmann R. (2009). Temporal and spatial control of germ-plasm RNAs. *Curr Biol.* **19**, 72-77.

Raucher D., Stauffer T., Chen W., Shen K., Guo S., York J.D., Sheetz M.P., Meyer T. (2000). Phosphatidylinositol 4,5-bisphosphate functions as a second messenger that regulates cytoskeleton-plasma membrane adhesion. *Cell* **100**, 221-228.

Raz E. (2004). Guidance of primordial germ cell migration. *Curr Opin Cell Biol* **16**, 169-73.

Richardson B.E., Lehmann R. (2010). Mechanisms guiding primordial germ cell migration: strategies from different organisms. *Nat Rev Mol Cell Biol.* **11**, 37-49.

Reichman-Fried M., Minina S., Raz E. (2004). Autonomous modes of behavior in primordial germ cell migration. *Dev Cell* **6**, 589-596.

Roberts R.Z., Morris A.J. (2000). Role of phosphatidic acid phosphatase 2a in uptake of extracellular lipid phosphate mediators. *Biochim Biophys Acta.* **1487**, 33-49.

Rupp R.A., Snider and L., Weintraub H. (1994). "Xenopus embryos regulate the nuclear localization of XMyoD." *Genes Dev* **8**, 1311-1323.

## S

Saitou M., Barton S.C., Suran M. A. (2002). A molecular programme for the specification of germ cell fate in mice. *Nature* **418**, 293 -300.

Saitou M. (2009). Germ cell specification in mice. *Curr Opin Genet Dev.* **19**, 386-395.

Saitou M, Yamaji M. (2010). Germ cell specification in mice: signaling, transcription regulation, and epigenetic consequences. *Reproduction* **139**, 931-942.

Saitou M., Yamaji M. (2012). Primordial germ cells in mice. *Cold Spring Harb Perspect Biol.* **4(11)**, a008375.

Sanger F., Nicklen S., Coulson A.R. (1977). DNA sequencing with chain-terminating inhibitors. *Proc Natl Acad Sci U S A* **74**, 5463-5467.

Sambrook J., F. E. F., Maniatis T. (1989). Molecular cloning. *A laboratory manual, 2d edition.*

Cold Spring Harbour. Cold Spring Harbour Laboratory Press.

Santos A.C., Lehmann R. (2004a). Germ cell specification and migration in Drosophila and beyond. *Curr Biol.* **14**, R578-589.

Santos A.C., Lehmann R. (2004b). Isoprenoids control germ cell migration downstream of HMGCoA reductase. *Dev Cell.* **6**, 283-293.

Sasaki H., Matsui Y. (2008). Epigenetic events in mammalian germ-cell development: reprogramming and beyond. *Nat Rev Genet.* **9**, 129-140.

- Schedl T. (1997). Developmental genetics of the germ line. In *C. elegans II* (eds. D. L. Riddle, T. Blumenthal, B. Meyer and J. R. Priess), pp. 241-269. Cold Spring Harbor: Cold Spring Harbor Laboratory Press.
- Schneider D., Tarantola M., Janshoff A. (2011). Dynamics of TGF-beta induced epithelial-to-mesenchymal transition monitored by Electric Cell-Substrate Impedance Sensing. *Biochimica Et Biophysica Acta-Molecular Cell Research* **1813**, 2099-2107.
- Sechi A.S. and Wehland J. (2000) The actin cytoskeleton and plasma membrane connection: PtdIns(4,5)P(2) influences cytoskeletal protein activity at the plasma membrane. *J. Cell Sci.* **113**, 3685–3695.
- Seervai R.N., Wessel G.M. (2013). Lessons for inductive germline determination. *Mol Reprod Dev.* doi: 10.1002/mrd.22151. [Epub ahead of print].
- Servant G., Weiner O.D., Herzmark P., Balla T., Sedat J.W., Bourne H.R. (2000). Polarization of chemoattractant receptor signaling during neutrophil chemotaxis. *Science* **287**, 1037–1040.
- Sharp P.A., Sugden B., Sambrook J. (1973). "Detection of two restriction endonuclease activities in Haemophilus parainfluenzae using analytical agarose--ethidium bromide electrophoresis." *Biochemistry* **12**, 3055-3063.
- Singh H., Sarathi S.P. (2012). Insight of Lectins- A review. *IJSER* **3**, 813-821.
- Singh M.K., Dadke D., Nicolas E., Serebriiskii I.G., Apostolou S., Canutescu A., Egleston B.L., Golemis E.A. (2008). A novel Cas family member, HEPL, regulates FAK and cell spreading. *Mol Biol Cell* **19**, 1627-1636.
- Staton A.A., Knaut H., Giraldez A.J. (2011). miRNA regulation of Sdf1 chemokine signaling provides genetic robustness to germ cell migration. *Nat Genet.* **43**, 204-211.
- Stebler J., Spieler D., Slanchev K., Molyneaux K.A., Richter U., Cojocaru V., Tarabykin V., Wylie C., Kessel M., Raz E. 2004. Primordial germ cell migration in the chick and mouse embryo: the role of the chemokine SDF-1/CXCL12. *Dev Biol.* **272**, 351-361.
- Stürzenbaum S.R., Kille P. (2001). Control genes in quantitative molecular biological techniques: the variability of invariance. *Comp Biochem Physiol B Biochem Mol Biol.* **130**, 281-289.
- Su Q., Cai Q., Gerwin C., Smith C.L., Sheng Z.H. (2004). Syntabulin is a microtubule-associated protein implicated in syntaxin transport in neurons. *Nat Cell Biol.* **6**, 941-53.
- Swan L.E., Wichmann C., Prange U., Schmid A., Schmidt M., Schwarz T., Ponimaskin E., Madeo F., Vorbruggen G., Sigrist S.J. (2004). A glutamate receptor-interacting protein homolog organizes muscle guidance in Drosophila. *Genes Dev.* **18**, 223–237.
- T**
- Taguchi A., Takii M., Motoishi M., Orii H., Mochii M., Watanabe K. (2012). Analysis of localization and reorganization of germ plasm in Xenopus transgenic line with fluorescence-labeled mitochondria. *Dev Growth Differ.* **54**, 767-776.
- Takamiya K., Kostourou V., Adams S., Jadeja S., Chalepakis G., Scambler P.J., Haganir R.L., Adams R.H. (2004). A direct functional link between the multi-PDZ domain protein GRIP1 and the Fraser syndrome protein Fras1. *Nat. Genet.* **36**, 172–177.

- Takeuchi T., Tanigawa Y., Minamide R., Ikenishi K., Komiya T. (2010). Analysis of SDF-1/CXCR4 signaling in primordial germ cell migration and survival or differentiation in *Xenopus laevis*. *Mech Dev.* **127**, 146-158.
- Tam P.P., Zhou S.X. (1996). The allocation of epiblast cells to ectodermal and germ-line lineages is influenced by the position of the cells in the gastrulating mouse embryo. *Dev. Biol.* **178**, 124 -132.
- Tanaka S.S., Yamaguchi Y.L., Tsoi B., Lickert H., Tam P.P. (2005). IFITM/Mil/fragilis family proteins IFITM1 and IFITM3 play distinct roles in mouse primordial germ cell homing and repulsion. *Dev Cell* **9**, 745-756.
- Tanaka T., Nakamura A. (2008). The endocytic pathway acts downstream of Oskar in *Drosophila* germ plasm assembly. *Development* **135**, 1107-1117.
- Tarbashevich K. (2007). Molecular mechanisms of germ cell specification and migration in *Xenopus laevis*. PhD thesis, IMPRS/ Georg-August University of Goettingen.
- Tarbashevich K., Koebernick K., Pieler T. (2007). XGRIP2.1 is encoded by a vegetally localizing, maternal mRNA and functions in germ cell development and anteroposterior PGC positioning in *Xenopus laevis*. *Dev Biol.* **311**, 554-565.
- Tarbashevich K., Dzementsei A., Pieler T. (2011). A novel function for KIF13B in germ cell migration. *Dev Biol.* **349**, 169-178.
- Tenenhaus C., Subramaniam K., Dunn M.A., Seydoux G. (2001). PIE-1 is a bifunctional protein that regulates maternal and zygotic gene expression in the embryonic germ line of *Caenorhabditis elegans*. *Genes Dev.* **15**, 1031-1040.
- Terayama K., Kataoka K., Morichika K., Orii H., Watanabe K., Mochii M. (2013). Developmental regulation of locomotive activity in *Xenopus* primordial germ cells. *Dev Growth Differ.* **55**, 217-228.
- Thelen M. (2001). Dancing to the tune of chemokines. *Nat. Immunol.* **2**, 129-134.
- Thorpe J.L., Doitsidou M., Ho S.Y., Raz E., Farber S.A. (2004). Germ cell migration in zebrafish is dependent on HMGCoA reductase activity and prenylation. *Dev Cell* **6**, 295-302.
- Tranquillo R.T., Zigmond S.H., Lauffenburger D.A. (1988). Measurement of the chemotaxis coefficient for human neutrophils in the under-agarose migration assay. *Cell Motil Cytoskeleton* **11**, 1-15.
- Tsuda M., Sasaoka Y., Kiso M., Abe K., Haraguchi S., Kobayashi S., Saga Y. (2003). Conserved role of nanos proteins in germ cell development. *Science* **301**, 1239–1241.
- V
- Van Doren M., Broihier H.T., Moore L.A., Lehmann R. (1998). HMG-CoA reductase guides migrating primordial germ cells. *Nature* **396**, 466-469.
- Van Haastert P.J., Veltman D.M. (2007). Chemotaxis: navigating by multiple signaling pathways. *Sci STKE.* **346**, pe40.
- Varlamova O., Spektor A., Bresnick A.R. (2001). Protein kinase C mediates phosphorylation of the regulatory light chain of myosin-II during mitosis. *J. Muscle Res. Cell Motil.* **22**, 243–250.
- Venkataraman T., Dancausse E., King M. L. (2004). „PCR-based Cloning and Differential Screening of RNAs from *Xenopus* Primordial Germ Cells, Cloning Uniquely Expressed RNAs from Rare Cells.” *In Methods in*

*Molecular Biology: Germ Cell Protocols (Molecular Embryo Analysis, Live Imaging, Transgenesis and Cloning)*, Vol. 2, edited by H. Schatten, pp. 67-78. Totowa: Humana Press.

Venkatarama T., Lai F., Luo X., Zhou Y., Newman K., King M.L. (2010). Repression of zygotic gene expression in the *Xenopus* germline. *Development* **137**, 651-660.

Venkateswarlu K., Hanada T., Chishti A.H. (2005). Centaurin- $\alpha$ 1 interacts directly with kinesin motor protein KIF13B. *J Cell Sci.* **118**, 2471-2484.

Vincent S.D., Dunn N.R., Sciammas R., Shapiro-Shalef M., Davis M.M., Calame K., Bikoff E.K., Robertson E.J. (2005). The zinc finger transcriptional repressor Blimp1/Prdm1 is dispensable for early axis formation but is required for specification of primordial germ cells in the mouse. *Development* **132**, 1315-1325.

## W

Wang J.F., Park I.W., Groopman J.E. (2000). Stromal cell-derived factor-1 $\alpha$  stimulates tyrosine phosphorylation of multiple focal adhesion proteins and induces migration of hematopoietic progenitor cells: roles of phosphoinositide-3 kinase and protein kinase C. *Blood* **95**, 2505-2513.

Webb D.J., Zhang H., Horwitz, A.F. (2005). Cell migration: an overview. *Methods Mol. Biol.* **294**, 3-11.

Wegener J., Keese C.R., Giaever I. (2000). Electric cell-substrate impedance sensing (ECIS) as a noninvasive means to monitor the kinetics of cell spreading to artificial surfaces. *Exp Cell Res.* **259**, 158-166.

Weidinger G., Stebler J., Slanchev K., Dumstrei K., Wise C., Lovell-Badge R., Thisse C., Thisse B., Raz E. (2003). dead end, a novel vertebrate germ plasm component, is required for zebrafish primordial germ cell migration and survival. *Curr Biol.* **13**, 1429-1434.

Whittington P.M., Dixon K.E. (1975). Quantitative studies of germ plasm and germ cells during early embryogenesis of *Xenopus laevis*. *J Embryol Exp Morphol.* **33**, 57-74.

Wylie C. (1999). Germ cells. *Cell* **96**, 165-74.

Wylie C.C., Heasman J. (1976). The formation of the gonadal ridge in *Xenopus laevis*. *J Embryol Exp Morphol.* **35**, 125-138.

Wylie C.C., Roos T.B. (1976). The formation of the gonadal ridge in *Xenopus laevis*. III. The behaviour of isolated primordial germ cells in vitro. *J Embryol Exp Morphol.* **35**, 149-157.

Wylie C.C., Heasman J. (1982). Effects of the substratum on the migration of primordial germ cells. *Philos Trans R Soc Lond B Biol Sci.* **299**, 177-183.

Wylie C.C., Heasman J. (1993). Migration, proliferation, and potency of primordial germ cells. *Semin Dev Biol.* **4**, 161-170.

## X

Xu H., Kardash E., Chen S., Raz E., Lin F. (2012). G $\beta$  $\gamma$  signaling controls the polarization of zebrafish primordial germ cells by regulating Rac activity. *Development* **139**, 57-62.

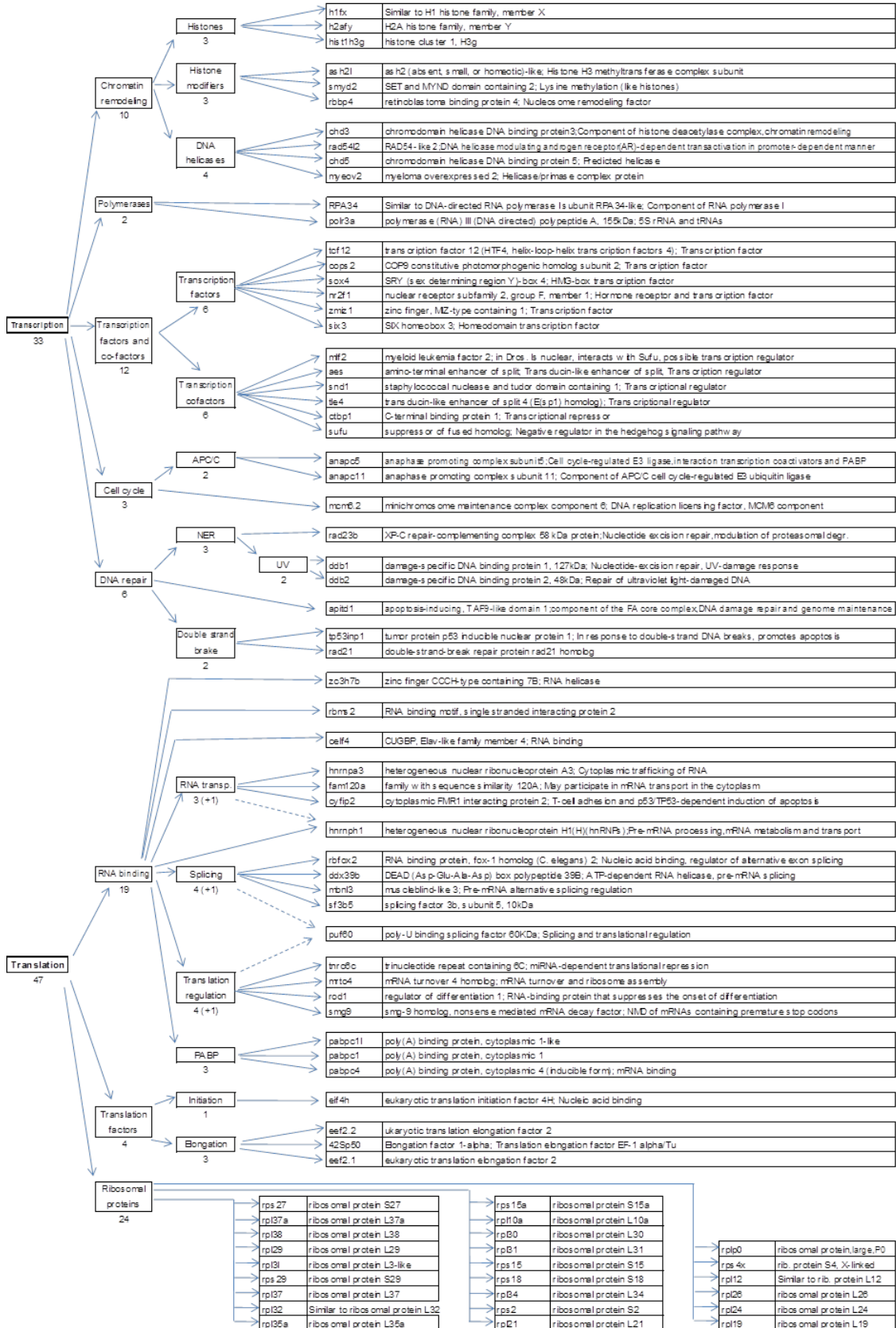
## Y

- Yabuta Y., Kurimoto K., Ohinata Y., Seki Y., Saitou M. (2006). Gene expression dynamics during germline specification in mice identified by quantitative single-cell gene expression profiling. *Biol. Reprod.* **75**, 705-716
- Yamada K.H., Hanada T., Chishti A.H. (2007). The effector domain of human Dlg tumor suppressor acts as a switch that relieves autoinhibition of kinesin-3 motor GAKIN/KIF13B. *Biochemistry* **46**, 10039-10045.
- Yamaji M., Seki Y., Kurimoto K., Yabuta Y., Yuasa M., Shigeta M., Yamanaka K., Ohinata Y., Saitou M. (2008). Critical function of Prdm14 for the establishment of the germ cell lineage in mice. *Nat Genet.* **40**, 1016-1022.
- Yin H.L. and Janmey P.A. (2003) Phosphoinositide regulation of the actin cytoskeleton. *Annu. Rev. Physiol.* **65**, 761-789.
- Ying Y., Liu X.M., Marble A., Lawson K.A., Zhao G.Q. (2000). Requirement of Bmp8b for the generation of primordial germ cells in the mouse. *Mol Endocrinol.* **14**, 1053-1063.
- Ying Y., Zhao G.Q. (2001). Cooperation of endoderm-derived BMP2 and extraembryonic ectoderm-derived BMP4 in primordial germ cell generation in the mouse. *Dev Biol.* **232**, 484-492.
- Yisraeli J.K., Sokol S., Melton D.A. (1990). A two-step model for the localization of maternal mRNA in *Xenopus* oocytes: involvement of microtubules and microfilaments in the translocation and anchoring of Vg1 mRNA. *Development* **108**, 289-298.
- Yoo S.K., Deng Q., Cavnar P.J., Wu Y.I., Hahn K.M., Huttenlocher A. (2010). Differential regulation of protrusion and polarity by PI3K during neutrophil motility in live zebrafish. *Dev Cell* **18**, 226-36.
- Youngren K.K., Coveney D., Peng X., Bhattacharya C., Schmidt L.S., Nickerson M.L., Lamb B.T., Deng J.M., Behringer R.R., Capel B., Rubin E.M., Nadeau J.H., Matin A. (2005). The Ter mutation in the dead end gene causes germ cell loss and testicular germ cell tumours. *Nature* **435**, 360-364.

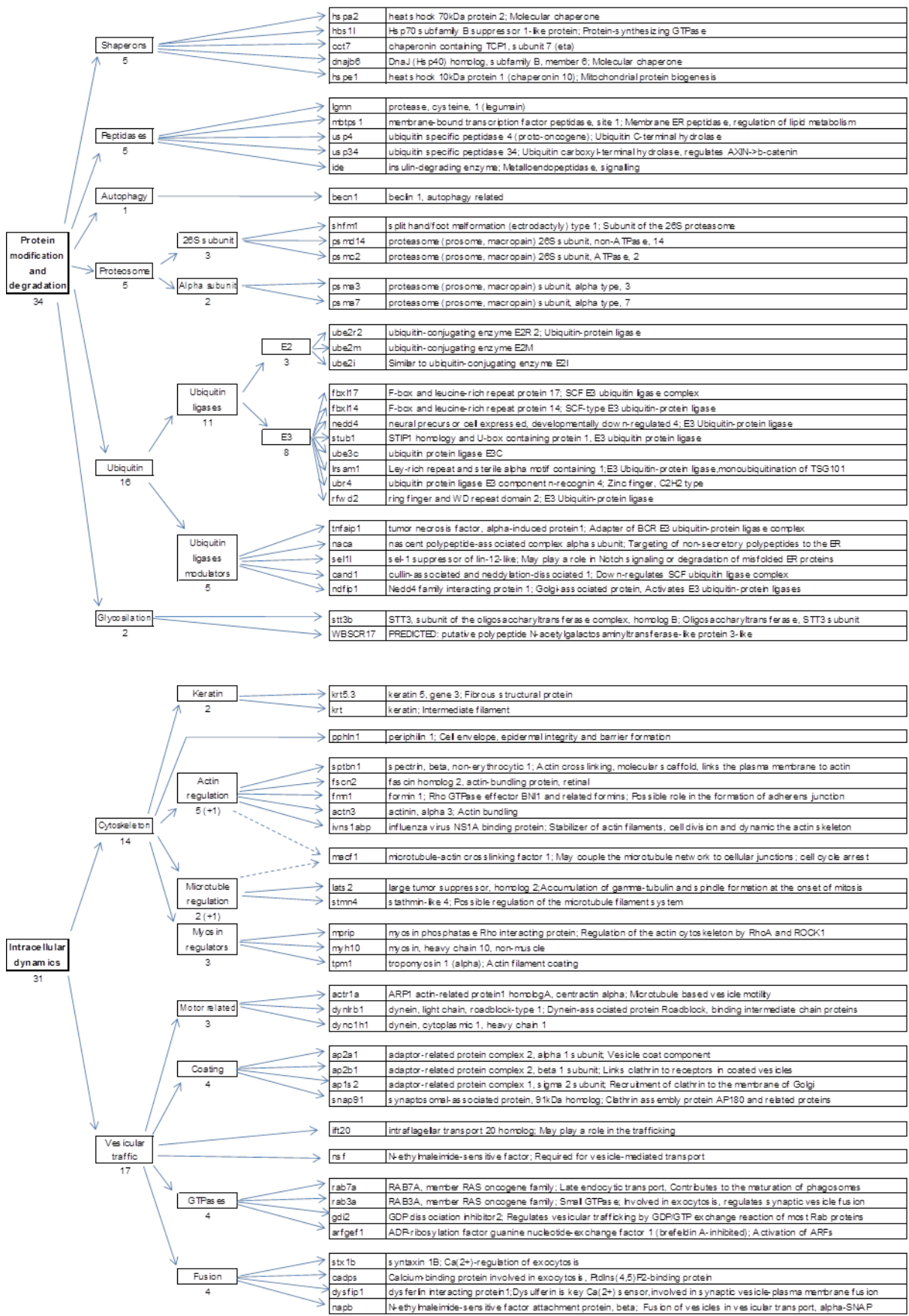


Supplementary material

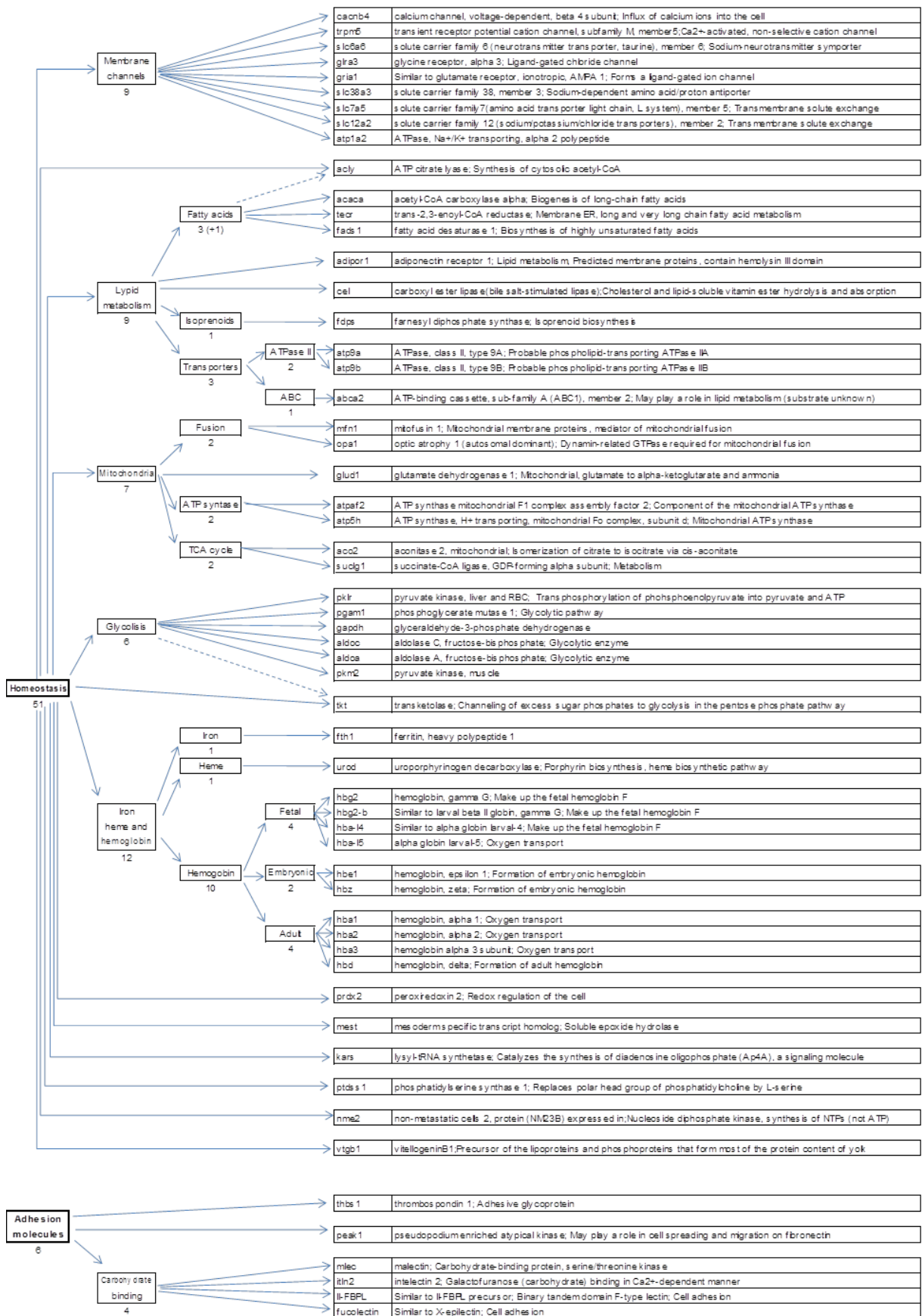
PGC upregulated genes



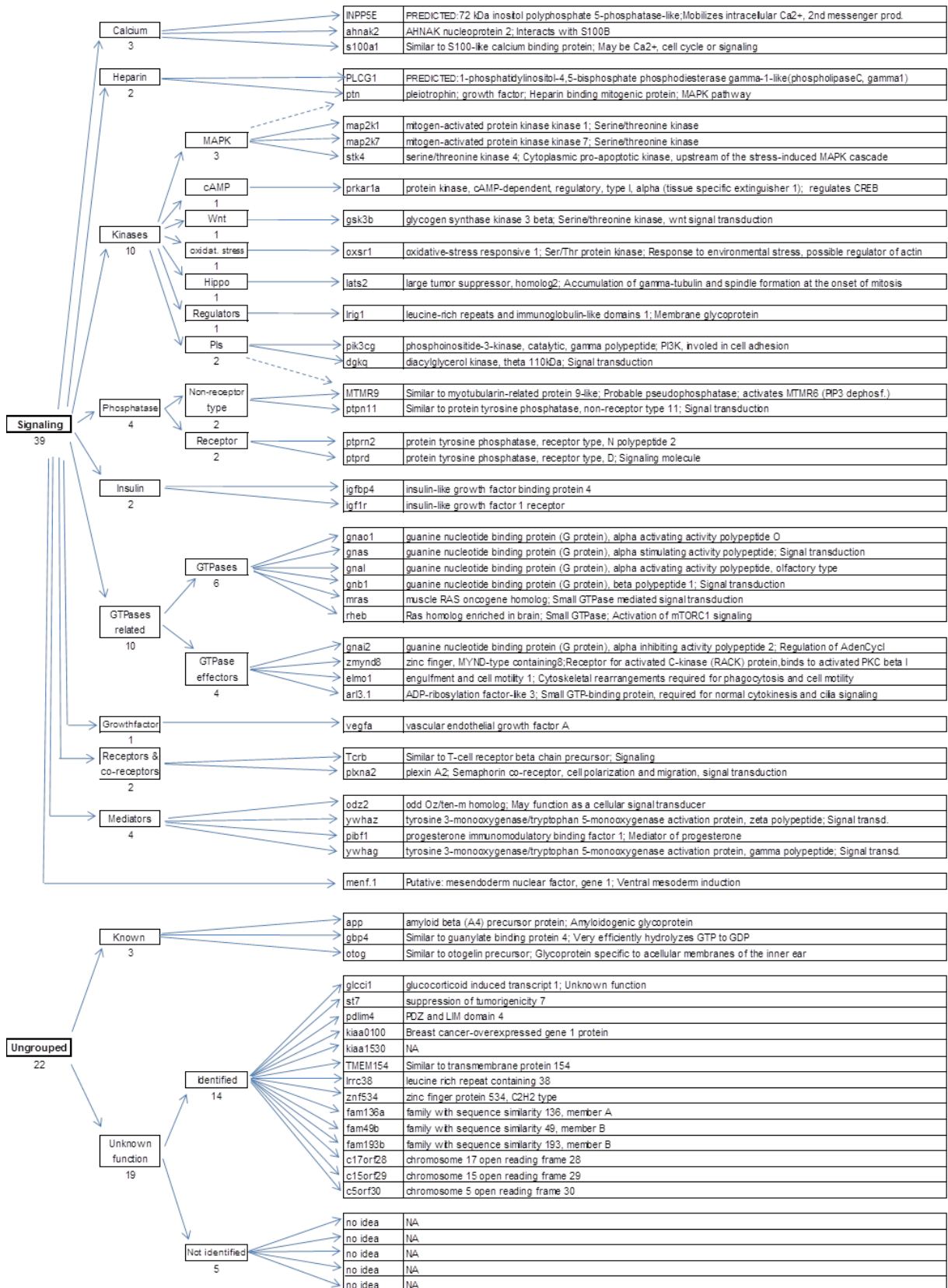
PGC upregulated genes



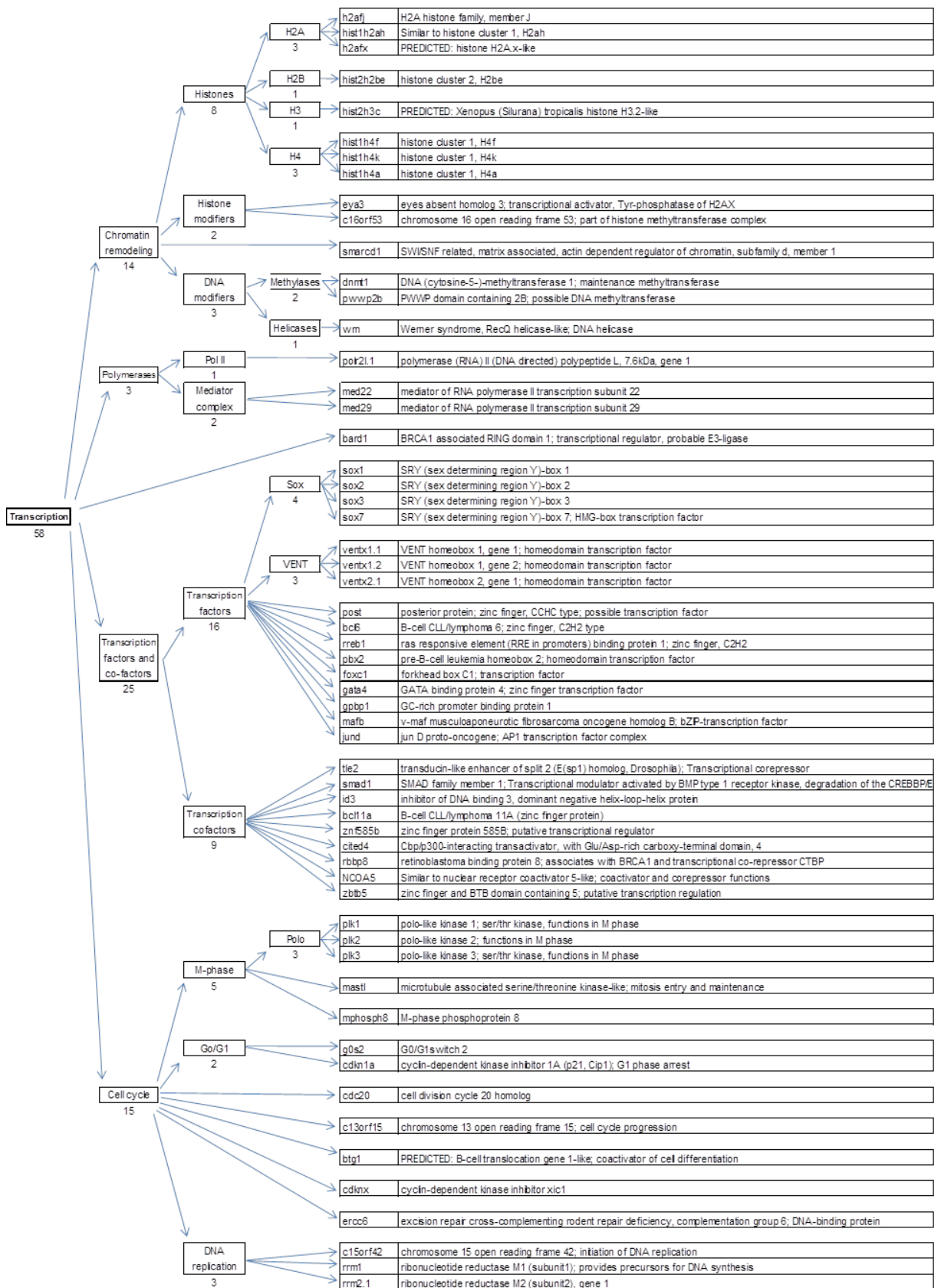
PGC upregulated genes



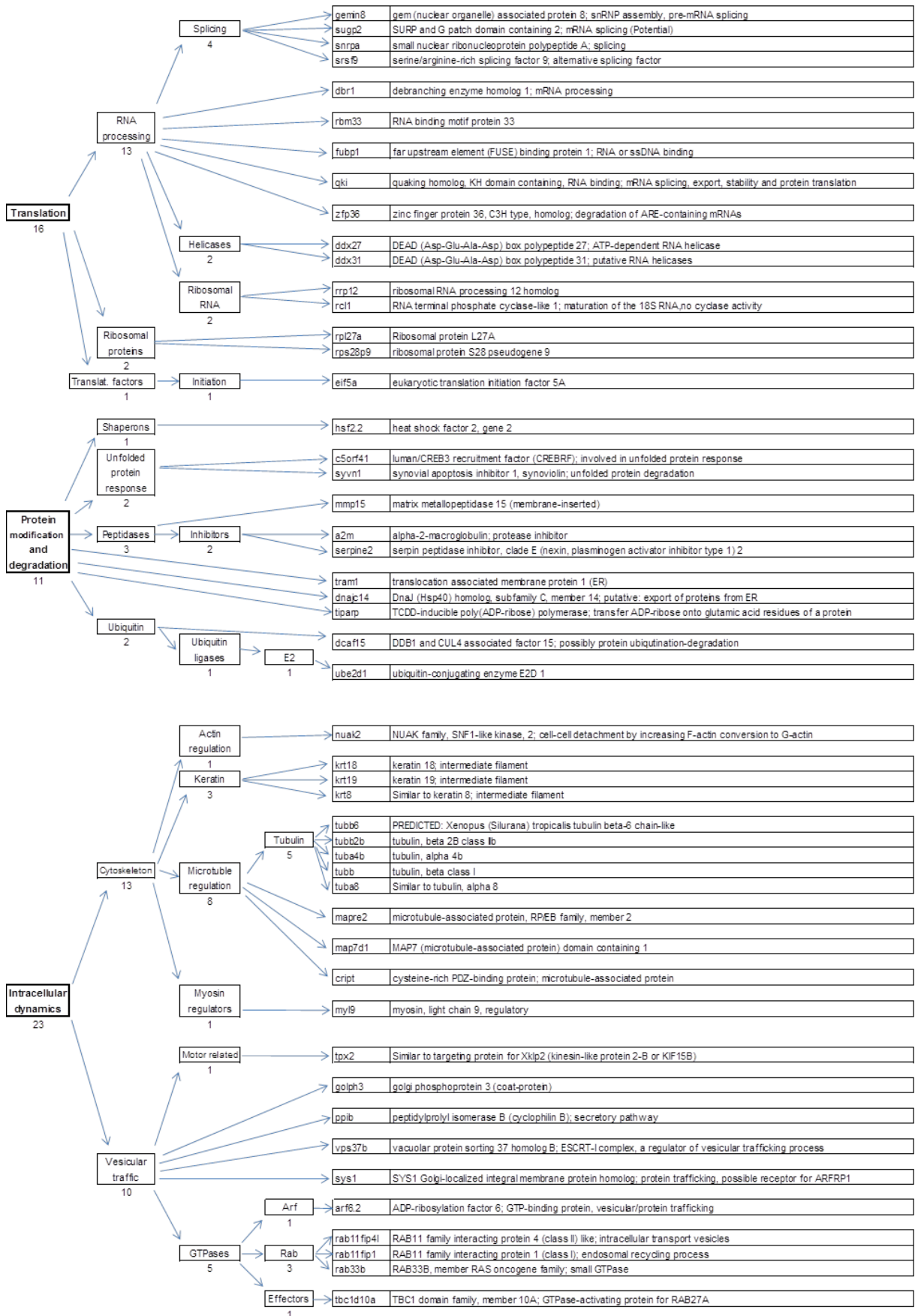
PGC upregulated genes

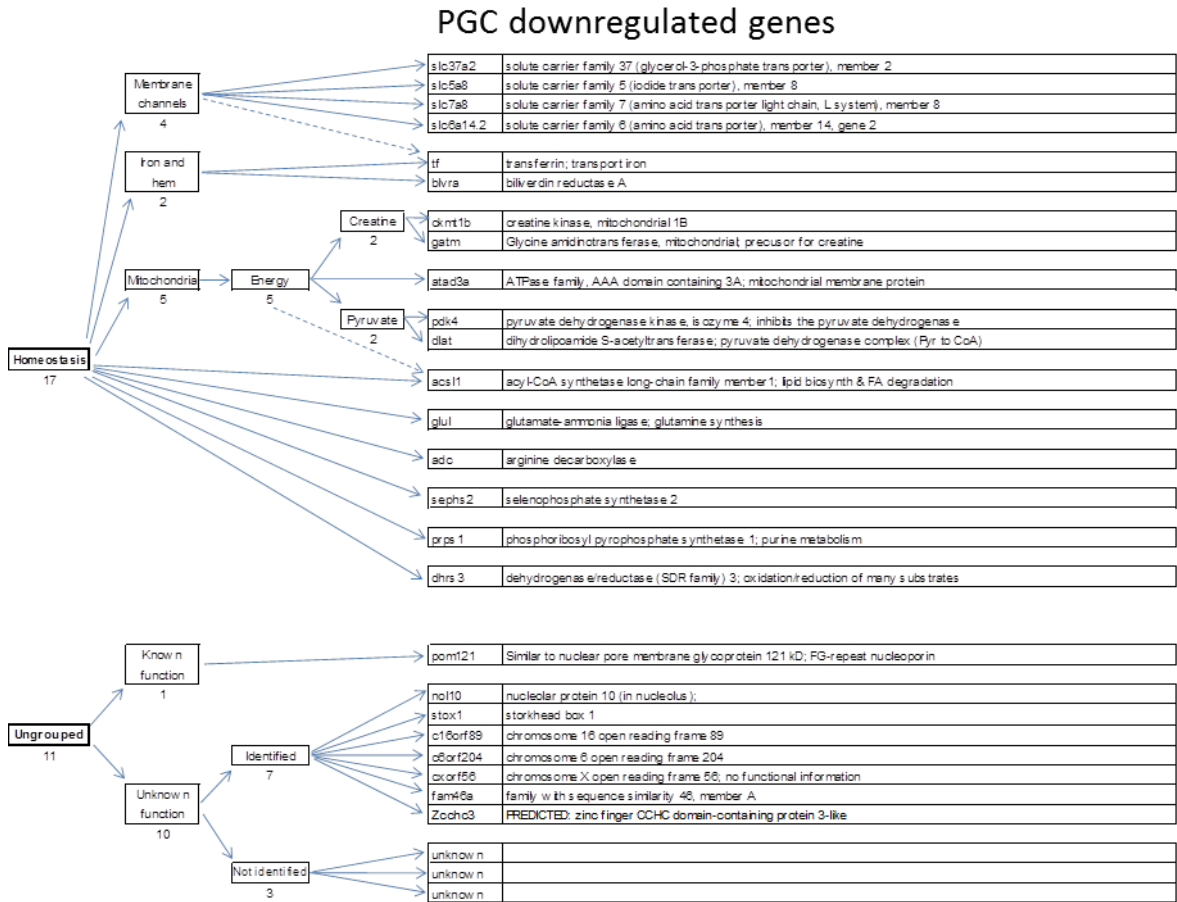


PGC downregulated genes

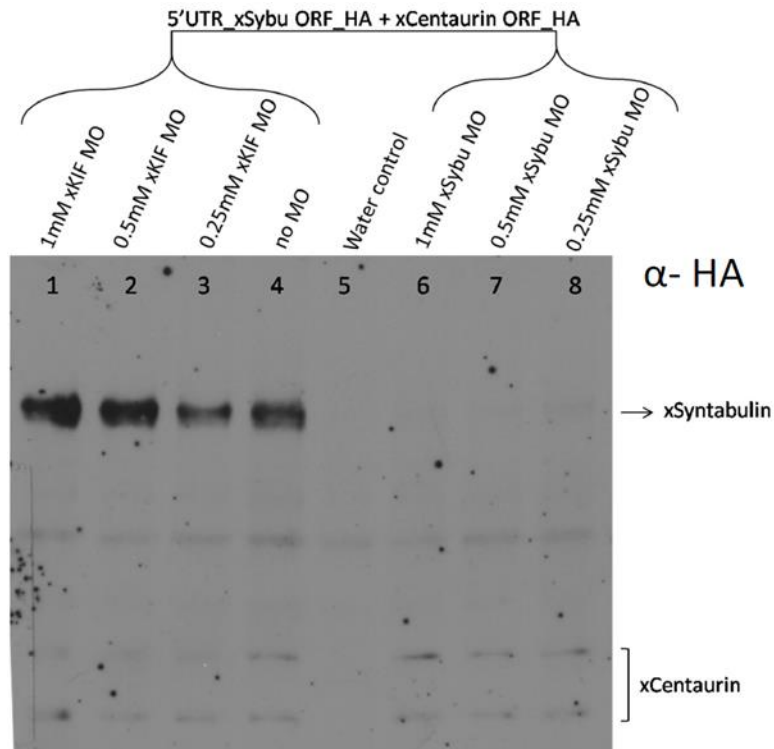


PGC downregulated genes





**Suppl. Fig. 1. Groups of differentially up- and downregulated genes in PGCs isolated from tailbud stage versus PGCs isolated from neurula stage *X. laevis* embryos.** Data obtained after next generation sequencing analysis were used to identify differentially expressed genes, upregulated or downregulated in migratory (tailbud, stage 28-30) versus pre-migratory (neurula, stage 17-19) PGCs. Genes were grouped according to the function in the cell and homology. Number below each group name corresponds to the number of genes in the group.



**Suppl. Fig. 2. Specificity of xSybu MO.** Different concentrations of xSyntabulin antisense morpholino (xSybu MO) were used for knockdown of xSyntabulin expression *in vitro*. HA-tagged xSyntabulin protein was produced by in vitro transcription and translation (TNT) of the pCS2+\_5'UTR\_xSybu\_HA construct (lane: 1-3, 5-8). The TNT reaction was allowed to occur in the presence of xSyntabulin morpholino (xSybu MO) of varying concentrations (0.25mM, 0.5mM, 1mM) or xKIF13B morpholino (xKIF MO) as control (lane: 1-3). xCentaurin protein was also produced similarly in the same reaction, to check for specificity of the xSybu MO (lane: 1-3, 5-8). Additionally, a water control was also used (lane: 4).



## Curriculum vitae

**Name:** Aliaksandr Dzementsei

**Date of birth:** 23<sup>th</sup> May 1985

**Place of Birth:** Minsk, Belarus

**E-mail:** dzementsei@gmail.com

### EDUCATION

**1991-2000** Gymnasium 171, Minsk, Belarus

**2000-2002** Lyceum of Belarusian State University, Minsk, Belarus

**2002-2007** Belarusian State University, Faculty of Microbiology, speciality biotechnology, Minsk, Belarus

**2007-present** MSc/PhD Molecular Biology Program, University of Goettingen and International Max Plank Research School, Goettingen, Germany

**2009-present** PhD work in the Department. of Developmental Biochemistry, GZMB, Göttingen, Germany

### RESEARCH EXPERIENCE

**2003-2006** Course project in Dept. of Microbiology, Biological faculty, Belarusian State University.

Research topic: "The study of phenomenon caused by the mutation in gene *pelW* of bacterium *Erwinia carotovora* subsp. *atroseptica* that results in unusual production of pectinolytic enzymes".

**2006-2007** Diploma project in Dept. of Microbiology, Biological faculty, Belarusian State University.

Research topic: "The study of the minor phytopathogenicity and virulence factors of *Erwinia carotovora* subsp. *atroseptica*".

**07-09. 2007** Junior scientific assistant in the Laboratory of xenobiotic degradation and bioremediation of natural and industrial media, Institute of Microbiology, National Academy of Sciences of Belarus

**01-03.2008** Intern student in Dept. of Developmental Biology, Center for Biochemistry and Molecular Biology, George August University Goettingen. Research topic: "Cloning of *Tribolium* genes homologous to *Drosophila* members of the Wingless and Dpp pathways".

**03-05.2008** Intern student in Dept. of Developmental Biochemistry, Center for Biochemistry and Molecular Biology, George August University Goettingen.

Research topic: "Germ cells development and migration in *Xenopus laevis*".

**05-07.2008** Intern student in Neurobiology Department, Max Planck Institute of Biophysical Chemistry, Goettingen, Germany.

Research topic: "Cloning, expression and purification of Nod1 and Nod2 CARD and LRR domains".

**2008-2009** Master student at Dept. of Developmental Biochemistry, Center for Biochemistry and Molecular Biology, George August University Goettingen.

Research topic: "Mapping of xKIF13B domains in the context of the primordial germ cell migration in *Xenopus laevis* embryos".

**2009-up to date** PhD student at Dept. of Developmental Biochemistry, Center for Biochemistry and Molecular Biology, George August University Goettingen.

Research topic: "Role of cellular dynamics, adhesion and polarity in the context of primordial germ cell migration in *Xenopus laevis* embryos".

### SCHOLARSHIPS

**2002-2007** Scholarship of Belarusian State University

**2007-2008** Stipend of the Excellence Foundation for the Promotion of the Max Planck Society